SOIL WATER DYNAMICS UNDER FIELD CROPS

by

Stephen Sunday Nwabuzor, B.Sc.

A thesis submitted for the degree of Doctor of Philosophy
of the University of London in the Faculty of Engineering

October 1984

Public Health & Water Resource Engineering
Department of Civil Engineering
Imperial College of Science & Technology
London

ABSTRACT

Soil water models are of use in predicting the temporal and spatial distribution of soil moisture which is of considerable importance in agricultural and water resources planning.

A number of soil water models are reviewed. It is seen that these have in general not been validated to an appropriate extent. This study evaluates some of the postulated soil water models using field data and on the basis of the results provides a better understanding of the interplay of parameters involved in the prediction of soil water status.

The evaluated models consider the physical processes governing soil moisture transport along the soil-root-atmosphere pathway and those that relate actual evapotranspiration rate to potential evapotranspiration rate as a function of soil moisture conditions.

Evaluation of the models is preceded by field instrumentation and experimentation under different agricultural crops in the same climatic and soil environments. The importance of the neutron probe calibration for experimental sites is demonstrated. A technique is proposed for the evaluation of the soil hydraulic parameters and an optimisation procedure for the estimation of root hydraulic parameters is indicated.

The physically-based soil water model is assessed for a 45-day period and shown to perform well. The performance is improved if the root hydraulic resistance is increased.

The two single-layer empirical models are shown to predict soil moisture status, however they cannot account for recharge during deficit conditions. The assignment of a single field capacity value to represent the moisture profile is believed to account for this deficiency. The dynamic response of the soil profile can be better described by a multi-layer approach.

The most noble application of the mind of
man is the study of the works of his Creator

DEDICATION

This thesis is dedicated

to

my parents

brothers

sisters and to

well-wishers

ACKNOWLEDGEMENTS

The work presented in this thesis was carried out under the supervision of Dr H.S. Wheater whom the author sincerely thanks for his encouragement, patience, criticism and advice.

I would also like to thank the staff of the Soil Physics section of the Institute of Hydrology, Wallingford, Oxon, for providing installation equipment for the neutron probe access tubes. Emeritus Professor A.J. Rutter is specially thanked for his interest and assistance while at the Imperial College Field Station, Ascot.

My colleagues in the Water Resources Engineering Section have contributed to making these years of research most enjoyable and profitable. In a special manner, I want to mention Dave Sherratt for his help with the field instrumentation and with whom many hours of valuable discussion was shared.

Several people have contributed in diverse ways to the successful completion of this work and I want to express my appreciation to all of them; in particular, Biodun Ilumoka who showed great understanding and provided the much needed moral support through the period of this work.

The author is grateful to the European Economic Community for awarding a scholarship that made this work possible. Miss Anne Officer and Mrs Fiona Newman of the British Council, who acted as Programme Officers are thanked for their interest and regular enthusiasm to help. Also the National Cereals Research Institute, Ibadan, Nigeria, is acknowledged for granting a study leave for this work. Finally, my thanks to Miss Judith Barritt for typing the thesis.

CONTENTS

		Page
	ABSTRACT	2
	ACKNOWLEDGEMENTS	5
	CONTENTS	6
	LIST OF TABLES	10
	LIST OF FIGURES	12
CHAPTER 1	GENERAL INTRODUCTION	17
1.1	Background	17
1.2	Objectives of Study	19
CHAPTER 2	CONCEPTS OF SOIL WATER MOVEMENT	21
2.1	Introduction	21
2.2	Soil Water Storage	21
2.2.1	Capillarity	21
2.2.2	Adsorption	23
2.3	Soil Water Characterisation	23
2.4	The Soil Moisture Characteristics	25
2.5	Soil Water Movement	28
2.6	Application of the Water Flow Equation	33
2.6.1	Infiltration and Redistribution	33
2.6.2	Redistribution	38
2.6.3	Evaporation from a Bare Soil Surface	40
2.7	Conclusions	42
CHAPTER 3	A REVIEW OF PLANT WATER RELATIONS	43
3.1	Introduction	43
3.2	Plant Water Relations	43
3.2.1	The Soil-Plant-Atmosphere Continuum	43
3.2.2	The Leaf-Air Interface	44
3.2.2.1	Measurement of Actual Evapotranspiration	48
3.2.2.2	Potential Evaporation	52
3.2.2.3	The Penman Formula	54
3.2.2.4	Modification of the Combination Approach to Estimate Actual Evaporation	56

		Page
3.2.3	Soil-Root Interface	58
3.2.3.1	The Microscopic Approach	58
3.2.3.2	The Macroscopic Approach	60
3.3	Empirical Models	69
3.4	Comparison of Physical and Empirical Models	79
3.5	Conclusions	81
CHAPTER 4	THE STRUCTURE OF ADOPTED SOIL WATER MODELS	82
4.1	Introduction	82
4.2	Choice of a Physically-Based Soil Water Model	82
4.3	The Physically-Based Soil Water Model: Structure and Dynamics	84
4.3.1	Soil Water Dynamics and Extraction Model	84
4.3.2	Boundary Conditions	90
4.3.3	Selection of Time Step	90
4.3.4	Initial Conditions and Model Calculation Procedure	91
4.3.5	Optimisation of the Crown Potential	94
4.4	Limitations and Capabilities of the Physical Soil Water Model	95
4.5	Choice of Empirically-Based Soil Water Model	96
4.6	The Dynamics of the Empirically-Based Model	98
4.7	Conclusions	102
CHAPTER 5	FIELD EXPERIMENTATION TO MONITOR SOIL MOISTURE AT SILWOOD PARK	103
5.1	Introduction	103
5.2	Soil Moisture Measurement Techniques	104
5.2.1	Moisture Measurement Techniques	104
5.2.1.1	Gravimetric Technique	104
5.2.1.2	Electromagnetic Technique	105
5.2.1.3	Nuclear Technique	105
5.2.2	Soil Moisture Potential Measurement	109
5.2.2.1	Tensiometer	109
5.2.2.2	Porous Blocks	109
5.2.3	Remote Sensing	110
5.3	Choice of Soil Moisture Measurement Techniques	110

		Page
5.4	The Field Experiments	111
5.4.1	Experimental Area	111
5.4.2	Particle Size Analysis	111
5.4.3	The Soil Profile	114
5.4.4	The Field Crops	116
5.5	Instrumentation	118
5.5.1	Access Tubes	118
5.5.2	Tensiometers	119
5.5.3	Weather Station	119
5.6	The Neutron Probe Calibration	120
5.6.1	Bulk Calibration	120
5.6.2	Surface Calibration	122
5.7	Bulk Density	125
5.8	Data Collection and Observation	127
5.9	Conclusions	128
CHAPTER 6	FIELD ESTIMATION OF SOIL HYDRAULIC PARAMETERS	130
6.1	Introduction	130
6.2	Determination of the Unsaturated Hydraulic Conductivity	130
6.2.1	Theoretical Calculations	130
6.2.2	Laboratory Measurement	131
6.2.3	In situ Technique	132
6.2.3.1	Infiltration Technique	132
6.2.3.2	The Internal Drainage Technique	134
6.2.3.3	Natural Balance Method	138
6.3	Determination of the Soil Moisture Characteristics	145
6.4	Analyses of Data	146
6.4.1	Neutron Probe Readings	147
6.4.2	Tensiometer Readings	148
6.5	Results and Discussion	149
6.5.1	Unsaturated Hydraulic Conductivity	149
6.5.2	Soil Moisture Characteristics	180
6.6	Conclusions	180

		Page
CHAPTER 7	EVALUATION OF THE PHYSICAL SOIL WATER MODEL	183
7.1	Introduction	183
7.2	Soil Hydraulic Resistance	183
7.3	Root Hydraulic Resistance	185
7.3.1	Procedure for Estimating Cortex Hydraulic Resistance	185
7.3.1.1	Water Balance	186
7.3.1.2	Calculation of Crown Potential	191
7.4	Description of Input Data to Physical Soil Water Model	194
7.5	Computer Program	194
7.6	The Model Behaviour	195
7.6.1	The Relationship of Actual/Potential Crown Potential and Soil Hydraulic Resistance	197
7.6.2	Simulation of Layer Moisture Contents	198
7.6.3	Sensitivity of Model Output to Root Hydraulic Resistance	202
7.6.4	Actual Evapotranspiration and Drainage	207
7.6.5	Simulated Hydraulic Head Profiles	207
7.7	Conclusions	210
CHAPTER 8	THE EVALUATION OF EMPIRICAL DRYING CURVES	212
8.1	Introduction	212
8.2	The Determination of Field Capacity and Soil Moisture Deficit	212
8.3	Determination of Available Water Capacity	216
8.3.1	Linear Drying Curve	218
8.3.2	The Exponential Drying Curve	220
8.4	Simulation Results	221
8.5	Recharge Estimation	237
8.6	Spatial Variability of SMD's	238
8.7	Conclusions	239
CHAPTER 9	CONCLUSIONS	241
REFERENCES		244
APPENDIX A	COMPUTER PROGRAM OF PHYSICALLY-BASED SOIL WATER MODEL	
APPENDIX B	COMPUTER PROGRAM OF EMPIRICALLY-BASED SOIL WATER MODEL	

LIST OF TABLES

Page

CHAPTER 5

Table 5.1 Average values of soil physical properties 115

Table 5.2 Planting and harvesting dates 1980-1982 118

Table 5.3 Rooting depth observation 128

CHAPTER 6

Table 6.1a Water content and storage during the drying cycle, summer 1980 (permanent grass) and the unsaturated hydraulic conductivity 159

Table 6.1b Water content and storage during the drying cycle, summer 1980 (permanent grass) and the unsaturated hydraulic conductivity 160

Table 6.1c Water content and storage during the drying cycle, summer 1980 (permanent grass) and the unsaturated hydraulic conductivity 161

Table 6.2a Water content and storage during the drying cycle, summer 1981 (permanent grass) and the unsaturated hydraulic conductivity 162

Table 6.2b Water content and storage during the drying cycle, summer 1981 (permanent grass) and the unsaturated hydraulic conductivity 163

Table 6.2c Water content and storage during the drying cycle, summer 1981 (permanent grass) and the unsaturated hydraulic conductivity 164

Table 6.3a Water content and storage during the wetting cycle, summer 1981 (permanent grass) 170

Table 6.3b Water content and storage during the wetting cycle, summer 1981 (permanent grass) 171

Table 6.3c Water content and change in storage during the wetting cycle, summer 1981 (permanent grass) 172

Table 6.4 Unsaturated hydraulic conductivity data (permanent grass) 175

Table 6.5 Regression constants describing $k(\theta)$ for different layers 176

Page

CHAPTER 7

Table 7.1 Root density distribution 184

Table 7.2 Observed actual evapotranspiration 191

CHAPTER 8

Table 8.1 Field capacity values 216

Table 8.2 Linear depletion curve - optimised available water capacity 220

Table 8.3 Exponential drying curve - optimised root constant 221

Table 8.4 Recharge estimates 237

Table 8.5 Standard deviation of measured SMD's 239

LIST OF FIGURES

Page

CHAPTER 2

Fig. 2.1 Capillary rise 22

Fig. 2.2 Attraction of water molecule to clay micelle 22

Fig. 2.3 Soil moisture characteristics for different soil types 27

Fig. 2.4 Hysteresis and hysteresis loop 27

Fig. 2.5 Conductivity-suction relationship for different soils 30

Fig. 2.6 Rectangular unit volume of soil 30

Fig. 2.7 Infiltration moisture profile 35

Fig. 2.8 Redistribution following irrigation in a medium-textured soil profile 39

CHAPTER 3

Fig. 3.1 Schematic representation of transpiration through the stomata and the cuticle 45

Fig. 3.2 Illustration of a leaf section with open and closed stomata 45

Fig. 3.3 General shape of the sink term as a function of soil water content 67

Fig. 3.4 Variation of the sink term with depth 67

Fig. 3.5 Types of assumed relationships between plant-available soil moisture and AE/PE rate 71

Fig. 3.6 Temporal decrease of transpiration for crops having different root densities 72

Fig. 3.7 Relationship between actual and potential soil moisture deficit 74

Fig. 3.8 Ratio of actual to potential transpiration as a function of soil moisture 76

CHAPTER 4

Fig. 4.1 Model Structure 85

Fig. 4.2 Representation of a root system as a resistance network 88

Fig. 4.3 Flow diagram of physical soil water model 93

Fig. 4.4 Flow diagram for calculating soil moisture deficit 99

Fig. 4.5 Regulating functions used to determine actual evaporation from potential for the study site 100

Page

CHAPTER 5

Fig. 5.1 The field station Silwood Park 112

Fig. 5.2 Instrument network 113

Fig. 5.3 Summary of soil profile 117

Fig. 5.4 The Neutron probe 121

Fig. 5.5 Neutron probe bulk calibration curve 123

Fig. 5.6 Institute of Hydrology calibration curves 124

Fig. 5.7 Neutron probe surface calibration curve 126

CHAPTER 6

Fig. 6.1 Diagram of hydraulic head profiles 139

Fig. 6.2 Hydraulic head and moisture profiles (drying cycle) 141

Fig. 6.3 Hydraulic head and moisture profiles (wetting cycle) 144

Fig. 6.4 Hydraulic head profile, Grass (1/08/80) 150

Fig. 6.5 Hydraulic head profile, Grass (4/08/80) 151

Fig. 6.6 Hydraulic head profile, Grass (8/08/80) 152

Fig. 6.7 Hydraulic head profile, Grass (26/06/81) 153

Fig. 6.8 Hydraulic head profile, Grass (30/06/81) 154

Fig. 6.9 Hydraulic head profile, Grass (6/07/81) 155

Fig. 6.10 Hydraulic head profile, Grass (11/07/81) 156

Fig. 6.11 Hydraulic head profile, Grass (24/07/81) 157

Fig. 6.12 Hydraulic head profile, Grass (27/07/81) 158

Fig. 6.13 Hydraulic head profile, Grass (1/05/81 - wetting cycle) 165

Fig. 6.14 Hydraulic head profile Grass (8/05/81 - wetting cycle) 166

Fig. 6.15 Hydraulic head profile Grass (11/05/81 - wetting cycle) 167

Fig. 6.16 Hydraulic head profile Grass (19/05/81 - wetting cycle) 168

Fig. 6.17 Hydraulic head profile Grass (3/08/81 - wetting cycle) 169

Fig. 6.18 Moisture profiles Grass - wetting cycle 173

Fig. 6.19 Unsaturated hydraulic conductivity - wetness relationship 177

Fig. 6.20 Unsaturated hydraulic conductivity - wetness relationship 178

Page

Fig. 6.21 Unsaturated hydraulic conductivity - wetness relationship 179

Fig. 6.22a Soil moisture characteristics 181

Fig. 6.22b Soil moisture characteristics 181

Fig. 6.22c Soil moisture characteristics 181

Fig. 6.22d Soil moisture characteristics 181

CHAPTER 7

Fig. 7.1a Hydraulic head profiles permanent grass (1981) 187

Fig. 7.1b Hydraulic head profiles permanent grass (1981) 188

Fig. 7.1c Hydraulic head profiles permanent grass (1981) 189

Fig. 7.1d Hydraulic head profiles permanent grass (1981) 190

Fig. 7.2 Simulated optimised crown potentials using different cortex hydraulic resistances 193

Fig. 7.3 Simulated optimised crown potentials using different cortex hydraulic resistances 193

Fig. 7.4 Simulated optimised crown potentials using different cortex hydraulic resistances 193

Fig. 7.5 Temporal distribution of potential and actual crown potentials 196

Fig. 7.6 Relationship of actual/potential crown ratio vs soil resistance 199

Fig. 7.7a Simulated vs observed moisture content 0-15 cm layer 200

Fig. 7.7b Simulated vs observed moisture content 15-25 cm layer 200

Fig. 7.7c Simulated vs observed moisture content 25-35 cm layer 200

Fig. 7.7d Simulated vs observed moisture content 35-45 cm layer 200

Fig. 7.7e Simulated vs observed moisture content 45-55 cm layer 201

Fig. 7.7f Simulated vs observed moisture content 55-65 cm layer 201

Fig. 7.7g Simulated vs observed moisture content 65-75 cm layer 201

Fig. 7.7h Simulated vs observed moisture content 75-85 cm layer 201

Fig. 7.8a Simulated vs observed moisture content 0-15 cm layer, at cortex resistance of 500 day 203

Fig. 7.8b Simulated vs observed moisture content 15-25 cm layer, at cortex resistance of 500 day 203

Page

Fig. 7.8c Simulated vs observed moisture content 25-35 cm layer, at cortex resistance of 500 day 203

Fig. 7.8d Simulated vs observed moisture content 35-45 cm layer, at cortex resistance of 500 day 203

Fig. 7.8e Simulated vs observed moisture content 45-55 cm layer, at cortex resistance of 500 day 204

Fig. 7.8f Simulated vs observed moisture content 55-65 cm layer, at cortex resistance of 500 day 204

Fig. 7.8g Simulated vs observed moisture content 65-75 cm layer, at cortex resistance of 500 day 204

Fig. 7.8h Simulated vs observed moisture content 75-85 cm layer, at cortex resistance of 500 day 204

Fig. 7.9a Simulated vs observed moisture content 0-15 cm layer, at cortex resistance of 1500 day 205

Fig. 7.9b Simulated vs observed moisture content 15-25 cm layer, at cortex resistance of 1500 day 205

Fig. 7.9c Simulated vs observed moisture content 25-35 cm layer, at cortex resistance of 1500 day 205

Fig. 7.9d Simulated vs observed moisture content 35-45 cm layer, at cortex resistance of 1500 day 205

Fig. 7.9e Simulated vs observed moisture content 45-55 cm layer, at cortex resistance of 1500 day 206

Fig. 7.9f Simulated vs observed moisture content 55-65 cm layer, at cortex resistance of 1500 day 206

Fig. 7.9g Simulated vs observed moisture content 65-75 cm layer, at cortex resistance of 1500 day 206

Fig. 7.9h Simulated vs observed moisture content 75-85 cm layer, at cortex resistance of 1500 day 206

Fig. 7.10 Cumulative evapotranspiration 208

Fig. 7.11 Simulated hydraulic head profiles 209

Fig. 7.12 Simulated hydraulic head profiles 209

Fig. 7.13 Simulated hydraulic head profiles 209

Fig. 7.14 Simulated hydraulic head profiles 209

CHAPTER 8

Fig. 8.1 Distribution of total profile moisture with time 215

Page

Fig. 8.2 R^2 contours for two response surfaces 219

Fig. 8.3a Simulated vs observed SMDs (Grass 1980) 222

Fig. 8.3b Simulated vs observed SMDs (Grass 1981) 222

Fig. 8.3c Simulated vs observed SMDs (Grass 1982) 223

Fig. 8.4a Simulated vs observed SMDs (Wheat 1980) 224

Fig. 8.4b Simulated vs observed SMDs (Wheat 1981) 224

Fig. 8.4c Simulated vs observed SMDs (Wheat 1982) 225

Fig. 8.5a Simulated vs observed SMDs (Orchard 1980) 226

Fig. 8.5b Simulated vs observed SMDs (Orchard 1981) 226

Fig. 8.5c Simulated vs observed SMDs (Orchard 1982) 227

Fig. 8.6a Simulated vs observed SMDs (Field Bean 1980) 228

Fig. 8.6b Simulated vs observed SMDs (Field Bean 1981) 228

Fig. 8.7a Simulated vs observed SMDs (Grass 1980)
- exponential curve 230

Fig. 8.7b Simulated vs observed SMDs (Grass 1981)
- exponential curve 230

Fig. 8.7c Simulated vs observed SMDs (Grass 1982)
- exponential curve 231

Fig. 8.8a Simulated vs observed SMDs (Wheat 1980)
- exponential curve 232

Fig. 8.8b Simulated vs observed SMDs (Wheat 1981)
- exponential curve 232

Fig. 8.8c Simulated vs observed SMDs (Wheat 1982)
- exponential curve 233

Fig. 8.9a Simulated vs observed SMDs (Orchard 1980)
- exponential curve 234

Fig. 8.9b Simulated vs observed SMDs (Orchard 1981)
- exponential curve 234

Fig. 8.9c Simulated vs observed SMDs (Orchard 1982)
- exponential curve 235

Fig. 8.10a Simulated vs observed SMDs (Field Bean, 1980)
- exponential curve 236

Fig. 8.10b Simulated vs observed SMDs (Field Bean, 1981)
- exponential curve 236

CHAPTER 1

GENERAL INTRODUCTION

1.1 Background

The study of soil water dynamics is of major importance in the fields of agriculture, hydrology and environmental engineering. The reason for this can be ascribed to the significant role which soil water plays in food production, groundwater reserves and in the modification of the environment.

From an agricultural perspective, soil water is important at various stages of crop growth including seeding, germination, flowering and harvesting stages, where excess or scarcity of water exerts deleterious effects on plant growth. Hydrological interest ranges from predicting overland flow, in order to estimate surface runoff occurrence, to the estimation of groundwater recharge. Groundwater resources provide a significant proportion of freshwater. This resource depends on percolated soil water for recharge. The rapid industrialisation, urbanisation and higher life expectancy in most developed countries demand that this resource be jealously guarded. However, in our search for adequate and increased food production, fertilizers, pesticides and herbicides are continually being applied to agricultural lands to improve growth and yield potential. These chemicals dissolve in soil water and eventually are mobilised to recharge groundwater. The quantity of leachates needs to be monitored if groundwater reserves are not to be polluted in the long term. In this respect, the dynamics of soil water become significant.

The foregoing diverse interests have led to the postulation of numerous soil water models. In recent years, this has been accentuated by the development of computer technology which offers a major advancement in our search for a fast and accurate solution to hitherto complex and time consuming algorithms. Soil water models are based either on a theoretical treatment of the processes involved in the hydrological balance of soils or on an empirical treatment of the atmospheric demand as a function of soil water status. These models

range from single to multi-parameter models. However, validation of these models is the exception rather than the rule. This is because the measurement of the intrinsic parameters is difficult and requires, in some cases, an extensive network of instruments and laborious experimentation. If and when attempts are made to evaluate the parameters, they are site specific and hence cannot be extrapolated to other areas. This latter fact has probably accounted for the proliferation of soil water models whose utility is confined to the modellers! The question therefore arises:- has a stage not been reached where a 'break' should be put to further model formulation and effort concentrated on evaluation of current models? It is believed this would provide a better understanding of the compatibility of concepts governing soil water flow with existing soil water models. For instance, along the soil-root-atmosphere pathway, a dichotomy in opinion exists regarding which component exerts significant influence on soil moisture hydraulics. A school of thought argues for the roots while the other advocates for the dominance of the soil.

Apart from the preceding, there is the problem of model complexity which is unresolved. The more parameters that are introduced into soil water models, the more difficult is their evaluation and the more time needed for solution. It is therefore necessary to understand what level of complexity is introduced for soil water models to perform efficiently. Simple, single parameter models have been developed (Penman, 1949) to simulate soil moisture status (Grindley, 1967), although the threshold point at which soil moisture supply diverges from satisfying the potential atmospheric demand has not been reconciled. This requires evaluation of the threshold point under different soil, crop and climatic environments. This would enable modellers to arrive at a consensus and form a basis for further improvement and recommendation for water resource planners, specifically in irrigation scheduling.

The limited validation of soil water models has been due to the difficulty of measuring flow parameters under field conditions. This is because apart from instrumentation, there are problems of field soil heterogeneity which poses problems of spatial variability. Also with plant root growth, techniques have not yet been developed to monitor the changing hydraulics of roots.

Consequently, the lack of widespread use of postulated soil water models can be attributed to the following:-

(a) The lack of validation studies in different climatic, soil and crop types.

(b) The difficulty of field instrumentation which is laborious and time consuming to install, operate and maintain.

(c) The problem of field soil heterogeneity and profile layerings which cause significant variability in soil water flow parameters.

1.2 Objectives of Study

Based on the above discussion and the lack of widespread applicability of postulated soil water models, this study has the following objectives:-

(1) To carry out extensive monitoring of soil water potential and soil moisture content under different agricultural crops.

(2) To determine the usefulness of the data collected in (1) above in evaluating soil and root hydraulic parameters.

(3) To evaluate a physically-based soil water model in the presence of plant roots, by comparing simulation results with observed field data. This shall include sensitivity analysis to examine the relative dominance of the root and soil resistances to moisture flow.

(4) To evaluate two single-layer, empirically-based soil water models for their predictive abilities under the different crops. This is expected to provide a better understanding regarding the threshold point where potential atmospheric demand diverges from actual supply of moisture by the soil.

To accomplish these objectives, in Chapter 2 the fundamental concepts governing soil water movement are reviewed. In Chapter 3 the plant-water interaction processes are reviewed and an account given of existing soil water models. The structures and operational behaviours of the adopted physically-based and empirically-based soil water

models are presented in Chapter 4. The details of the experimentation and soil moisture measurement techniques are discussed in Chapter 5. In Chapter 6, the technique proposed for the evaluation of the soil hydraulic parameters is indicated, while in Chapters 7 and 8 the performance of the adopted physically and empirically-based soil water models is evaluated. Finally, the conclusions of the study are presented in Chapter 9.

CHAPTER 2

CONCEPTS OF SOIL WATER MOVEMENT

2.1 Introduction

Water is a dynamic constituent of the soil. It affects to a very large extent the physico-chemical properties of the soil. The proportion of the soil volume occupied by water determines the degree of aeration which has important implications for the growth of plants and soil microbial population (Brady, 1974). Apart from its agricultural importance, soil water determines the replenishment of groundwater reserves and is a controlling factor in the occurrence of runoff and consequent intermittent flood disasters.

This chapter gives a description of the pertinent theory and processes governing soil water movement and storage.

2.2 Soil Water Storage

Water is primarily held in soils by the processes of adsorption and capillarity. These processes generally cannot be distinguished from each other in field soils.

Although the electronegative property of clays confers greater significance to adsorption in clay soils than in sandy soils, the important mode of water retention in soils is by capillarity.

2.2.1 Capillarity

The pressure difference between the water in a capillary tube and the atmosphere (Figure 2.1) is given by Hillel (1980a) as:-

$$\Delta P = (2T\cos\alpha)/r \qquad (2.1)$$

where ΔP = pressure difference which is equal to $P_A - P$ in Figure 2.1

T = surface tension between liquid and the air (force/unit length)

α = contact angle between liquid and capillary tube

r = radius of capillary

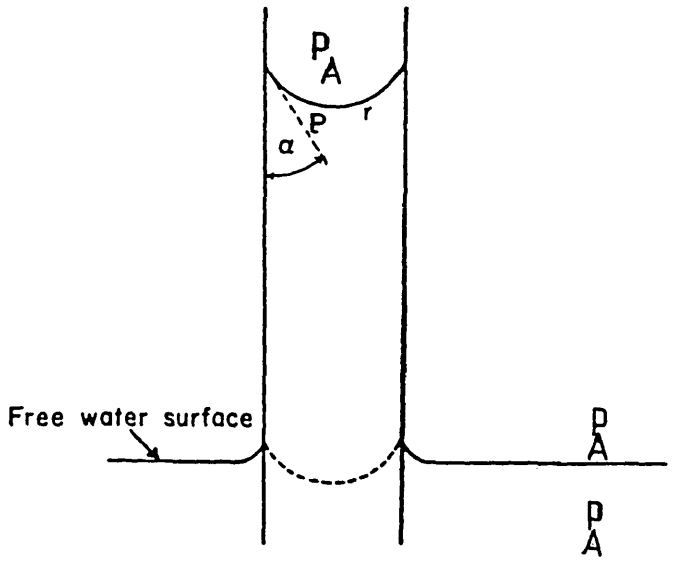

FIG. 2.1 Capillary rise.

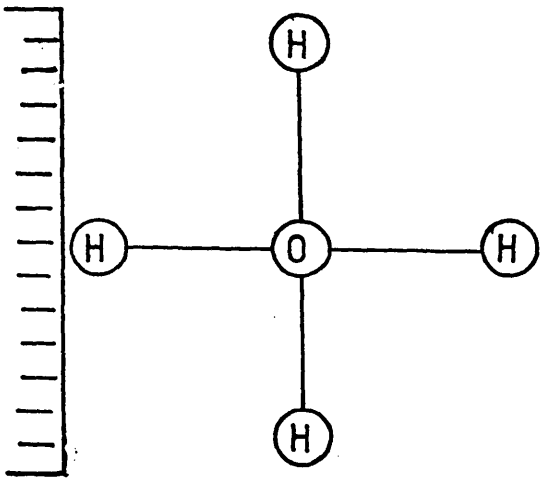

FIG.2.2 Attraction of water molecule to clay micelle.

The pressure difference in a soil pore requires two radii of curvatures r_1 and r_2 lying in planes normal to each other because of the non-spherical shape of the water-air interface, hence pressure difference is specified as:-

$$\Delta P = T(\frac{1}{r_1} + \frac{1}{r_2}) \qquad (2.2)$$

Equation 2.2 above infers that the capillary retention increases as the pore-size decreases. This explains the occurrence of more rapid drainage in sandy soils as opposed to slow prolonged drainage encountered in clay soils.

2.2.2 Adsorption

This is the adhesion of water to solid surfaces consequent upon the attraction that occurs at the molecular level. The dipolar nature of water molecules results in attraction to charged surfaces (Figure 2.2). This explains the very high suction obtained in clays when soil water is limited.

2.3 Soil Water Characterisation

Soil water is normally specified in terms of volume (or mass) relative to that of the soil or with reference to its energy state.

Mass wetness is specified by:-

$$\theta_g = M_w/M_s \qquad (2.3)$$

where θ_g = moisture content on a dry weight basis

M_w = mass of water

M_s = mass of dry soil

Volume wetness on the other hand is specified by:

$$\theta_v = V_w/V_b \qquad (2.4)$$

where θ_v = moisture content on a volume basis

V_w = volume of water

V_b = bulk volume of soil

Energy of soil water

The total soil water energy is often equated with its potential energy. This is because the kinetic energy of soil water is negligible. The potential energy is defined as the work that is required to move a unit mass of water from a given reference point at atmospheric pressure to another point under consideration.

Generally the total potential of soil water consists of gravitational, osmotic and pressure potentials. Thus:-

$$\phi_t = \phi_g + \phi_o + \phi_p \qquad (2.5)$$

where ϕ_t = total potential

ϕ_g = gravitational potential

ϕ_o = osmotic potential

ϕ_p = pressure potential

The gravitational potential is the energy due to the earth's gravitational field. It is determined by the height of a body above a given reference point. It can be specified in terms of potential energy per unit volume as:-

$$\phi_g = \rho g z \qquad (2.6)$$

where g = acceleration due to gravity

z = height above a reference

ρ = density of water

The osmotic potential occurs in the presence of a membrane whose permeability to water molecules differ from that of the molecules of dissolved salts. It is often ignored in soil water movement studies because it is assumed that the solute can move freely with the soil water. Hence:-

$$\phi_o = 0 \qquad (2.7)$$

where ϕ_o = osmotic potential

The above assumption may not be true in studies involving soil water plant interaction because the osmotic potential is likely to be an important component of the total potential.

The pressure potential is a consequence of the difference between atmospheric and soil water pressures. Below the water table, a positive hydrostatic pressure is obtained, thus for static equilibrium:

$$\phi_p = \rho g h \qquad (2.8)$$

where ϕ_p = pressure potential

ρ = density of water

g = acceleration due to gravity

h = submergence depth below free water surface

In the unsaturated zone, the pressure potential is negative as a result of the attractive forces of the soil matrix. The term capillary potential is used to indicate the potential that results from capillary effects (Buckingham, 1907). However, due to the importance of adsorption especially in clay soils as previously discussed, the term matric potential is often used.

2.4 The Soil Moisture Characteristic

The relationship between matric potential and soil water content for given soil types is presented graphically in what is commonly termed the soil moisture characteristic curve (Childs, 1940).

There are many empirical equations that have been proposed to describe the soil moisture characteristic curve. Among them are:-

$$\phi_p = -a(f-\theta)^b/\theta^c \qquad \text{Visser (1966)} \qquad (2.9)$$

$$\phi_p = -a\theta^{-b} \qquad \text{Gardner } \underline{\text{et al.}} \text{ (1970)} \qquad (2.10)$$

$$(\phi_e/\phi_p)^f = -(\theta-\theta_r)/(\theta_m-\theta_r) \qquad \text{Brooks and Corey (1966)} \qquad (2.11)$$

where a, b and c are empirical constants

f = porosity

θ = volumetric wetness

ϕ_e = air entry suction

ϕ_p = matric potential, a negative value

θ_m = maximum wetness

θ_r = residual wetness

The moisture characteristic curve is an essential component of physically based models. Different soils exhibit inherent characteristics as shown in Figure 2.3. The application of any of the relevant moisture characteristic curves requires the determination of the relevant empirical constants. However, the field measurements are compounded by the problems of field soil heterogeneity. Consequently many readings are needed before any meaningful application of the curve is made. The acquisition of such data is laborious and time consuming, hence the application of the soil moisture characteristic curve to the analysis of field soils has been limited.

The shape of the moisture characteristic curve is a function of pore size distribution. The larger the pore size as obtained in sandy soils, the lower the suction at which desorption takes place. Clay soils have finer and relatively uniform pores and during desorption, shrinkage occurs coupled with simultaneous adsorption and capillarity. In the latter soil, high suctions are required for desorption to occur.

The slope of the soil-moisture characteristic curve is known as the specific water capacity and is given by:-

$$C_\theta = d\theta/d\phi_p \qquad (2.12)$$

The specific water capacity is useful in providing information on soil moisture storage and soil water availability to plants.

Hysteresis

During desorption or sorption in field soils, different soil moisture characteristics are normally obtained for a particular soil type. This results in different equilibrium moisture contents at a given suction. The moisture content is greater in desorption than during sorption. The phenomenon which gives rise to such a soil condition is referred to as hysteresis. The continuous path of the two curves is called a hysteresis loop (Figure 2.4).

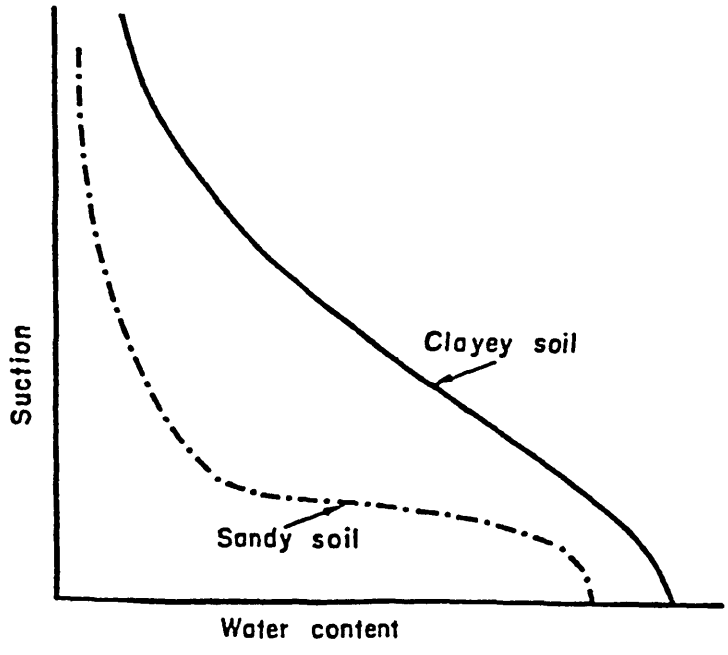

FIG.2.3 Soil moisture characteristics for different soil types.
(After Hillel,1980a)

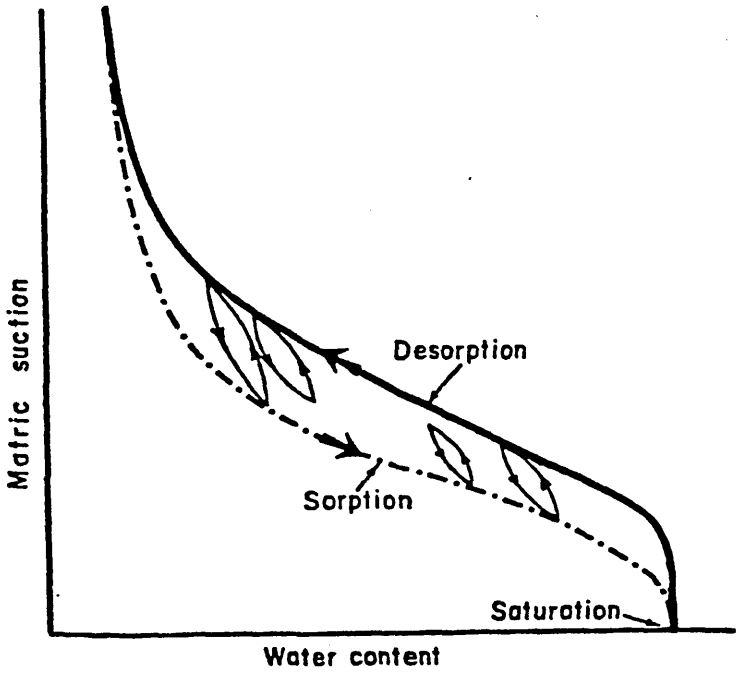

FIG.2.4 Hysteresis and Hysteresis loop
(After Hillel,1980a)

The factors that cause hysteresis in soils have been discussed by Haines (1930) with reference to the 'ink bottle' effect. Other causes include the effect of contact angle which is greater in advancing than receding menisci, air entrapment and swelling and shrinking of soils. These factors are difficult to quantify under natural field conditions where irregular alternating wet and dry conditions prevail. As such, hysteresis is often disregarded in soil water flow models. The non-inclusion of hysteresis effects in soil water models can probably be justified in monotonic conditions only.

2.5 Soil Water Movement

Soil water moves through the pores in the soil. This movement is activated by mechanical, electrical and molecular forces; and can take place in the liquid and vapour phases. The dominant mode of water movement is through the liquid phase, the vapour phase attaining some significance when high thermal gradients occur.

The liquid movement occurs either in saturated or unsaturated soils.

Saturated flow occurs when all the micro- and macro-pores are filled with water. The pressure at which water is held is generally positive pressure.

Unsaturated flow occurs when the pores are not completely filled with water causing an air-water interface to occur. Consequently, tension occurs and the processes of capillarity and adsorption are important.

The movement of water in saturated or unsaturated soils is governed by the total potential which can also be referred to as the hydraulic head. The hydraulic head can be specified thus:-

$$H = -h + z \qquad (2.13)$$

where H = hydraulic head

h = matric suction head

z = elevation head

The classical equation of flow employs a macroscopic approach credited to Darcy (1856). It is given in differential form for saturated flow as:-

$$V_x = -K_x \partial H/\partial x \quad (2.14)$$

$$V_y = -K_y \partial H/\partial y \quad (2.15)$$

$$V_z = -K_z \partial H/\partial z \quad (2.16)$$

where V_x, V_y, V_z are the flux in the directions x, y and z.

K_x = saturated hydraulic conductivity in the x-direction.

If it is assumed that $K_x = K_y = K_z = K$ in saturated flow conditions, then Equations 2.14, 2.15 and 2.16 can be given as:-

$$V = -K\nabla H \quad \text{Slichter (1899)} \quad (2.17)$$

where ∇H is the gradient of the hydraulic head in three dimensional space.

The Darcy equation was originally conceived for saturated flow. In this flow, the hydraulic conductivity depends on the pore size rather than the number of pores. This explains the higher conductivity in sands and gravels relative to clays despite the greater number of pores in the latter.

The unsaturated flow condition occurs as a result of evaporation, root abstraction and drainage within the soil profile. The movement of water takes place along gradients of increasing negative potential. The drying of soils that results in unsaturated flow allows the specification of a relationship between the hydraulic conductivity and moisture content or matric potential. This is because as large pores empty, only small and finer pores transmit water. This leads to a more tortuous path through which flow has to take place. As such, the hydraulic conductivity decreases by several orders of magnitude.

Typical conductivity-suction relationships for different soils are shown in Figure 2.5

It is apparent from Figure 2.5 that sandy soils initially have a higher conductivity which decreases rapidly as large pores empty. On the other hand, clay soils have less rapid decrease because of a wider spread of pore sizes. This probably explains why clays may act

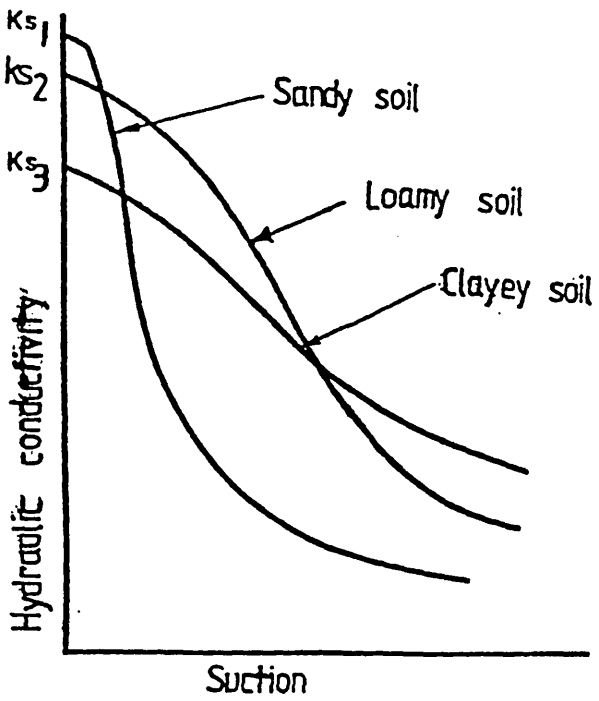

FIG.2.5 Conductivity-suction relationships for different soils (log-log)

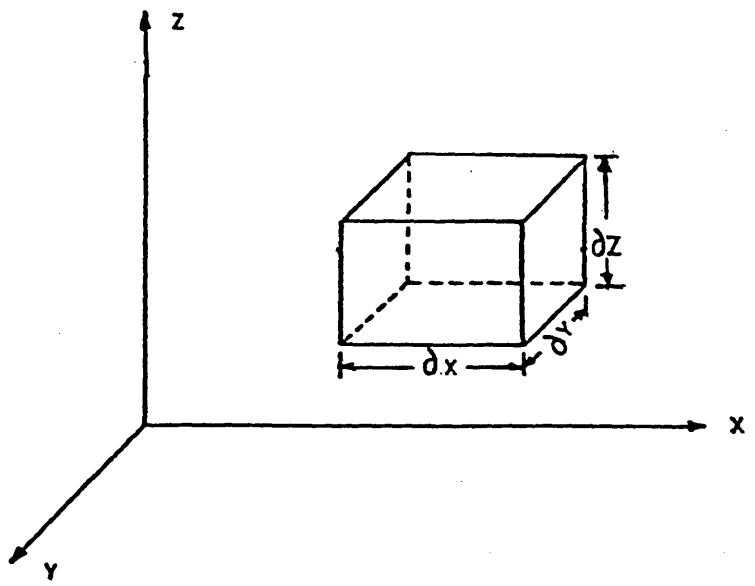

FIG.2.6 Rectangular unit volume of soil

as a barrier to flow when soil is saturated and why sands impede flow when soil dries.

Some empirical equations have been presented to describe the conductivity-moisture content or matric potential relationship by Gardner (1960a):-

$$K(\phi_p) = a/\phi_p^{\,n} \qquad (2.18)$$

$$K(\phi_p) = a/(b + \phi_p^{\,n}) \qquad (2.19)$$

$$K(\theta) = a\theta^{c} \qquad (2.20)$$

$$K(\theta) = K_s(\theta/f)^{c} \qquad (2.21)$$

where a, b, c and n are constants

K_s = saturated hydraulic conductivity

f = porosity

ϕ_p = matric potential, a negative value

Hysteresis is known to affect these functions but it is less pronounced in the $K(\theta)$ than for the $K(\phi_p)$ function (Hillel, 1980).

Another constraint to the unsaturated flow of water relates to the law of conservation of matter, which states that matter is neither created nor destroyed. Hence, the equation of flow is combined with the equation of continuity. Thus:-

Inflow = Outflow + change in storage

If a unit volume of soil is considered in an X, Y, Z coordinate space with dimensions dx, dy and dz (Figure 2.6), the total flow going through the given phases is the net accumulation of water within the unit volume of soil.

The total flux of water going IN =

$$V_y dzdx + V_z dxdy + V_x dydz \qquad (2.22)$$

The total flux of water going OUT =

$$(V_y + \frac{\partial V_y}{\partial y} dy)dzdx + (V_z + \frac{\partial V_z}{\partial z} dz)dxdy + (V_x + \frac{\partial V_x}{\partial x} dx)dydz \qquad (2.23)$$

Hence, storage change:-

$$dxdydz \frac{\partial \theta}{dt} = - (\frac{\partial V_y}{\partial y} dydzdx + \frac{\partial V_z}{\partial z} dzdydx + \frac{\partial V_x}{\partial x} dxdydz) \qquad (2.24)$$

If the above occurs over a given period for the volume element of soil, there is a change in moisture content with time. Thus we have the equation of continuity which is given as:-

$$\frac{\partial \theta}{\partial t} = -(\frac{\partial V_y}{\partial y} + \frac{\partial V_x}{\partial x} + \frac{\partial V_z}{\partial z}) \qquad (2.25)$$

Equation 2.25 can be written in vector form to give

$$\frac{\partial \theta}{\partial t} = - \nabla \vec{V} \qquad (2.26)$$

where $\vec{V}$ = the vector flux.

The above equation 2.26 is normally combined with Darcy's equation as given in equation 2.17 to give the unsaturated flow equation (Richards, 1931) thus:-

$$\partial\theta/\partial t = -\nabla.K\nabla H \qquad (2.27)$$

The above equation can be written in the form of a diffusion equation. This converts the flow equation into a form similar to the heat and diffusion equations, by introducing a diffusivity term D. The diffusivity term is the ratio of the hydraulic conductivity to specific water capacity and is given by Childs and Collis-George (1950) as:-

$$D(\theta) = K(\theta) \frac{d\phi_p}{d\theta} \qquad (2.28)$$

where $\frac{d\phi_p}{d\theta}$ = reciprocal of the specific water capacity

It then follows therefore that in the vertical direction, equation 2.27 can be written as:-

$$\partial\theta/\partial t = \frac{\partial}{\partial z}[D(\theta)\frac{\partial\theta}{\partial z}] + \frac{\partial K(\theta)}{\partial z} \qquad (2.29)$$

Equation 2.29 has in-built errors in its application due to the non-inclusion of hysteresis effects and fails to account for the occurrence of thermal gradients. This is because under the preceding conditions, soil water flow is not consistently related to decreasing water content gradient. However, the hydraulic diffusivity ($D(\theta)$) has the advantage of having more limited variation of diffusivity with moisture content than that which obtains in the hydraulic conductivity moisture content relationship.

2.6 Application of the Water Flow Equation

Several processes that involve soil water movement are normally described by the flow equation. Some of these processes include infiltration and redistribution, lateral flow and drainage.

2.6.1 Infiltration and Redistribution

Infiltration is the entry of water into the soil through the surface, while redistribution is the post-infiltration movement of water in the soil profile. In practice, it is difficult to differentiate between infiltration and redistribution within the profile.

The infiltration rate has implication in flood and erosion control studies. This is because whenever rainfall rate exceeds infiltration rate, surface ponding occurs which leads to surface runoff. Runoff is important in soil conservation techniques, as it washes away the top soil which in agricultural practice contains most of the plant nutrients. It is also important in soil water management because it represents a loss of profile moisture and hence affects soil water balance calculations.

The maximum rate of infiltration at a given time is designated the infiltration capacity and is dependent on several factors, some of which are:-

(i) The antecedent soil moisture content which determines the suction gradient prevalent at the onset of infiltration. Higher infiltration rates are normally associated with the occurrence of large gradients in a dry soil.

(ii) The hydraulic conductivity; this becomes important at the latter stages of infiltration when the initial higher suction gradients decrease as the soil gets wetter. The infiltration rate at this stage being controlled by gravity and the hydraulic conductivity of the soil.

(iii) The structure and texture of the soil surface affects infiltration rate significantly. When rain falls on soil, the drops cause soil impaction and surface crusting. These lead to the closure of pores and consequently prevents the entry of water into the soil profile. Soil profile layering also affects infiltration rate especially when impeding layers are present.

The soil cover affects infiltration rate by the type of vegetation on the soil surface. This is as a result of foliage which prevents surface compaction and the root growth which breaks up impeding layers; thus creating passages within the soil. This enhances the infiltration rate.

Infiltration rates decrease asymptotically with time to a steady infiltration capacity as a result of surface crusting and decreasing hydraulic gradients.

Bodman and Coleman (1944) in working with hard homogeneous soils first described the moisture profile during infiltration; when they applied a constant head of water (figure 2.7). The following components were identified in their study; a surface zone of saturation which is underlain by a zone of rapid decrease in moisture content; the transition zone. This passes into a transmission zone; a zone where the moisture content remains constant; and bounded at the bottom by a zone of rapid decrease in moisture content; the wetting zone. The wetting front defines the limit of infiltration.

Infiltration moisture profiles were reproduced by Youngs (1958); when comparing empirical profiles derived from experiments with slate dust and glass beads with profiles predicted by the Richards equation. Youngs suggested that the Bodman and Coleman surface saturation layer does not exist; and that it might have been caused by a bad structured soil surface.

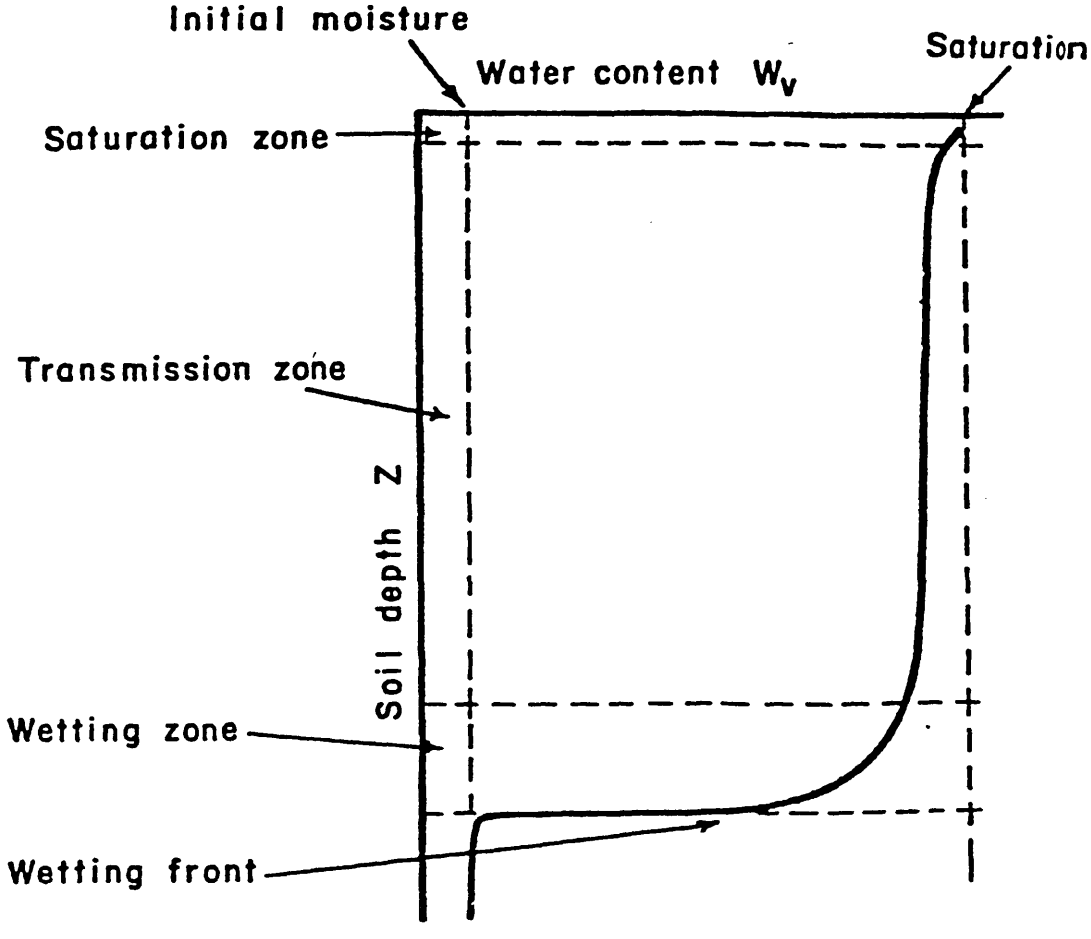

FIG.2.7 Infiltration moisture profile
(After Hillel,1980b)

Several equations have been proposed for predicting infiltration rates. Generally these equations can be grouped into three major classes; empirical, semi-empirical and theoretical.

The best known empirical equations are those of Kostiakov and Horton (Childs, 1969); and Holtan (1961). Kostiakov's (1932) equation states that

$$I = Bt^{-n} \tag{2.30}$$

where I = infiltraton capacity

B and n are constants

Horton (1940) states that

$$I = Ic + (Io - Ic)e^{-kt} \tag{2.31}$$

where Ic = steady infiltration rate

Io = initial capacity

k = constant

t = time

while Holtan's equation is

$$I = Ic + b(m - Iac)^{n} \tag{2.32}$$

where m = soil storage capacity

Iac = accumulated infiltration

b,n = constants

The equation proposed by Green and Ampt (1911) is semi-empirical and states that

$$Ic = Ks(Ho - Hf + Lf)/Lf \tag{2.33}$$

where Ks = saturated hydraulic conductivity

Ho = pressure head at the entry surface

Hf = effective pressure head at the wetting front

Lf = the length of the wetting zone

Equation 2.33 was derived by applying Darcy's law to the situation of an idealised infiltration profile from an excess surface water supply from time zero. The Green and Ampt equation (2.33) has predictable parameters that have physical significance; but they can only be determined by experimentation. Philip (1957a) solved the flow equation analytically for infiltration into a dry soil to produce

$$Iac = \lambda t^{1/2} + \chi t^{2/2} + \psi t^{3/2} + \omega t^{4/2} + \delta \qquad (2.34)$$

λ, χ, ψ and ω = functions of diffusivity; δ = correction term.

The above equation (2.34) is a power series in $t^{\frac{1}{2}}$ and it is for vertical flow. The Philip's equation produces a good fit to observed data and predicts the general shape of the infiltration time curve, however computing the parameters are difficult (Mein and Larson, 1973).

In practice, equation 2.34 is generally approximated to

$$I = \lambda t^{-\frac{1}{2}} + B \qquad (2.35)$$

A practical approach to predicting infiltration rates from flow theory involves the numerical solutions of the flow equation by finite difference techniques. A finite difference solution; for non-ponding; pre-ponding and ponding conditions; was solved by Rubin (1966). Mein and Larson (1973) solved a two-stage model for pre-ponded conditions, the first stage predicting the volume of infiltration to the moment at which surface ponding begins while the second stage uses a modified Green-Ampt model to provide information on cumulative infiltration and the mean suction at the wetting front.

Rubin and Mein and Larson did not consider hysteresis and soil profile layering. Miller and Gardner (1962) studied infiltration into layered soils and suggested that the Philip equation may be inadequate because wetness and conductivity exhibit abrupt discontinuities at inter layer boundaries. Hanks and Bowers (1962) numerically provided solutions for layered soils which agreed with experimental results of Colman and Bodman (1944) and Green et al. (1964). The Hanks and Bowers solution also applies to non-homogeneous soils (Wang and Lakshminarayana, 1968). Their computations indicated that the least

permeable layer governs the infiltration rates, once the wetting front had passed that layer.

Despite the above studies of infiltration theory, there has been limited verification of existing theories. There are problems of soil heterogeneity; irregular alternating dry and wet conditions which cause swelling and shrinking and cracking. It is thus common to find that field application of infiltration theory very much relies on empirical measurement of infiltration capacities for differing soil-vegetation combinations.

2.6.2 Redistribution

This is a process that occurs consequent upon the cessation of infiltration. In practice however, it is difficult to separate both processes. The redistribution process affects the quantity of water that is retained at various times by different soil layers within the profile; its rate and duration determines the effective soil water storage and the quantity of leachates out of the root zone.

Some laboratory investigations (Youngs, 1958; Hillel, 1980) have been carried out to determine the redistribution of water following infiltration into a dry soil. Typical redistribution profiles are shown in Figure 2.8.

In general, redistribution of water in the soil profile comprises of an upper wetted layer underlain by an unwetted layer. The rate and duration of redistribution being dependent on the hydraulic conductivity, initial wetting depth and relative dryness of the bottom layers.

Youngs (1958) showed that in an initially dry soil with a shallow wetting depth, the suction gradient augments the gravitational gradient to give a rapid rate of redistribution, while a soil with a deep wetting is predominantly dominated by the gravitational gradient. In both conditions, the Bodman and Coleman's transmission zone becomes a draining zone.

Gardner et al. (1970) provided an approximate solution of the flow equation for long time periods to give a logarithmic expression of the form

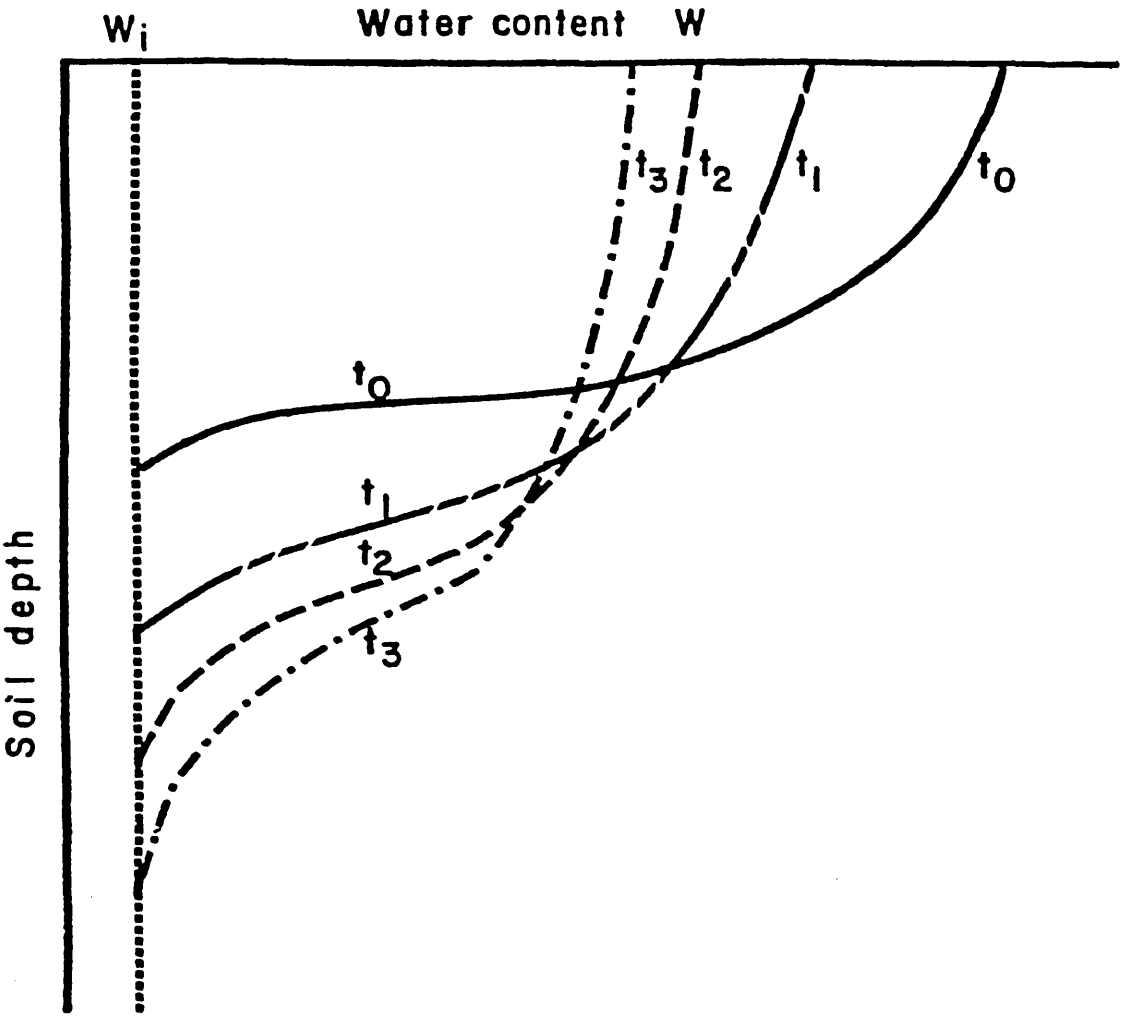

FIG.2.8 Redistribution following irrigation in a medium-textured soil (After Hillel,1980b)

$$\log w = \log a - c \log t \qquad (2.36)$$

where w = the water content of the upper part of the profile

a and c = constants

t = time

Gardner et al. found that the initially wetted zone drains monotonically, while the lower depths alternately wetted and dried.

It is difficult to obtain satisfactory analytical description of the redistribution process because of hysteresis effects. However, numerical solutions have been attempted and have been found to give good agreement with observed profiles in laboratory columns (Remson et al., 1965; Rubin, 1967; and Staple, 1969). The problems discussed under infiltration also apply for redistribution and hence make it rather difficult to apply the solutions under field conditions.

2.6.3 Evaporation from a Bare Soil Surface

The evaporation of moisture can either take place from plant surfaces, open water or directly from soil surfaces. The following discussion shall focus on the latter.

In a saturated bare soil, the meteorological conditions control the evaporation rate while soil moisture hydraulics become significant with progressive drying out of the soil. A similarity exists between evaporation and infiltration since in both cases moisture moves from a wet soil to a relatively dry soil. The difference in the case of evaporation being the gravitational gradients opposition to the suction gradients.

The steady-state upward flow of moisture (E) from a high water table is conventionally described by:-

$$E = -K(\phi_p)\left[\frac{d\phi_p}{dz} - 1\right] \qquad (2.37)$$

where $K(\phi_p)$ = conductivity-suction relationship

$\frac{d\phi_p}{dz}$ = suction gradient

Equation 2.37 can also be given as:-

$$z = \int_{o}^{z} \frac{d\phi_p}{1 + E/K(\phi_p)} \qquad (2.38)$$

where z = height from water table.

The latter equation has been used to obtain suction distributions with height for different fluxes from a water table (Gardner, 1958).

Generally in field conditions, significant evaporation loss only occurs when the water table is near the surface.

Three main stages have been recognised in the evaporation process (Idso et al., 1979). Stage I is the constant evaporation rate stage. This occurs from an initially wet soil, when the soil conductivity is high enough to satisfy the potential evaporation as induced by the prevailing meteorological conditions. The duration of this stage is dependent on the relative magnitude of the potential evaporation; the higher the rate, the shorter the duration.

Stage II is the falling evaporation rate stage, where the soil evaporation rate lags behind the potential rate. This occurs because of the progressive drying out of the surface zone moisture content. The rate limiting factor at this stage being the soil hydraulic properties. Stage III is a consequence of the dessication of the surface zone. The resultant effect is the effective cessation of liquid water movement through the surface soil; moisture being lost by vapour diffusion.

Several workers (Black et al., 1969; Klute et al., 1965; Rose, 1966 and Ritchie, 1972) have applied the flow equation under field conditions to predict evaporation from a bare soil surface. Cumulative evaporation was described to be a function of the square root of time. They all reported good agreement between calculated and measured amounts of cumulative evaporation from a bare soil surface and lysimeter experiments were used to validate the calculated evaporation.

Gardner et al. (1970) studied simultaneously the redistribution and evaporation processes theoretically and in laboratory columns. They found that evaporation did not significantly affect redistribu-

tion and deep drainage processes; although the latter reduced evaporation by up to 75%.

Despite the efforts that have been made to predict evaporation from a bare soil surface, much work is still needed to monitor the effects of non-isothermal conditions, soil cracking and the effects of surface cover, for example mulching, before the theoretical derivations can be applied with any degree of confidence in field situation.

2.7 Conclusions

The preceding discussion highlighted the basic theory and different processes involved in soil water movement and storage. It has become apparent that:-

(a) Capillarity is the major mode of water retention.

(b) The movement of unsaturated soil water is along gradients of increasing negative potential.

(c) The major processes of infiltration, redistribution and evaporation of soil water can be described by the Darcy-Richards equation of flow, if soil hydraulic parameters are known. These parameters are the soil moisture characteristics and the unsaturated hydraulic conductivity-moisture content relationship.

However, apart from considering the influence of the above processes in soil water distribution in this study, the assessment of moisture distribution in the presence of plant roots is also studied. A discussion of the way in which moisture is being lost directly from plants coupled with postulated soil water models within the last two decades follows in Chapter 3.

CHAPTER 3

A REVIEW OF PLANT WATER RELATIONS

3.1 Introduction

The actual rate of soil moisture loss is dependent on a complex interaction of atmospheric, soil and plant factors. Consequently, this chapter presents the processes involved in soil moisture loss to the atmosphere via plant roots. It also presents a review of soil water models postulated within the last two decades, highlighting their limitations and advantages.

3.2 Plant Water Relations

The actual loss of soil moisture to the atmosphere induced by meteorological variables can either be by direct evaporation or via vegetation. In the latter case, the loss is referred to as transpiration. The combined loss of soil moisture by evaporation and transpiration is known as evapotranspiration.

Quantitative description of soil moisture loss through plants has generally been approached in two ways, either by the application of physically-based or empirically based concepts. The physically-based concept regards moisture flow from soil through the plant to the atmosphere as being due to soil and plant hydraulics. Empirically-based models, on the other hand, specify relationships between soil moisture status and the actual evapotranspiration rates. This latter relationship is commonly termed a drying curve.

3.2.1 The Soil-Plant-Atmosphere Continuum

Philip (1966) used the term "soil-plant-atmosphere-continuum" to describe the dynamic nature of water movement from the soil to the plant and finally to the atmosphere as a physically integrated process. The concept is based on the principle that the potential difference existing between the atmosphere and the soil provides the main driving force for soil water flux via the plant. Across each segment involved in the transportation of soil water to the atmosphere, there are potential differences which have corresponding resistances that control the flux magnitude within a given segment.

Van den Honert (1948) was the first to describe moisture movement through the plant as being similar to that of the flow of electric current through a series of resistance networks. The basic principle in this analogy is that the rate of water flow through the plant is assumed to be proportional to the potential difference across a given pathway within the plant and inversely proportional to the resistance of that pathway. Thus:-

$$Q_p = -\frac{H_l - H_r}{R_p} \qquad (3.1)$$

where Q_p = flux of moisture within the plant

H_l = leaf water pressure head

H_r = root water pressure head

R_p = resistance to flow within the plant.

Water movement from the soil to the atmosphere can be studied both at the leaf-air interface and at the soil-root interface. The leaf-air interface has the greatest potential drop and the leaf also provides the stomata which control moisture loss to the atmosphere. The stomatal control of moisture loss is dependent on the flux magnitude obtained at the soil-root interface. Consequently, a full description of plant water use must generally consider both the leaf-air and soil-root interfaces.

3.2.2 The Leaf-Air Interface

The leaf-air interface controls the rate of plant water loss because of the stomatal control mechanism in the leaf; Figure 3.1. This control can be described in terms of the resistance to flow across the potential difference prevailing at the interface. The measurement of this resistance allows the use of either the aerodynamic or combination formulae, discussed in a later section, for the calculation of the transpiration rate.

The leaf resistance comprises two main resistances in parallel, the cuticular and stomatal resistances. When the stomata are open, the vapour flux through the cuticle is negligble while the cuticular transpiration becomes significant when the stomata are fully closed.

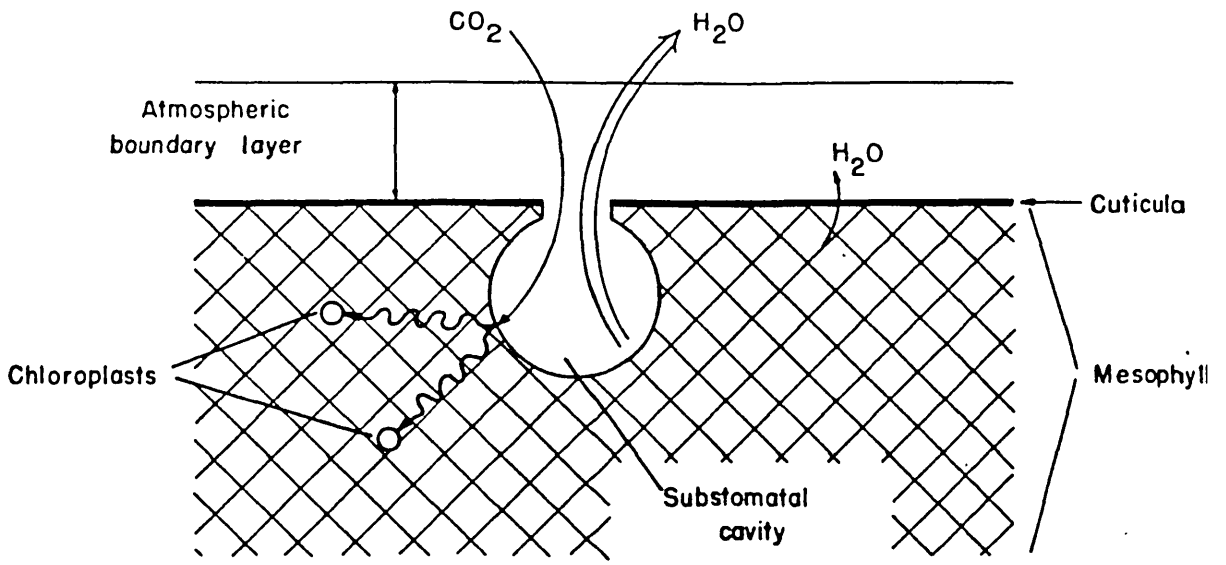

Fig. 3.1 Schematic representation of transpiration through the stomate and the cuticle, and of the diffusion of CO_2 into the stomate and through the mesophyll to the chloroplasts. (After Hillel,1980b)

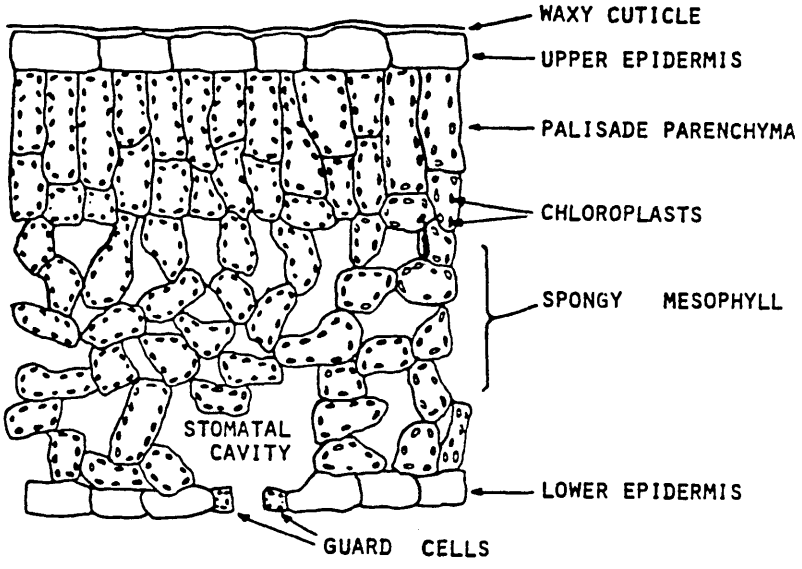

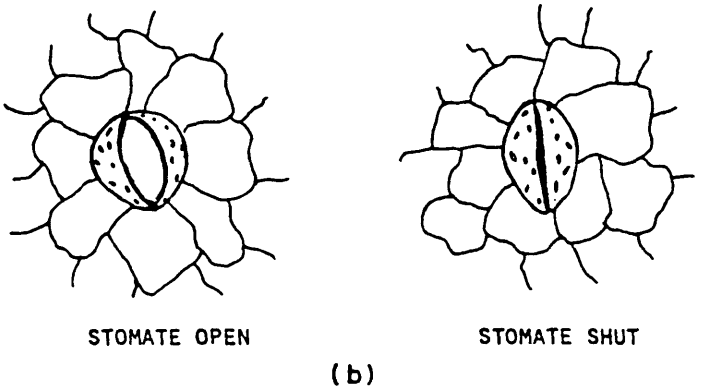

Fig3.2 Illustration of a leaf section with open and closed stomate: (a) transverse view, (b) surface view. (After Hillel,1980b)

Stomatal resistance is a combination of three component resistances, substomatal, stomatal pore and mesophyll resistances. Stomatal resistance is often used to describe the vapour transport from saturated vapour pressure in the substomatal cavities through the stomatal apertures. In practice, the stomatal resistance is approximated by the pore resistance (Rose, 1966) which is controlled by the guard cells surrounding the stomatal aperture (Figure 3.2).

Whenever the guard cells lose turgor as a consequence of plant water stress, their geometry changes reducing the stomatal aperture (Figure 3.2), increasing the pore resistance and ultimately limiting the vapour flux magnitude. Apart from the sensitivity of the guard cells to plant water status, the stomatal aperture is also affected by carbon dioxide concentration, wind and temperature.

The flow of moisture from the soil through the plant to satisfy the prevailing atmospheric demand as soil moisture deficit develops entails that the leaf suction increases (Gardner, 1960b). This is essential to maintain enough potential gradient to create the desired flux. Increasing soil moisture deficits lead to correspondingly higher leaf suctions until wilting is reached (Hillel, 1980b). Wilting is the limit when the leaf suction can no longer increase, demand exceeds supply, plant water deficit results and the guard cells lose their turgidity and, ultimately, the stomata close to regulate water loss. Wilting therefore depends on a combination of factors, namely, soil hydraulic conductivity, soil water content, transpirational demand and root density.

Carbon dioxide combines with plant water in the presence of sunlight energy in the leaf of plants to produce starch. This process is known as photosynthesis. The stomata are sensitive to carbon dioxide concentration and tend to close in the presence of high carbon dioxide concentration whereas low concentrations induce opening. Increased carbon dioxide production is associated with high temperatures. This explains the temporary closure of stomata normally obtained at midday under high temperature conditions. Wind also indirectly affects the stomata by changing the concentration of carbon dioxide. High winds lower the concentration and consequently induce stomatal opening.

The rate of moisture loss through the stomata is directly proportional to the vapour pressure difference between the substomatal cavity and the atmosphere, and inversely proportional to the resistance encountered along the diffusion path. Thus:-

$$Fs = (VPa - VPL)/Dr \qquad (3.2)$$

where Fs = stomatal flux

VPa = vapour pressure of air

VPL = saturated vapour pressure at leaf temperature

Dr = diffusion resistance

The diffusion resistance (Dr) is composed of an external diffusion resistance known as the boundary resistance and the stomatal and cuticular resistances. Hence

$$Dr = r_{bl} + \left[\frac{1}{r_s} + \frac{1}{r_{cu}}\right]^{-1} \qquad (3.3)$$

where r_{bl} = boundary layer resistance

r_s = stomatal resistance

r_{cu} = cuticular resistance

The stomatal and cuticular resistances when combined is known as the leaf resistance (Rose, 1966).

The leaf resistance is independent of windspeed while the magnitude of the boundary layer resistance is dependent on windspeed. Low values are obtained at high windspeeds and high values result from low windspeeds. In normal field situations with moderate wind when the stomata are open, the boundary layer resistance usually exceeds the leaf resistance. However in windy conditions, which favour higher rates of evaporation, the stomatal resistance may exceed that of the boundary layer (Rose, 1966).

The atmospheric boundary layer is almost always a turbulent layer, although this has a small laminar sub-layer. As such the final resistance encountered by the transpiration stream is imposed by the external atmosphere. A diffusion porometer is often used to obtain values for the stomatal pore resistance. The instrument measures the stomatal aperture of the leaf in the field; by measuring the viscous

resistance to air flow through the pores of the leaf (Slatyer et al., 1965).

The preceding discussion focussed on the mechanisms and factors governing the actual loss of water from a plant via the leaf to the atmosphere. The latter is known as actual transpiration rate.

3.2.2.1 Measurement of Actual Evapotranspiration

Actual evapotranspiration can be estimated directly from either of the following three techniques;-

(a) Moisture flux measurement above an evaporating surface,

(b) Energy balance approach,

(c) Utilising the law of continuity.

(a) Moisture flux:

Although many techniques have been proposed for measuring moisture flux above an evaporating surface, the measurement techniques are broadly divided into three approaches. The simplest method entails the enclosure of small plant communities for subsequent monitoring of the changes in humidity within the enclosure (Stark, 1968). It is obvious that the results obtained by this approach may not be representative. This is because atmospheric wind turbulence, aerodynamic roughness and vapour pressure will not be duplicated within the enclosure.

The aerodynamic approach (Shuttleworth, 1979) presents another category for the estimation of moisture flux. It involves the analysis of the vertical profiles of humidity and horizontal windspeed to estimate moisture loss. Implicit in this approach are the following assumptions:-

(a) that the principle of similarity obtains (Tanner, 1968) which states that the transfer coefficients for water vapour and momentum are equal;

(b) the shear stress is constant with height;

(c) the windspeed is described by a logarithmic profile.

The first two assumptions seem to hold while the third probably applies when neutral atmospheric equilibrium prevails (Rijtema, 1965). Another limitation of this approach stems from the dependence of the windspeed function on a displacement height and on an aerodynamic roughness parameter, both of which are expected to vary with windspeed. The aerodynamic approach as delineated above has not gained current usage primarily because the accuracy required, by the measurement of the profiles, are difficult to achieve due to fetch requirements (Shuttleworth, 1979). However the principle of the approach has been integrated into a "combination technique" which is discussed in a later section in this chapter.

Another method for moisture flux estimation is the "eddy correlation" technique (Swinbank, 1951). This approach is based on the principle that within the turbulent boundary layer, water vapour is transferred by the process of turbulent diffusion. Consequently, different wind velocities come into play in the process and for moisture flux to occur, a humidity gradient must be present. The concurrent measurements of the fluctuations in windspeed normal to the evaporating surface and the fluctuations in humidity content of the air measured at the same point can then be related to evaporation loss. Thus, if w, the instantaneous vertical air velocity is replaced by a temporal mean, $\bar{w}$, and a turbulent fluctuation, w' and q_h is the specific humidity,then according to Eagleson (1970):-

$$w = \bar{w} + w' \tag{3.4}$$

$$q_h = \bar{q}_h + q_h' \tag{3.5}$$

and $$E = \overline{\rho w' q_h'} \tag{3.6}$$

where E = vertical flux of water vapour g $cm^{-2} sec^{-1}$

ρ = density of air

There are practical difficulties encountered in using the eddy correlation technique, these include;

(i) The difficulty of creating sensors capable of recording measurements of the fluctuating windspeed and humidity (or temperature), at rates that are high enough to encompass all the higher frequencies involved in turbulent flux and to also provide at the same time, enough reliability to measure lower frequencies.

(ii) The analysis of the sensor outputs is complex in real time (Shuttleworth, 1979). This is because the data sampled is so vast and occur at a time duration which is about half the sensor time response. This latter difficulty however can be obviated by the use of cheap digital processors which are currently available.

The measurement techniques involved in eddy correlation principles are still largely experimental, however, the technique is regarded as possessing great potential for the direct measurement of actual evapotranspiration (Baier, 1967). This is because it is the method, of all the meteorological techniques, with the minimum of theoretical assumptions and with the least dependence on surface conditions (Shuttleworth, 1979). Despite this apparent superiority of the technique, doubts still remain regarding the extrapolation of point measurements to areal estimates.

(b) Energy Balance:

This method is based on the principle of the conservation of energy. It can be represented by the following:-

$$Rn = S + \lambda E + H + N + \Delta Storage \qquad (3.7)$$

where Rn = net radiation

S = soil heat flux

λ = latent heat of vaporisation

H = turbulent heat flux

N = energy of photosynthesis

E = evaporation rate

For practical applications, N is normally assumed to be negligible (Rijtema, 1966) and Rn and S can be measured with some degree of accuracy. As such, the fundamental obstacle to using this approach resides in the determination of H and λE. These terms are, as a consequence, separated by using the Bowen ratio (Bowen, 1926), β, which requires the time-averaged measurements of the vertical temperature and vapour pressure gradients. The ratio can be represented thus:-

$$\beta = H/\lambda E \tag{3.8}$$

$$= \gamma \frac{(Ts-Ta)}{(e_s-e_a)} \tag{3.9}$$

where γ = psychrometric constant $\simeq 0.66$ mb $^{o}C^{-1}$ (Shuttleworth, 1979)

Ts,Ta = the surface and air temperatures

e_s, e_a = the surface and air vapour pressures

This ratio of the vertical gradients of temperature and vapour pressure can directly be determined in the form of a differential measurement (McNeil and Shuttleworth, 1975) or as the ratio of tangents fitted to empirical temperature and humidity profiles (Stewart and Thom, 1973). If the ratio of the two energy fluxes are determined, then the sum of the fluxes, A, also known as the available energy is given by:-

$$A = H + \lambda E \tag{3.10}$$

Equation (3.7) can then be rewritten in the following form:-

$$\lambda E = A \mid (1+\beta) \tag{3.11}$$

From equation 3.11 above, it is evident that when A approximates zero and β equals -1, the energy balance approach breaks down. However, this latter situation is only realised at low flux intensities and hence it is not considered to be a serious limitation.

A more specific drawback of the energy balance approach relates to the unsuitability of the technique under advective heat transfer, especially when moisture status of contiguous areas have significant effect on local evaporative demand. Despite this limitation, the inherent assumptions in the approach are less than the assumptions made in the aerodynamic approach and on this score it has an edge.

In the application of both aerodynamic and energy balance principles to the estimation of losses from field crops and forest, Tachjman (1971) found satisfactory agreement between losses obtained for alfalfa and potatoes but not for forest. The apparent discrepancy in estimated losses for forest may be linked to the assumption of windspeed being described by a logarithmic profile which implies that the aerodynamic approach should not be used near tall vegetation (Thom et al., 1975). Both approaches however suffer from the difficulty of obtaining surface vapour pressure and surface temperature measurements from the surface of an evaporating crop.

(c) Continuity:

This approach is similar to the energy balance technique, except that it involves the determination of the water balance of either a large-scale catchment or small experimental plots. For the latter, the technique entails the monitoring of soil moisture storage on a short-term basis and consequently allows estimates of evapotranspiration to be made (Dunin, 1969).

Lysimeters are normally employed for the determination of the moisture loss from a soil sample with vegetative cover, and thus if rainfall and drainage outputs are known, the evapotranspiration can be calculated as a residual from the water balance equation. A major limitation to the lysimeter technique is the lack of representativeness of the soil samples to duplicate the wider field area. Also, the vegetation development may be atypical.

3.2.2.2 Potential Evaporation

Most of the soil water models that have been postulated as described later in Sections 3.2.3 and 3.3 depend for their input on assessment of the potential atmospheric demand. Potential evaporation is a measure of the "thirst" of the atmosphere for water. It has been defined (Penman, 1956) as the evaporation from an extended surface of short green crop, actively growing, completely shading the ground, of uniform height and not short of water. Essentially, this definition implies that the potential evaporation is not influenced by soil moisture content but is dependent on the energy available for the potential evaporation process. The drawbacks of the potential eva-

poration concept have been given by Shuttleworth (1979), however, the concept as defined cannot be fully realistic since advective effects, which influence atmospheric demand, are considered insignificant. Whatever the deficiencies inherent in the concept, it has generally been utilised as an estimate of atmospheric evaporative demand upon which the influence of surface control are normally superimposed.

Potential evaporation values can be estimated by direct measurement of loss or from an empirical relationship that is dependent on climatological data as utilised by Penman (1956) and Thornthwaite (1948) formulae. The direct measurement of moisture flux is either by measuring changes in the water level of an open water surface like an evaporation pan (Denmead and Shaw, 1959) with appropriate correction or by assessing the losses from a moist vegetated surface, for example an irrigated lysimeter, by a water balance procedure (Boonyatharokul and Walker, 1979).

The preceding methods have been used to estimate potential evaporation values under United Kingdom weather conditions and their relative performance discussed by Ward (1963), Smith (1964) and Pegg and Ward (1972). Rijtema (1966) also compared sunken pan evaporation with results obtained from meteorological data in the Netherlands using a modified Penman (1948) equation. On the whole, the Penman formula is preferable to the Thornthwaite formula and good agreements are observed between the measured evaporation from water pans and those calculated from meteorological data utilising the Penman (1948) formula. For the latter, however, the agreement seems to hold for duration of greater than five days as divergence becomes noticeable when shorter periods are considered.

Generally, the evidence reveals that the Penman formula and evaporation pans can give equivalent results for potential evaporation. In practice, the Penman formula has enjoyed greater applicability in the United Kingdom, primarily because the climatic data required in computation is readily available from the British Meteorological Office network of stations and secondly, the weather of the British Isles is akin to the conditions in which the equation was derived (S.E. England). However, since some of the more complex evapotranspiration models are offshoots of the Penman formula, a discussion of the equation is given in the following section.

3.2.2.3 The Penman Formula

Penman (1948) synthesised the moisture flux and energy balance approaches that were previously described in Sections 3.2.2.1a and 3.2.2.1b respectively to calculate evaporation from an open water surface. This synthesis obviates the need to take surface measurements, the latter being the major difficulty to utilising the individual approaches on a routine basis. Although the equation as originally conceived is for the calculation of evaporation from an open water surface, subsequent modification, by using a reduction factor, allows for the equation to be employed to estimate potential evapotranspiration from a short green crop that is adequately supplied with water.

The estimation of potential evaporation by the Penman formula requires as input standard meteorological data. These include:- saturation deficit of the air, air temperature and vapour pressure, radiation and windspeed at 2 m elevation. Essentially, two basic steps are involved in the Penman equation, first the evaluation of the net gain of radiation energy and second the determination of how this latter energy is partitioned in heating the air and in evaporation. Greater weighting is given to the radiation term (Penman, 1956) with the consequence that 100% overestimate of the atmospheric term gives only 10% overestimate of the total figure (Penman, 1956).

The Penman (1948) equation for open water is presented as follows:

$$E = \frac{\Delta}{\Delta+\gamma}\left\{Ra(1-r)\left(a + b\frac{n}{N}\right)\right\}$$

$$- \frac{\Delta}{\Delta+\gamma}\left\{\sigma T_a^{\,4}(0.56-0.092\sqrt{e_d})\left(0.10 + 0.90\frac{n}{N}\right)\right\}$$

$$- \frac{\gamma}{\Delta+\gamma}\left\{0.35(e_s - e_d)\left(1 + \frac{\mu}{100}\right)\right\} \qquad (3.12)$$

where E = potential evaporation (mm/day)

Δ = rate of change of saturated vapour pressure with temperature

γ = psychrometric constant

Ra = Angot value of short wave radiation

r = albedo

a,b = regression constants in relation to incoming solar radiation to duration of bright sunshine

n = duration of bright sunshine

N = maximum possible duration of bright sunshine

σT_a^4 = black body radiation (cal/cm²/day)

u = wind runs in miles/day at 2 m

e_s = saturation vapour pressure at temperature Ta (mm Hg)

e_d = vapour pressure at height Z (mm Hg)

Equation 3.12 has been the subject of some criticisms basically because of the empiricisms inherent in its derivation. Consequently, some improvements have been suggested which relate to the inclusion of a heat storage term, the use of a measured value for the radiation term rather than estimated and the utility of a better described wind function. Expanding on Penman's concepts, Van Bavel (1966) introduced aerodynamic principles which utilised a wind function that included surface roughness and measured net radiation, thus eliminating the empiricisms in the Penman approach. The results obtained by Van Bavel give good agreement between measured and calculated potential evaporation in the arid environment in which the model was applied.

There are several models that have been developed to calculate potential evapotranspiration which include that of De Bruin and Labians (1980) as reported by Belmans et al. (1981) and Thom and Oliver (1977). These models are extensions of the Penman formula. In the United Kingdom, the model developed by Monteith (1965) which introduced aerodynamic and surface resistances into the Penman formula has been adopted for estimating potential evapotranspiration by the British Meteorological Office, provided a minimum constant value of surface resistance is specified (Thompson et al., 1981). This surface resistance is expected to vary for different crops. However for the purpose of this study, the Penman formula is applied for estimating potential evapotranspiration primarily because the meteorological data needed for its application are readily available in the United Kingdom.

3.2.2.4 Modification of the Combination Approach to Estimate Actual Evaporation

The combination technique earlier discussed for the estimation of potential evaporation has been subjected to a series of modifications to estimate actual evapotranspiration (Shuttleworth, 1976, 1978). This apparent flexibiity of the technique stems from the Penman and Schofield (1951) idea of using stomatal resistance as an index of plant physiological response to the evaporation process. This latter idea has been incorporated by Monteith (1965) into the so-called Penman-Monteith equation for estimating actual evapotranspiration. In the Monteith version of the Penman model is included the aerodynamic resistance computed from wind velocity profile and atmospheric profiles of temperature, humidity and windspeed and the stomatal resistance.

Rijtema (1965) demonstrated that for practical purposes, actual evapotranspiration not only depends on aerodynamic and energy balance approach but also is dependent on crop and soil properties. Consequently, the equation for actual evapotranspiration (E_a) is given according to Rijtema (1969) as:-

$$E_a = \frac{\Delta Hnt/L + \gamma\{u(Zo,d)(e_s-e_d)\}}{\Delta + \gamma\{1 + u(Zo,d)*Dr\}} \qquad (3.13)$$

where Hnt = net radiation

L = latent heat of evaporation

Zo = roughness length of the evaporating surface

d = zero plane displacement relative to the earth's surface

Dr = the diffusion resistance of the crop.

The diffusion resistance Dr takes into account the geometry of the evaporating surface and considers the effect of both stomatal opening and transport resistances in the flow path. It follows therefore that the value of the diffusion resistance depends on the soil cover and leaf area (Rc^c); light intensity (Rc^l) and soil moisture conditions (Rc^ψ). Although these factors are independent of each other, the combined effect can be expressed as:-

$$Dr = f\left(Rc^{c},\ Rc^{l},\ Rc^{\psi}\right) \tag{3.14}$$

If Ra represents the resistance to liquid flow from the evaporating surface to the bulk air, $uf(Zo,d)(e_s-e_d)$ may be rewritten as $(e_s-e_d)/Ra$. Hence

$$E_a = \frac{\Delta Hnt/L + \gamma(e_s-e_d)/Ra}{\Delta + \gamma\{1 + RaDr\}} \tag{3.15}$$

The experimental evaluation of crop roughness and surface resistance has been attempted by Rijtema (1965); Szeicz and Long (1969) and by Russell (1980).

Although the combination approach is approved of by several workers (Federer, 1982; Thompson, 1982), reservations remain regarding its general application, especially since the research leading to its derivation and subsequent modification has been carried out in small plots with associated microclimates. This leads to the problem of assigning specific resistance term values in other locations. This is because the resistance terms are dependent on a variety of factors, which include plant type, rooting habits and proliferation, plant cover and leaf senescence, light intensity, soil properties, soil moisture content and evaporative demand, that are variable with time. As a consequence of the empirical relations of the resistance terms, inherent in the application of the combination technique to estimate actual evapotranspiration, doubts persist regarding whether satisfactory results would be obtained for other crops in specific locations and for certain climatic conditions where insufficient data are evident.

The various techniques given above for the estimation of the actual evapotranspiration rate provide a single value for water loss from soil through the plant. They do not account for the processes involved in the extraction and relative distribution of moisture loss within the soil profile. Consequently, consideration shall be given in the following to the soil-root interface.

3.2.3 Soil-Root Interface

The application of classical physical laws to describe soil water extraction by plant roots has been generally approached in two ways, (a) the microscopic and (b) the macroscopic models.

3.2.3.1 The Microscopic Approach

This was first proposed by Philip (1957b) and later expounded by Gardner (1960b) and Cowan (1965). The basic philosophy involved is the idealisation of a single root as an infinitely long cylinder of uniform radius and water absorbing properties. The soil water within the cylinder is assumed to move radially. A modification of the diffusion equation is normally used to describe this idealised condition as shown in the following expression by Gardner (1960b):-

$$\partial\theta/\delta t = \frac{1}{r}\frac{\partial}{\partial r}(rD\frac{\partial\theta}{\partial r}) \qquad (3.16)$$

where θ = volumetric moisture content

D = diffusivity

t = time

r = radial distance from axis of the root

Analytical solutions of the above equation (3.16) were attempted by Gardner (1960b) using data obtained for three soil types Pachappa sandy loam, Indio loam and China clay, and by Cowan (1965) for steady rate flow. Tinker (1976) however intimated that considering the limited knowledge currently available on soil-root hydraulics, a good numerical solution will be very nearly as accurate as an analytical solution and is more flexible.

Numerical solutions were presented by Molz *et al.* (1968) for radial flow of moisture to a vertical root in a New Jersey sandy loam and by Hillel *et al.* (1975) for the simultaneous movement of water and salt to a plant root.

In their analytical solution of the radial flow equation (3.16), Gardner (1960b) and Cowan (1965) predicted the occurrence of large suction gradients between the root surface and the surrounding soil. They also predicted a higher rhizosphere resistance (impedance encountered by water movement in the soil within the immediate vici-

nity of the root) relative to the pararhizal resistance (impedance imposed by the bulk soil). It is worth mentioning however that certain assumptions were made in their approximate methods. These include the use of an average water uptake rate by the plants, the assumption of a dense rooting system which absorbs water uniformly from an infinite soil volume and also the non-inclusion of hysteresis effects. Newman (1969), Lawlor (1972) and Arya et al. (1975) have presented theoretical and experimental evidence to show that the rhizosphere resistance is not appreciable. They argued for the dominance of the root hydraulic resistance over the soil hydraulic resistance. The conflicting results obtained can be ascribed to various factors. In their calculations, Gardner and Cowan assigned large values to the average water uptake rate and this can lead to an overestimation of the suction gradients (Newman, 1969). Furthermore, the use of an average water uptake rate is assumed to be equivalent to the prevailing transpiration rate. The latter fails to account for the possibility of water storage within the plant and this casts doubt on the use of a constant plant water uptake rate. A further complication is introduced when it is realised that uptake rate within the entire root system may not be uniform. This, according to Brouwer (1965) as reported by Tinker (1976), is due to the variation of the uptake rate with the suction in the xylem. This suction is dependent on the distance from the root tip. The possibility of differential uptake from surface soil horizon, occasioned by relatively dense root distribution, is not accounted for in the average uptake rate assumption. Weatherley (1976) analysed data obtained from plants grown in water cultures and theoretically showed that the soil-root interface constitutes a high resistance barrier to water flow. Weatherley further showed qualitatively that the root is a major site of variable resistance. These latter properties can be argued to be a function of both soil and root properties. According to Huck et al. (1970) and Tinker (1976), poor root-soil contact, a consequence of differing root and soil geometries is a factor which leads to variable absorption of water by the roots. Another possibility however is the shrinkage of roots caused by water stress in plants (Weatherley, 1976) which has been known to lead to about 40% shrinkage of roots in sunflower. This latter effect will result in low hydraulic conductance and hence higher root resistance.

The limitations of utilising the microscopic principle to developing practical soil water models were laid out by Molz and Remson (1970) and Molz (1981). These are the difficulties encountered in the measurement of detailed root geometries which are spatially and temporally variable, the interaction effects of other roots in the root system and the changes in root permeability that continually occur along the root length throughout its life-cycle. Consequently most soil water models that are being developed adopt a macroscopic approach.

3.2.3.2 The macroscopic approach to modelling root water uptake presents the whole root system as a spatially and temporally variable diffuse sink, ignoring the flow of soil water toward individual roots.

Mathematical description of the macroscopic approach normally involves the addition of a volumetric sink term to the Darcy-Richards equation and it is expressed for one-dimensional vertical flow thus:-

$$\partial\theta/\partial t = \frac{\partial}{\partial Z}\left(K(\theta)\frac{\partial H}{\partial Z}\right) - S \qquad (3.17)$$

where θ = volumetric water content of soil

$K(\theta)$ = unsaturated hydraulic conductivity

H = total soil hydraulic head

Z = elevation

S = sink term, representing water uptake by roots

The utilisation of extraction functions to calculate water uptake by plant roots has been widely recognised and applied by several workers (Molz, 1971; Feddes and Rijtema, 1972; Hillel et al., 1976, Rowse, et al., 1978). The forms of the sink term proposed by these various workers have either been empirical, semi-empirical or physical in their orientation.

The electrical analogy of Van den Honert (1948) has been the foundation on which subsequent formulation of physically based sink terms are built. The extraction term is normally assumed to be proportional to the pressure difference existing between the soil and the plant and inversely proportional to the total resistance encountered

in both the soil and plant segments of the transpiration stream. Thus:-

$$S = -(Hp - Hs)/(Rs + Rp) \qquad (3.18)$$

where Hp = plant water hydraulic head, assumed to apply at base of stem

Hs = soil water hydraulic head

Rs = soil hydraulic resistance

Rp = plant hydraulic resistance

Earlier formulation and utility of the extraction term by Gardner (1964) neglected the inclusion of the plant resistance in the above equation and expressed the resistance to water movement in the soil by

$$Rs = 1/BKL \qquad (3.19)$$

where B = an empirically determined constant

K = unsaturated hydraulic conductivity

L = length of roots per unit volume of soil

Consequently equation (3.18) above is expressed by Gardner (1964) as

$$S = BKL(Hp - Hs) \qquad (3.20)$$

Whisler *et al.* (1968) and Feddes *et al.* (1974) presented the following to express the extraction function:-

$$S = -A(Z).K(Hp-Hs) \qquad \text{Whisler } et\ al.\ (1968) \qquad (3.21)$$

$$S = -K(\theta).(Hp-Hs)/b \qquad \text{Feddes } et\ al.\ (1974) \qquad (3.22)$$

where A(Z) = root density function

$K(\theta)$ = unsaturated hydraulic conductivity, a function of volumetric moisture content

b = empirical function representing the geometry of flow

The extraction functions presented above in equations (3.20), (3.21) and (3.22) neglect the root resistance term. This is inconsistent with the evidence of Newman (1969), Lawlor (1972) and Rowse *et*

al. (1978) who indicate that the root resistance should be an important component of soil water movement through plant roots. Other workers (Nimah and Hanks, 1973; Hillel et al., 1976; Herkelrath et al., 1977 and Rowse et al. (1978), took cognisance of the root resistance and subsequently formulated extraction functions which considered this component. Their respective functions are in agreement with current knowledge available on soil-root hydraulics, since they encompass parameters which quantitatively describe the soil and plant segments of moisture movement through roots (Molz, 1981).

The following are the proposed extraction terms formulated by:

Nimah and Hanks (1973):-

$$S = -\frac{[Hr + (PRES.Z) - H(Z,t) - S(Z,t)]RDF(Z)K(\theta)}{\Delta X \Delta Z} \qquad (3.23)$$

where Hr = internal root pressure head at the soil surface where Z is zero

Z = depth

PRES = head loss coefficient for longitudinal water flow in the root xylem

H(Z,t) = soil pressure head

S(Z,t) = soil osmotic head

RDF(Z) = proportion of total active roots in depth increment ΔZ

$K(\theta)$ = soil hydraulic conductivity

ΔX = distance between roots

Hillel et al. (1976):-

$$S = (Hs-Hp)/(Rs+Rr) \qquad (3.24)$$

where Hs = total soil hydraulic head

Hp = plant water head at base of stem

Rs = soil hydraulic resistance, assumed to be equal to equation (3.19)

Rr = hydraulic resistance of the roots to water movement

Herkelrath et al. (1977)

$$S = \frac{\theta}{\theta_s} \rho l(Hs-Hr) \qquad (3.25)$$

where θ = volumetric water content

θ_s = saturation water content

ρ = root permeability per unit length of root

l = length of roots per unit volume of soil

Hs = soil water pressure head

Hr = root water head

Rowse et al. (1978):-

$$S = \Delta ZL((Hs-Hp)/(Rs+Rp)) \qquad (3.26)$$

where ΔZ = thickness of soil layer

L = length of roots per unit soil volume

Hs = bulk soil water head

Hp = plant water head assumed constant throughout the root xylem

Rs = soil resistance to root water uptake per unit length of root

Rp = plant resistance to water uptake per unit length of roots

From the above equations, Feddes et al. (1974) in making an analogy between the extraction terms and Darcy's law, defined a coefficient of proportionality as being proportional to the specific area of the soil-root interface and inversely proportional to the impedance of the soil-root interface. This coefficient of the sink term is defined in different ways and is represented by the term 1/b in equation (3.22) and defined by Gardner (1964) as LB in equation (3.20), A(Z) by Whisler et al. (1968), while Nimah and Hanks (1973) use RDF(Z)/$\Delta X \Delta Z$ as in equation (3.23). The coefficient is difficult to evaluate because the physics involved in soil water extraction by plant roots has not been thoroughly understood. There is little information available regarding the determination of the proportionality coefficient because direct experimental measurement of the various factors involved is extremely difficult.

However, Feddes (1971) as reported by Feddes et al. (1974) tried to compute values for the proportionality coefficient from field measurements of vertical flow in the presence of red cabbage by using a finite difference approximation of equation (3.22). Feddes found that the coefficient of proportionality is a variable dependent on the rooting depth and proportional to the root mass. Nimah and Hanks (1973) found that the proportionality coefficient over the entire rooting depth sums to unity while Feddes et al. (1974) intimated that this might not be so. In order to reconcile the disparity in values obtained by Nimah and Hanks (1973) and Feddes et al. (1974), Feddes et al. (1974) carried out a sensitivity analysis by using values of coefficient of proportionality derived from field data by Feddes (1971), and those derived using Nimah and Hanks (1973) calculation procedure (where the coefficient of proportionality equals unity over the entire rooting depth) in equation (3.22). They observed that the transpiration increased from 8.7 cm to 9.0 cm and that the soil evaporation decreased from 1.3 cm to 1.2 cm for the Nimah and Hanks (1973) and Feddes (1971) models respectively. Their result showed that the coefficient of proportionality has an insignificant influence on the model output. Consequently in this study where a physical extraction term is being tested against field data, the empirical constant is assumed to be unity. This is in agreement with other workers (Hillel et al.,1976; Belmans et al., 1979).

Hillel et al. (1976) developed a simulation model which considered the simultaneous movement of water and solute to plant roots using equation (3.24). Their extraction term is similar to the Gardner and Ehlig (1962) formulation, the difference occurring in the procedure employed in the calculation of the root resistance term. The root resistance is assumed to be composed of a coefficient of absorption and a coefficient of conduction (Hillel et al., 1976). Belmans et al. (1979) disregarding the solute component of Hillel et al. simulation model tested equation (3.24) by adopting an alternative calculation strategy for the root resistance component, which disregarded the conduction component of the root resistance. Belmans et al. in their study worked with a homogeneous soil packed in pots under laboratory conditions in which rye grass was grown. The soil was initially wetted and subjected to continuous drying. Belmans et al. observed that an increase in the root resistance values gave better

prediction of the soil moisture content distribution with depth when compared with measured values. They concluded that the root resistance term is likely to be an important factor in improving model predictions. This latter point was confirmed by Herkelrath et al. (1977) who showed that prediction of moisture content with the radial flow equation (Gardner, 1960b) when compared with the results of divided root experiments, obtained by growing winter wheat in cylinders packed with Plainfield sand, performed very poorly. However the prediction was improved and better agreement obtained when the Herkelrath et al. (1977) extraction function in equation (3.25) was utilised. The apparent improvement was the inherent assumption in their extraction function which stipulates that the effective area of contact between the root and soil decreased as the soil water content decreased; confirming the results of earlier workers (Newman, 1969; Lawlor, 1972 and Taylor and Klepper, 1975) that the major resistance to water uptake was in the root and not in the soil.

Molz (1971) using data obtained by Gardner (1964) computed the effective root distribution for sorghum to show the effects the latter distribution has on root water uptake. Molz found that root distribution is a spatially and temporally variable parameter. Computed root distributon was shown to compare favourably with actual root distribution as soil moisture deficit increases; initial divergence being obtained at high soil water contents. This similarity in observed and calculated root distribution as soil dries can be explained by the fact that as plant tension increases, it induces a root uptake pattern that becomes more representative of the actual root distribution. The initial divergence obtained showed that significant impedance to water flow within the plant might occur even when the soil is moist.

So far the discussion has focussed on the extraction functions that have been formulated employing mainly physical parameters and in some instances empirical characteristics. The extraction functions differ in their complexities depending on the number of parameters and the difficulties encountered in measuring these parameters under field conditions. Consequently, Feddes et al. (1976) argue with some justification that complex sink terms are, in most cases not applicable under field conditions because they require expensive and time con-

suming experimentation to assess the spatial and temporal variability of the inherent terms. An empirical volumetric sink term was proposed by Feddes et al. (1976)(Figure 3.3).

The sink term was allowed to vary with soil moisture content in accordance with known critical pressure heads for root water uptake. For practical application, Feddes et al. (1976) expressed the actual transpiration (E_a) by the following expression

$$E_a = \int_0^{-W} S(z,t)dz \qquad (3.27)$$

where W = rooting depth

t = time

$\int_0^{-W} S$ = sink term approximated to triangle OZS (Figure 3.4))

If $S(\theta) = \alpha(\theta)S_{max}$ (Figure 3.3) the sink term is then represented by equation (3.28) if the integral of equation (3.27) is approximated by the area of triangle OWS_{max} (Figure 3.4).

Hence $$S(\theta) = \alpha(\theta)\frac{2E_p}{W} \qquad (3.28)$$

where $\alpha(\theta) = S(\theta)/S_{max}$ (Figure 3.3)

E_p = potential transpiration rate

Feddes et al. applied an implicit finite difference solution to the above extraction term using data obtained from field experiments on which red cabbage was the test crop in a heavy clay soil. Their result did not accurately predict the distribution of soil water content with depth but simulates the cumulative effect over the entire profile.

There is an obvious similarity in Feddes et al. (1976) model with empirical drying curves as will be shown in the section on empirical studies. However a major limitation of utilising the preceding principle is the problem of determining the point at which the actual transpiration rate lags behind the potential.

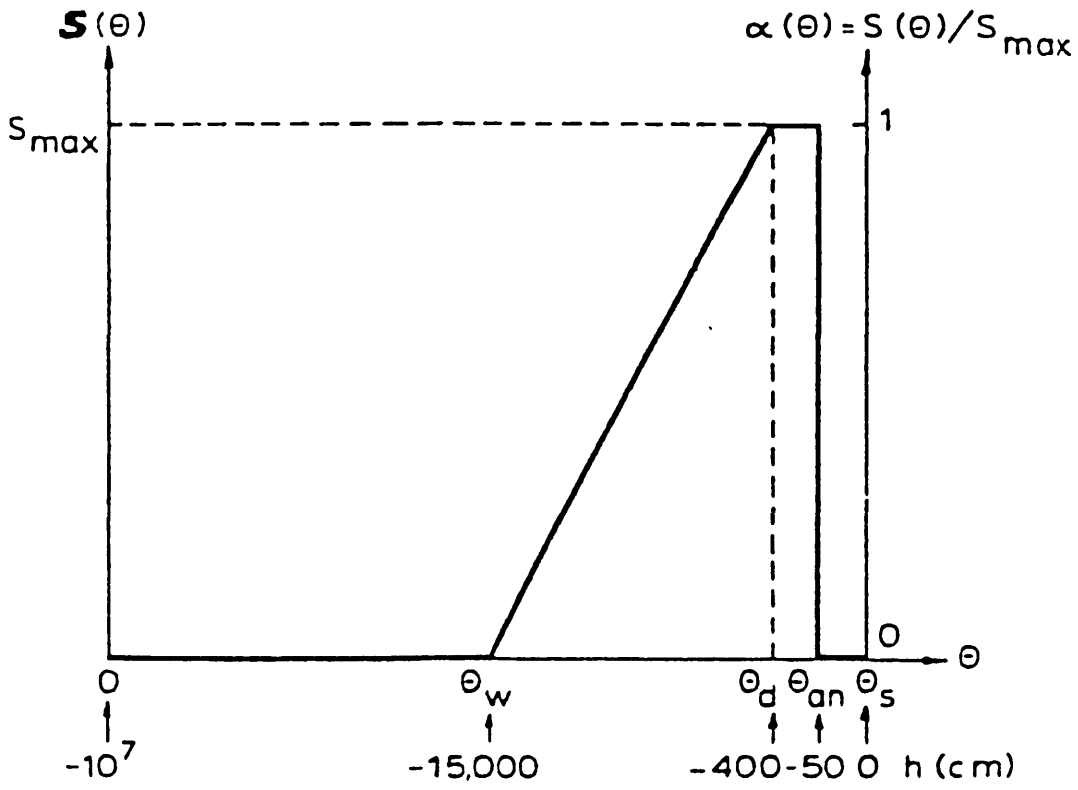

FIG.3.3 General shape of the sink term as a function of soil water content (After Feddes et al,1976)

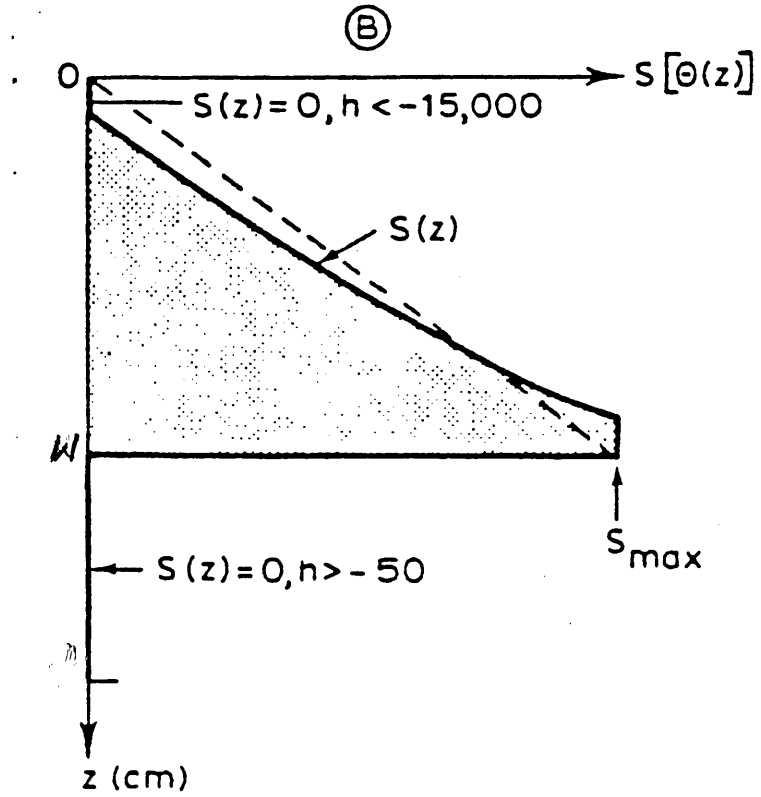

FIG.3.4 Variation of the sink term with depth

(After Feddes et al,1976)

Walley and Hussein (1982) provide a model which compromised between a physical treatment and an empirical treatment of root water extraction. Their model subdivides the soil profile into three distinct layers. Allowance is made for moisture flux occurrence between the layers according to the following equation which is similar to the Darcy equation:-

$$V_{12} = K_{12}(\phi_m) \left[\frac{H_1 - H_2}{(d_1+d_2)/2}\right] \qquad (3.29)$$

where V_{12} = moisture flux between layers 1 and 2

$K_{12}(\phi_m)$ = average unsaturated hydraulic conducitvity, a function of soil water potential (matric)

H_1 = total soil water head in layer 1

H_2 = total soil water head in layer 2

d_1 and d_2 = depths of layers 1 and 2 respectively

The root extraction function is represented by a semi-empirical equation given by:-

$$S = N(H_1 - Hs)/\left[\frac{r}{K+Kr} + \frac{r_d}{tr}\right] \qquad (3.30)$$

where N = an empirical parameter representing root density times soil layer thickness

H_1 = leaf water pressure head

Hs = soil water pressure head

r = a parameter representing the combined effect of root radius and radius of influence of individual roots

K = unsaturated hydraulic conductivity

Kr = root coefficient

r_d = rooting depth

tr = parameter representing the transmissivity of the root and stem systems.

Walley and Hussein also provide an empirical equation which accounts for rapid percolation into lower layers when excess rainfall occurs. Although they intimated that the model is simple and can pro-

vide a reasonable simulation of soil moisture status, validation tests by other workers have not been carried out.

3.3 Empirical Models

The prior discussions emphasised predominantly the soil water models that consider the distribution and movement of water within the soil profile. The following shall consider the prediction of soil moisture with regard to the effect on relative evapotranspiration rate.

Drying Curves:-

The use of empirical studies to describe plant water uptake normally entails deriving a relationship between the actual evapotranspiration and potential evaporative demand of the atmosphere as a function of soil moisture status. This relationship is referred to as a drying curve and can be expressed as follows

$$E_a/E = f(M) \qquad (3.31)$$

where E_a = actual evapotranspiration
E = potential evapotranspiration

and M is an index of soil water content. This index can be expressed as matric potential (Feddes et al., 1976); soil moisture deficit (Penman, 1949) or as the available water capacity in the rooting zone (Calder et al., 1983). The available water is defined as the moisture content held at suctions between field capacity and permanent wilting point for a particular crop (Israelsen and Hansen, 1967).

A lack of consensus emerges from the literature regarding the disposition of actual evapotranspiration relative to the potential evapotranspiration rate as a function of soil moisture content. This is evidenced by the number of drying curves proposed by several workers (Veihmeyer and Hendrickson, 1955; Thornthwaite and Mather, 1955; Slatyer, 1956, Denmead and Shaw, 1962 and Gardner and Ehlig, 1963). The main controversy centres between the views postulated by Veihmeyer and Hendrickson and that of Thornthwaite and Mather (Figure 3.5). Veihmeyer and Hendrickson from lysimeter results suggested that equivalent values of actual and potential evapotranspiration are

obtained until permanent wilting point is attained. On the other hand, Thornthwaite and Mather employing data from vapour and temperature profiles proposed a linear reduction of the relative evapotranspiration with increasing soil matric potential. In between these two latter views is an exponential form given by Pierce (1958).

These earlier conflicts of ideas have been explained by Slatyer (1956); Denmead and Shaw (1962) and Gardner and Ehlig (1963). In working with sorghum, Slatyer found that the actual evaptoranspiration rate is virtually equal to the potential evapotranspiration rate for a wider range of moisture contents than realised for peanuts and cotton which are sparsely rooted. Denmead and Shaw observed from corn grown in pots that at high potential evapotranspiration rate, the reduction of AE/PE occurred at lower soil suction than at lower potential evapotranspiration rate. The magnitude of this relative reduction is expected to be different under varying crop and soil types. As such Gardner and Ehlig using Birds' Foot Trefoil observed a reduction in relative evapotranspiration at a higher moisture content in clay than sand. Zahner (1967) presented similar results to that of Gardner and Ehlig by fitting idealised soil water extraction functions in a forest environment. Zahner's idea has been criticised for the complexity introduced in including soil textural and climatic differences (Rutter, 1975).

The effect of environmental factors on the shape of the drying curve for different transpiration rates and root densities has been theoretically reproduced by Cowan (1965), Figure 3.6. This latter representation has been criticised by Newman (1969) specifically in relation to the assumed root densities utilised in the computation which Newman believes may lead to an underestimation of the root resistance term.

Although the drying curve concept has been around for some time and some qualitative descriptions of environmental influences have been given, there has been limited field application. This is due to a lack of quantitative guidelines and the fact that most of the drying curves have been derived from pot experiments and lysimeters with homogeneous soil and well formed root systems which may not fully replicate the natural environment. Despite the limited applications

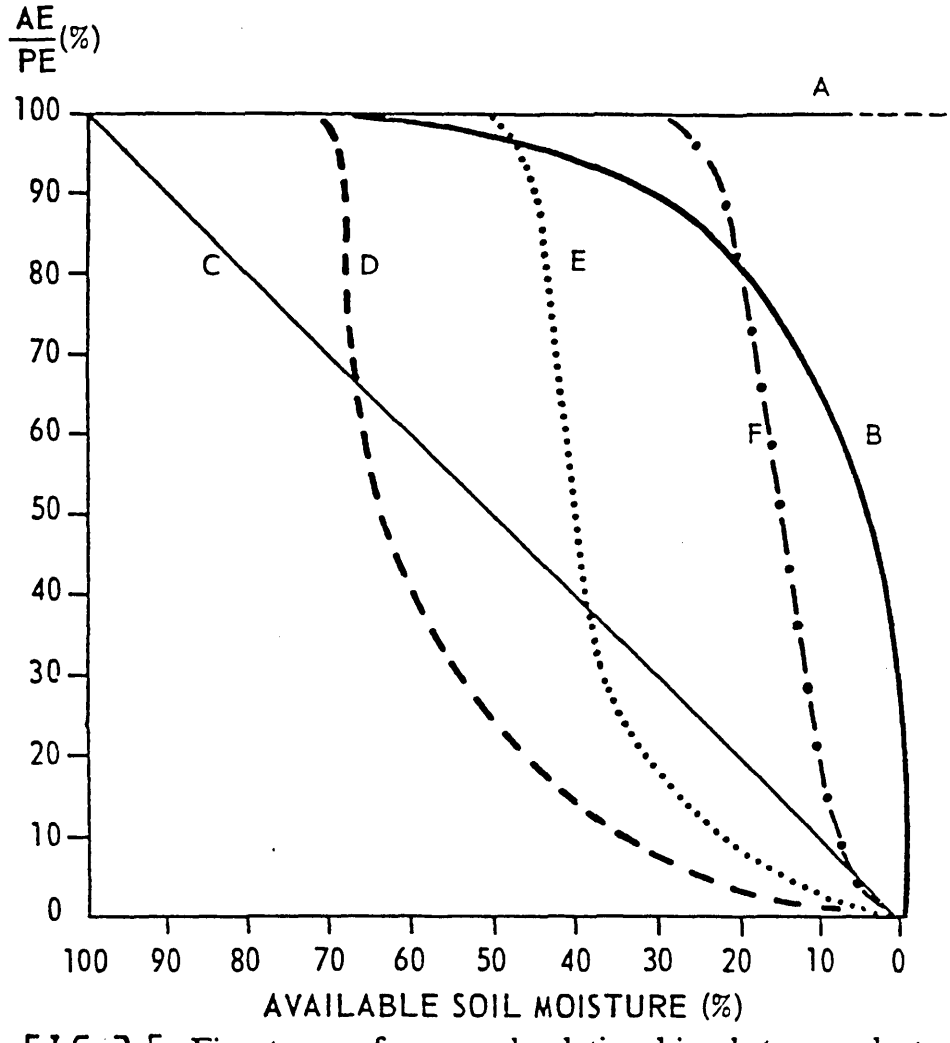

FIG. 3·5 Five types of assumed relationships between plant-available soil moisture and *AE/PE* rate. (After Baier and Robertson, 1966)

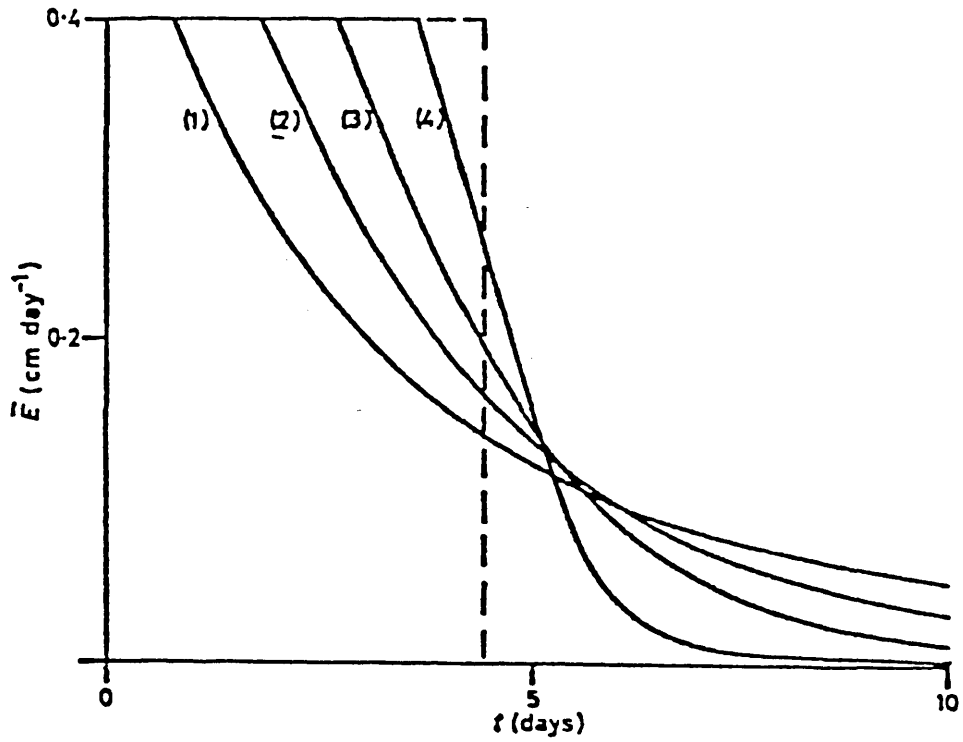

FIG.3.6 Temporal decrease of transpiration rate for crops having different root densities (After Cowan,1965)

of the drying curve concept, there exists a handful of empirically based soil water models that utilise the concept. In the following, such models are discussed.

Empirical models will be defined strictly within the context of the application of the drying curve concept to predict soil moisture status.

The majority of empirical models that have been proposed represent the soil profile as being comprised of one or more layers of finite available water capacity. The rate of moisture extraction from any layer is assumed to depend on both the potential extraction rate and the quantity of available water remaining in that layer. The potential extraction rate is normally equated with the potential transpiration for either one or double layer models. In multi-layer models, the potential transpiration is subdivided between the layers on a percentage basis in accordance with the root density distribution within each layer.

A single layer model was developed by Penman (1949) and was later utilised by Grindley (1967) to predict regional soil moisture status in the United Kingdom. Essentially, the model incorporates a drying curve based on the relationship between actual and potential deficit within the layer (Figure 3.7). Actual soil moisture deficit is expressed as the quantity of water extracted by evapotranspiration and is normally assumed to be equal to the amount of water required to return the layer to field capacity. The potential deficit is the difference between Penman evapotranspiration and rainfall. When no deficit is apparent, any rainfall in excess of evapotranspiration is regarded as being lost to runoff or groundwater via deep percolation.

Holmes and Robertson (1959) proposed a two-layer model based on the concept of soil moisture deficit. The model has an upper layer to which rainfall input is assigned and which is assumed to be depleted at the potential evaporation rate. When the upper layer is depleted, extraction from the lower layer takes place at a slower rate. This rate is described by a stepped function which varies during the growing season in accordance with root proliferation (Figure 3.8).

A multi-layer model was developed to predict evapotranspiration in the Idaho corn belt of the United States by Shaw (1963). Shaw

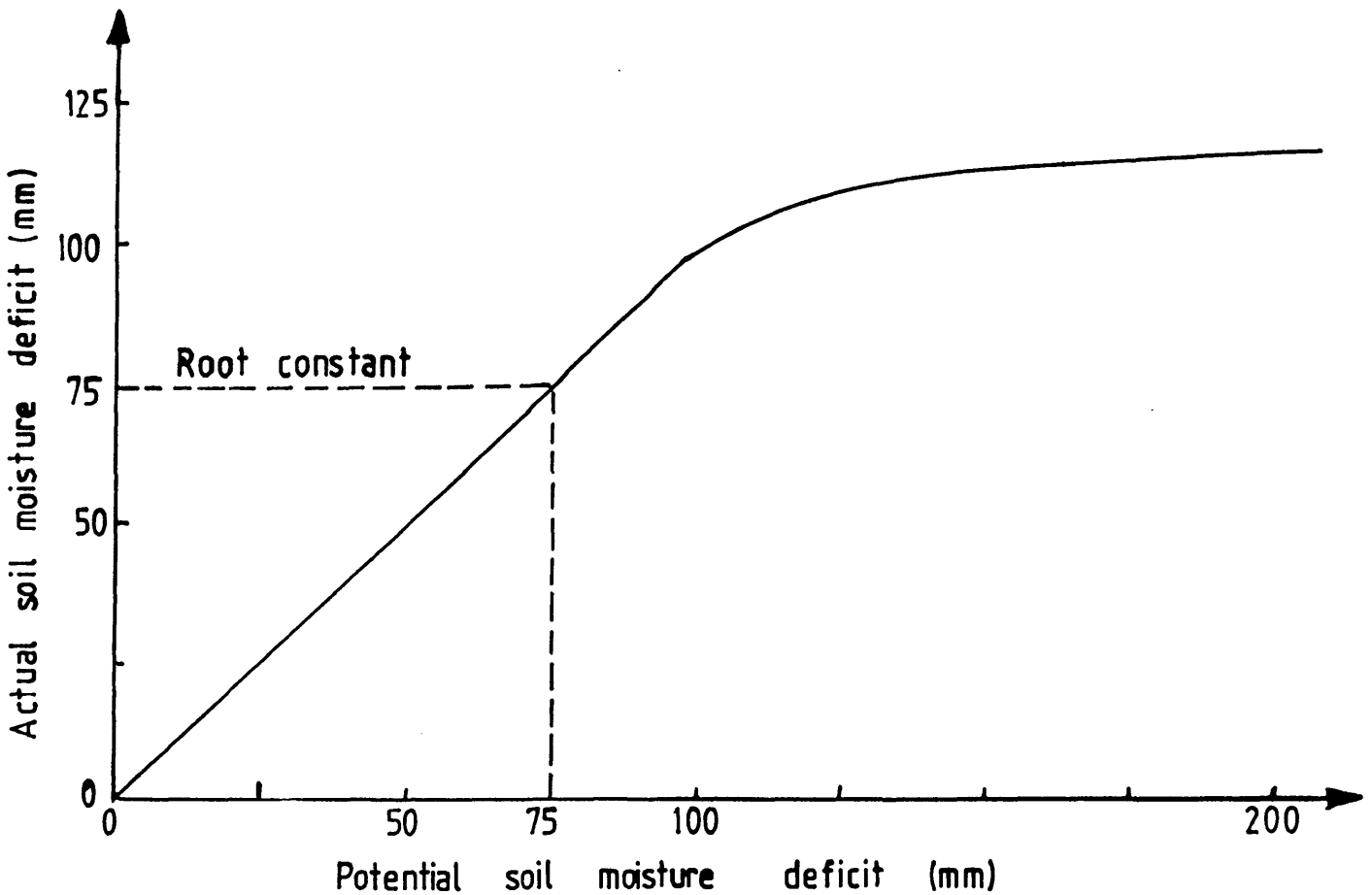

FIG. 3·7 DRYING CURVE FOR 75MM ROOT CONSTANT.

divided the soil profile into several layers with each layer supplying a percentage of the total potential demand as calculated from a standard class A evaporation pan. The relative evapotranspiration rate is controlled by a drying curve identical to that of Denmead and Shaw (1962). The latter curve is based on the remaining available water in the profile. Shaw computes runoff by utilising a runoff coefficient which is based on Kohler and Linsley (1951) equation and infiltration is represented by the progressive accretion of water in the surface layers.

A multi-layer "New Versatile Budget" model was also developed by Baier and Robertson (1966). This latter model is an extension of the Holmes and Robertson (1959) model which has been earlier discussed. In this model, the soil profile is divided into six layers, each with its own corresponding drying curve, and with water being withdrawn concurrently from all the layers. The total extraction rate is given by:-

$$AE_i = \sum_{j=1}^{N} [K_j \frac{S_{j(i-1)}}{S_j} Z_j PE_i e^{-w(PEi-\overline{PE})}] \qquad (3.32)$$

where AEi = actual transpiration for day i

K_j = coefficient for plant and soil characteristics in the jth zone

$S_j(i-1)$ = available water in the jth zone at the end of day i-1

S_j = available water capacity in the jth zone

Z_j = adjustment factor for different types of soil dryness curves

PE_i = potential evapotranspiration for day i

w = adjustment factor accounting for the effects of varying PE rates on the AE/PE ratio

$\overline{PE}$ = average PE for the month or season

In the above equation (3.32), the maximum extraction from a layer is determined by the coefficient K, and the proportion of PE_i accounted for by each layer and also is determined by a linear drying curve. The drying curve is dependent on the available water remaining within the layer ($S_{j(i-1)} \mid S_j$) and is modified by Z_j, which is the difference between the linear relationship and any of the series of cur-

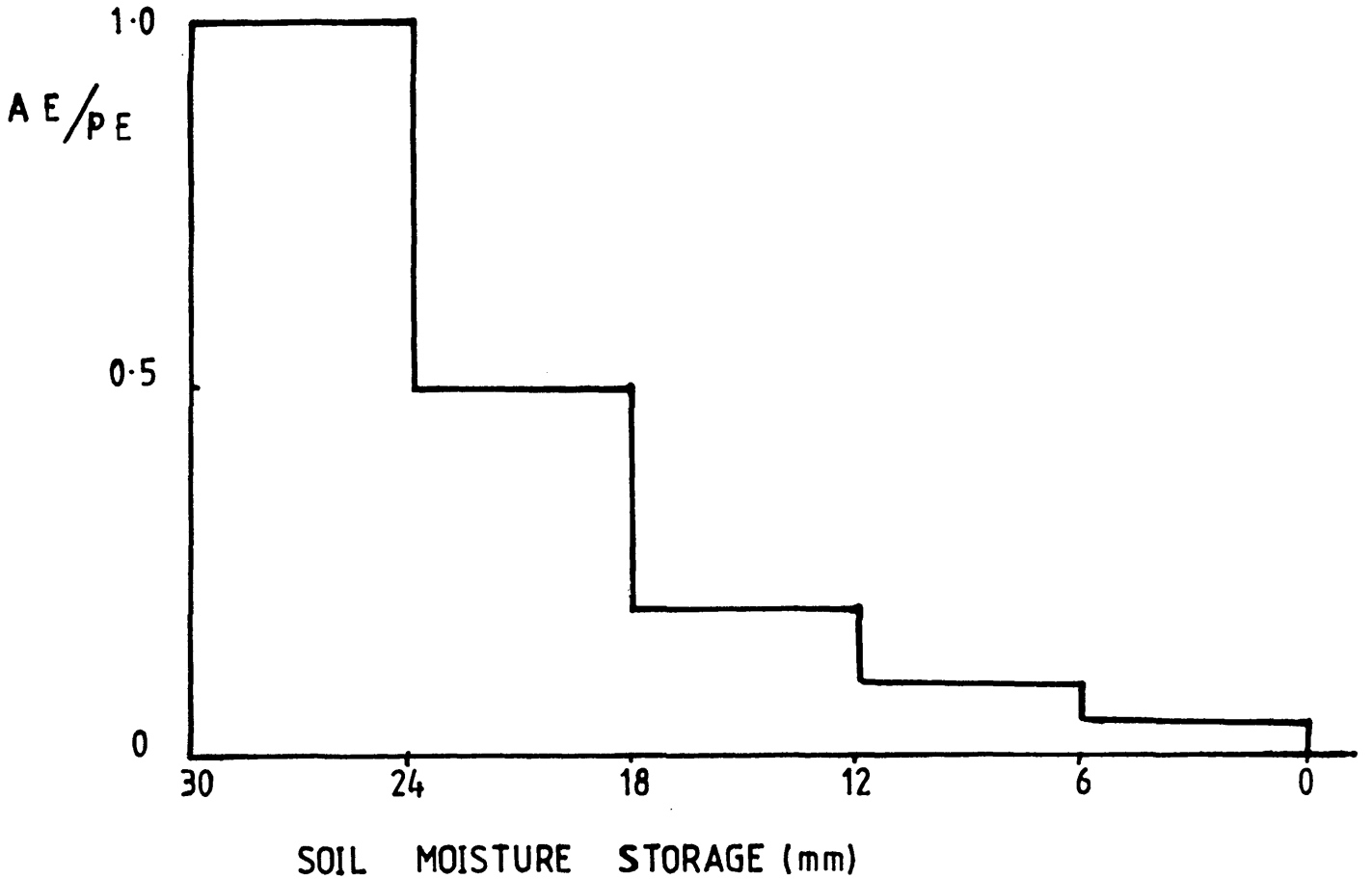

FIG. 3.8 RATIO OF ACTUAL TO POTENTIAL TRANSPIRATION AS A FUNCTION OF SOIL MOISTURE (After Holmes and Roberston, 1959)

ves in Figure 3.5. The effect of transpiration rate is taken care of by $e^{-w(PEi-\overline{PE})}$. In common with most multi-layer models, the respective layers are sequentially filled and any surplus is deemed to go to drainage. Runoff is computed by utilising a regression equation derived from rainfall and moisture content in the surface layer. Although the "New Versatile Budget" model attempts to encompass both soil and plant characteristics, it disregards redistribution within the layers and prolonged drainage which normally occurs in most soils.

A predominantly empirical model which contains a theoretical description of redistribution, drainage and capillary rise was developed by Saxton et al. (1974). Their model encompasses the following:- a subdivision of the potential evapotranspiration into soil evaporation and plant transpiration which is influenced by a canopy shading percentage which varies throughout the year. The potential evaporative demand is being controlled by the plant as dictated by the percentage of the canopy that is actively transpiring. The soil profile is split into twelve layers with the evaporation occurring predominantly in the uppermost layer, and the redistribution of the extraction within the layers being controlled by the root density. Implicit in the model, in common with the Baier and Robertson (1966) model, is the possession by each layer of its own drying curve. An observed improvement in the Saxton et al. technique is the inclusion of moisture redistribution between the layers. The latter is achieved by utilising the one-dimensional vertical Darcy equation of flow. Also included in the model is a bottom layer in the profile which is assumed to remain at field capacity and controls the drainage from and capillary rise to the profile.

A rather more comprehensive model that has been developed is that of Makkink and Van Heemst (1975) which considered the simulation of moisture status in the presence of a water table. Their model was calibrated and tested in the Rottegats Polder region of the Netherlands. In contrast to other empirical models which assume that the soil profile is an amalgam of discrete, finite capacity layers, their technique assumed the soil profile to be composed of dynamic zones. The model can simulate interception, groundwater table fluctuations, transpiration and the rehydration and dehydration of micellular water. In essence, the Makkink and Van Heemst model splits

the soil profile into saturated and unsaturated zones of variable water capacities. The unsaturated zone is characterised by a hydrostatic equilibrium moisture content which is dependent on moisture tension values obtained from a moisture characteristic and height above the water table. This equilibrium moisture is further subdivided into available and unavailable moisture with the latter being obtained at moisture held above 15 bar suction.

The evaporation zone is assigned a maximum capacity and represents a bare soil moisture store which is presumed to be depleted by evaporation only. The transpiration zone is made up of the crop available water which has a varying capacity as the crop develops. A deficit is allowed to occur only in the transpiration zone while drainage takes place both in the transpiration zone and the lower part of the unsaturated zone. A reduction factor which is dependent on the residual available water in the transpiration zone modifies the actual extraction relative to the potential demand.

The magnitude of the infiltrated rainfall and the quantity of excess water in the unsaturated zone control the recharge of the saturated zone. Slow drainage is dependent on the amount of excess water in the unsaturated zone and on the height of this surplus above the water table. The latter is expressed as follows:

$$\text{Percolation} = \text{Surplus}/f(\text{HFV}) \qquad (3.33)$$

where HFV = height of surplus from the water table.

Capillary rise is computed in a similar fashion to the above by accumulating the deficit in the transpiration zone at the top of the profile and also computing the height above the water table.

Although the Makkink and Van Heemst model described in the preceding provides a fairly realistic simulation of profile water balance in the presence of a water table, it requires the evaluation of a large number of empirical parameters for each environmental condition. This latter point is likely to hinder the widespread applicability of the model, since a handful of theoretical models exists which possess few and easily identified parameters and which are likely to produce equal or better simulation results.

In the United Kingdom, the British Meteorological Office adapted a double layer-model which is a modification of the Grindley (1967) model. The model predicts soil moisture deficit, runoff and slow dainage (Thompson, 1981). A drying curve that relates the surface resistance in the Penman-Monteith evaporation formula to soil moisture deficit as suggested by Russell (1980) is employed to compute actual evaporation. Basically, the model splits the soil profile into two layers:- TOP and BOTTOM. The two layers are assigned coresponding available water capacities with the moisture in the top layer readily available to the plant for transpiration. The moisture in the bottom layer is less accessible to the plant. The relative available water capacity of the bottom layer is given as 1.5 times the capacity of the top layer designated as MAX. When the two layers are filled, 40% of the available water is apportioned to the top layer and 60% to the bottom, and the soil moisture content under this condition is defined as being at field capacity. The maximum deficit allowed is equal to the available water capacity which is 2.5 MAX. Deficit conditions are when either or both layers are not full, i.e. below field capacity. Implicit in the Meteorological Office model is the soil moisture deficit threshold known as MAX and which is referred to as the root constant (Penman, 1949). The root constant concept entails that soil moisture is transpired at the potential evapotranspiration rate until this threshold is reached. The root constant values are expected to vary for each soil and crop types. However, the assignment of these values have been largely based on conjecture for different land uses (Arnott and Wales Smith, 1978). Consequently there is a need to evaluate the values for each soil and crop type before a full assessment of the Meteorological Office model can be made.

3.4 Comparison of Physical and Empirical Models

The preceding sections discussed the two principal approaches available to describing soil moisture extraction by plants; (a) the physical (based on soil and plant hydraulic characteristics); (b) the empirical (based on soil water content modulation via drying curves).

The relative advantages of these approaches have been given by Feddes *et al.* (1976) who showed that both yield comparable results. In comparing finite difference models containing simple and complex

extraction functions with a finite element simulation; Feddes et al. (1976) showed that both provided inadequate simulation of the extraction distribution, with none of the model exhibiting any degree of superiority.

Although physical models have been judged to provide a realistic simulation of soil water processes, primarily because they are based on proven physical theory governing soil water flow (Cowan, 1965; Molz, 1981), it may be argued that unless such models take into full account the problem of hysteresis, fissure flow and spatial heterogeneity, empirical models may also perform equally well. In discussing the predictions from a finite difference simulation model, Rowse et al. (1978) observed the inability of the model to account for moisture movement through root cracks. The utility of empirical models is normally justified because of the limited knowledge required of the soil hydraulic parameters. The latter is probably true for simple models like that of Thornthwaite and Mather (1955), Grindley (1967), Doorenbos and Pruitt (1977) and the British Meteorological Office (MORECS) model (Thompson, 1981); but may not be applicable to those of Saxton et al. (1974) and Makkink and Van Heemst (1975).

Generally, however, the application of both physical and empirical soil water models has been limited by the lack of experimental validation studies. The models of Feddes et al. (1976) and Rowse et al. (1978) are still probably the only physical models that have been subjected to extensive testing and have enjoyed some applicability in the field (Molz, 1981). Empirical models, on the other hand, although normally calibrated for a specific crop and soil combination have not been tested widely. In most cases, validation has been carried out in grass plots and extension to other crops is necessary for a well-substantiated evaluation of the models. For instance, in the United Kingdom, the validations of the Grindley model are found in Wheater and Weaver (1980), Hall and Heaven (1979) and in Wheater et al. (1982), while MORECS comparisons with field data has been confined to that of Gardner and Bell (1980) and Gardner (1981).

There are limited comparative studies of physical and empirical models available in the literature, particularly in the same climatic and edaphic environment. Parkes and O'Callaghan (1980) compared the

finite element model of Feddes et al. (1974) with Baier and Robertson (1966) Versatile Budget Model. Both models were observed to underestimate root extraction during high evaporative demands and failed to account for fissure flow. However, Parkes and O'Callaghan concluded that if slow drainage is incorporated, the empirical model can be a more practicable technique.

3.5 Conclusions

Thus far the two main approaches to estimate soil water extraction have been discussed. The various plant and soil hydraulic parameters that interplay in the processes of evapotranspiration, redistribution and drainage have been highlighted. It has been apparent from the literature that the efficiency of the models for general applicability has so far not been demonstrated. This has been due to the inclusion of parameters; for example root hydraulic resistance; plant potential; which are not easily measured in the field and are generally site and crop specific. In the empirical models, an application for regional soil moisture prediction has been shown, although the reconciliation of which drying curve is suitable for any particular environment has not been achieved. Consequently, this study attempts to carry out field validation of some of the postulated soil water models under different crop types and similar soil type. It is believed this shall afford a better understanding of the interplay of parameters and hence give guidelines for future soil water management.

CHAPTER 4

THE STRUCTURE OF ADOPTED SOIL WATER MODELS

4.1 Introduction

Discussions in Chapter 3 concentrated on the review of the two main approaches to modelling soil water in the presence of plant roots. It has been apparent that physical soil water models can be said to replicate the currently available concepts of soil-root hydraulics because they are based on proven physical laws. On the other hand, empirical models require little knowledge of soil hydraulic parameters but the use of any given drying curve for a particular environment has not been reconciled.

The objectives of this study as given in Chapter 1 include the evaluation of the relative performance of physically-based and empirically-based soil water models. This is carried out by comparison of the simulated moisture profiles with field measured data. This chapter focusses on the choice of a physically-based and an empirically-based soil water model for this study. It presents the structure and operational dynamics of the models used, highlighting the limitations and capabilities.

4.2 Choice of a Physically-based Soil Water Model

The utility of models to simulate soil water fluxes within the soil profile and through plant roots depends on several criteria. These criteria include: the objectives of the study; the conceptual framework of the model; the number of parameters to be evaluated and the availability of relevant data.

Soil water simulation models in most cases have as their objectives the prediction of soil water status and associated physico-biological parameters at any given time. This provides quantitative information on the management of water resources; either in irrigation planning, groundwater recharge or in the prediction of drought and flood occurrence. These objectives determine to a large extent the type of model to be employed and the level of detail involved.

The two main physically-based approaches to modelling soil water as discussed in Chapter 3 are the microscopic and macroscopic techniques. The limitations of the microscopic approach have also been discussed in Chapter 3. The major difficulties in utilising the technique have been the problem of the prescription of boundary conditions for the individual roots and the lack of adequate measurement techniques to monitor the water content and water potential around individual roots. The macroscopic level of description has normally been preferred (Gardner, 1964; Nimah and Hanks, 1973; Hillel et al., 1976; Herkelrath et al., 1977 and Rowse et al., 1978) because it considers the entire root system as a diffuse sink for soil water, and hence eliminates the problems associated with the microscopic approach.

It is evident from the previous chapter that a number of physically based macroscopic soil water models have been postulated. These models vary in their complexity depending on the number of parameters. A model like that of Nimah and Hanks (1973) introduces an internal root pressure head, a head loss coefficient for longitudinal water flow in the root xylem and soil osmotic potential while that of Herkelrath et al. (1977) considers a root permeability factor. These latter parameters are expected to vary with time depending on soil water content, meteorological conditions and age of roots. In considering the current state of in situ measurement of plant physiological response, it would be impossible to measure the root parameters in the field without introducing errors which are likely to invalidate the model results. It is therefore believed by this author that in choosing a particular model for performance testing, it is necessary that a balance be struck between the degree of complexity introduced into physical soil water models and the available measurement techniques. This is to minimise the errors that may be accumulated from parameter estimation. A model structure similar to that of Hillel et al. (1976) and Rowse et al. (1978) has distinct advantages over Nimah and Hanks and that of Herkelrath et al. models. This is because the models of Hillel et al. and Rowse et al. embody the internal root pressure head; the head loss coefficient for longitudinal water flow and osmotic potential (Nimah and Hanks, 1973) and root permeability factor (Herkelrath et al., 1977) into one parameter; the root resistance term. This latter parameter is consistent with the current

view of soil-root hydraulics that the roots impose a resistance to flow of water from soil to plant (Molz, 1981). The Hillel et al. and Rowse et al. models also allow for flexibility (allowance made for the prescription of different boundary conditions) to account for variable root distributions and soil profile layering and variable climatic regimes. It was decided therefore to follow the modelling approach of Hillel et al. (1976) which is similar in many respects to that of Rowse et al. (1978). Such an approach will allow for the prediction of soil moisture distribution with respect to different depths within the root zone and allow for quantitative estimation of the root resistance and soil resistance terms. The latter will allow further understanding of the dominance or otherwise of the root resistance term over the soil resistance term.

4.3 The Physically-based Soil Water Model: Structure and Dynamics

The physically-based soil water model described in the following uses soil and plant hydraulic parameters to describe the temporal distribution of soil water with depth. The use of the model allows for an evaluation of its performance and provides quantitative estimation of the root and soil resistance terms. The model consists of numerical solutions of the Darcy-Richard equation describing soil water fluxes in the soil profile. The latter equation is coupled with a sink term representing plant water uptake. As the solution employs a finite difference method, the soil profile is divided into a number of layers. This number and the individual thickness of each layer can be varied arbitrarily. A uniform layer thickness of 10 cm was selected below 15 cm depth to correspond to field measurement depths of both soil moisture content and soil moisture potential. The number of soil layers is ten as shown in Figure 4.1, with the root zone confined to the uppermost three layers.

4.3.1 Soil Water Dynamics and Extraction Model

The distribution of soil water is given by Darcy's law as in the following:-

$$V = -k(\theta)\,\partial H/\partial Z \qquad (4.1)$$

where V = soil water flux

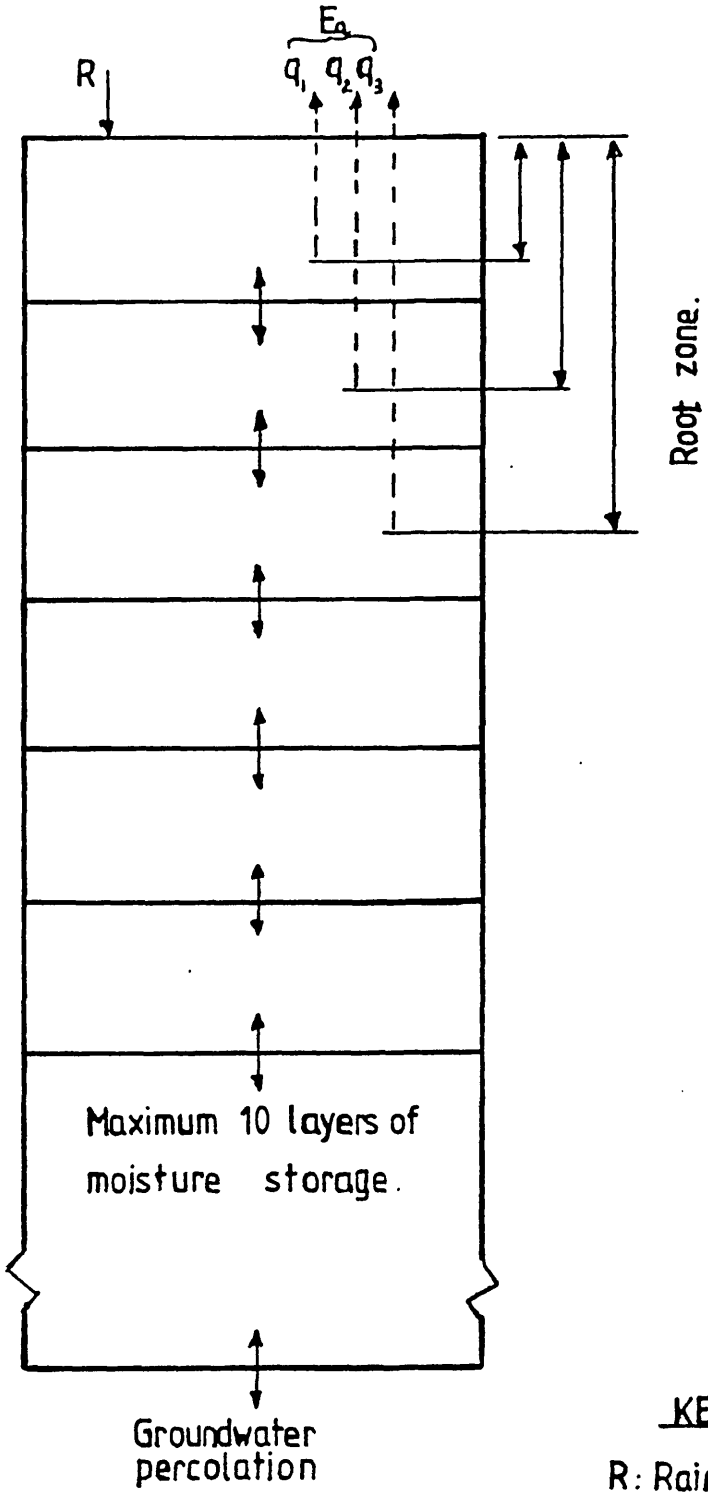

KEY.

R: Rainfall.

Ea: Actual evapotranspiration

q_i: Root abstraction from layer 1.

FIG. 4.1 MODEL STRUCTURE.

$K(\theta)$ = hydraulic conductivity-wetness relationship

$\partial H/\partial Z$ = hydraulic head gradient

The above equation (4.1) is combined with the conservation equation to give the vertical transient-state flow of water as:-

$$\frac{\partial \theta}{\partial t} = \frac{\partial}{\partial Z}\left[K(\theta)\frac{\partial H}{\partial Z}\right] - S \qquad (4.2)$$

where θ = volume wetness

t = time

Z = elevation

S = sink term representing extraction by plant roots

The soil water potentials are determined from a polynomial function of the volumetric moisture content. This is expressed by Gardner et al. (1970) as:-

$$\phi_p = -a\theta^{-b} \qquad (4.3)$$

where ϕ_p = soil water potential

θ = volumetric water content

a and b are empirical constants.

The above equation (4.3) is not normally applicable for saturated and wilting conditions (Hillel, 1980b). These extreme conditions are not considered in this study and hence there is a limit to the range of volumetric moisture contents for which the soil water potential can be calculated. However, since the empirical parameters a, b are obtained during the summer months when the above conditions are not likely to occur, equation 4.3 should be adequate. Hysteresis is not considered in the above equation. This is because in field conditions, the spatial variability of the soil moisture characteristics is often too large to prevent the modelling of hysteresis (de Wit and van Keulen, 1972).

Hydraulic conductivity-wetness relationship:- It is evident from equation (4.2) that a knowledge of the hydraulic conductivity as a

function of volumetric moisture content is necessary. Normally, if experimental data for the K(θ) relationship are unavailable, a predictive technique based on Green and Corey (1971) is employed (Goutzamanis and Connor, 1977). This technique is a modified pore-interaction model of Marshall (1958) which determines the K(θ) relationship by separating the soil moisture characteristics into pore classes. However, for this exercise, a "natural balance" technique is used to evaluate the K(θ) relationship. The following expression given by Hillel (1980b) is used:-

$$K = ae^{b\theta} \tag{4.4}$$

where a and b are empirical constants obtained by fitting regression lines through plots of K versus θ.

Equation (4.2) is the governing equation of the physically-based soil water model. However, before it can be used, the sink term which represents the root uptake of soil water has to be defined.

Extraction Model:- The analogy between root water uptake and flow of electric current through a series of resistors (van den Honert, 1948) has been discussed in Chapter 3. Figure 4.2 gives a schematic representation of the root system as a resistance network. This analogy has been the basis on which the model sink term (S) in equation 4.2, used in this study is built.

Consequently, the rate of water extraction by the plants from a unit volume of soil can be given as:-

$$S = \frac{POTH - POCR}{RS + RR} \tag{4.5}$$

where POTH = total head of soil water

RS = soil hydraulic resistance to moisture movement

RR = root hydraulic resistance to moisture absorption and conduction

POCR = the plant water potential, in head units, at a point where all roots converge

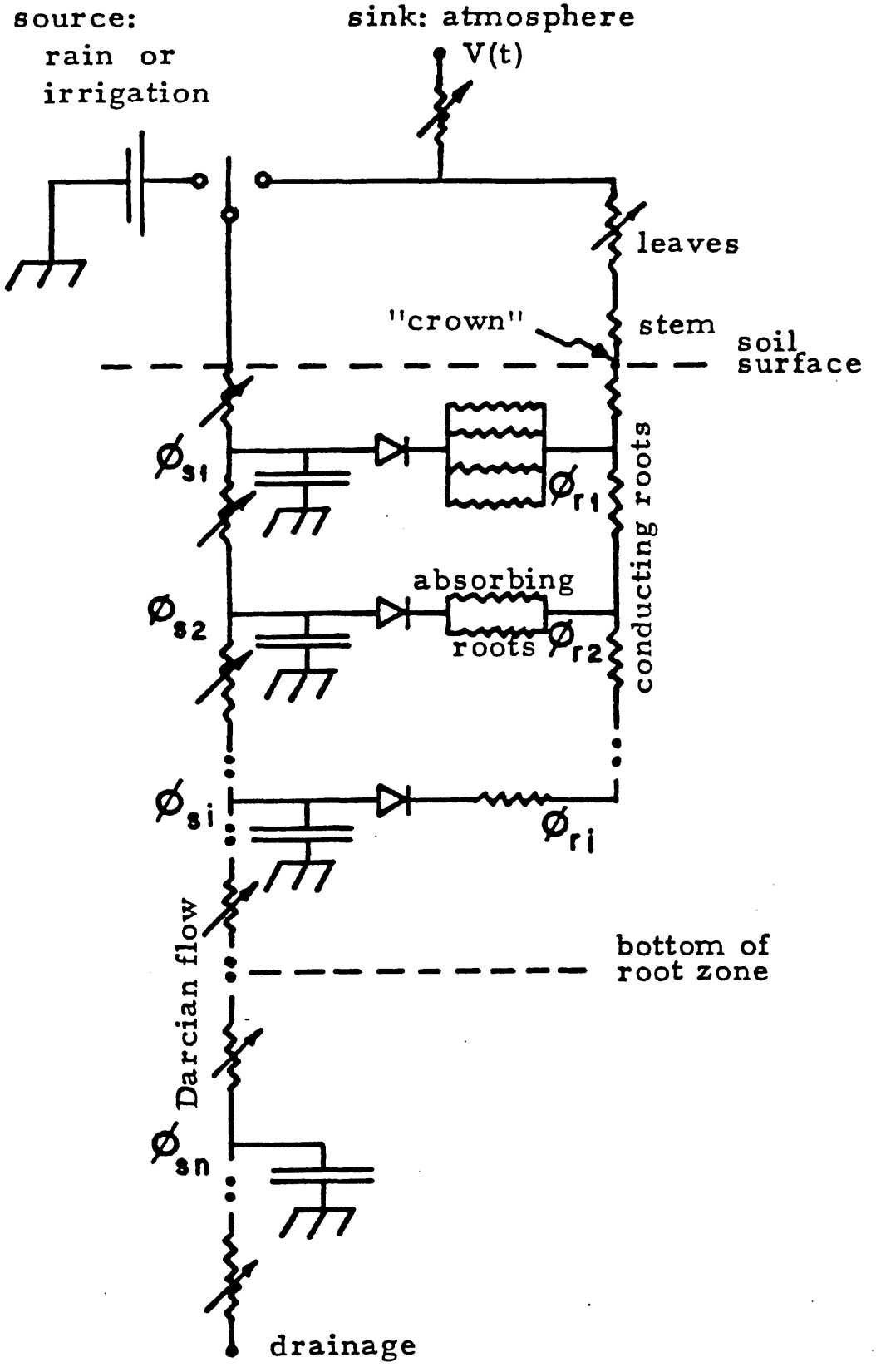

Fig. 4.2 Representation of a root system as a resistance network
(After Hillel, 1977)

This implies that the plant emerges from the soil with a single water potential which can also be referred to as the "crown potential" (Hillel, 1977).

Gardner (1964) from theoretical and experimental studies defined the soil hydraulic resistance (RS) as inversely proportional to the unsaturated hydraulic conductivity (K), a function of volumetric moisture content and the total length of active roots in the unit volume of soil. Hence:-

$$RS = 1/BKL \qquad (4.6)$$

where B is an empirical constant which represents a root length activity factor. A value of unity is assigned to this constant as discussed in Chapter 3. L is the length of active roots per unit volume of soil.

The root hydraulic resistance (RR) to moisture movement is composed of two resistances (Hillel et al., 1976). These resistances are:-

(1) absorptive resistance which is imposed by the epidermis, cortex and endodermis of the root to moisture movement;

(2) conductive resistance which is imposed by the xylem vessels in the transportation of moisture from the roots to the leaves. This resistance attains greater significance in tall plants where the conduction of water traverses a longer pathway. However in shallow rooted crops with short growth, the conductive resistance is neglected (Belmans et al., 1979 and Feyen et al., 1980). Consequently, in this study the conductive resistance is assumed negligible. The absorptive resistance is considered to be proportional to the specific hydraulic resistance of the cortex (R_u) and inversely proportional to the length of roots per unit volume of soil (Belmans et al., 1979). Hence:-

$$RR = R_u/L \qquad (4.7)$$

4.3.2 Boundary Conditions

The boundary conditions imposed at the surface of the profile are rainfall and the evapotranspiration rates. The latter gives an indication of the atmospheric demand for water. The estimation procedure used for deriving the potential evapotranspiration is the Penman (1956) combination formula as discussed in Chapter 3.

An objective of this study is the reconciliation of the dominance of either the soil or root hydraulic resistances. In order to achieve the latter objective, actual evapotranspiration rates are also given as surface boundary condition. This is necessary to monitor the actual flux predicted by the soil water model and obviates the need for deriving a relationship between the potential evapotranspiration rates and actual evapotraspiration rates.

At the bottom of the profile (105 cm), the redistribution occasioned by the differences in soil water potential at this depth is assumed to be negligible, hence only the gravitational effect is considered. It is thus assumed that at the bottom of the profile, the potential gradient equals unity. This is in agreement with van Bavel et al. (1968). This latter approximation contracts the Darcy equation to:-

$$V = K(\theta) \qquad (4.8)$$

4.3.3 Selection of Time Step

Rainfall is the most important meteorological factor that affects soil moisture status and it varies greatly with time. It is therefore desirable that when infiltration of rainfall is modelled, time steps of less than one-day be employed. However, the current state of rainfall data collection is commonly on a 24-hr basis and hence it is not feasible for general application to employ a time step that is less than one day.

Interception of rainfall by plants occurs and this process can only be treated if information on individual storm duration and intensity is available (Carbon and Galbraith, 1975). Since this information is not often available, the model presented here utilises the

total daily rainfall and hence assumes that all rainfall infiltrates the soil profile in one time-step. This assumption implies that no surface runoff occurs and that ponding at surface is non-existent.

4.3.4 Initial Conditions and Model Calculation Procedure

As previously discussed, the soil profile is split into ten layers. For each of the layers, initial values of volumetric moisture content are assigned. The daily rainfall values, daily potential evapotranspiration values and the daily actual evapotranspiration rates are given as input data. Soil water characteristic constants and the hydraulic conductivity-wetness relationships as given in equations 4.3 and 4.4 respectively are allocated to each layer.

The soil water potential is calculated for each layer according to the expression given in equation 4.3. The calculation of the layer soil water potential enables the total soil water head to be obtained for each layer according to the following equation.

$$POTH(I) = POTM(I) - DEPTH(I) \qquad (4.9)$$

where POTH = hydraulic head
POTM = matric suction head
DEPTH = distance of layer from soil surface
I = layer number

In utilising the finite difference form of the Darcy equation, the average or weighted values of the hydraulic conductivity between adjacent layers are normally chosen (Carbon and Galbraith, 1975). The arithmetic mean has been known to give realistic results (Wind and van Doorne, 1975), hence the average conductivity is computed thus:-

$$AVCON(I+1) = 0.5(HYC(I) + HYC(I+1)) \qquad (4.10)$$

where AVCON = average conductivity
HYC = hydraulic conductivity calculated according to equation 4.4
I = layer number

The application of equation 4.10 assumes that there is a smooth transition between the physical properties of two adjacent layers.

However, if the layer characteristics are significantly different, serious errors in simulation are likely to occur.

The soil and root hydraulic resistances are computed for each layer that comprise the root zone by using equations 4.6 and 4.7 respectively.

The distribution of soil moisture between the layers is carried out on the basis of a finite difference form of Darcy equation. Thus, neglecting the extraction term, the following expresses the moisture flux between layers.

$$FLW(I+1) = AVCON(I) \times [POTH(I) - POTH(I+1) \mid DIST(I)] \quad (4.11)$$

where FLW = vertical flow of moisture between adjacent layers
DIST = distance between the middle of adjacent layers

The abstraction of soil moisture by the plant roots is calculated by using equation 4.5 for the layers in which the plant roots are confined. Hence:-

$$ABST(I) = [(POTH(I) - POCR) \mid (RS(I) + RR(I)] \quad (4.12)$$

where ABST(I) = abstraction from layer I
POCR = crown potential

The procedure used for estimating the daily crown potential is described in a later section in this chapter.

Having obtained the moisture fluxes between the layers and the extraction of moisture by the roots, the new layer moisture contents are computed thus:-

$$NFLW(I) = FLW(I) - FLW(I+1) - ABST(I) \quad (4.13)$$

where NFLW(I) = net flow of moisture to layer I

The above operations are carried out daily for the simulation period. The flow chart which describes the model operations is shown in Figure 4.3. However for a successful application of the model to evaluate the resistance terms, it is essential to derive daily crown potential values. These latter values are deemed to be the driving

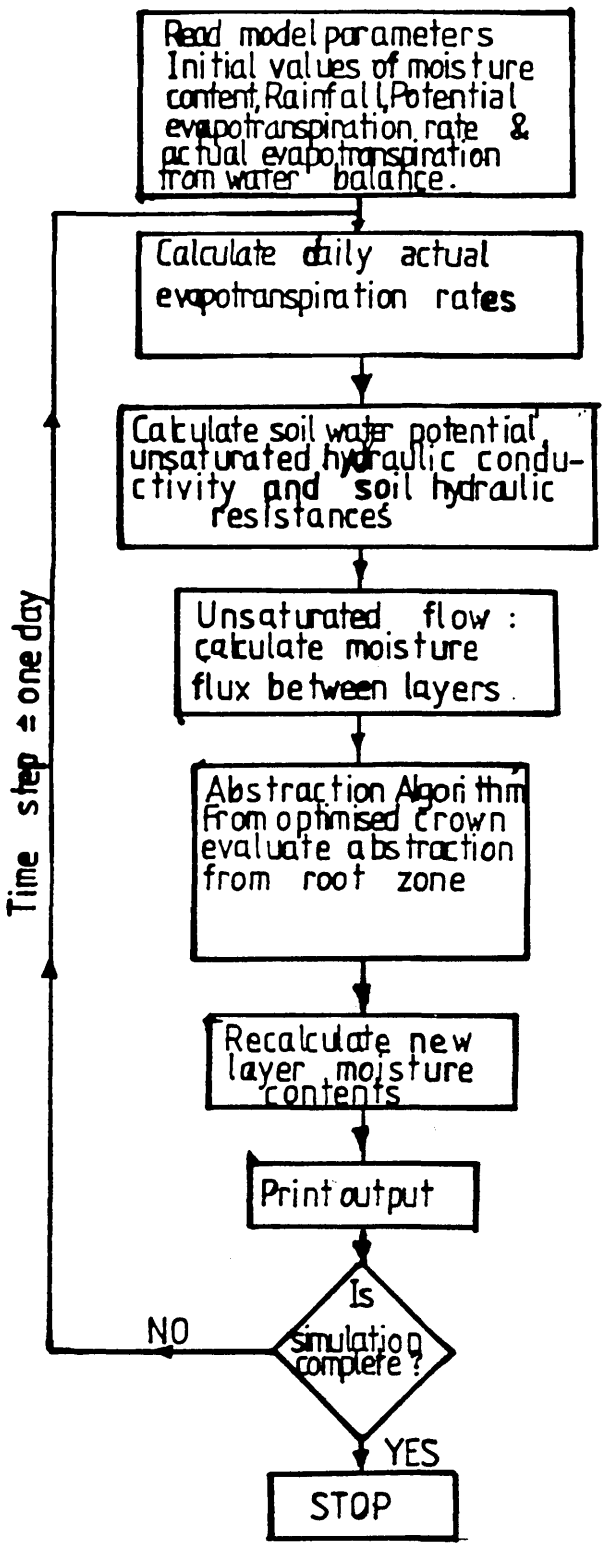

FIG 4·3 FLOW DIAGRAM OF PHYSICAL SOIL WATER MODEL

force for moisture movement from soil to roots. The crown potential in turn is dependent on atmospheric demand. Consequently, the following section describes the optimisation procedure used to search for the appropriate crown potential values.

4.3.5 Optimisation of the Crown Potential

(a) Actual evapotranspiration rates are derived from water balance studies by using the following expression:-

$$AE_i = AE_T \times (PE_i \mid PE_T) \qquad (4.14)$$

where AE_i = daily actual evapotranspiration rate

AE_T = total actual evapotranspiration rate obtained from water balance for the given interval

PE_i = daily potential evapotranspiration rate

PE_T = total potential evapotranspiration rate for same interval as AE_T

(b) Initial volumetric moisture contents for all layers are specified.

(c) The soil water potentials are calculated for each layer according to equation 4.3 and corresponding total soil water head calculated according to equation 4.9.

(d) The initial crown potential is set equal to the total soil water head in the first layer. Hence:-

$$POCR = POTH(1) \qquad (4.15)$$

(e) Specific root hydraulic resistance values are derived using same procedure described in section 7.3.1, and are assigned for each of the three layers comprising the rooting depth.

(f) The soil hydraulic resistance for the three layers as given in (e) above is calculated using equation 4.6.

(g) The redistribution between layers is calculated using equation 4.11.

(h) The daily total root abstraction (TABS) is calculated for three layers thus:-

$$TABS = ABST(1) + ABST(2) + ABST(3) \quad (4.16)$$

(i) The relative difference (DIF) between TABS and AE_i for a particular day is obtained from the following:

$$DIF = (TABS - AE_i) \mid AE_i \quad (4.17)$$

(j) If the absolute difference $\mid DIF \mid$ is less than or equal to 0.01, the crown potential for the given day is set to the current value, otherwise:-

$$POCR = POCR - (DIF \times POCR \times CF) \quad (4.18)$$

where CF is a correction factor set equal to 0.01 (Hillel et al., 1976). The extraction rates are calculated as in step (h) above using new POCR from equation 4.18 until (j) is satisfied.

The optimisation procedure described above allows for the evaluation of the daily actual crown potential that is appropriate to supply the actual evapotranspiration rate. Consequently, it would allow for the comparison of the simulation results with field measured values.

4.4 Limitations and Capabilities of the Physical Soil Water Model

The preceding model description shows that there are limitations in the model operation which can affect the model output. These limitations include:-

(a) The omission of the stomatal control mechanism by which the plant can regulate its transpiration during periods of high demand.

(b) The assignment of a single value to the crown potential. This disregards the potential distribution through the plant system, since the water potential in the leaves may be different from that in the stem.

(c) The portrayal of the root system as possessing a fixed root hydraulic resistance. This fails to consider the variations in root resistance which may be caused by root growth and ageing.

However, despite the above limitations, the model has the following advantages:

(a) Flexibility; the model can allow for the use of any type of root distribution and the imposition of different boundary conditions. The model can also be applied to as many number of layers as desired.

(b) The model can predict the root water withdrawal pattern from different layers and also predict the drainage to deep percolation.

(c) The model allows for the examination of the relative dominance of the respective soil and root hydraulic resistances. In the context of the objective of this study, the model satisfies this requirement.

(d) The model describes the processes involved in root water uptake and soil moisture distribution purely by physical theories which are in agreement with current knowledge of soil-root-atmosphere hydraulics.

4.5 Choice of an Empirically-Based Soil Water Model

It has been shown in a previous discussion in Chapter 3 that actual evapotranspiration can be calculated with a combined aerodynamic and energy balance approach if crop and soil factors are included. These factors require elaborate and sophisticated instrumentation and in some cases field experimentation to evaluate them. Coupled with this is the intrinsic drawback of extrapolating point measurements to assessing areal evapotranspiration losses for a range of field crops. However, the provision of sufficient data using the above approach would entail a network of instruments with back-up personnel which is believed would be beyond the resources of this study.

In the previous chapter, numerical soil water models were reviewed. It has become evident that the adoption of a modelling approach allows the use of a single climatological input (λE) to derive actual evapotranspiration losses for different crops. This advantage obviates the need for laborious and expensive instrumentation. A limitation apparent in the application of most soil water models,

however is the insufficient data available regarding plant physiological response. This latter fact is more acute when sophisticated models that require detailed description of the soil-plant-atmosphere hydraulics are used.

In adopting an empirically-based soil water model, a sophisticated approach cannot be justified if adequate data for the utility of the approach is not available.

Earlier review and discussion have also shown that most empirical models although calibrated for a particular application have not been widely tested and hence lack experimental validation. In the United Kingdom, the model developed by Penman (1949) and subsequently adapted by Grindley (1967) as discussed in Chapter 3 has been widely used. The model is simple and the conceptual framework is flexible, allowing for the adjustment of the drying curve (Goodhew, 1970). Estimates of root constant values for a range of land use are also available (Grindley, 1970). The model is based on potential evapotranspiration estimates which are readily obtained from standard climatic data in the United Kingdom. The major drawback is little experimental validation that exists regarding the assignment of root constant values for different categories of land use. However, the modelling philosophy requires the estimation of soil profile field capacity. This is because the accounting technique provides a direct estimate of soil moisture deficit which is relevant for assessing the irrigation needs of crops and also for assessing the onset of flood conditions.

It is evident from the foregoing discussion that, in using a particular drying curve for validation study, a compromise must be achieved between the number of parameters and the availability of the pertinent data. Models that consider detailed description of soil-plant-atmosphere like that of Rijtema (1965) and Monteith (1965) require considerable data input. The latter is also true for multi-layer models like that of Holmes and Robertson (1959), Baier and Robertson (1966) and that of Makkink and van Heemst (1975). A modelling approach similar to that of Penman (1949) apart from being simple allows for the use of different regulating functions. Evident from postulated drying curves is a threshold point beyond which actual

evapotranspiration (AE) rate falls below the potential evapotranspiration (PE) rate. The way in which AE falls below PE is still controversial. The exponential drying curve is a recent description of the Penman (1949) original empirical drying curve and has been employed by the British Meteorological Office (Calder et al., 1983). A linear depletion rate has been advocated in some cases beyond the threshold point. In order to reconcile the use of different drying curves, it has become an objective of this study to compare the exponential drying curve as utilised by the British Meteorological Office with the constant/linear depletion curve. This will allow for a comparative assessment of the soil moisture deficit simulations of both curves for different crops in the same soil type and climatic environment. It will also enable the validation of the root constant concept regarding the use of fixed quoted values. The description of the empirically-based model operations now follows.

4.6 The Dynamics of the Empirically-based Model

A major consideration in the adoption of the aforementioned model is the significance of evapotranspiration losses in determining soil moisture status prior to precipitation or irrigation inputs. The model assesses both actual evapotranspiration losses and estimates soil moisture status.

The calculation procedure involves the estimation of daily potential evapotranspiration values by using the Penman (1948) formula. The daily potential evapotranspiration values are given as input to the model and a time-step of one day is assumed for model calculation.

A flow diagram of the computer program that executes the empirically-based model is shown in Figure 4.4. The procedure for the assignment of the root constant values is by optimisation. This is discussed fully in a later chapter.

The soil moisture accounting procedure which provides estimates of actual evapotranspiration and soil moisture deficit is carried out for each crop type following the drying curves shown in Figure 4.5. The methodology for obtaining the available water capacity is reserved for later discussion in Chapter 7. The model assumes that the maximum

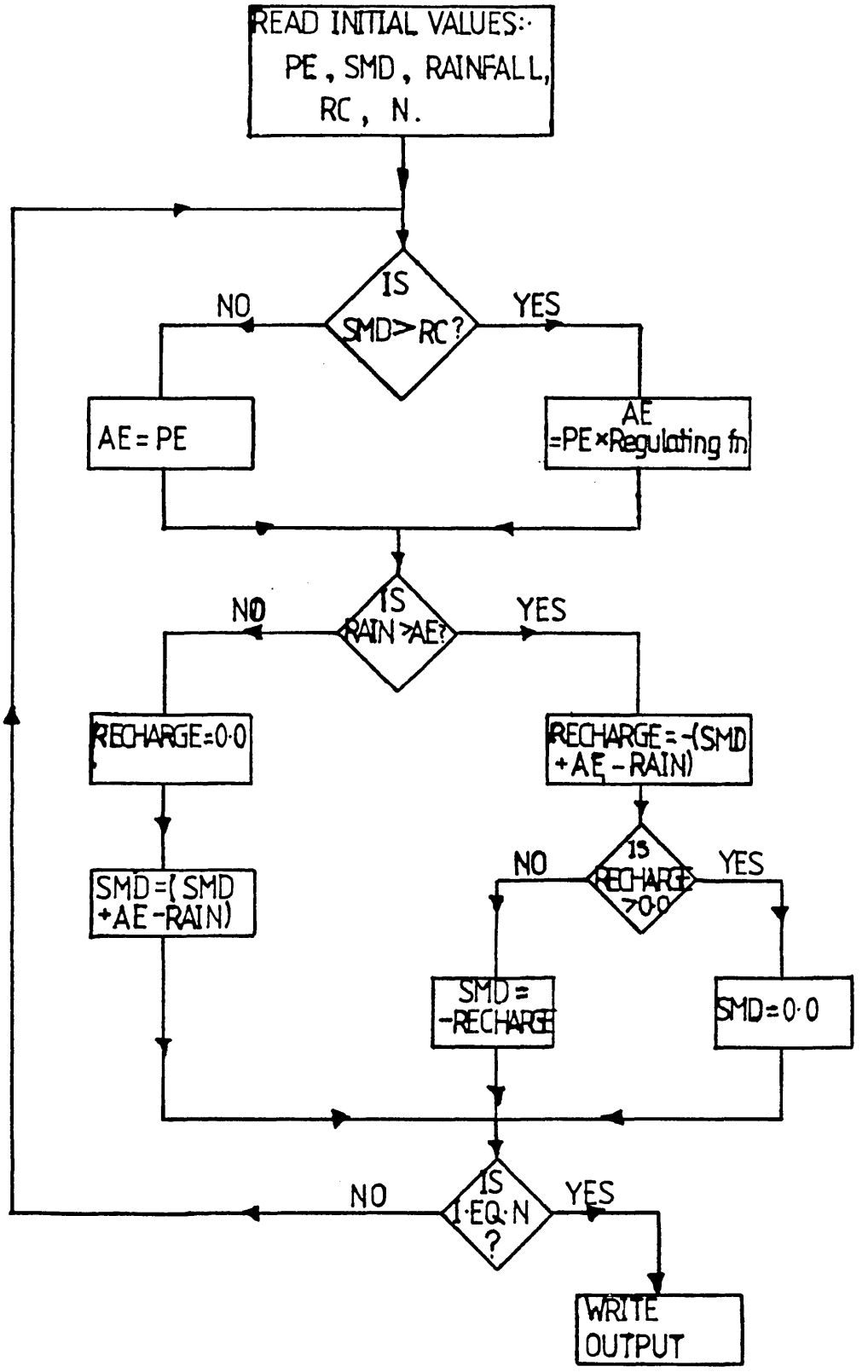

FIG. 4.4 FLOW DIAGRAM FOR CALCULATING SOIL MOISTURE DEFICIT.

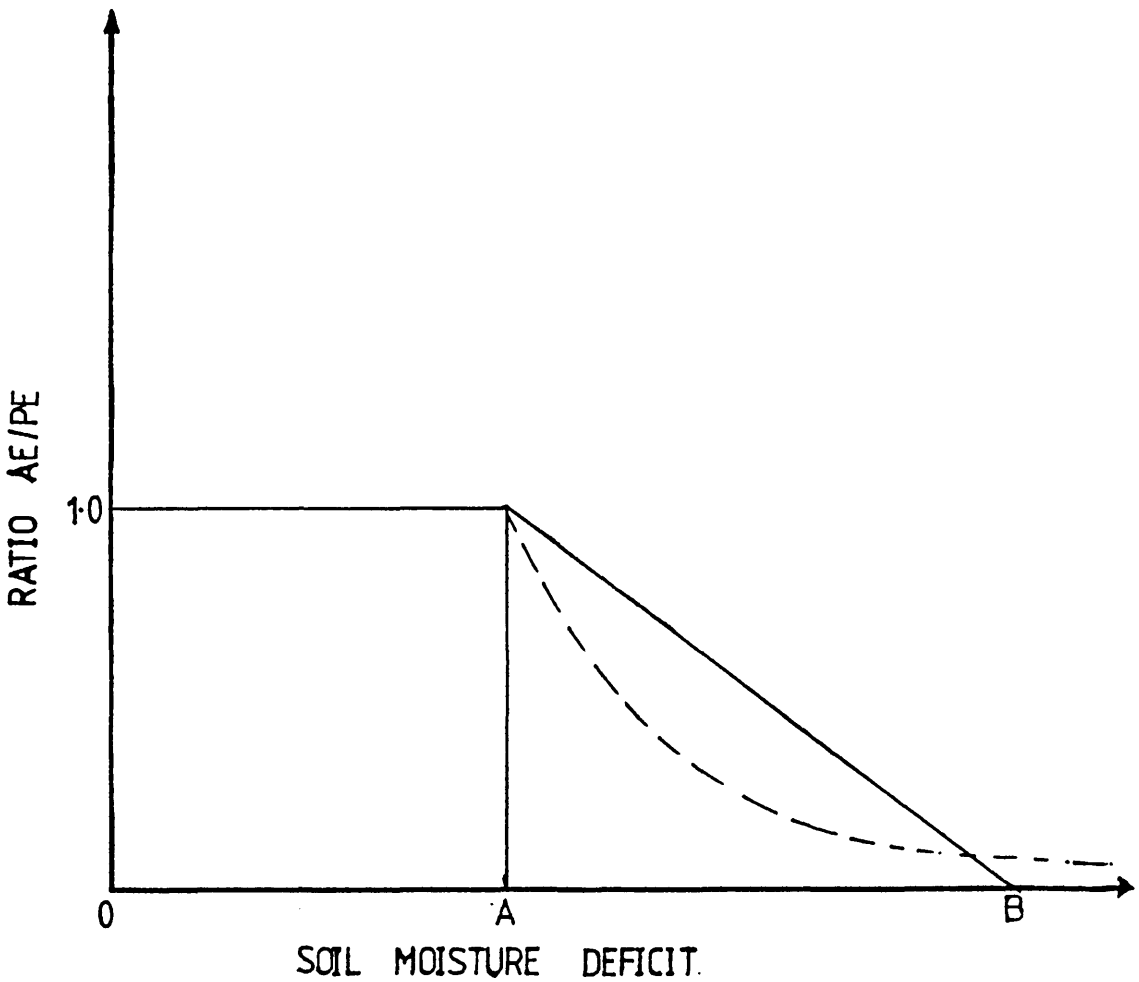

FIG 4.5. REGULATING FUNCTION USED TO DETERMINE ACTUAL EVAPORATION FROM POTENTIAL FOR THE STUDYSITE.

moisture storage is represented by the field capacity. The field capacity is defined as the maximum level of moisture which can be retained by the soil against drainage, so that subsequent moisture input is regarded as passing to runoff or recharge. The moisture level in the model is with reference to field capacity, hence any reduction from field capacity is regarded as soil moisture deficit. Initially, the soil moisture deficit (SMD) is set equal to zero. This latter condition is usually reasonable for the United Kingdom winter conditions when the soil is draining. If the soil moisture deficit is lower than the assigned root constant value, the actual evapotranspiration is set equal to the potential evapotranspiration value, otherwise, the actual evapotranspiration equals the following empirical equation similar to that used by the British Meteorological Office (Calder et al., , 1983):-

$$E = 1.9E_t \exp[-0.6523 \ SMD \mid RC] \qquad (4.19)$$

and $$E = E_t \quad \text{when} \quad SMD < RC \qquad (4.20)$$

where E = actual evapotranspiration
E_t = potential evapotranspiration
RC = root constant
SMD = soil moisture deficit

and alternatively, the equation similar to that of Woodhead (1976) which is linear is also utilised. It is of the form:-

$$E = E_t(1 - SMD/AW) \qquad (4.21)$$

where AW = available water capacity

If the actual evapotranspiration is greater than rainfall, the recharge to deep percolation is set equal to zero and the current soil moisture deficit equals the old soil moisture deficit plus the actual evapotranspiration minus rainfall. This is given as:-

$$SMD(I) = SMD(I-1) + E + R \qquad (4.22)$$

where I = current day number
R = rainfall

If the actual evapotranspiration is less than rainfall, the recharge is given by:-

$$\text{Recharge}(I) = R - SMD(I-1) - E \qquad (4.23)$$

The recharge can either be negative or positive depending on the current level of soil moisture deficit. If the recharge is greater than zero, the current soil moisture deficit is set to zero, otherwise, current soil moisture deficit equals

$$SMD(I) = - \text{Recharge}(I) \qquad (4.240$$

The two forms of the regulating functions, used in determining actual evapotranspiration from the potential evapotranspiration values for this study are shown in Figure 4.5.

4.7 Conclusions

The foregoing discussion highlights the factors governing the adoption of a physically-based soil water model and empirically-based soil water models for performance testing in this study.

The limitations and capabilities of the physical soil water model have been shown. The empiricisms inherent in most of the currently available computational techniques for estimating actual evapotranspiration from climatic data are noted. As such the preference of the author for conceptual model approach is indicated.

CHAPTER 5

FIELD EXPERIMENTATION TO MONITOR SOIL MOISTURE AT SILWOOD PARK

5.1 Introduction

The discussion in the preceding chapter centred on the operational dynamics of adopted physically and empirically-based soil water models. In order to validate the physical soil water model, it is essential to evaluate relevant hydraulic parameters. These parameters are the unsaturated hydraulic conductivity - wetness relationship and the soil moisture characteristics of the specific study site. Alternatively, if the measurements of soil moisture content and water potential are available, inference of the hydraulic parameters can be made given known boundary conditions.

Widespread application of previously published models has been limited by a paucity of data regarding the above flow parameters. This is because the generation of field data on soil moisture content and soil water potential entails laborious and time consuming instrumentation which is a prerequisite for high quality field data. It was therefore believed that an investigation of the local soil moisture response in the study site was essential to confirm the validity of the adopted models.

Field experiments to monitor soil moisture content and soil water potential under different agricultural crops exhibiting different rooting habits were carried out. The latter was necessary for calibration of the soil water parameters and for subsequent comparison with simulated soil moisture contents.

Consequently, this chapter describes the techniques that were employed for the *in situ* determination of soil moisture content and soil water potential profiles under the different crops in the experimental area. It also describes the experimentation carried out and the factors governing the choice of the test crops for the period 1980-1982 at Silwood Park, near Ascot in Berkshire, England.

5.2 Soil Moisture Measurement Techniques

There are several techniques available for the assessment of soil moisture response under field conditions. These techniques are categorised into two, the assessment of soil moisture content and the assessment of soil water potential.

Techniques in the first category enable the quantitative estimation of the total soil moisture in the profile. They also allow some qualitative estimation of moisture movement, when variation of moisture content with depth is considered for sequential profiles (McGowan and Williams, 1980). On the other hand, the determination of soil water potential allows the definition of potential gradients (Wellings and Bell 1980), thus giving the direction of moisture movement. The latter enables the separation of evapotranspiration and drainage components of the soil profile under certain conditions.

Whatever technique is employed, a comprehensive description of soil moisture response requires both moisture and tension data, although valuable information can be obtained from either independently.

5.2.1 Moisture Content Measurement

5.2.1.1 Gravimetric Technique

This is the simplest method of determining soil moisture content (Reynolds, 1970). The basic principle involves oven drying of a soil sample at $105^{o}C$ until constant weight is obtained. The method does not require expensive apparatus and produces an absolute value of moisture content. The disadvantages of this technique include: (i) the difficulty of obtaining representative moisture values in a heterogeneous soil profile, (ii) the technique is site destructive, this is because many samples are needed over long periods of time to monitor moisture movement, (iii) the soil profile is non-reproducible. Despite these limitations, the technique offers the most reliable standard against which other soil moisture determination techniques are calibrated.

5.2.1.2 Electromagnetic Technique

This involves the measurement of the variation of the soil electrical properties as induced by changes in soil moisture content. Schmugge et al. (1980) give a detailed description of the technique. The technique relies on the magnetic properties of soil particles and soil water. It consists of sensors which are responsive either to resistivity, capacitance or both. The sensors are placed at desired soil depths and careful calibration is required to give absolute values of soil moisture content. Although the technique is precise, it suffers from long-term unreliability as the calibration curve is influenced by the ionic concentration of soil water. This latter point and the high cost of the readout devices/interfaces have probably influenced the lack of widespread application.

5.2.1.3 Nuclear Technique

This involves the emission of radioactive materials into the soil and can be subdivided into two classes:-

(a) Gamma Ray Attenuation:- This relies on the principle that the scattering and absorption of gamma rays from a radioactive source are related to the soil density along their path (Ferguson and Gardner, 1962; Davidson et al., 1963). The changes in soil density are associated with moisture content changes hence the moisture content is determined from the soil density change. The method is suitable for smaller depth integrals than the neutron probe technique discussed in the next section. It also has the following advantages: (i) the system can be interfaced to accommodate automatic recording, (ii) the measurement is non-destructive. The system however has the following disadvantages: (i) it requires two tubes to be very precisely located in parallel which is difficult to achieve in the field, (ii) spatial resolution in stratified soils is difficult to achieve. This is a consequence of large variations in bulk density and moisture content.

(b) Neutron Scattering:- This revolves around the principle that high energy neutrons emitted from a radioactive source are effectively slowed down by the hydrogen nuclei in the soil.

The number of slowed neutrons is monitored by a sensor placed adjacent to the source. Soil water has a preponderance of hydrogen ions, hence there exists a relationship between slowed neutrons and soil water content. The neutron probe is the most widely used of the nuclear scattering techniques, and its installation, calibration and operation has been described by Bell (1976).

Essentially, the radioactive source emits fast neutrons radially into the soil which are moderated by hydrogen nuclei. In wet soil the emitted neutrons are slowed down before they get far from the source. Thus in a wet soil the density of slow neutrons surrounding the probe will be greater and will extend a shorter distance from the source, and vice versa for dry soil. It is therefore obvious that the calibration of the neutron probe must be carried out in order to account for the inherent variations which occur in field soils. Generally, there are three ways in which calibration can be carried out, theoretical calculations, laboratory experimentation and field measurements (Bell, 1976).

The effects of bulk density and soil chemical composition on the probe calibration have been studied by several workers (Lawless et al., 1963; Olgaard, 1965). Olgaard (1965) showed that a theoretical calibration can be obtained purely from soil analysis. The use of theoretical curve is generally not recommended because extensive and sophisticated chemical analysis is required. The results obtained must then be adjusted to account for bound water in the soil matrix.

Laboratory calibrations are normally performed in large drums where actual moisture content can be controlled and accurately measured. This is suitable for soils which are texturally and chemically homogenous and which can be repacked to reproduce their natural field situation. This latter technique is suitable for sands and gravels but cannot be applicable to highly structured soils.

The field calibration technique is the most commonly adopted procedure for calibrating the neutron probe. This procedure, according to Bell (1976), involves installing additional access tubes and obtaining a calibration by taking a number of undisturbed soil samples as close as possible to the tubes. The technique is site

destructive and if calibration data are required for specific depths, new access tubes must be installed. It is apparent that the technique is tedious and time consuming. In practice, calibration points are accepted where moisture content is invariant over a depth interval of 30-40 cm, or where there are linear changes with depth of moisture content over such an interval (Wheater, 1977). This latter fact adds a limitation to the number of calibration points that can be obtained from a given access tube.

Apart from the need for a bulk calibration for the neutron probe, there is the added complication of estimating surface effects. This is occasioned by the spherical emission of neutrons from the source. In effect, this means that the probe must operate within a finite sphere. This sphere is variable and depends on the soil moisture content. As a result, when the probe approaches the soil surface, a proportion of the emission is lost. It is apparent therefore that the shape of the moisture profile at the surface is signficant. This is because the relationship between the proportion of emission lost and depth is non-unique. In order to obtain the surface effect on the calibration curve surface measurements obtained at wet and dry ends of the soil moisture content can be used to define a surface calibration (Wheater, 1977). On the other hand, extension trays in which equivalent surface materials are packed can be placed over the access tube to remove the air interface while readings are taken (Bell, 1976). This procedure has the inherent difficulty of maintaining the tray at natural moisture levels, but theoretical adjustments are also unsatisfactory. Theoretical adjustments often involve the displacement and orientation of the calibration line which in general is dependent on the range of moisture content considered. It is evident that the preceding surface calibration techniques have inherent drawbacks. Hence, for this study a separate surface calibration is carried out. This involves installing a number of 40 cm long access tubes and obtaining a calibration, by taking a number of undisturbed soil samples at 10 cm depth, over a range of moisture contents.

The relationship used in expressing the neutron probe calibration is of the form

$$R = m\theta + C \qquad (5.1)$$

where R is the slow neutron count rate in the soil, m and C are constants while θ is the moisture volume fraction. However to prevent age drift, the linear calibration normally used is of the following form

$$R/Rs = m\theta + C \qquad (5.2)$$

where Rs is the standard count rate in water and m and C are constants different from those above.

The use of Rs ensures continuity of records and removes, apart from the age drift effect, the effects due to the following:-

(1) Repair of the probe which can lead to a different sensitivity.

(2) The use of more than one probe, since no two probes have exactly the same count rate. Water is normally used above any material as a standard because it is cheap and has no unpleasant characteristics (Bell, 1976).

The use of the neutron probe is however affected by random error occasioned by the randomness of radioactive decay. Normally, ratemeters or ratescalers are used for counting slowed neutrons. This count is displayed in digital form and is normally the mean count rate obtained over a preset 16 or 64 second integration time. The number of counts (N) recorded in a given time interval is expected to follow a normal distribution. Hence the standard deviation (σ_n) is given by:-

$$\sigma_n = N^{\frac{1}{2}} \qquad (5.3)$$

The count rate, R = N/t, where t is the counting time. The standard deviation of the count rate σ_r (actual digital reading obtained) is given by :-

$$\sigma_r = (R/t)^{\frac{1}{2}} \qquad (5.4)$$

Equation (5.4) shows that the larger the reading, as obtained from a wet soil, the larger the error. Hence the longer the counting time, the smaller the error.

5.2.2 Soil Moisture Potential Measurement

5.2.2.1 Tensiometer

This is an instrument used for measuring the soil water potential (Richards and Gardner, 1936). Essentially, it is composed of a liquid filled porous ceramic cup connected by a continuous liquid column to a manometer, vacuum gauge or pressure transducer. The soil suction removes water from the cup and produces a drop in the system's hydrostatic pressure which is then displayed on the manometer or gauge. The disadvantages of this method are that high tension readings are outside the range of the instrument which normally operates below 0.9 bars. Above 0.9 bars, the readings become erroneous and non-reproducible (Cooper, 1980). In the United Kingdom, surface readings can be lost in dry conditions.

The second limitation relates to the time lag of tensiometer response to soil suction changes. This lag is caused by (a) the hydraulic resistance of the cup and the soil in contact with it, (b) the sensitivity of the pressure measuring device. This latter point is given further consideration by Cooper (1980) who found that when tensiometers are close to the limit of their operational range, the readings rise rapidly after de-airing and then become steady after 2-3 days. Thereafter they decline until the next de-airing. De-airing is the flushing out of air bubbles also known as purging.

5.2.2.2 Porous Blocks

In common with the electromagnetic technique discussed above, the variation of the electrical resistance of porous blocks and moisture content changes offers another possibility for the indirect measurement of soil moisture potential. This procedure utilises nylon or gypsum blocks (Bouyoucos and Mick, 1948) buried in the soil which equilibrate with soil suction rather than with soil moisture content.

The calibration of the porous blocks involves the use of a pressure plate apparatus in which a predetermined suction is applied on a moist block. This moist block is embedded in a "representative" soil sample until equilibrium moisture content is attained. The blocks are cheap, simple to use and operate effectively at high suctions above that of the tensiometer range. They however have poor

sensitivities at low tension. The technique is useful in augmenting tensiometer readings in dry conditions. The major disadvantages of the porous blocks are (i) deterioration of the blocks in the long term, (ii) sensitivity to soil water salinity which affects the calibration curve, and (iii) individual calibration of the blocks are required which is time consuming.

5.2.3 Remote Sensing

This technique employs electromagnetic energy reflected or emitted from the soil surface (Schmugge, 1978). The approach includes (i) thermal infrared radiation which measures the diurnal range of surface temperature or measures the crop-canopy air temperature differential, (ii) microwave, based on the dielectric properties of the soil and measures the backscatter coefficient or the thermal emission from the soil surface.

A major disadvantage is that the surface condition only is sensed. Schmugge *et al.* (1980) presents a full review of the technique but it is evident that current methods are not yet fully developed or widely used.

5.3 Choice of Soil Moisture Measurement Techniques

For the purpose of the present field study, the readings of both moisture content and soil water potential are required. This is because both readings are necessary for the determination of the soil moisture characteristics and for the subsequent comparison with model predictions of the adapted soil water models. Furthermore, in the estimation of simple water budgeting techniques, the changes in soil moisture levels are necessarily coupled with the direction of the soil moisture movement. The soil water potential readings enable the definition of the latter. As a consequence, it is essential to utilise a non-destructive method to monitor changes in the soil profile with time. The neutron probe appears to offer the best approach for a complete profile description of soil moisture with a single instrument and the readings obtained integrate a given volume around the depth of measurement, i.e. are spatially representative. The only component left on site are a few access tubes which are robust and cause minimal inconvenience to normal cultivation practices. It is apparent there-

fore that the neutron probe has major advantages and it was therefore adopted for soil moisture determination. On the other hand, the mercury manometer tensiometers have the advantages of being easy to design and construct, cost relatively little and can provide information on temporal changes of soil moisture movement under saturated and unsaturated conditions. They also can normally be placed in the soil easily with little disturbance. Hence, the latter technique was employed for the measurement of tension readings in this study. However, because of the limited range of operation of the tensiometers, it became necessary to augment the manometer readings. Gypsum blocks were subsequently used as the augmenting technique.

5.4 The Field Experiments

5.4.1 Experimental Area

The experimental area is shown in Figure 5.1. It is located at Silwood Park, 40 km south west of London. It lies on lat. $51^{o}28'$N and it is about 220' above mean sea level.

The soil at the site belongs to the Fyfield series of typical argillic brown earths (Soil Survey of England and Wales, 1983). Efforts were made to dig a profile pit (1 m × 1.8 m × 1.6 m). A discussion of the result given in a later section showed that the profile soils are sandy brown earth with some restriction of subsoil permeability, caused by podsolisation below 1.2 m. This latter observation indicates that capillary rise may be important in these soils.

Generally, the experimental area has been used as a field station by Imperial College and a wide range of agricultural crops are grown.

5.4.2 Particle Size Analysis

The size distribution of soil particles affects the hydraulic characteristics of the soil. As such particle size analysis down the profile was carried out by using the Bouyoucos hydrometer method on samples obtained from locations shown in Figure 5.2.

Five soil samples were collected at each of different soil depths by using soil augers. The depths considered were 0-10, 10-20,

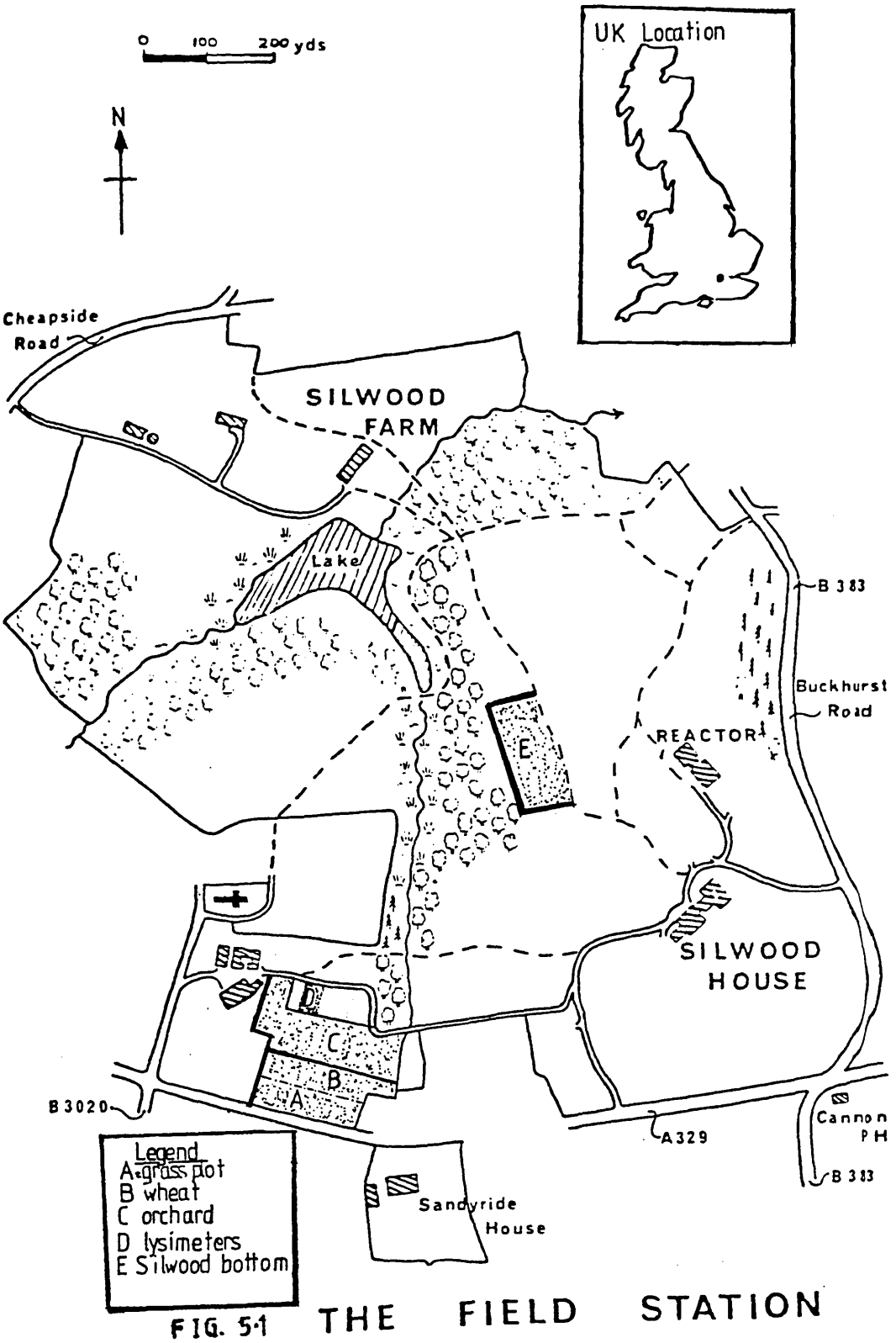

FIG. 5-1 THE FIELD STATION SILWOOD PARK

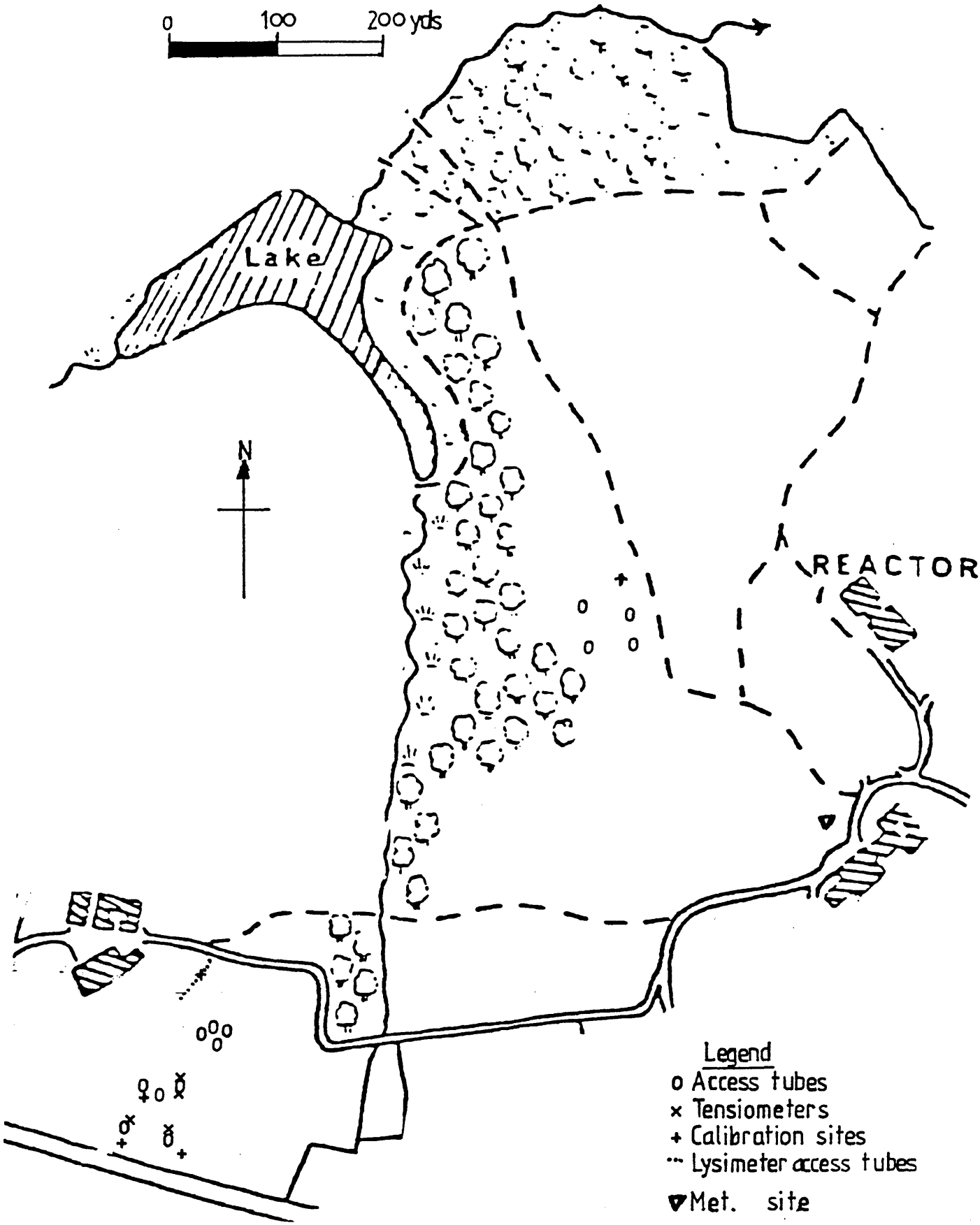

Fig. 5.2 Instrument network

20-40, 40-60, 60-80, 80-100 and 100-120 cm depths. The samples were air dried and broken with a pestel and mortar, and passed through a 2 mm sieve. From the samples, 50 gms were put in a 500 ml dispersion cup to which was added 200 ml distilled water and 15 ml 0.5 N sodium oxalate. This was allowed to soak for 15 mins before dispersion with a mechanical baffle for 10 mins. The soil suspension was transferred to a 1000 ml sedimentation cylinder and made up with distilled water to the 1000 ml mark. The cylinder was then vigorously shaken and allowed to stand.

The Bouyoucos hydrometer was used to obtain a reading at 5 min of silt and clay as g/litre. The cylinder was shaken and after 2 hrs a second reading obtained of clay only. The contents were then poured through a 0.20 mm sieve, to obtain the coarse sand component. The fine sand was then calculated as a residual.

A temperature correction of 0.3 g/litre was made for each degree above 20^{o}C and a zero correction for the hydrometer made by floating it in distilled water plus 15 ml 0.5 N sodium oxalate.

The average values of the physical properties are shown in Table 5.1. The particle size analysis show that the soil is composed predominantly of sand. This indicates that the hydraulic conductivity of the soils may be high, especially if soil is wet; since water flow will be predominantly through the larger pores.

5.4.3 The Soil Profile

Table 5.1 shows the change in texture down the profile obtained at locations indicated in Figure 5.2. This change shows the surface soil to be a loamy sand which graduates to a sand down to 100 cm, where the soil changes to a sandy loam. At 1.2 m, the soil changes to a sandy clay loam. Also shown in Table 5.1 are the coefficients of variation associated with the sand, silt and clay fractions. It is apparent that the clay fraction shows high coefficients of variation ranging from 12.9 to 77.5 percent. On the other hand, the fine sand fraction has low coefficients of variation ranging from 2.6 to 6.6 percent.

TABLE 5.1 : Average values of soil physical properties

Para meters	Depth (cm)	Coarse Sand 2-0.2 mm %	Fine Sand 0.2 0.02 mm %	Silt 0.02-0.002 mm %	Clay 0.002 mm %	Bulk Density g/cm^3
μ		25.6	62.0	6.4	6.0	1.54
σ	0-10	4.4	2.0	1.3	1.4	0.60
cv		17.2	3.2	20.3	23.3	39.1
μ		18.0	64.0	14.0	4.0	1.56
σ	10-20	2.5	2.2	2.9	1.1	0.13
cv		13.8	3.4	20.7	27.5	8.3
μ		12.6	65.4	18.0	4.0	1.60
σ	20-40	4.4	2.3	2.5	1.6	0.04
cv		34.9	3.5	13.3	39.5	2.3
μ		13.0	67.0	18.0	2.0	1.56
σ	40-60	2.2	1.7	1.9	1.5	0.17
cv		17.2	2.6	10.5	77.5	10.9
μ		12.3	65.7	16.0	6.0	1.44
σ	60-80	2.8	2.5	2.7	3.0	0.20
cv		22.9	3.7	16.5	50.2	13.8
μ		12.0	64.7	13.3	10.0	1.42
σ	80-100	3.2	3.5	2.5	2.3	0.42
cv		26.1	5.4	18.6	23.0	29.5
μ		2.0	67.5	8.5	22.0	1.48
σ	100-120	1.1	4.5	1.8	2.8	0.19
cv		54.8	6.6	21.0	12.9	12.8
μ						1.56
σ	120-140	-	-	-	-	0.24
cv						15.4

μ = mean of the sample population
σ = standard deviation
cv = coefficient of variation (percent)

Although the profiles are basically sandy, they are found to be non-uniform. This is also evident from the inspection of one of the soil profiles (Figure 5.3) by means of a pit which gave qualitative results. The surface layer down to 35 cm was black, indicating the presence of organic matter. It was hard to dig. However between 65 cm and 100 cm, the soil was yellow and much easier to dig. Below 120 cm, the soil was a patchy red and grey colour and was very hard to dig. Stones were encountered at varying degrees down to 100 cm especially in the surface layer and between 65 cm and 85 cm layers.

A summary of the profile is given in Figure 5.3.

5.4.4 The Field Crops

A range of crops was selected to investigate the relative water use and pattern of soil water depletion for different crops in the same soil series and climatological regime.

Five of the commonly grown crops in the study area were utilised as the test crops. The choice of these crops was governed by the rooting characteristics and whether they were annuals or perennials. The latter would afford insight into extraction patterns of the crops throughout the year. The crops used were wheat (spring and winter varieties), permanent grass, field beans, cabbage and an apple orchard. The apple orchard was well established, having been on site since 1963 (Rutter, personal comm; 1980). The other crops with the exception of permanent grass were annuals. The field beans and cabbage followed each other in a crop rotation at Silwood bottom (Figure 5.1). The other crops lie across the same slope (Figure 5.1). The plot sizes vary but were at least 75 m × 75 m in the wheat plot to 125 m × 75 m in the apple orchard. In addition to the field sites, nine drained lysimeters of 2 m^2 area and 0.8 m depth continuing the same soil series as under the field crops were put to rye grass in May 1980. Three treatments replicated three times were imposed on the lysimeters to monitor soil moisture response to natural precipitation, irrigation and drought conditions. This was to evaluate the effect the different moisture regimes would have on the relative disposition of actual evapotranspiration rate to the potential evapotranspiration rate and hence aid the evaluation of model parameters.

Depth (cm)	Ease of Digging	Texture Class	Stoney Nature	Colour
0				
	Hard	Loamy sand	A lot of stones	Very dark
35				
	Soft	Sand	A few stones	Dark
65				
	Soft	Sand	A lot of stones	Yellow, patches of white
85				
	Soft	Sand	A few stones	Yellow, patches of white
100				
	Hard	Sandy loam	No stones	Yellow, patches of white
120				
	Very hard	Sandy clay loam		red and grey patches

Figure 5.3 : Summary of soil profile

Table 5.2 gives the planting and harvesting dates associated with some of the field crops during the period of this study.

TABLE 5.2 : Planting and harvesting dates 1980-1982

Crop	Year	Planted	Harvested
Spring Wheat	1980	23/ 4/80	17/ 9/80
Winter Wheat	1980/1981	11/11/80	26/ 8/81
Summer Wheat	1981/1982	9/11/81	27/ 8/82
Field Beans	1980	22/ 4/80	15/ 9/80
Field Beans	1981	8/ 4/81	10/ 9/81
Field Beans	1982	13/ 5/82	15/ 9/82
Cabbage	1980	28/ 5/80	6/10/80
Cabbage	1981	1/ 6/81	20/10/81
Cabbage	1982	4/ 6/82	2/11/82

5.5 Instrumentation

5.5.1 Access Tubes

A number of access tubes were installed in the field plots under the crops discussed above. These access tubes were constructed from aluminium alloy tubing, with 44.5 mm outside diameter, 41.25 mm inside diameter and 1.6 mm wall thickness. The installation of the tubes was carried out following the procedure given by the Institute of Hydrology (Bell, 1976). The number of access tubes installed represented a compromise between the number of crop sites that could be monitored in a day using the neutron probe and the representativeness of the access tube location in the respective plots.

The access tubes installed were generally 1.8 m long and about 150-300 mm of the tubes were allowed to protrude from the soil surface. This effectively provided soil moisture profiles down to about 1.5 m. The relative distribution of the access tubes are: three tubes in the wheat plot, four in the orchard, two in the permanent grass, two in the cabbage, two in the field bean plot and nine in the lysimeters. The access tubes location is shown in Figure 5.2.

5.5.2 Tensiometers

Apart from access tubes, duplicate sets of mercury-manometer tensiometers were installed in the permanent grass and wheat plots. The tensiometers were installed 50 cm from each access tube in the permanent grass crop at depths 10 cm, 20 cm, 30 cm, 40 cm, 50 cm, 70 cm, 90 cm, 110 cm, 130 cm and 150 cm. The depths in the wheat are 10 cm, 20 cm, 30 cm, 40 cm, 60 cm, 80 cm and 100 cm. The depth intervals were increased at deeper layers as a compromise between the number of tensiometers that can be made and the magnitude of flux changes in the profile since all the tensiometer sets were constructed by this author with the assistance of a colleague. The 50 cm distance from the access tubes of the tensiometer sets was believed to be far enough not to interfere with the moisture readings and yet close enough to monitor the same soil mass. The reasons for duplicate sets are to ensure that at least one full set of tensiometers was always working adequately and to minimise any unnoticed instrument or reading errors and also to indicate spatial variation. To prevent missing data during extremely dry conditions, gypsum blocks were installed at depths of 10, 20, 30, 40 and 50 cm respectively in the wheat and grass plots. These depths are believed to be the depths where tensiometers may fail to respond in very dry conditions. The location of the tensiometers are also shown in Figure 5.2.

5.5.3 Weather Station

The monitoring of soil moisture content entails that precipitation input and other climatic variables which affect moisture loss be measured. In the field station, there is a meteorological site at which daily rainfall, temperature and humidity data are collected. Windspeed and radiation data are not collected. The meteorological site is within 500 m of all instrumented plots. An attempt was made to install a rain gauge on the lysimeter site. However the frequency of the rainfall readings in the latter, once a week, made the use of the rainfall data impracticable because they were affected by evaporation losses. Hence, the daily rainfall data from the field station's meteorological site was used for all analysis in this study. Temperature (wet and dry bulbs), windspeed, and sunshine hours data were obtained from the British Meteorological Office for the

Easthampstead site (Grid Reference SU865677) a distance of about 10 km from the experimental area.

5.6 The Neutron Probe Calibration

The Wallingford neutron probe was employed for monitoring soil moisture content in this study. The probe has a ratescaler and gives a reading of observed count rate over a 16 or 64 second time interval. The instrument is shown in Figure 5.4. The radioactive source of fast neutrons is Americium-Berylium and the detector is a boron trifluoride proportional counter (Bell, 1976). As discussed earlier in Section 5.2.1.3, the calibraton of the probe was carried out for both bulk and surface soil profiles. Consequently, the neutron probe described above was calibrated in the field as follows.

5.6.1 Bulk Calibration

This calibration was obtained for soil profile depths greater than 20 cm. For this purpose, a total of five additional access tubes were installed in the field sites (Figure 5.2). Gravimetric samplings were carried out on one access tube at a time, spanning a range of conditions in conjunction with the neutron probe. The samplings involved using a cylindrical sample core of size 6 cm × 3.3 cm diameter. On each sampling occasion, six soil core samples from 10-15 cm around the access tube for a given depth in which uniform moisture profile was located were obtained. The mean of the gravimetric results of the six soil samples from the given depth was converted to moisture volume fraction and plotted against neutron probe counts simultaneously obtained during sampling. The neutron probe counts were normalised by the standard count in water. The latter involved obtaining a probe count in water by using a plastic container (50 cm deep × 60 cm diameter) filled with water. Inserted in the middle of the container was an access tube sealed at the bottom. The neutron probe was lowered down the access tube and count rate reading over a 64 sec time interval was carried out. This was repeated ten times and the mean of the ten count rate readings was designated the standard count in water. The standard count in water was repeated four times during the experimental period. This showed very little variation. The values obtained ranged between 966 and 977 counts with a coefficient of variation of 0.32%, the average standard count in water used was 972.0.

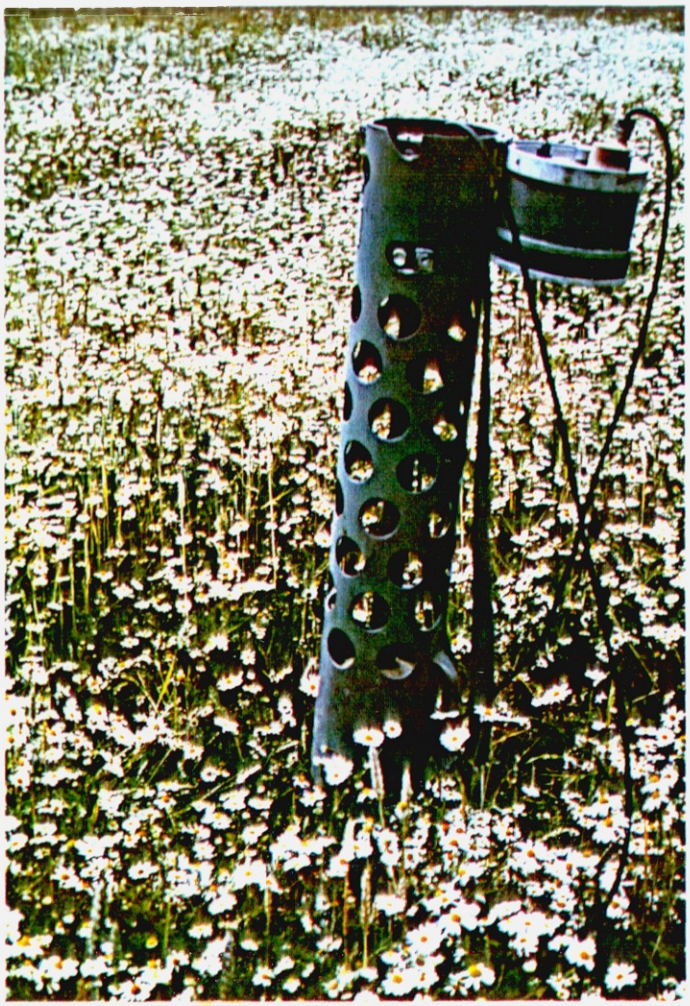

Fig. 5.4 The Neutron Probe

The plot of the bulk calibration from depths of 20 cm and below is shown in Figure 5.5. A linear regression on the data gave reasonable correlation coefficient of 0.87. This demonstrates that there is little variation in soil moisture characteristics in the different field plots. It therefore indicated that the technique used for sampling was satisfactory.

In the United Kingdom, the Institute of Hydrology (Bell, 1976) have used the Wallingford probe extensively over a range of soils. Their study showed that there was little variation over the entire range of soils (Figure 5.6). A comparison of their calibration curve for a comparable soil type as that of the study site shows the IH equation as:-

$$\theta = 0.79\ R/Rs - 0.024 \qquad (5.5)$$

while in this study, the calibration obtained is

$$\theta = 0.63\ R/Rs + 0.051 \qquad (5.6)$$

where θ is the moisture volume fraction and R/Rs is the count ratio.

The preceding implies that the Institute of Hydrology curve, equation 5.5 will give a calculated soil moisture content that is 11.98% higher than the soil moisture content obtained from the derived site calibration. This latter implication emphasises the need to carry out specific site calibrations especially in studies where absolute values of moisture content are desired. As a result of the good correlation coefficient obtained from the site data, the calibration curve derived in this study, equation 5.6 was used to interpret the neutron probe count rates obtained in this study at 20 cm and below.

5.6.2 Surface Calibration

This was applicable to the 0-20 cm layer in the field site. The procedure used involved the installation of nine 40 cm long access tubes at different locations in the field site. The method of sampling was similar to that used for the bulk calibration section 5.6.1, except that sampling was at 10 cm depth. For each calibration point, six known volume cores were taken around the tube at 10 cm depth; and precise count rates obtained, taking an average of ten 64

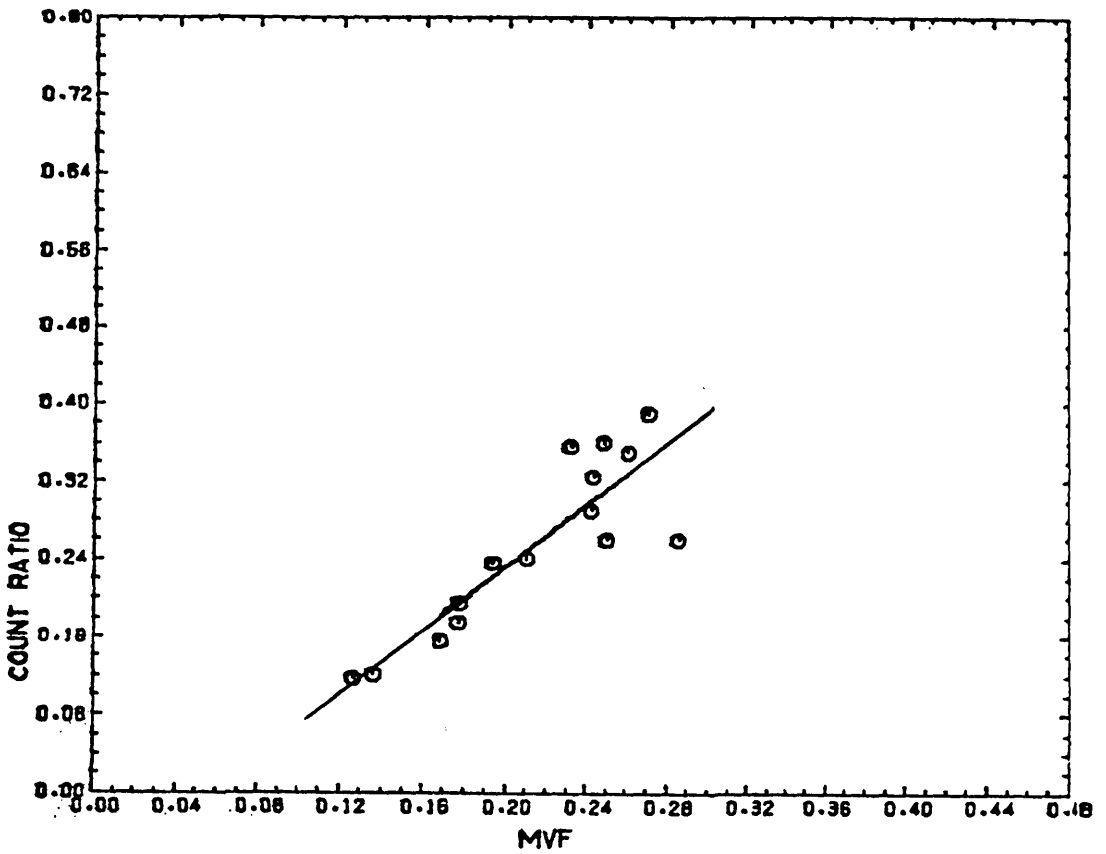

FIG. 5.5 NEUTRON PROBE BULK CALIBRATION CURVE

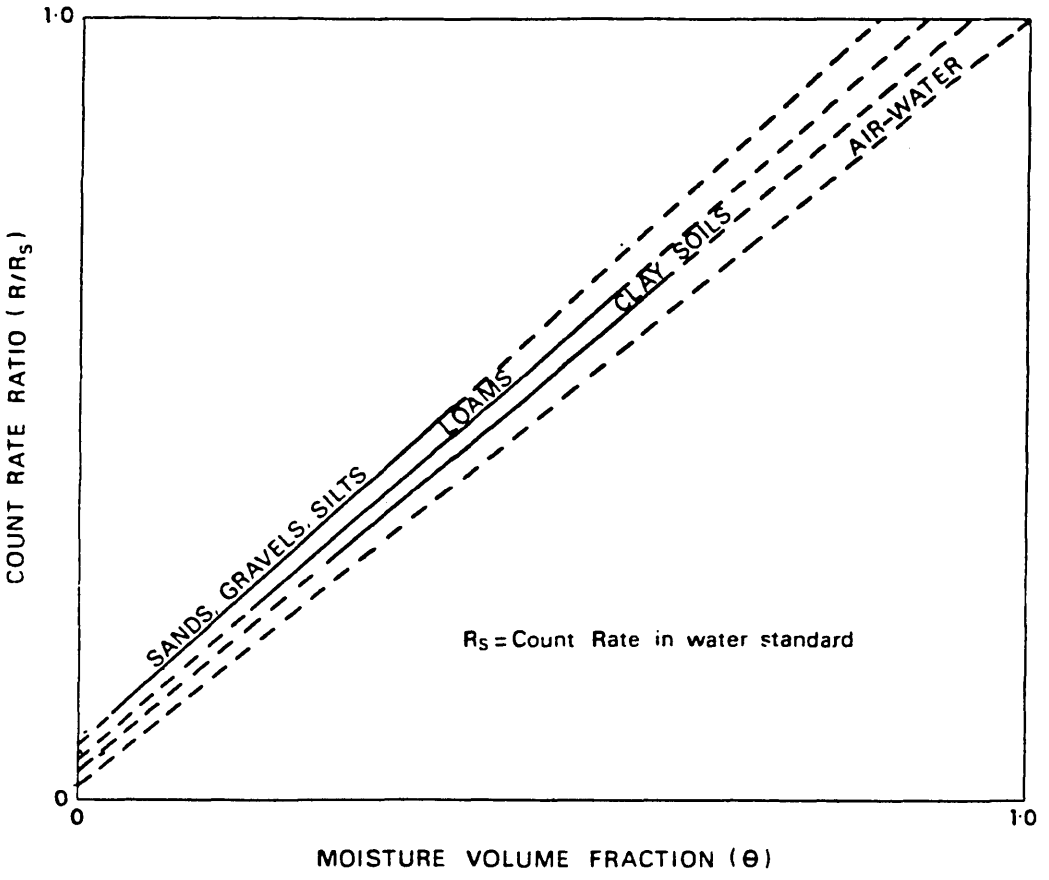

FIG. 56 INSTITUTE OF HYDROLOGY CALIBRATION CURVES (After Bell, 1976)

second integration time readings. The plot of the neutron probe count rates normalised by the probe count in water is shown in Figure 5.7. The coefficient of correlation is 0.93. This shows that for the soil moisture range measured in the field, the technique adopted for the surface calibration proves adequate. The linear regression equation for the surface soil as derived is given thus:-

$$\theta = 1.25\ R/Rs - 0.05 \qquad (5.7)$$

where θ and R/Rs is as defined in equation 5.6. Equation 5.7 was used in this study for interpreting surface neutron probe data.

A comparison of both derived surface and bulk calibration curves shows a steeper gradient for the surface than obtained for the bulk soil. As such for a given count ratio, the surface soil has a higher level of moisture content. This is expected since a proportion of emitted radiation is lost.

5.7 Bulk Density

During the field calibration of the probe, the gravimetric sampling technique used further allowed the calculation of bulk density for the field site. Again, six soil core samples were obtained around the access tubes used for calibration at given depths. The depths were 0-10, 10-20, 20-40, 40-60, 60-80 and 80-100, 100-120 and 120-140 cm respectively. The profile of bulk density with depth was obtained by using the mean of the six core samples for a given depth from five locations shown in Figure 5.2.

Although the soil profiles were predominantly sandy they were found to be non-uniform with depth as previously discussed. This latter fact was also demonstrated by the bulk density profile (Table 5.1). A higher bulk density was obtained for the 0-60 cm layers, between 1.54-1.60 g/cm^3 while lower values were obtained for the 60-100 cm layer, approximately 1.44 g/cm^3. The result confirmed the sandy texture of the profiles as a value of 1.61 g/cm^3 for a sandy-textured soil has been quoted (Marshall and Holmes, 1979). The lower bulk density obtained at deeper layers could be ascribed to the soils being of more uniform size and an increase in clay content; especially between 80-100 cm and 100-120 cm layers. The binding effect of the

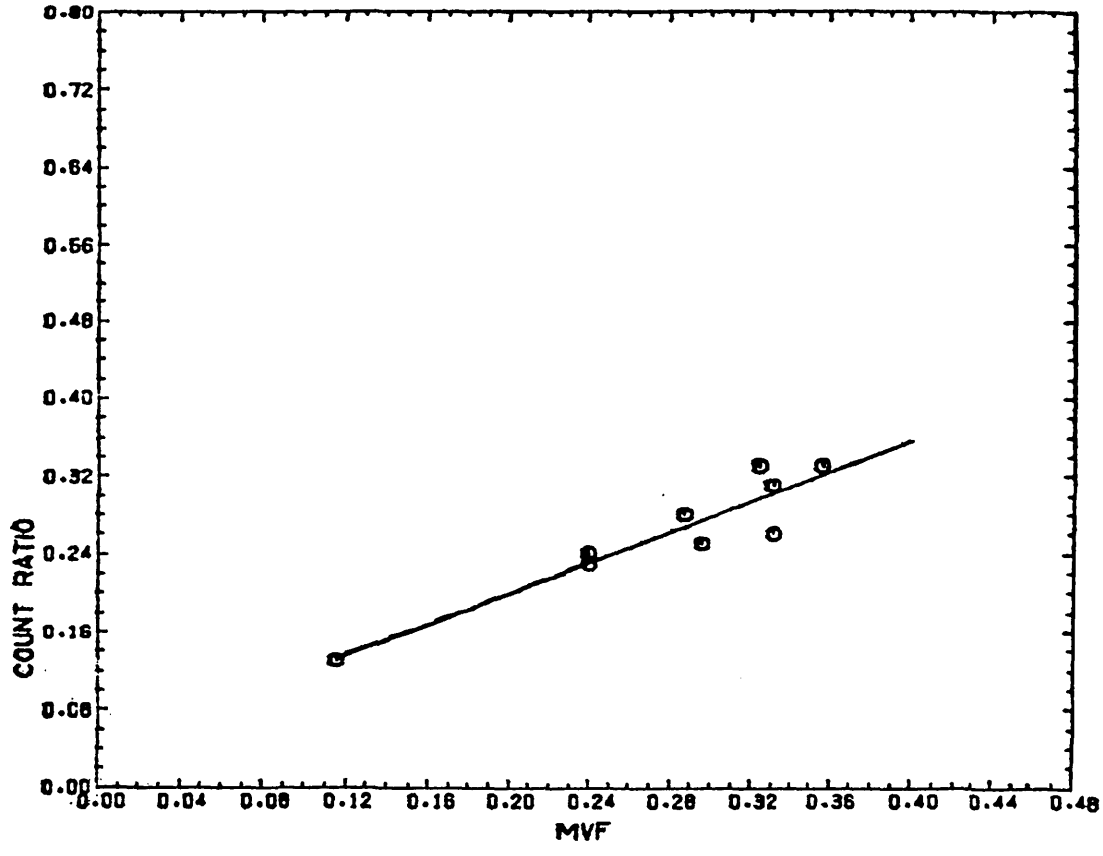

FIG. 5-7 NEUTRON PROBE SURFACE CALIBRATION CURVE

clay could be assumed to be responsible for the rather hard nature encountered while digging between these depths. Below 120 cm, the bulk density was more typical of a sandy subsoil, however the very hard nature of it could be attributed to the increased clay content. This latter fact probably accounts for the restriction of subsoil permeability below the 120 cm depth.

The variability of the bulk density for the different sampling sites are also shown in Table 5.1. The highest coefficient of variability (39.1%) was obtained for the 0-10 cm layer. This high coefficient of variability in the 0-10 cm layer, reflect the variable concentration of stones obtained in this layer for all sampling sites. For other layers (10-60 cm) however, the coefficients of variation were rather low, showing a similarity of the bulk densities for these layers.

5.8 Data Collection and Observation

The frequency of the neutron probe readings was twice weekly during the summer months and once a week during the autumn, winter and spring months. This was the case for all the field plots. The tensiometer readings were obtained thrice weekly during the summer months of 1980 and two times a week in the summer months of 1981. As stated earlier, the tensiometers were installed in the permanent grass and wheat plots. As such, tension readings were available from the grass and wheat plots only.

In some instances however, there were some missing data. This was the case for the soil moisture content readings between 21 February 1981 - 19 March 1981. The latter was caused by the failure of the neutron probe during this period. During the heavy snow storms that occurred between November 1981 to January 1982 soil moisture content readings were not observed since not much variation was likely to occur. For the tension readings, two major reasons were responsible for missing data. These were cracked rubber bungs and leakage of tensiometers at the porous pot-plastic tubing connection. The cracked rubber bungs allow air into the capillary tubing and hence make readings obtained under this condition suspect. The leakage encountered in the tensiometers was mainly caused by problems in construction. The latter was the case for the 1980 cropping season, however

better construction overcame these problems in the 1981 cropping season.

Apart from moisture content and tension readings collected in this study, attempts were also made to observe rooting depths under the various crops used, during the growing season. The root sampling was carried out by digging around four stands on each occasion until the whole root-soil mass was exposed. The roots were later washed free of soil and the lengths measured. Table 5.3 shows the mean of the rooting depth observation for the growing season of 1981 and 1982.

TABLE 5.3 : Rooting Depth Observation

Crop	1981	Mean Rooting Depth (cm)	1982	Mean Rooting Depth (cm)	Root Distribution
Wheat	2/6/81	10.8	19/6/82	9.6	Distribution of roots is located below 2.5 cm. The density of roots is uniform below this depth.
	16/6/81	17.4	30/6/82	11.9	
	2/7/81	20.6	17/7/82	18.2	
	16/7/81	19.2			
Field Beans	16/6/81	17.5	-	-	Root system is tap root. More dense between 2½-8 cm of main root length axis.
	2/7/81	24.3	-	-	
	16/7/81	25.1	-	-	
Permanent Grass	2/6/81	18.3	19/6/82	15.7	Roots are adventitious and more evenly distributed.
	2/7/81	25.7	30/6/82	24.1	
	16/7/81	20.4	17/7/82	28.8	

5.9 Conclusions

The preceding discussion showed the peculiarities of the experimental site, the measurement techniques used for assessing soil moisture levels and the field crops adopted as the test crops. It has become apparent that:-

(1) The soils were predominantly sandy and non-uniform with depth - as shown by the particle size analysis, qualitative description

of the soil profile and bulk density profile.

(2) The neutron probe technique was superior to other soil moisture measurement techniques and was adopted in this study.

(3) Mercury manometer tensiometers can be used for monitoring soil water potential.

(4) In situations where absolute values of soil moisture content are required, the field calibration of the probe is essential.

Having decided on the techniques for assessing soil moisture levels, the following chapter proceeds to evaluate the soil hydraulic parameters needed in the operations of the physical soil water model described in Chapter 4.

CHAPTER 6

FIELD ESTIMATION OF SOIL HYDRAULIC PARAMETERS

6.1 Introduction

The generally recognised soil hydraulic properties are the moisture characteristic and the relationship of hydraulic conductivity with moisture content and/or suction. These properties, as previously discussed in Chapters 2 and 4, are necessary for the accurate prediction of the soil moisture distribution with depth and through time in different soil types. Specifically, accurate estimation of the moisture characteristics and the relationship of hydraulic conductivity with moisture content are pertinent for the successful operation of the soil-water model whose structure is described in Chapter 4.

In consequence, this chapter reviews the current available methods for the determination of the two latter properties and subsequently indicates the techniques proposed for the estimation of the hydraulic properties of the soil in the study area. The results obtained from application of these techniques are also presented.

6.2 Determination of the Unsaturated Hydraulic Conductivity

Numerous methods have been proposed for the determination of the unsaturated hydraulic conductivity function. They broadly fall into three categories.

6.2.1 Theoretical Calculations

These calculations are based on the capillary tube analogy of soil to predict the unsaturated hydraulic conductivity function. Childs and Collis-George (1950) first proposed a calculation procedure based on the pore-size distribution obtained from the soil moisture characteristic curve. Their model assumed that randomly distributed pores of various radii are contained within the soil matrix, and that when adjacent pores are in contact, the overall hydraulic conductance across them depends on the number of interconnected pores and their geometry. The conductance of each pair of interconnected pores is determined by the narrower of the two. As such, the total permeability due to all possible combinations of interconnections is given by:

$$k = \frac{\rho}{\eta} g M \sum_{\lambda=0}^{\lambda=R} \sum_{r=0}^{r=R} r^2 f(\lambda)\delta r f(r)\delta r \qquad (6.1)$$

where k = unsaturated hydraulic conductivity

ρ = density of the conducting fluid

η = viscosity of the conducting fluid

g = acceleration due to gravity

M = matching factor obtained from experimentally found values of $k(\theta)$

r and λ = radii of two pores forming a sequence

R = radius of the largest pore which remains full of water

$f(\lambda)\delta r$ = fraction of the cross-sectional area occupied by pores of radius r to $r+\delta r$

Other methods of calculation have been based on the above theory with some improvements and simplifications being made to the calculation procedure (Kunze et al., 1968; Green and Corey, 1971 and Jackson, 1972). It is evident that the theoretical approach applies more to coarse-grained rather than fine-grained soils. This is because the theory is based mainly on capillarity and not on adsorption and also because the use of the theory neglects the hysteretic nature of the soil moisture characteristic curve. The limited application of the theoretical calculation in predicting the hydraulic conductivity-wetness relationship can be ascribed to the preceding drawbacks inherent in the approach.

6.2.2 Laboratory Measurement

This method relies on the solution of Darcy's equation. Essentially, it consists of computing the unsaturated hydraulic conductivity as a function of moisture content from data obtained from the amount of water that flows from a soil sample placed in a pressure plate apparatus (Gardner, 1956). In this technique, the unsaturated hydraulic conductivity can be obtained either from steady-state flow or transient flow data. The details of the computational technique are given by Gardner (1956), Peck (1964) and Youngs (1964).

Although laboratory resolution is achieved in this technique, it is obvious that the use of discrete samples, to determine hydraulic

parameter values which are extrapolated to flow prediction studies, does not adequately represent the macro-structure of soil as obtained in the field.

Other disadvantages include the failure to account for pressure plate membrane impedance (Kirkham and Powers, 1972) and the labour and time required to obtain samples from different soil depths. Consequently, in situ methods are preferred since bulk soil hydraulic properties are estimated (Davidson et al., 1969).

6.2.3 In Situ Technique

Current advances in soil water measurement techniques in the field as described in Chapter 5 have bolstered the wide applicability of this technique. The technique accounts for the spatial and vertical heterogeneities that occur in the soil hydraulic properties down the profile. Consequently the derived unsaturated hydraulic conductivity-wetness relationship approximates the bulk soil hydraulic parameter values in their natural state (Hillel et al., 1972).

Variants of the in situ technique exist. The type selected for use depends on the degree of heterogeneity inherent in the soil profile, the level of sophistication of the array of measuring instruments at hand and ultimately on the time available for the study. Generally, two principal methods emerge:-

6.2.3.1 Infiltration Technique

This involves the constant supply of water to the soil at a rate lower than the effective saturated hydraulic conductivity of the soil profile (Hillel and Benyamini, 1974; Poulovassilis et al., 1974). This method has been employed by Youngs (1964) in laboratory soil columns.

The application of water to the soil results in the establishment of a steady-state flux regime within the soil profile and the consequent development of a unit hydraulic gradient in the upper part of the profile. Once the latter state is reached, the hydraulic conductivity becomes equal to the rate of water supply into the soil. In a uniform soil, the suction gradients will tend to zero. It is important to measure the suction gradients in layered soils since suction

gradients may not be zero. Each application rate of water results in one value of $k(\theta)$, hence for different values of $k(\theta)$, a series of successively increasing application rates are used, assuming that the soil is initially dry.

The disadvantages of applying the constant application technique are (i) it requires elaborate equipment to be maintained in continuous operation for long duration (Amerman et al., 1970 and Rawitz et al., 1972), (ii) problems of surface sealing occasioned by drop impact which prevents infiltration, (iii) lateral flow to surrounding drier soil, (iv) the vertical flow assumption is invalidated in soils where impeding layers are present and, (v) a very long time is required for the attainment of steady-state at low water application intensities which makes it difficult to obtain $k(\theta)$ values at low values of moisture content (Poulovassilis et al., 1974) consequently only $k(\theta)$ values at the wet range of the curve are obtained (Hillel and Benyamini, 1974).

The preceding infiltration technique can also be applied across an impeding layer at the soil surface, thus creating a boundary condition for a desired flux (Hillel and Gardner, 1970). In the impeding layer technique, Hillel and Gardner explained that the saturated hydraulic conductivity of the impeding layer will be smaller than that of the subsoil. Consequently, if steady-state conditions are established, the hydraulic gradient through the impeding layer will be greater than unity and this leads to high suction development in the subsoil. The magnitude of this latter suction then increases with increasing hydraulic resistance of the impeding layer. Finally, when steady-state infiltration is achieved, the flux and conductivity of the subsoil become equal. In order to obtain a series of $k(\theta)$ values, it is essential to progressively lower the hydraulic resistance of the impeding layer.

Bouma et al. (1971) utilised the impeding layer principle with success by employing ring infiltrometers and by puddling the soil surface to achieve the desired boundary condition. Tensiometers were used to monitor the vertical and horizontal suction changes in the infiltrating profile. The advantage of the impeding layer technique over the constant water application rate is the simplicity of the

experimental system since it obviates the need for elaborate instrumentation. Despite the relative advantage of the technique, it is not suitable for general application because of the "unstable flow phenomenon" which has been reported to occur for some soil profiles (Hillel, 1980). This phenomenon, which is normally pronounced during infiltration in soils which exhibit a transition from a fine textured zone to coarse textured zone shows that the advance of infiltrating water may not be even in such soils and that flash flows take place at certain locations where intrusions are present (Raats, 1973). This instability in the progression of the wetting front has been a subject of recent study (Diment and Watson, 1983).

6.2.3.2 The Internal Drainage Technique

This method is a progression of the laboratory transient flow technique for soil columns applied to field situations (Watson, 1966). It is based upon the monitoring of the potential gradient and transient flux values within an initially saturated profile that is gradually depleted of moisture by drainage. This assumes that there is no further irrigation and evaporation from the soil profile. Following Ogata and Richards (1957); Rose et al. (1965), Watson (1966), van Bavel et al. (1968), Davidson et al., (1969) and Hillel et al. (1972) described in detail the application of the internal drainage technique under field conditions. The basic theory underlying the technique is presented below.

The water balance for a unit cross-sectional area of a soil profile during a given period of time can be represented as follows:

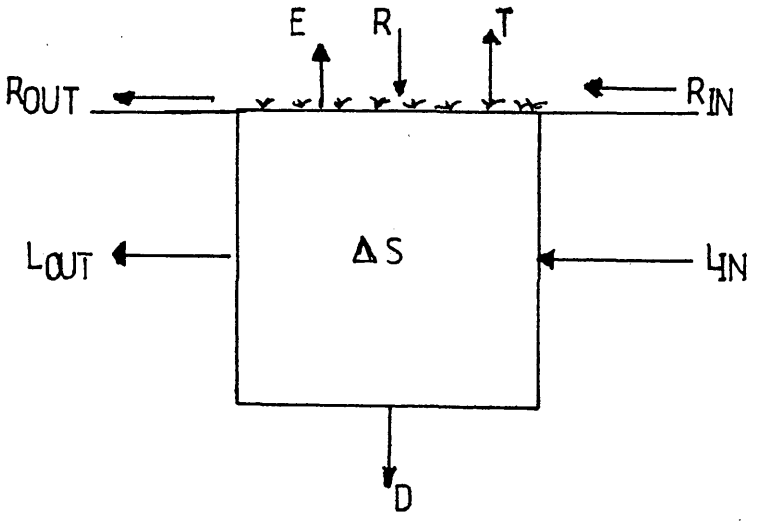

where R = rainfall

E = evaporation

T = transpiration

L_{IN} = subsurface lateral inflow

L_{OUT} = subsurface lateral outflow

R_{IN} = run on

R_{OUT} = runoff

ΔS = change in volumetric water storage of the soil profile

D = drainage

The components above are in units of depth or volume.

For the equation of continuity to be satisfied, the water balance can be given thus:-

$$R + R_{IN} + L_{IN} - R_{OUT} - L_{OUT} - E - T - D = \Delta S \qquad (6.2)$$

If only vertical flow is assumed to take place, equation 6.2 becomes

$$R - E - T - D = \Delta S \qquad (6.3)$$

When the soil surface is covered to preclude rainfall infiltration, evaporation and transpiration, we have

$$-D = \Delta S \qquad (6.4)$$

If the volumetric water content (θ) is measured down the profile at a given time (t), the moisture storage (S) of the entire profile to a given depth (Z) is determined by integration, hence

$$S = \int_{o}^{z} \theta \, dz \qquad (6.5)$$

Differentiating equation 6.4 with respect to time gives

$$-\frac{dD}{dt} = \frac{dS}{dt} \qquad (6.6)$$

The velocity of flow in the soil is given by Darcy's equation, consequently

$$+\frac{dD}{dt} = -k(\theta)\frac{dH}{dz} \qquad (6.7)$$

Substituting equations 6.5 and 6.7 into equation 6.6 gives

$$k(\theta)\left[\frac{dH}{dz}\right]_z = \frac{d}{dt}\left(\int_o^z \theta\, dz\right) \qquad (6.8)$$

Consequently,

$$k(\theta) = \left[\frac{dS}{dt}\right]_z \Bigg/ \left[\frac{dH}{dz}\right]_z \qquad (6.9)$$

Concurrent measurements of soil water potential and soil moisture content enable the determination of the hydraulic head gradient at any depth (z) and subsequently allow for the calculation of $k(\theta)$ or alternatively $k(\phi_p)$ (hydraulic conductivity-suction relationship).

To apply the above principle, it is a prerequisite that the soil profile is initially saturated. This is normally obtained by ponding until steady-state conditions are indicated by the constancy of tensiometer readings (Davidson et al., 1969) and of the moisture content as assessed by the neutron probe (Poulovassilis et al., 1974). The prevention of evaporation and rainfall infiltration is achieved by covering the surface of the soil profile with plastic sheets (Davidson et al., 1969 and Hillel et al., 1972). As water content gradually diminishes due to drainage, a series of $k(\theta)$ values are obtained either by assessing integrated fluxes over a given time interval and therefore deducing a mean value of k corresponding to a mean value of moisture content at the particular depth of the profile considered (Rose et al., 1965), or by utilising an instantaneous fluxes procedure (Watson, 1966).

From the preceding, it is clear that apart from the internal drainage technique possessing some of the advantages inherent in the infiltration method, it possesses other qualities which include the avoidance of extrapolating steady-state methods to transient state processes and also allows for the determination of the soil moisture characteristic without installing additional instruments (Hillel et

al., 1972). In spite of the superiority of the internal drainage technique over other in situ techniques, certain limitations however exist. These are the non-applicability of the technique in conditions where lateral movement is appreciable especially in soils where impervious layers are evident and the $k(\theta)$ values derived may not give layer representative values.

Poulovassilis et al. (1974) theoretically demonstrated the impracticability of this technique in a soil profile which exhibits an upper fine layer underlain by a relatively coarse one. This is because static equilibrium may be obtained in the upper profile thereby restricting the range of $k(\theta)$ values that can be obtained. However, Poulovasilis et al. suggests that in such a situation, if the plot is uncovered, the surface loses water by evaporation and the $k(\theta)$ relationship for that layer can be determined. A final constraint to the application of the internal drainage technique relates to the fact that suctions greater than 0.9 bar cannot be measured by the technique if tensiometers are used.

Thomson (1981) attempted to derive the $k(\theta)$ relationship for different layers in the experimental study site by using the internal drainage technique as delineated by Hillel et al. (1972). The results obtained by Thomson show the non-homogeneous nature of the soil profile as evidenced by the variations in moisture characteristics down the profile to a depth of 1.5 metres. Thomson's results further reveal that the technique appears to be markedly affected by the diurnal temperature variations. The latter appeared to affect the suction gradients measured at the surface and in consequence it was difficult to apply the technique to derive the $k(\theta)$ relationship between the soil surface and a depth of 37.5 cm for the particular profile. Furthermore, Thomson produced $k(\theta)$ values at the wetter end of the soil profile, consequently the relationships obtained may be questionable if extrapolated to drier conditions.

Based on results of Thomson (1981) for the study site and the apparent inadequacies revealed by them, it became imperative for this author to adopt an alternative technique. A "natural balance method" which is a slight modification of the Arya et al. (1975) technique is used to determine the unsaturated hydraulic conductivity function for the study site.

6.2.3.3 Natural Balance Method

Essentially, this technique involves the continuous monitoring of the natural changes in moisture content and soil water potential for a prolonged dry period (drying cycle) or wet period (wetting cycle).

(a) Drying Cycle

During a prolonged dry period in the field, soil moisture storage is depleted by evaporation and drainage. Consequently, at some time it is presumed that a zero-flux plane exists which separates the zone of upward and downward fluxes (Wellings and Bell, 1980). This zone is located on the maximum of the hydraulic head profile where dH/dZ = 0 (Figure 6.1c). As drying proceeds, the depth of the zero-flux plane will increase with time.

This procedure must be used in conjunction with rainfall data which allows the definition of the dry spells during the summer months. Under these conditions, the moisture profiles and hydraulic head profiles at two selected times, t_1 and t_2 can be approximated by those shown in Figure 6.2, while $Z_o(t_1)$ and $Z_o(t_2)$ are the zero flux plane (ZFP) depths at times t_1 and t_2 respectively. The mean zero-flux plane depth is calculated thus:-

$$\bar{Z}_o = \frac{Z_o(t_1) + Z_o(t_2)}{2} \qquad (6.10)$$

It is assumed that there is no flux between times t_1 and t_2 at depth $\bar{Z}_o$.

If any level Z located above $\bar{Z}_o$, during the time interval t_1 to t_2 is considered, then the average upward flux from the ZFP passing through the given depth (Z) is given by:-

$$q = \frac{-|\Delta S|_{\bar{Z}_o}^{Z}}{\Delta t} - C \qquad (6.11)$$

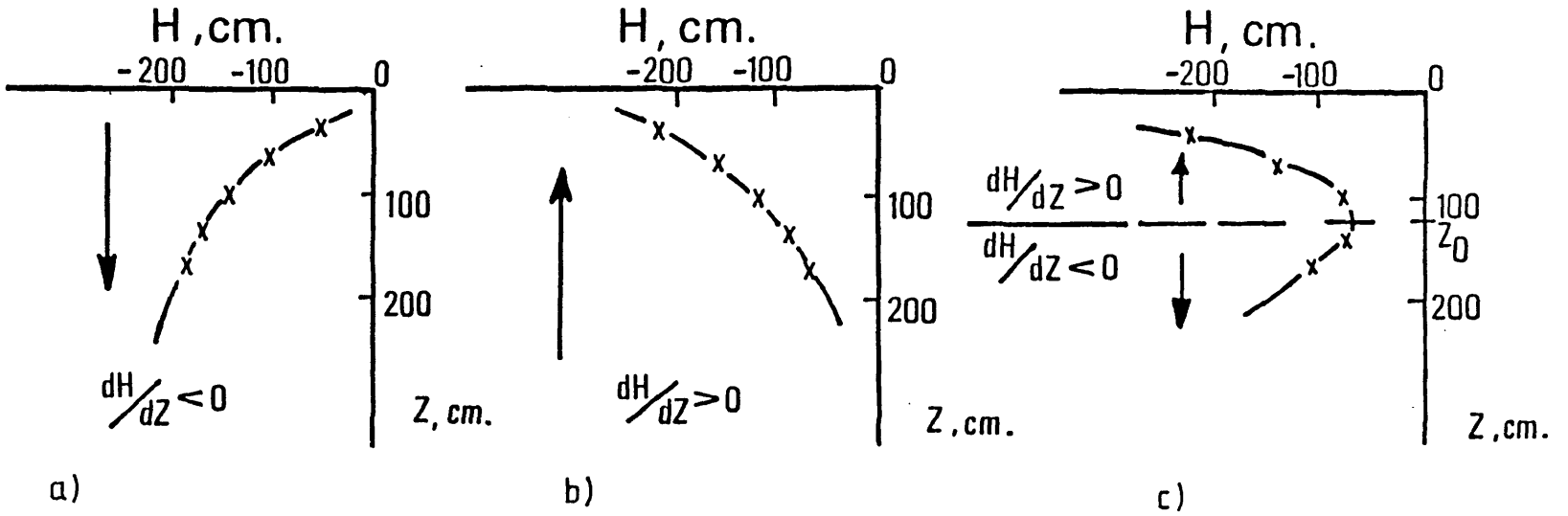

FIG.6.1 DIAGRAM OF HYDRAULIC HEAD PROFILES

where $|\Delta S|_{\overline{Z}_o}^{Z}$ is the variation in moisture storage between $\overline{Z}_o$ and Z during the interval considered as shown in the shaded area of Figure 6.2; C is the error associated with the flux. This error is primarily due to the inclusion of the root extraction term in the moisture storage variation in the above equation 6.11.

Similarly, the downward flux passing through any given depth (Z_L) located below Z_o is given by:-

$$q = \frac{-|\Delta S|_{Z_L}^{\overline{Z}_o}}{\Delta t} \qquad (6.12)$$

where $|\Delta S|_{Z_L}^{\overline{Z}_o}$ represents the change in moisture between $\overline{Z}_o$ and Z_L in the time interval considered. Since the flux can be related to the mean moisture content at Z and Z_L between t_1 and t_2, then let $\theta_1(t_1)$ and $\theta_2(t_2)$ be the moisture contents measured at the given depths in t_1 and t_2. The mean moisture content (θ_z) will be thus:-

$$\overline{\theta}_z = \frac{\theta_z(t_1) + \theta_z(t_2)}{2} \qquad (6.13)$$

To compute the average hydraulic gradient $(\overline{\frac{dH}{dz}})$ obtained at z between t_1 and t_2, the hydraulic head profiles for the respective time periods are drawn and the slopes read from them. As such, the mean hydraulic gradient obtained during the time interval at z is given as

$$\left|\overline{\frac{dH}{dz}}\right|_z = \frac{\left|\frac{dH}{dz}\right|_{t_1} + \left|\frac{dH}{dz}\right|_{t_2}}{2} \qquad (6.14)$$

The unsaturated hydraulic conductivity as a function of the mean moisture content obtained in the time interval at any given depth is calculated by Darcy equation, hence

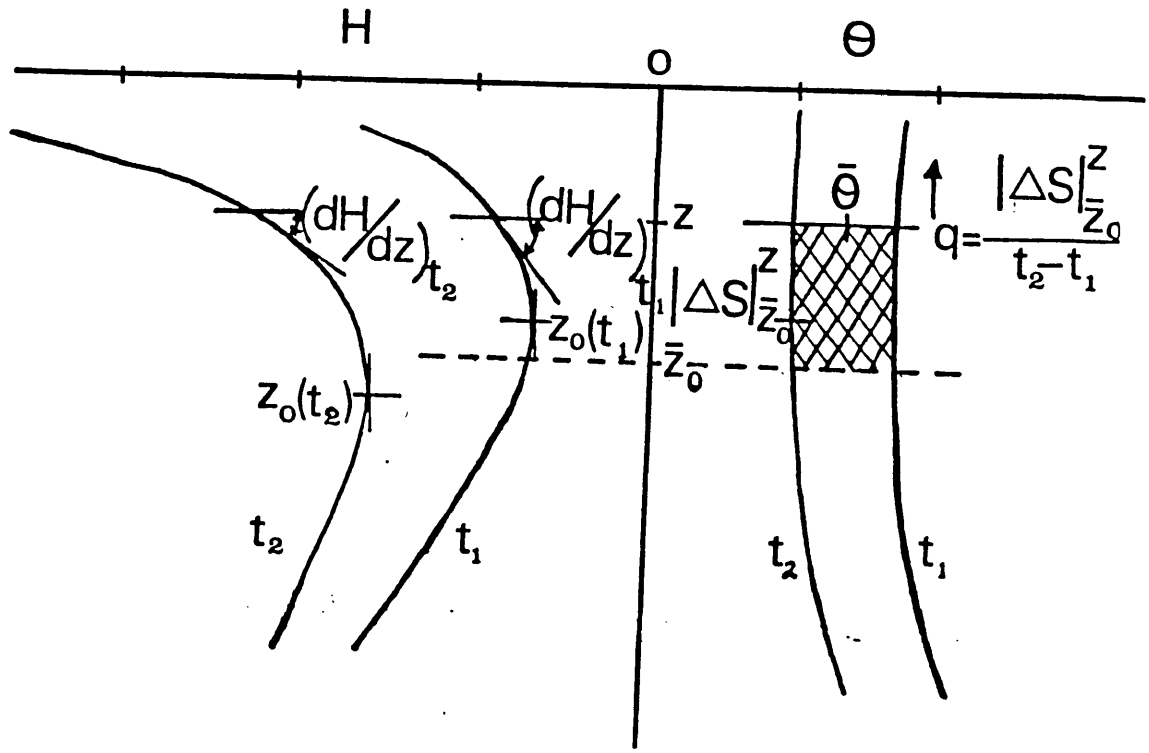

FIG.6.2 HYDRAULIC HEAD AND MOISTURE PROFILES (DRYING CYCLE)

$$k(\bar{\theta}) = q \left| \frac{d\bar{H}}{dz} \right| \qquad (6.15)$$

where q is as defined in equation 6.11.

The drying cycle method has been developed primarily for the total evaporation and drainage components of the soil profile. This can be noted if two levels z = 0 (soil surface) and Z = L (base of the profile) are considered between t_1 and t_2, the values

$$\left| \Delta S \right|_{Z_o}^{z=0} \quad \text{and} \quad \left| \Delta S \right|_{Z=L}^{z=0}$$

give the total evaporation and drainage components respectively, hence the natural balance technique. The above equation is applied in this study for vegetated soils in the evaluation of the $k(\theta)$. This is because the moisture and tension profiles obtained were from cropped surfaces. The latter obviously presents an error in the $k(\theta)$ values derived for the soil profile, especially above the zero flux plane depth. This is because root extraction and evaporation are simultaneously taking place. Consequently, the changes in moisture storage above the ZFP for the duration considered would be higher than that which would have been obtained if only evaporation from a bare soil profile was considered. The error calculated as a result of the preceding for the moisture profiles considered ranges from 8 to 33.1%. The latter shows that overestimation of the $k(\theta)$ values at depths above the ZFP would result. This overestimation is expected to be higher at depths nearer the soil surface due to preferential uptake of moisture by the roots from the surface. The preceding is a drawback of the natural balance technique when applied to cropped surfaces.

(b) The Wetting Cycle

In this circumstance, the natural variation in water content and water potential is monitored during a period when an initially dry soil is steadily wetted to a considerable depth by natural precipitation or irrigation.

Under this condition, water advances into the soil exhibiting a wetting front whose depth gradually increases with time. Consequently, for a given interval, there is an initially wet upper

surface overlying a drier subsurface. With time, the wetting front disappears and subsequently all flow is downward.

The wetting cycle is also carried out in conjunction with rainfall data to indicate the progress of the wetting up process.

If two times t_1 and t_2 are selected, then the profiles of hydraulic head and water content as measured with tensiometers and neutron probe respectively can be approximated with those shown in Figure 6.3.

Consider a level Z located above the wetting front Z', the average downard flux passing through the level at a time interval (t_2-t_1) will be given as:-

$$q = \left[\frac{\left| \Delta S \right|_{Z'}^{Z}}{\Delta t} - (C + D) \right] \qquad (6.16)$$

where $\left| \Delta S \right|_{Z'}^{Z}$ is the moisture storage change between Z' and Z during the interval considered as shown in the shaded area of Figure 6.3 and D is drainage error.

Similar procedures for calculating the mean moisture content (θ) and mean hydraulic gradient $(\frac{dH}{dZ})$ as used in the drying cycle are employed and these values are subsequently related to the flux. The $k(\theta)$ is finally obtained from equation 6.15. However, the utility of the wetting cycle as described above neglects the evaporation and drainage fluxes. The latter presents obvious problems relating to the evaluation of the flux at any given level in the profile using the wetting cycle procedure. In the use of the technique for the purpose of this study, it is considered that during and following a period of rainfall, actual evapotranspiration rate is equal to the potential evapotranspiration rate. Consequently, the surface inflow by precipitation is reduced by the potential evapotranspiration rate. The change in storage down to a given depth is calculated from soil moisture data and the drainage component is obtained as a residual. In this study, for the wetting cycle duration considered, the drainage from the profile ranges between 0.06 mm/day to 0.75 mm/day. The neglect of the drainage component therefore will have the effect of

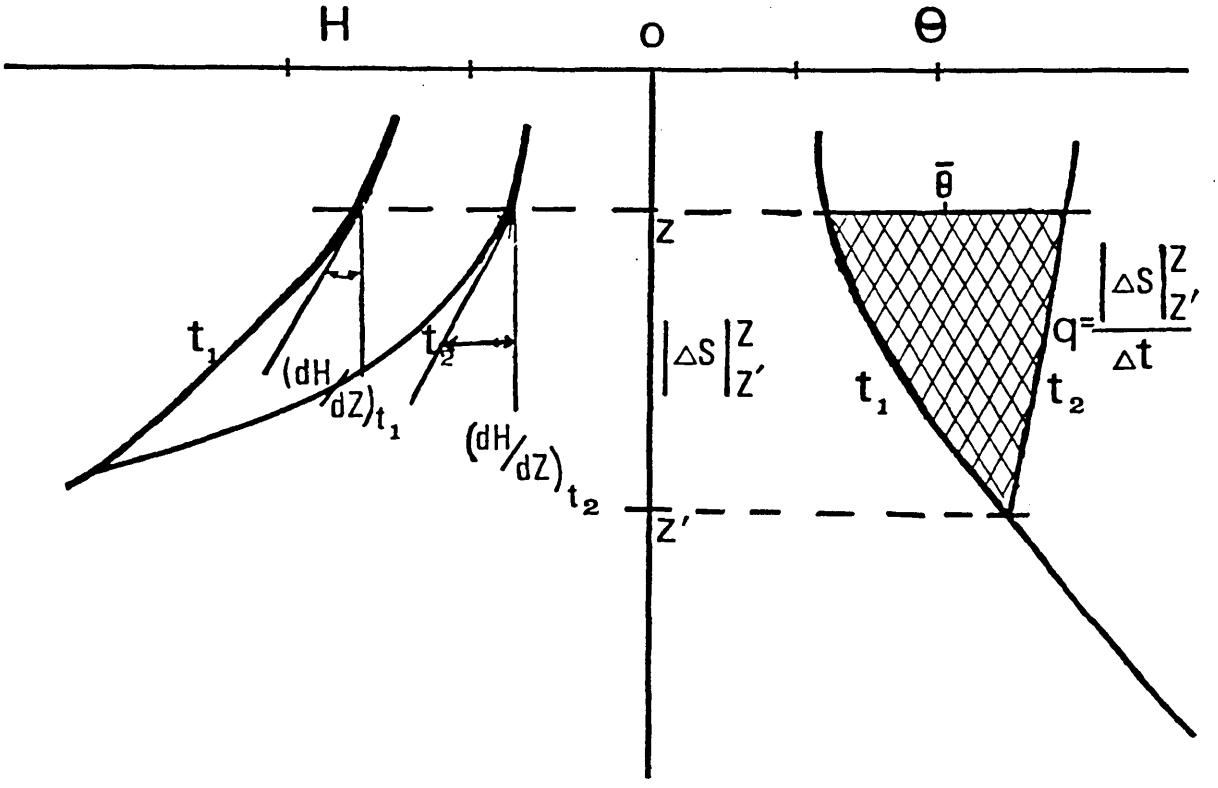

FIG.6.3 HYDRAULIC HEAD AND MOISTURE PROFILES (WETTING CYCLE)

underestimating the k(θ) values obtained by up to 25.7%. However the evapotranspiration component neglected in the wetting cycle technique may be significant in the upper layers, as to lead to overestimation of derived K(θ) values.

From the preceding description of the natural balance technique, it is evident that certain conditions must be fulfilled before the technique can be applied in field situations. These are that the soil moisture profile must exhibit the occurrence of ZFP depths and wetting front development as revealed by the simultaneous monitoring of soil water pressure and soil moisture content respectively. The technique circumvents the use of facilities required by the infiltration and internal drainage techniques in that ponding equipment and plastic sheets are not needed. Consequently all that is needed are the neutron probe and tensiometers. However, before the technique can reproduce actual unsaturated k(θ) values, the following have to be considered. These are that the drainage component be included in the calculation of the change in storage for the wetting cycle technique and that bare soil surface be used. The latter avoids the problem of transpiration neglected in the utility of these techniques as described in this study.

Generally however, the natural balance technique can be applied in all types of soils and eliminates the difficulty posed by layered soils as discussed earlier. Finally the k(θ) values obtained are within the moisture content range that will occur for transient-flux processes and hence are more pertinent for use in model testing and development.

6.3 Determination of the Soil Moisture Characteristics

Prior to the development of the neutron probe technique and the tensiometer for the monitoring of soil moisture content and soil water potential respectively, the soil moisture characteristic was determined mainly under laboratory conditions (Rose, 1966). The laboratory procedure utilises suction plate or pressure membrane apparatus. In either case, soil samples are placed on a porous plate and a known pressure is applied until equilibrium water content is attained. At this equilibrium state, the soil sample is either weighed or moisture outflow measured to calculate the moisture content

at the known equilibrium suction. The above procedure is repeated for a series of known pressures to obtain different moisture contents.

The criticisms levelled against the use of either the pressure membrane apparatus or suction plate are similar to those on the laboratory procedure for determining k(θ) relationship as discussed in the previous section. Particularly important, however, is the lack of field representativeness of the samples employed and the fact that the procedure is relevant either in desorption or sorption only. The latter does not allow the technique to account for hysteresis.

In consequence, an *in situ* technique has normally been preferred (Hillel and Benyamini, 1974; Arya *et al.*, 1975). This involves the use of the neutron probe technique and tensiometers *in situ* in the field. The procedure does not require additional instrumentation and in fact the soil moisture characteristics can be obtained from the soil moisture content and soil water potential readings used for the determination of the k(θ) relationship. As such, it is common in most field studies that both the moisture characteristic and k(θ) estimation are carried out simultaneously (Hillel *et al.*, 1972; Poulovassilis *et al.*, 1974).

The limitation to the use of the above technique has been imposed by the tensiometer range limit of 0-0.9 bar. For the purpose of this study, it was believed consistent to utilise the soil moisture readings and soil water potential data simultaneously obtained in the field for the derivation of the soil water potential versus soil moisture content relationship. The data thus obtained cut across both the drying and wetting phases of the soil moisture profile.

6.4 Analyses of Data

Rainfall data collected during the cropping seasons of 1980 and 1981 were inspected in order to isolate periods when dry spells occurred. Furthermore, the inspection facilitated the observation of periods when the dry spells were broken with the consequence that the profile was being wetted up to a considerable depth. Having isolated the dry and wetting up periods, it became mandatory to inspect the neutron probe and tensiometric data bank gathered during the two seasons to observe whether the isolated periods coincided with days on

which the soil water readings were taken. From the visual inspection, the following periods were isolated for the estimation of the $k(\theta)$ relationship under the permanent grass and wheat plots. These plots were simultaneously monitored for moisture content and soil water potential readings as discussed in Chapter 5.

The following days were isolated for

(a)	Drying cycle:	1/8/80 - 4/8/80
		4/8/80 - 8/8/80
		1/8/80 - 8/8/80
		26/6/81 - 30/6/81
		6/7/81 - 11/7/81
		24/7/81 - 27/7/81
(b)	Wetting cycle	27/7/81 - 3/8/81
		8/5/81 - 11/5/81
		11/5/81 - 19/5/81

6.4.1 Neutron Probe Readings

The data was converted by using the calibration curves derived for surface and bulk soil as given in equations 5.7 and 5.6 respectively to moisture volume fraction.

The next phase was to calculate the layer moisture contents. This entails the multiplication of the individual moisture volume fraction by a layer factor to give the moisture content of the layer, expressed as a depth of water in millimetres. The layer factor is the distance between half intervals on either side of the relevant measuring depth. The surface layer is an exception however and in this case the layer factor is taken from the surface to the half interval below the measurement depth. Thus the total water content of the profile to any given depth is the sum of the individual layer water contents. Consequently, the readings that were taken at 10, 20, 30, 40 ..... 150 cm give layer water contents for 0-15, 15-25, ... 145-155 cm respectively (a file called VOLL is created for the output).

As shown in the previous chapter, the random counting error at 64 secs is less than that at 16 secs, and hence the neutron probe

readings considered for the estimation of the k(θ) relationship were taken at the 64 secs counts throughout the cropping season. As such the random error obtained (1.04%) for the readings may not be significant in influencing the results obtained.

6.4.2 Tensiometer Readings

The data was put in a file called TENS. Since there were no field measurements at 60, 80, 100 and 120 cm depths as described earlier on, the missing readings were obtained by interpolation between 50, 70, 90, 110 and 150 cm readings. This was carried out by hand since some interpretation of the data was required. For each reading, the soil matric potential and total potential were calculated and put into separate data files MATPO and TOTPO respectively. The soil water matric potential was calculated according to the following equation in centimetres water:-

$$h_p = Y + Z - 12.6X \qquad (6.17)$$

where h_p = matric potential

Y = height (cm) above ground level of the mercury level in the mercury reservoir

Z = depth to middle of tensiometer porous cup (cm)

X = height of mercury above reservoir (cm)

The total head was calculated by adding the gravitational head as defined by equation (2.13).

The hydraulic gradient was calculated from hydraulic head profiles by defining tangents to the curves and the slopes were derived for the same depths as was the profile water content.

For the tension readings utilised, there were no missing values and the usual problem posed by cavitation was alleviated by "purging" the tensiometers of air bubbles at least two days before any reading was taken. The purging was carried out by distilled water from a syringe. Furthermore, for the drying cycle period considered, the tensiometer limit range was not exceeded.

6.5 Results and Discussion

6.5.1 Unsaturated Hydraulic Conductivity

The natural balance method as described in equations 6.10-6.16 was used to derive the k(θ) relationship.

(a) Drying Cycle

The hydraulic head profiles for the selected intervals during the 1980 and 1981 cropping seasons are shown in Figures 6.4-6.12 for the permanent grass plot location (Figure 5.1). Tangents to the curves were defined at the depths of measurements of the soil water potential and the hydraulic gradients read. From the change in arithmetic sign from positive to negative of the estimated hydraulic gradient values, the zero flux plane depths were located for each hydraulic head profile. The mean of successive zero flux plane depths for the specific duration considered was designated as the mean zero flux plane depth (Z_o). The mean ZFP depths are indicated in Table 6.1a, 6.1b, 6.1c and 6.2a, 6.2b, 6.2c. Also shown in Tables 6.1a, 6.1b, 6.1c and 6.2a, 6.2b, 6.2c are the mean hydraulic gradient values (dH/dz).

Employing the computational technique already described in 6.2.3(iii), the values of water storage at the dates of measurement and the variations in storage between mean ZFP depth at each time interval and selected depths were calculated. The data and associated average volumetric moisture content are shown in Tables 6.1a, 6.1b, 6.1c and 6.2a, 6.2b, 6.2c coupled with the corresponding flux and k(θ) values obtained for each given layer.

(b) Wetting Cycle

A similar procedure to that used under the drying cycle was employed to obtain hydraulic gradients from hydraulic head profiles for selected intervals (Figures 6.13-6.17) during the wetting cycle. The values obtained are shown in Tables 6.3a, 6.3b, 6.3c. The associated moisture profiles indicating the wetting fronts for the duration 11/5/81-19/5/81 is shown in Figure 6.18 for the permanent grass plot. The downward flux, mean hydraulic gradients, unsaturated hydraulic conductivity and corresponding average volumetric moisture contents are also shown in Tables 6.3a, 6.3b and 6.3c.

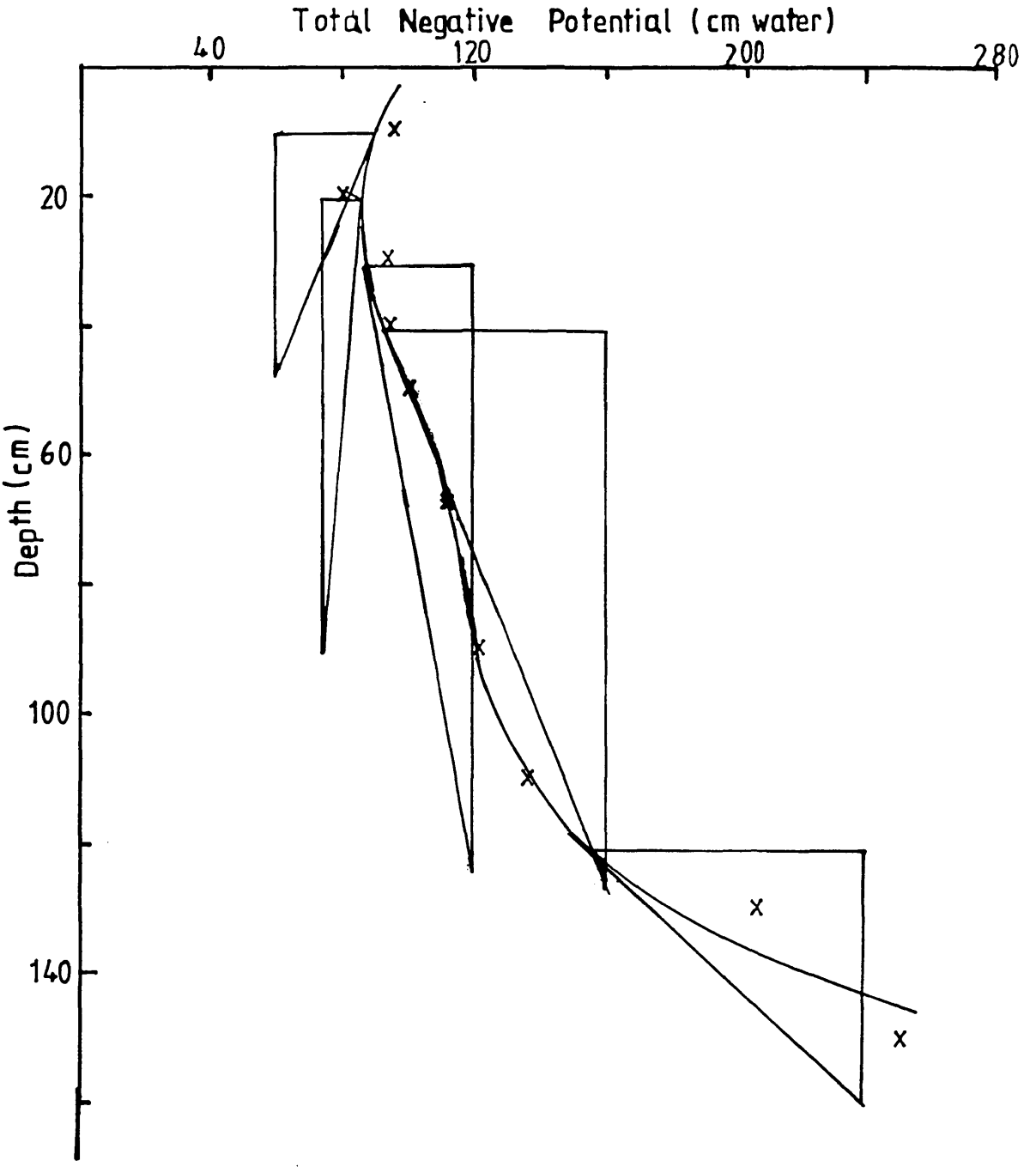

FIG. 6·4 HYDRAULIC HEAD PROFILE
GRASS - 1/08/80

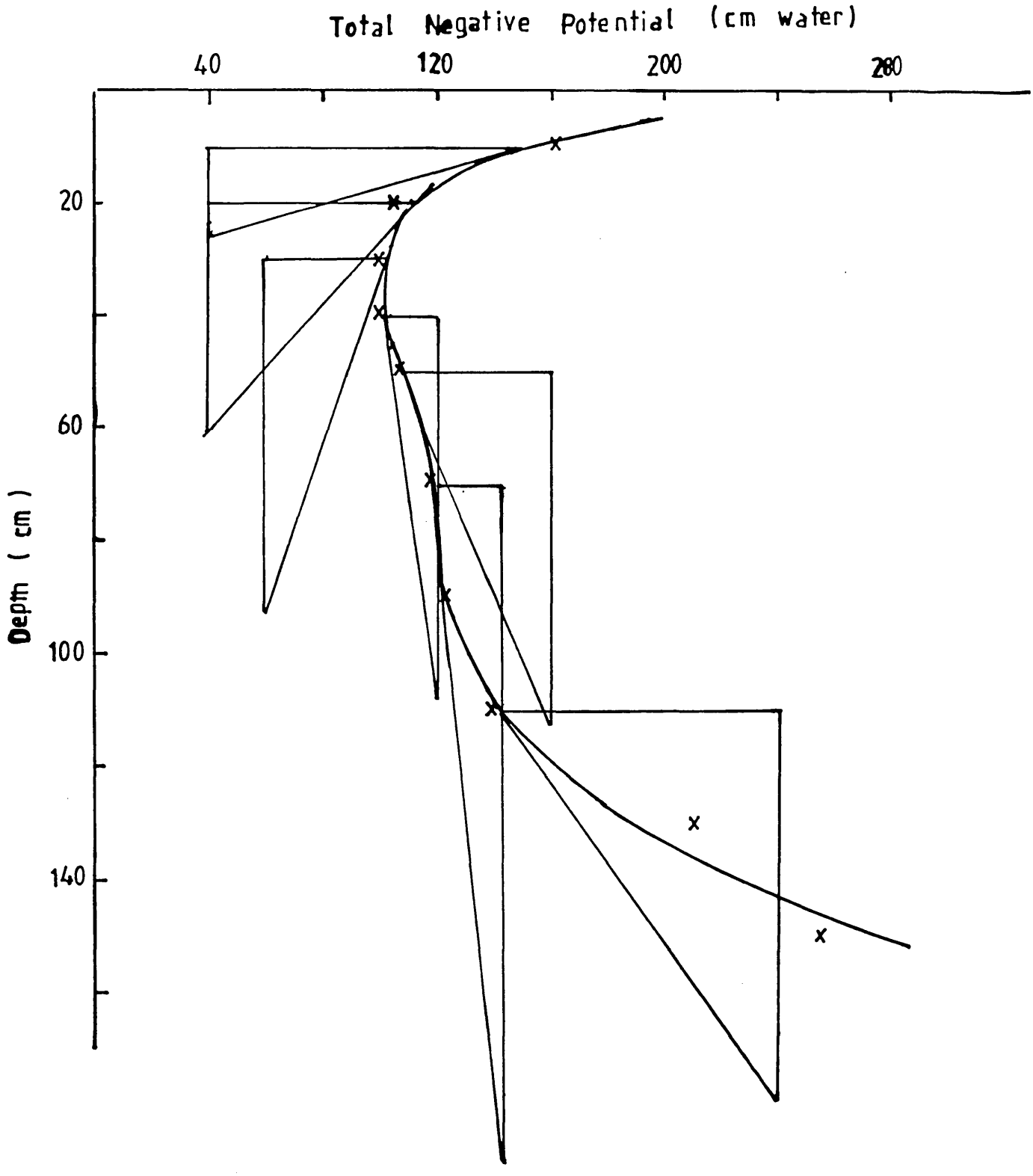

FIG. 6·5 HYDRAULIC HEAD PROFILE
GRASS - 4/08/80

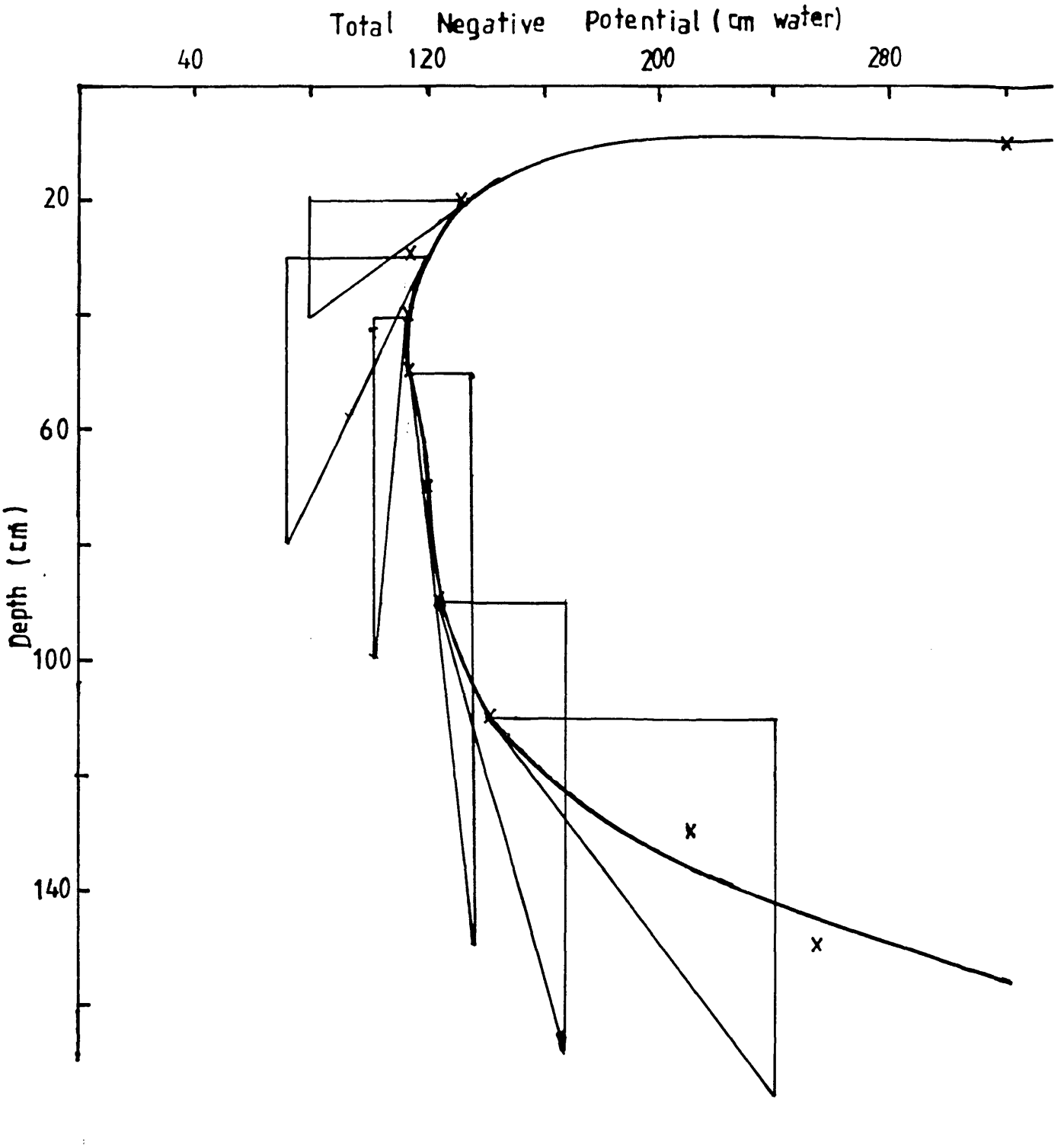

FIG. 6-6 HYDRAULIC HEAD PROFILE
GRASS - 8/08/80

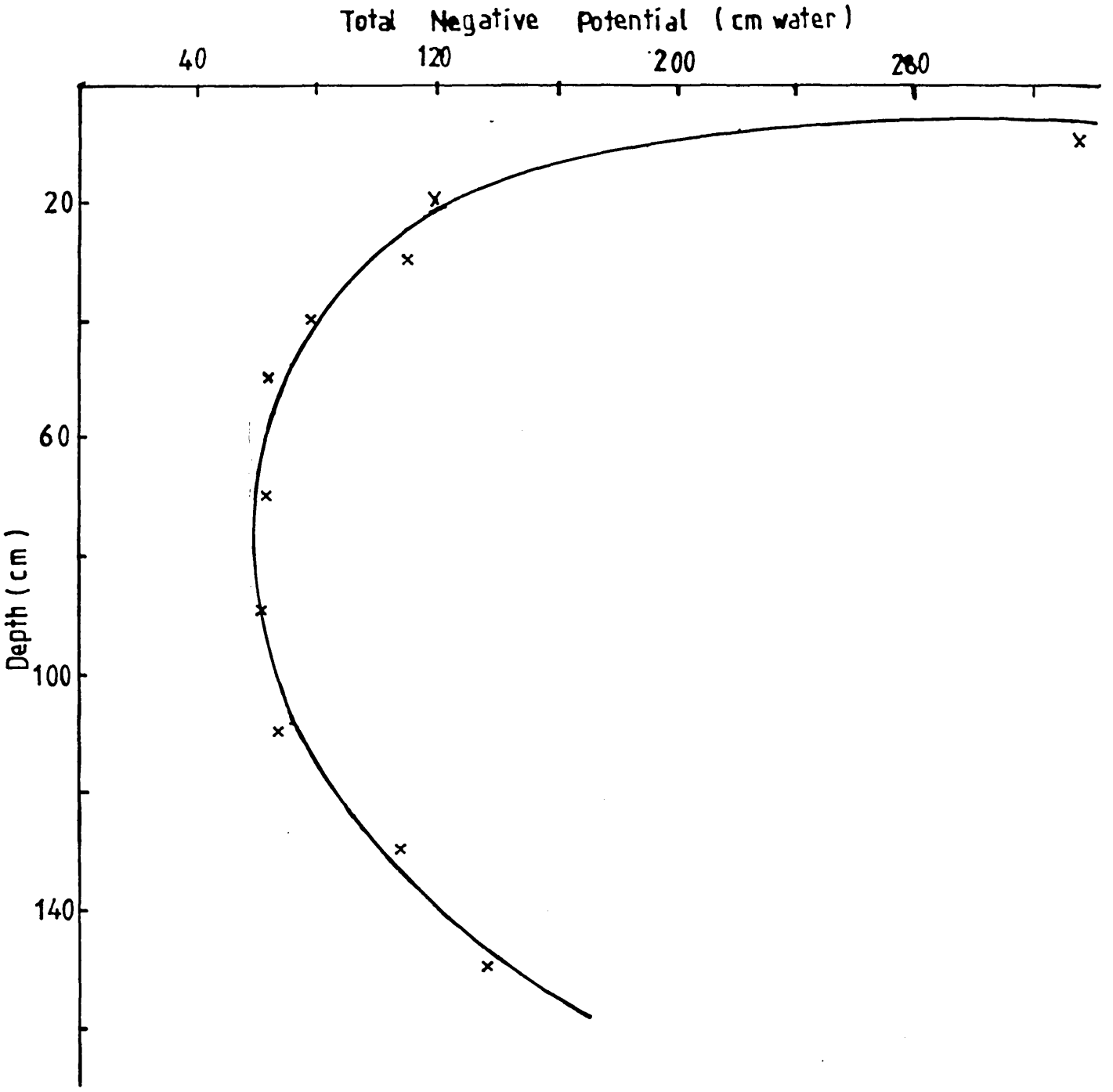

FIG. 6·7 HYDRAULIC HEAD PROFILE
GRASS - 26/06/81

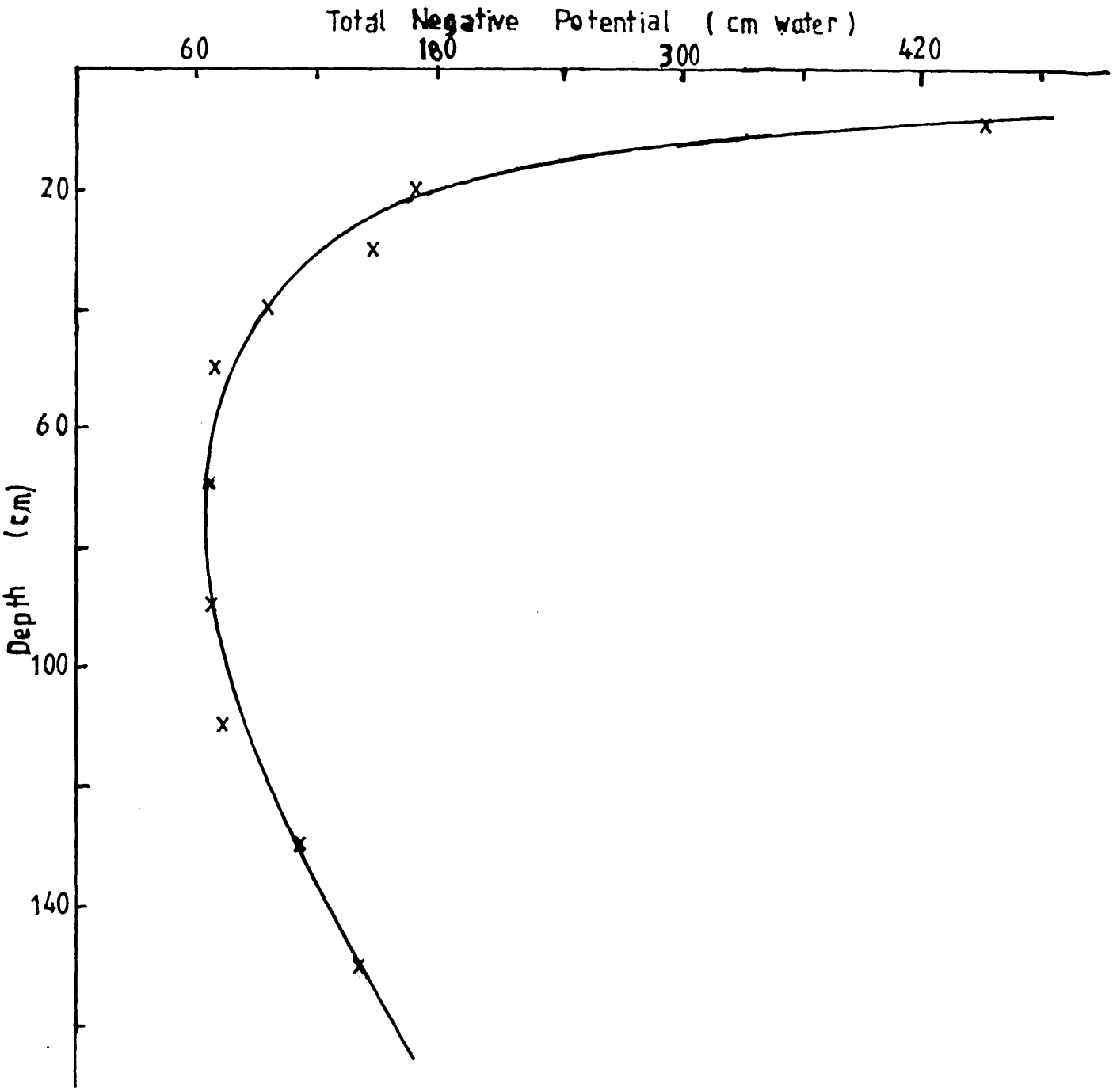

FIG. 6-8 HYDRAULIC HEAD PROFILE
GRASS - 30/06/81

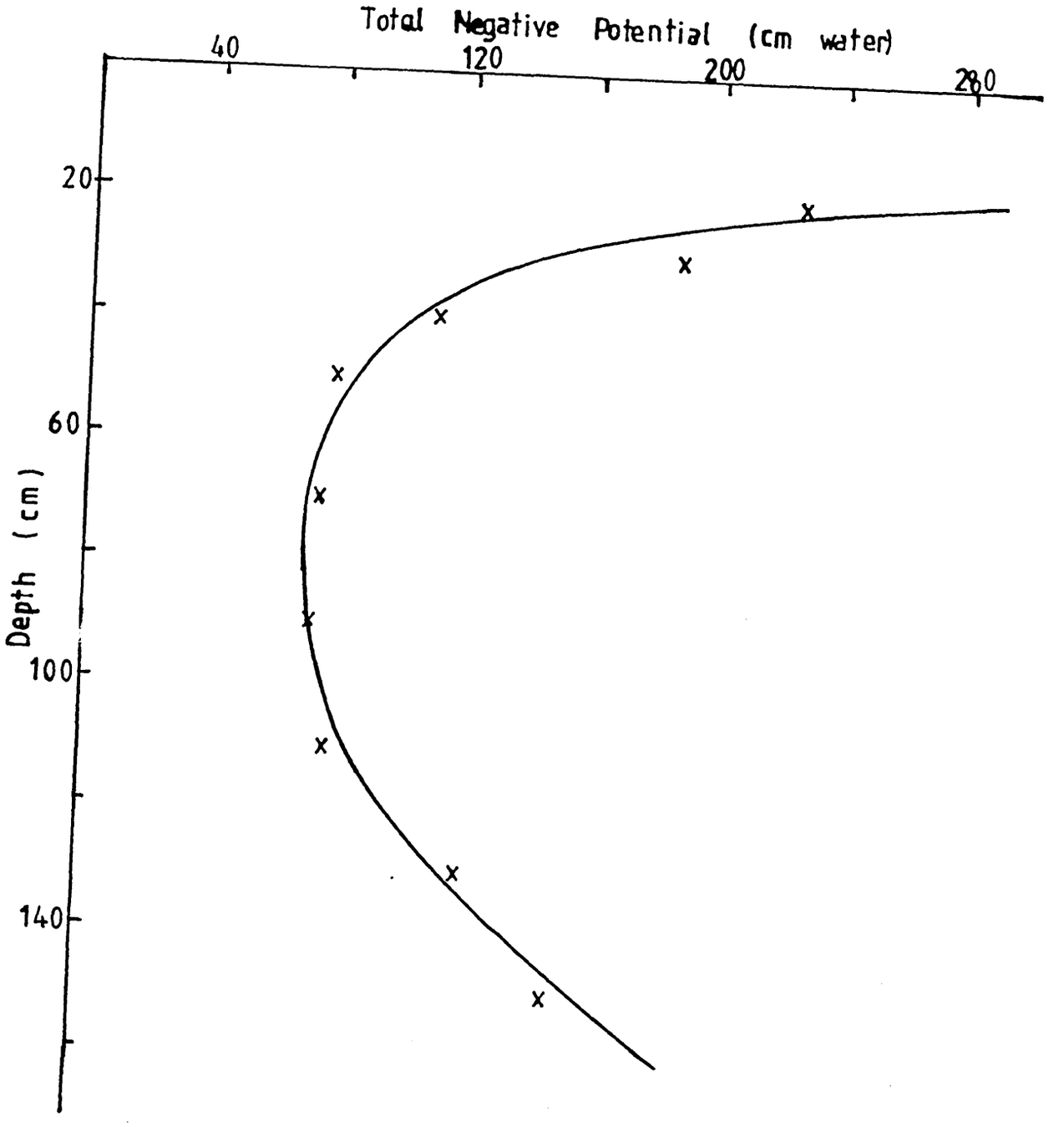

FIG. 6-9 HYDRAULIC HEAD PROFILE
GRASS - 6/07/81

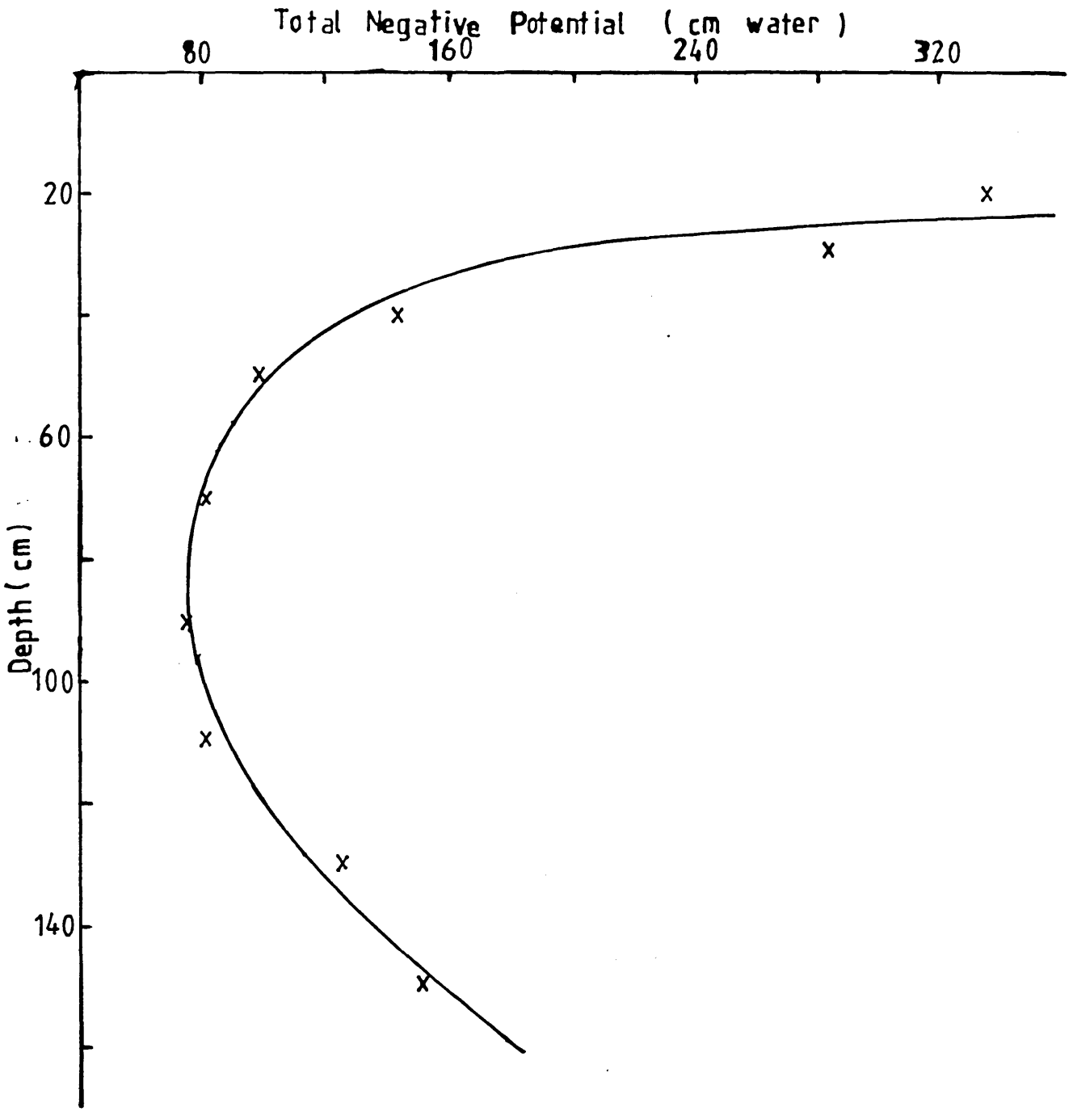

FIG. 6·10 HYDRAULIC HEAD PROFILE
GRASS - 11/07/81

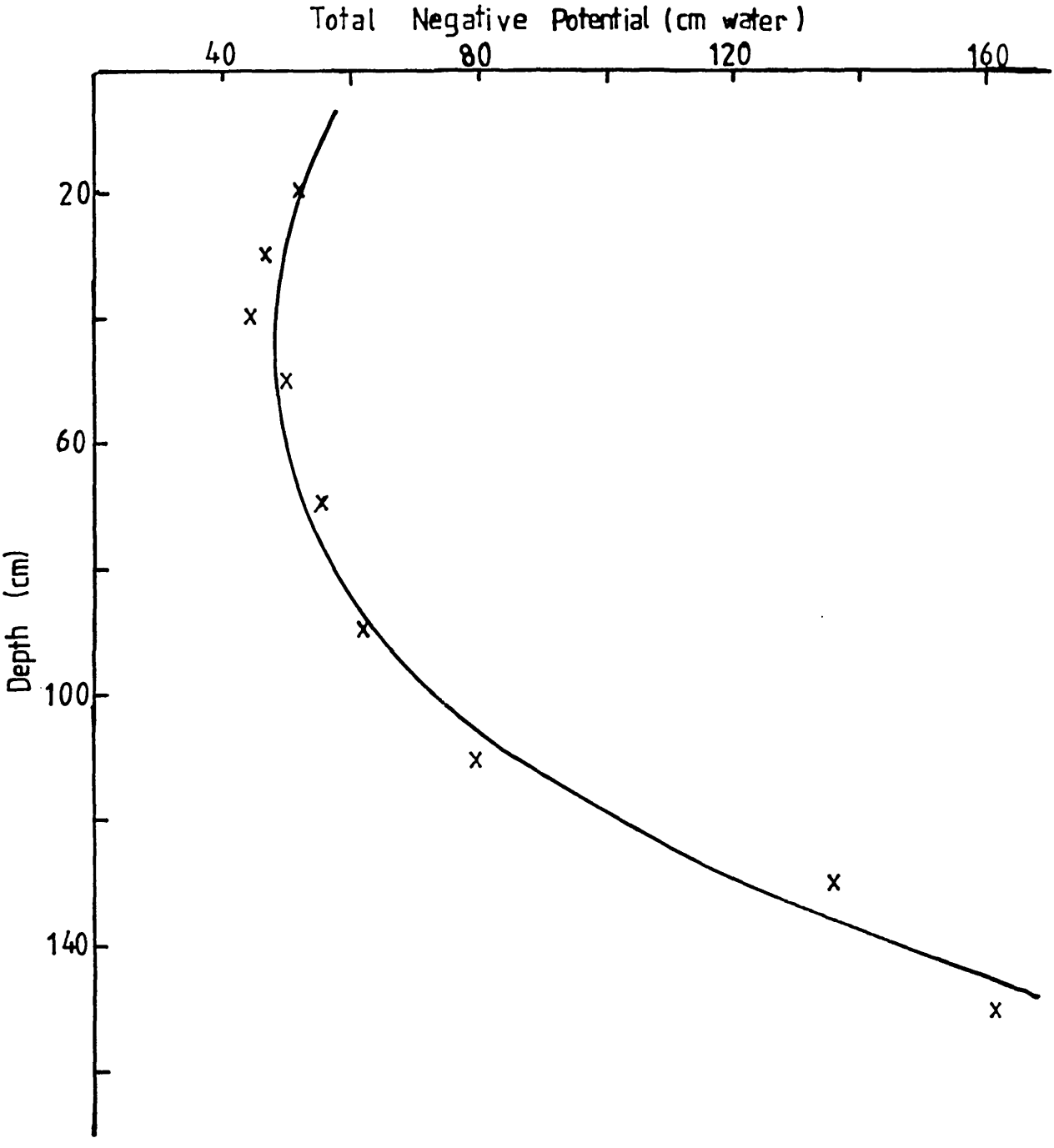

FIG. 6.11 HYDRAULIC HEAD PROFILE
GRASS - 24/07/81

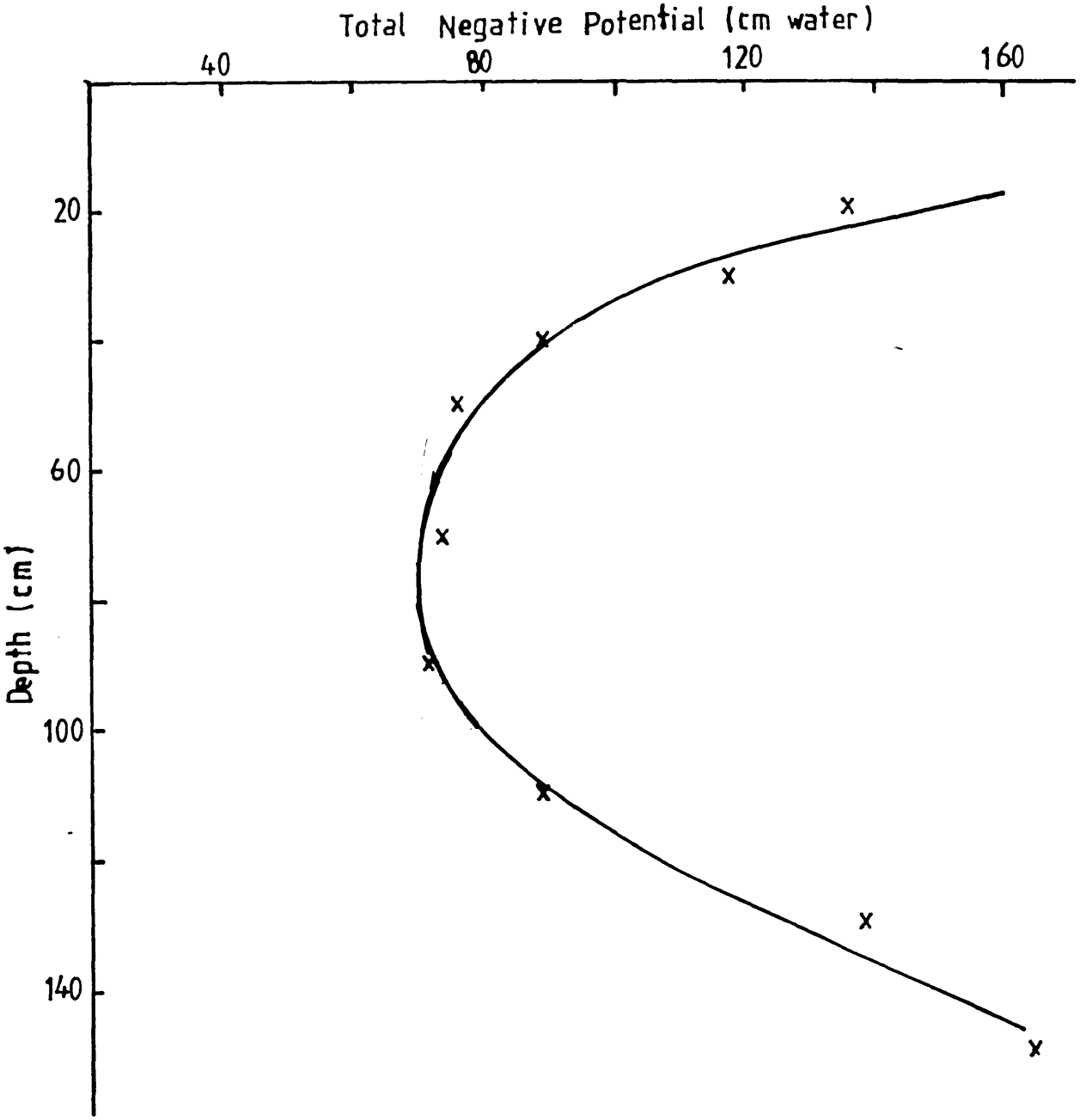

FIG. 6·12 HYDRAULIC HEAD PROFILE
GRASS - 27/07/81

TABLE 6.1a : Water content and change in storage during the drying cycle, summer 1980 (permanent grass) and the unsaturated hydraulic conductivity

Depth (cm)	Layer Moisture (mm) 10880	40880	ΔS (mm)	Mean (mm)	ΔS/t (mm/day)	$\frac{(dH)}{dZ}$ (cm/cm)	K (mm/day)	θ (cm^3/cm^3)
0-15	45.19	36.19						
			-1.11					
15-25	24.37	23.80		-0.85	-0.28	0.99	0.27	0.241
			-0.54					
25-35*	22.66	21.58						
			-0.54					
35-45	21.65	20.57		-1.08	-0.36	-0.57	0.63	0.211
			-1.62					
45-55	20.00	19.62		-1.81	-0.60	-0.77	0.77	0.198
			-2.00					
55-65	18.42	18.48		-1.97	-0.66	-0.51	1.29	0.185
			-1.94					
65-75	17.59	17.66		-2.11	-0.70	-0.32	2.19	0.176
			-2.27					
75-85	17.28	17.41		-2.01	-0.67	-0.33	2.03	0.174
			-1.74					
85-95	21.08	19.81		-2.38	-0.79	-0.49	1.61	0.205
			-3.01					
95-105	28.10	26.20		-3.96	-1.32	-0.79	1.67	0.272
			-4.91					
105-115	36.27	35.32		-5.34	-1.78	-1.39	1.28	0.358
			-5.86					
115-125	33.80	32.15		-6.69	-2.23	-2.15	1.03	0.329
			-7.51					
125-135	34.18	33.04						

* ZFP mean depth

TABLE 6.1b : Water content and change in storage during the drying cycle, summer 1980 (permanent grass) and the unsaturated hydraulic conductivity

Depth (cm)	Layer (mm) 10880	Moisture 80880	ΔS (mm)	Mean (mm)	ΔS/t (mm/day)	$\frac{(dH)}{dZ}$ (cm/cm)	K (mm/day)	θ (cm^3/cm^3)
0-15	45.19	30.94						
			-3.51					
15-25	24.37	22.22		-2.44	-0.34	+1.39	0.25	0.233
			-1.36					
25-35*	22.66	19.94						
			-1.36					
35-45	21.65	19.37		-2.50	-0.35	-0.52	0.68	0.205
			-3.64					
45-55	20.00	18.99		-4.15	-0.59	-0.42	1.40	0.195
			-4.65					
55-65	18.42	18.29		-4.72	-0.67	-0.35	1.92	0.184
			-4.78					
65-75	17.59	16.90		-5.13	-0.73	-0.30	2.44	0.173
			-5.47					
75-85	17.28	17.59		-5.32	-0.76	-0.38	2.00	0.174
			-5.16					
85-95	21.08	20.70		-5.35	-0.76	-0.53	1.43	0.209
			-5.54					
95-105	28.10	26.27		-6.46	-0.92	-0.82	1.12	0.272
			-7.37					
105-115	36.27	35.25		-7.88	-1.12	-1.41	0.79	0.358
			-8.39					
115-125	33.80	32.53		-9.03	-1.29	-2.20	0.58	0.332
			-9.66					
125-135	34.18	33.10						

* ZFP mean depth

TABLE 6.1c : Water content and change in storage during the drying cycle, summer 1980 (permanent grass) and the unsaturated hydraulic conductivity

Depth	Layer Moisture (mm)		ΔS	Mean	ΔS/t	$\left(\frac{dH}{dZ}\right)$	K	θ
(cm)	40880	80880	(mm)	(mm)	(mm/day)	(cm/cm)	(mm/day)	(cm^3/cm^3)
0-15	36.19	30.94						
			-3.22					
15-25	23.80	22.22		-2.43	-0.61	2.2	0.27	0.230
			-1.64					
25-35*	21.58	19.94						
			0.00					
35-45	20.57	19.37						
			-1.20					
45-55	19.62	18.99		-1.52	-0.38	-0.49	0.77	0.193
			-1.83					
55-65	18.48	18.29		-1.93	-0.48	-0.41	1.17	0.184
			-2.02					
65-75	17.66	16.90		-2.40	-0.60	-0.16	3.75	0.173
			-2.78					
75-85	17.14	17.59		-2.69	-0.67	-0.38	1.76	0.175
			-2.60					
85-95	19.81	20.70		-2.16	-0.54	-0.52	1.03	0.203
			-1.71					
95-105	26.20	26.27		-1.68	-0.42	-0.83	0.50	0.262
			-1.64					
105-115	35.32	36.25		-1.68	-0.42	-1.43	0.29	0.358
			-1.71					
115-125	32.15	32.53		-1.52	-0.38	-2.25	0.17	0.323
			-1.33					
125-135	33.04	33.10						

* ZFP mean depth

TABLE 6.2a : Water content and change in storage during the drying cycle, summer 1981 (permanent grass) and the unsaturated hydraulic conductivity

Depth (cm)	Layer Moisture (mm) 260681	300681	ΔS (mm)	Mean ΔS	ΔS/t (mm/day)	$\frac{dH}{dZ}$ (cm/cm)	K (mm/day)	θ (cm^3/cm^3)
0-15	31.69	23.62						
			-2.73					
15-25	22.53	21.27		-2.1	-0.53	6.33	0.08	0.219
			-1.47					
25-35	20.13	20.13		-1.47	-0.37	3.00	0.12	0.201
			-0.90					
35-45	19.05	18.48		-1.19	-0.30	1.71	0.17	0.188
			-0.39					
45-55	18.86	18.35		-0.65	-0.16	1.13	0.14	0.186
			-0.19					
55-65	18.62	18.42		-0.29	-0.07	0.59	0.11	0.185
			0.00					
65-75*	17.90	17.53						
			-0.19					
75-85	18.86	17.85		-0.70	-0.18	-0.14	1.28	0.184
			-1.20					
85-95	23.04	20.57		-2.44	-0.61	-0.50	1.22	0.218
			-3.67					
95-105	28.35	27.34		-4.18	-1.05	-0.68	1.54	0.279
			-4.68					
105-115	35.82	36.01		-4.59	-1.15	-0.98	1.17	0.359
			-4.49					
115-125	35.13	34.75		-4.68	-1.17	-1.30	0.90	0.349
			-4.87					
125-135	35.19	35.63						

* ZFP mean depth

TABLE 6.2b : Water content and change in storage during the drying cycle, summer 1981 (permanent grass) and the unsaturated hydraulic conductivity

Depth (cm)	Layer Moisture (mm) 60781	110781	ΔS (mm)	Mean ΔS	ΔS/t (mm/day)	$\frac{(dH)}{dZ}$ (cm/cm)	K (mm/day)	θ (cm^3/cm^3)
0-15	23.44	18.94						
			-5.98					
15-25	20.89	19.11		-5.09	-1.02			
			-4.20					
25-35	19.68	18.04		-3.38	-0.68	9.0	0.08	0.189
			-2.56					
35-45	17.97	17.03		-2.09	-0.42	3.05	0.13	0.175
			-1.62					
45-55	17.78	17.47		-1.47	-0.29	1.72	0.16	0.176
			-1.31					
55-65	18.16	17.41		-0.94	-0.19	0.92	0.20	0.178
			-0.56					
65-75	17.28	17.03		-0.44	-0.09	0.50	0.18	0.172
			-0.31					
75-85*	17.15	16.84						
			0.00					
85-95	20.06	20.00						
			-0.06					
95-105	25.63	25.13		-0.31	-0.06	-0.67	0.08	0.254
			-0.56					
105-115	36.33	34.75		-1.35	-0.27	-1.14	0.23	0.355
			-2.14					
115-125	34.81	34.11		-2.49	-0.50	-1.58	0.32	0.345
			-2.84					
125-135	35.82	35.00						

* ZFP mean depth

TABLE 6.2c : Water content and change in storage during the drying cycle, summer 1981 (permanent grass) and the unsaturated hydraulic conductivity

Depth (cm)	Layer Moisture (mm) 240781	270781	ΔS (mm)	Mean ΔS	ΔS/t (mm/day)	$\frac{(dH)}{dZ}$ (cm/cm)	K (mm/day)	θ (cm^3/cm^3)
0-15	28.12	25.87						
			-5.67					
15-25	22.15	20.70		-4.95	-1.65	2.39	0.69	0.214
			-4.22					
25-35	20.82	19.37		-3.50	-1.17	1.53	0.76	0.201
			-2.77					
35-45	19.24	17.41		-1.86	-0.62	0.65	0.95	0.183
			-0.94					
45-55	18.10	17.47		-0.63	-0.21	0.42	0.50	0.178
			-0.31					
55-65*	17.72	17.41						
			0.00					
65-75	16.84	16.65						
			-0.19					
75-85	17.28	17.03		-0.32	-0.11	-0.33	0.33	0.172
			-0.44					
85-95	19.75	18.99		-0.82	-0.27	-0.62	0.43	0.194
			-1.20					
95-105	25.38	25.82		-0.98	-0.33	-1.00	0.33	0.256
			-0.76					
105-115	35.38	35.38		-0.76	-0.25	-1.64	0.15	0.354
			-0.76					
115-125	34.24	35.99						
125-135	34.62	34.56						

* ZFP mean depth

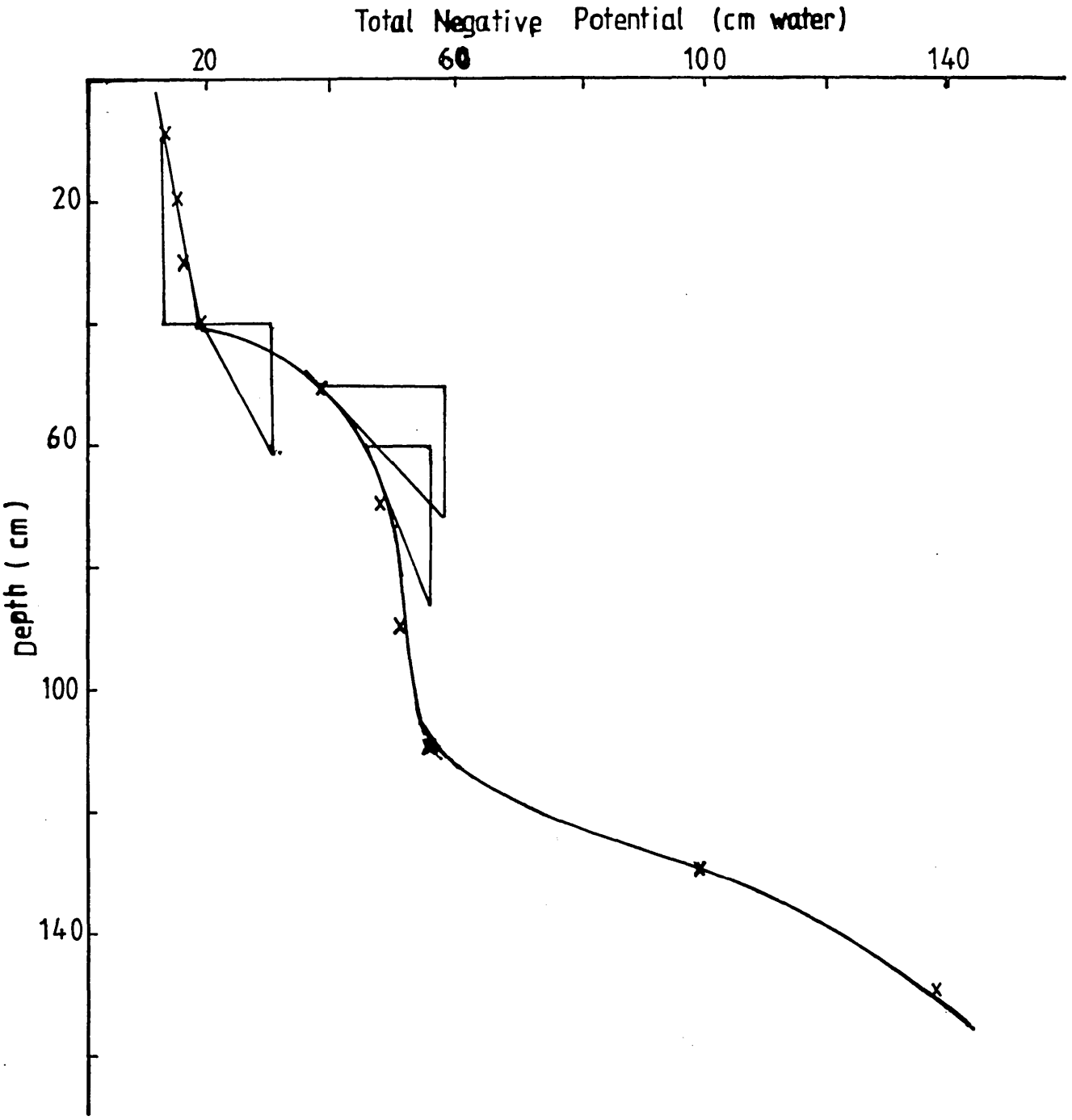

FIG. 6·13 HYDRAULIC HEAD PROFILE
GRASS - 1/05/81 (WETTING CYCLE)

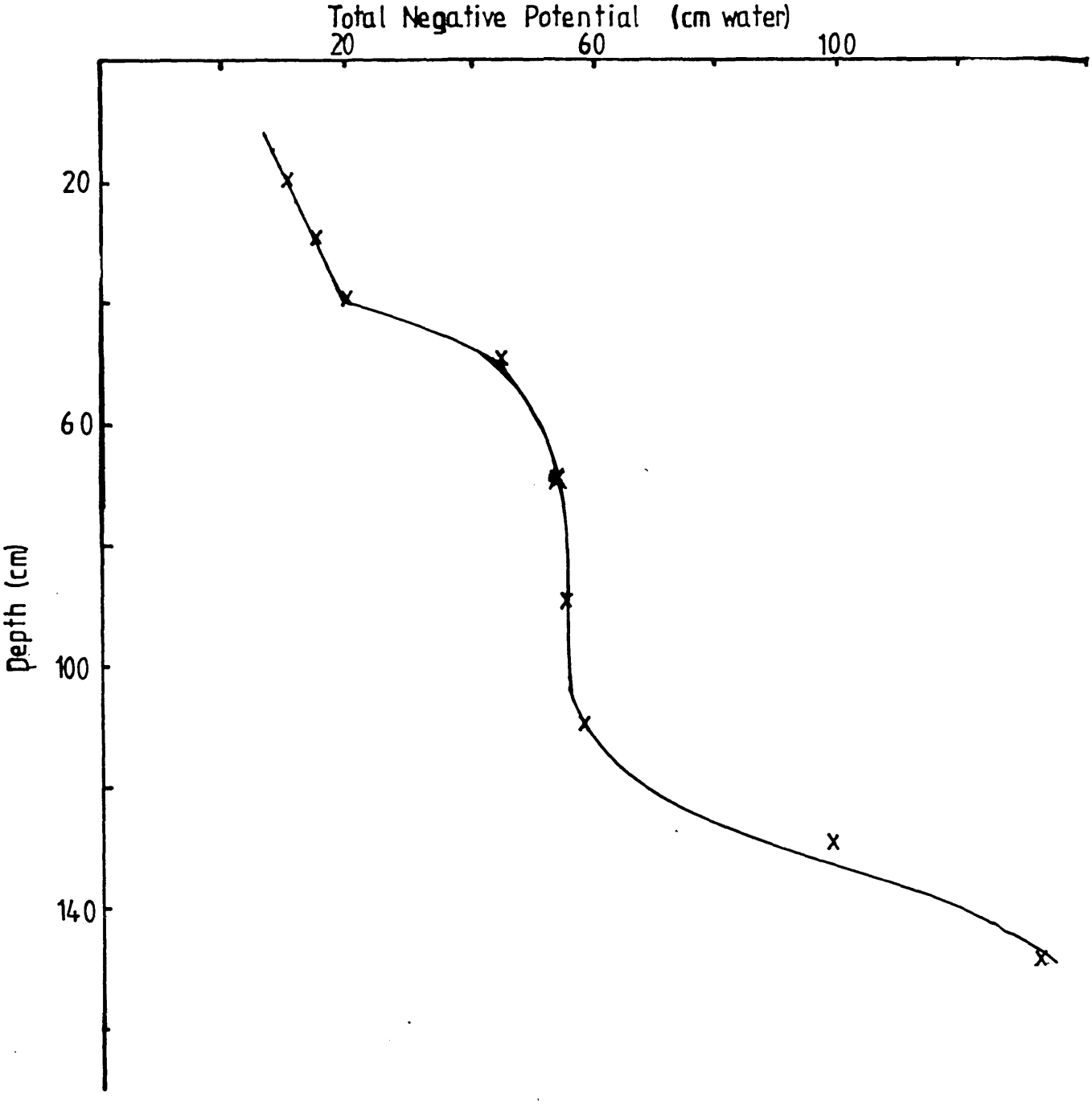

FIG. 6-14 HYDRAULIC HEAD PROFILE
GRASS - 8/05/81

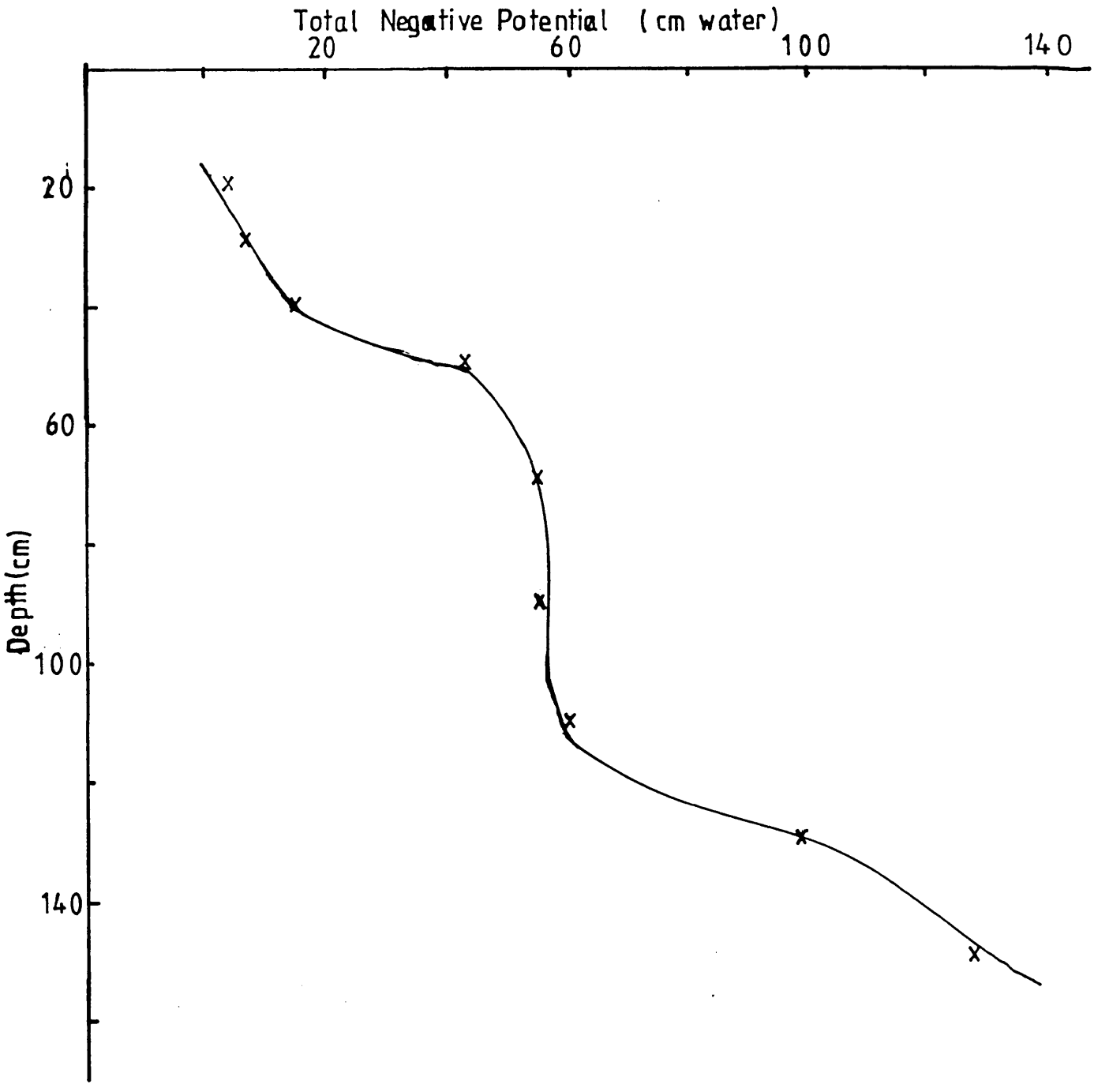

FIG. 6·15 HYDRAULIC HEAD PROFILE
GRASS - 11/05/81 (WETTING CYCLE)

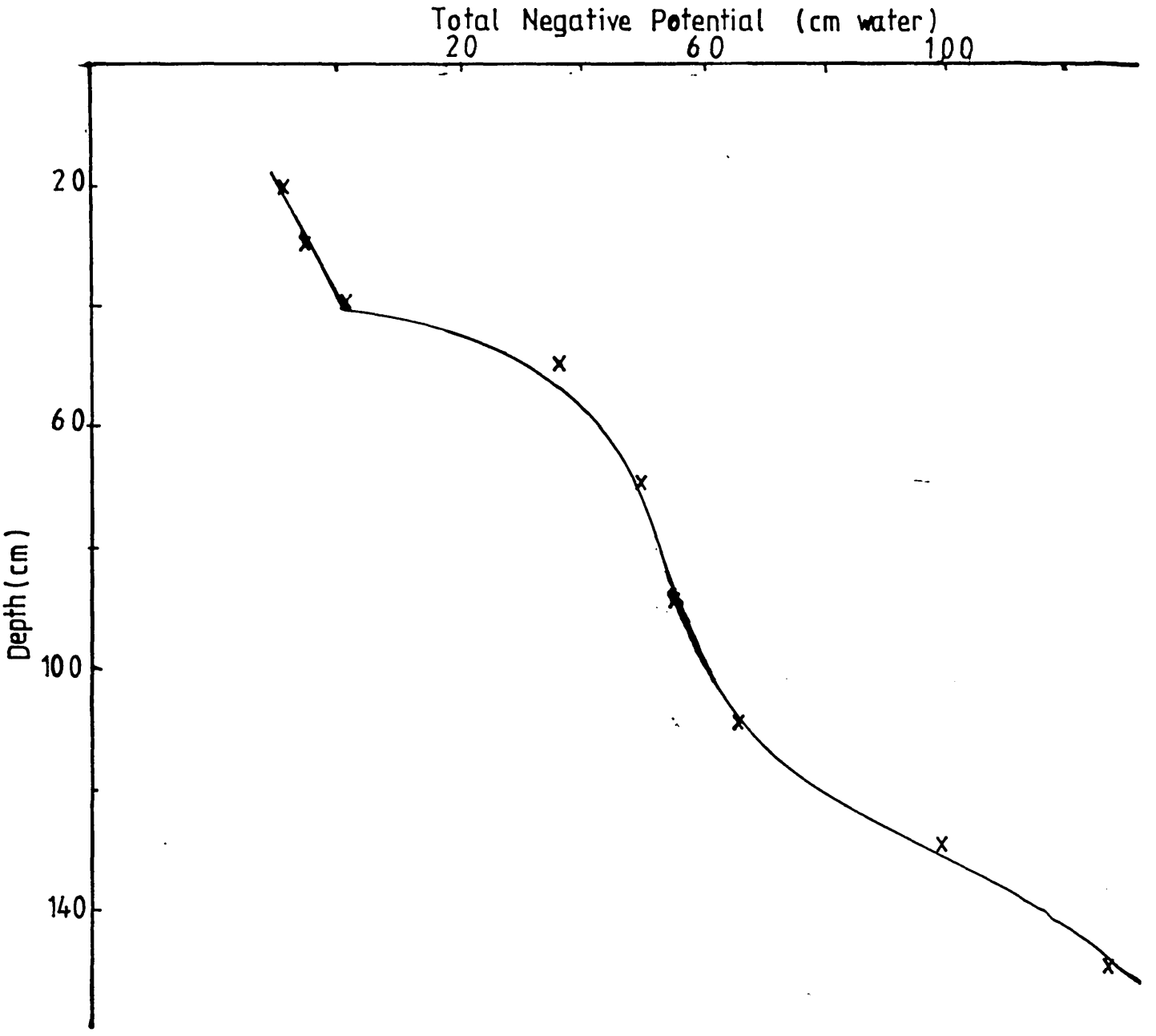

FIG. 6.16 HYDRAULIC HEAD PROFILE
GRASS- 19/05/81 (WETTING CYCLE)

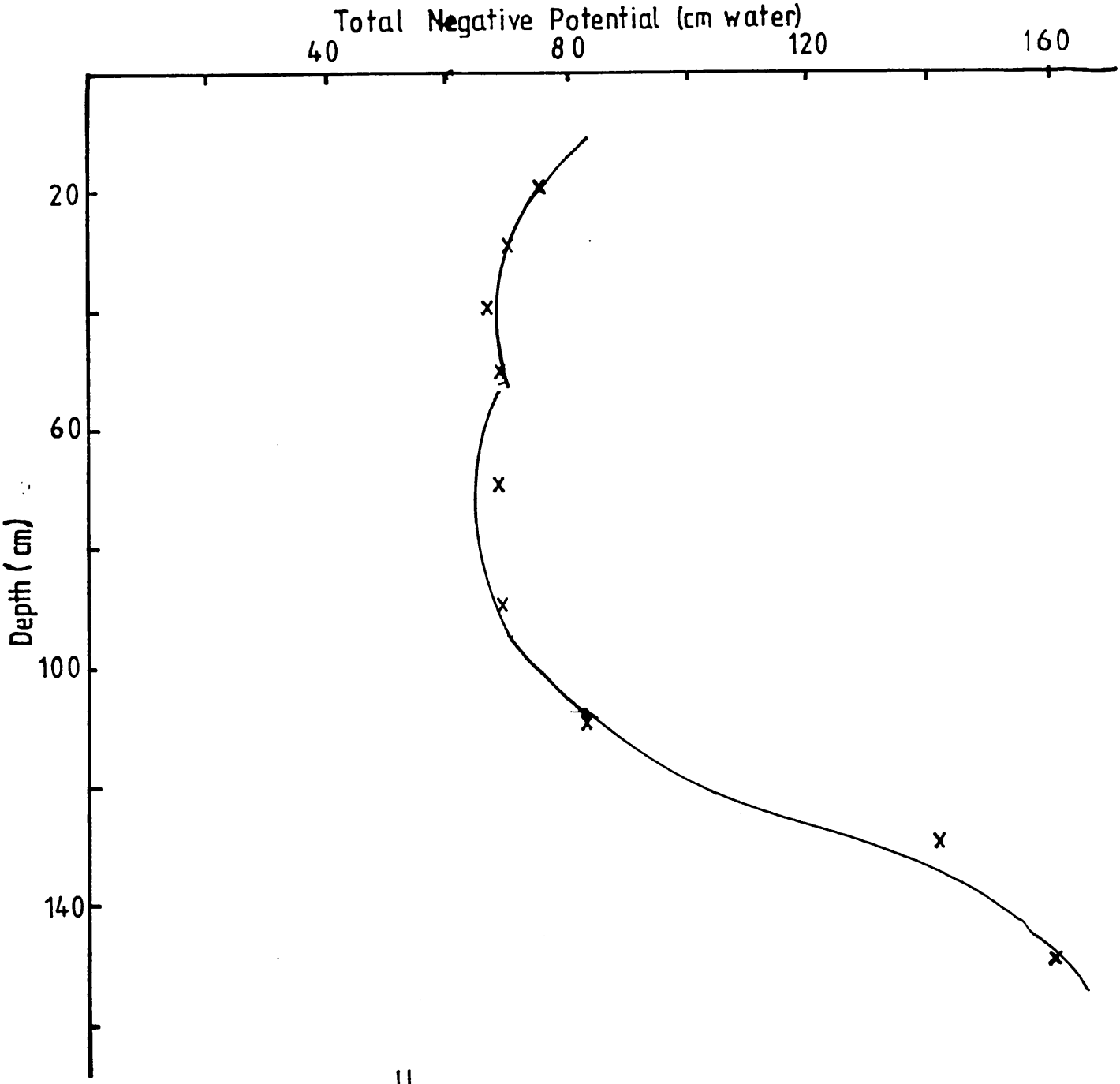

FIG.6.17 HYDRAULIC HEAD PROFILE
GRASS - 3/08/81 (WETTING CYCLE)

TABLE 6.3a : Water content and change in storage during the wetting cycle, summer 1981 (permanent grass)

Depth (cm)	Layer Moisture (mm) 80581	110581	ΔS (mm)	Mean ΔS	ΔS/t (mm/day)	$(\overline{\frac{dH}{dZ}})$ (cm/cm)	K (mm/day)	$\overline{\theta}$ (cm^3/cm^3)
0-15	49.50	53.25	3.11					
15-25	27.25	28.20	2.16	2.64	0.88	0.52	1.69	0.277
25-35	24.47	25.17	1.46	1.81	0.60	0.52	1.15	0.248
35-45	22.82	23.71	0.57	1.02	0.34	1.13	0.30	0.232
45-55	20.86	21.43	0.00	0.29	0.10	1.61	0.06	0.212

TABLE 6.3b : Water content and change in storage during the wetting cycle, summer 1981 (permanent grass)

Depth (cm)	Layer Moisture (mm) 110581	190581	ΔS (mm)	Mean ΔS	ΔS/t (mm/day)	$(\overline{\frac{dH}{dZ}})$ (cm/cm)	K (mm/day)	$\overline{\theta}$ (cm^3/cm^3)
0-15	53.25	57.56	9.75					
15-25	28.20	30.23	7.72	8.74	1.09	0.79	1.38	29.18
25-35	25.17	26.88	6.01	6.87	0.86	0.54	1.59	25.99
35-45	23.17	25.36	4.36	5.19	0.65	1.14	0.57	24.50
45-55	21.43	22.44	3.35	3.86	0.48	2.01	0.23	21.90
55-65	19.22	22.57	0.00	1.68	0.20	0.60	0.33	20.90
65-75	18.84	18.77						

TABLE 6.3c : Water content and change in storage during the wetting cycle, summer 1981 (permanent grass)

Depth (cm)	Layer Moisture (mm) 270781	30881	ΔS (mm)	Mean ΔS	ΔS/t (mm/day)	$(\overline{\frac{dH}{dZ}})$ (cm/cm)	K (mm/day)	$\overline{\theta}$ (cm^3/cm^3)
0-15	25.87	34.50	8.97					30.19
15-25	20.74	23.46	6.25	7.61	1.08	2.62	0.41	22.10
25-35	19.41	20.92	4.74	5.50	0.78	1.68	0.46	20.17
35-45	17.44	18.77	3.41	4.08	0.58	0.77	0.75	18.11
45-55	17.51	18.01	2.91	3.16	0.45	0.37	1.21	17.76
55-65	17.44	18.01	2.34	2.63	0.37	0.36	1.03	17.73
65-75	16.68	17.06	1.96	2.15	0.30	0.13	2.30	16.87
75-85	17.06	17.44	1.58	1.77	0.25	0.11	2.27	17.25
85-95	19.03	20.23	0.38	0.98	0.14	0.42	0.33	19.63
95-105	25.86	26.24	0.00	0.19	0.02	0.81	0.02	26.05

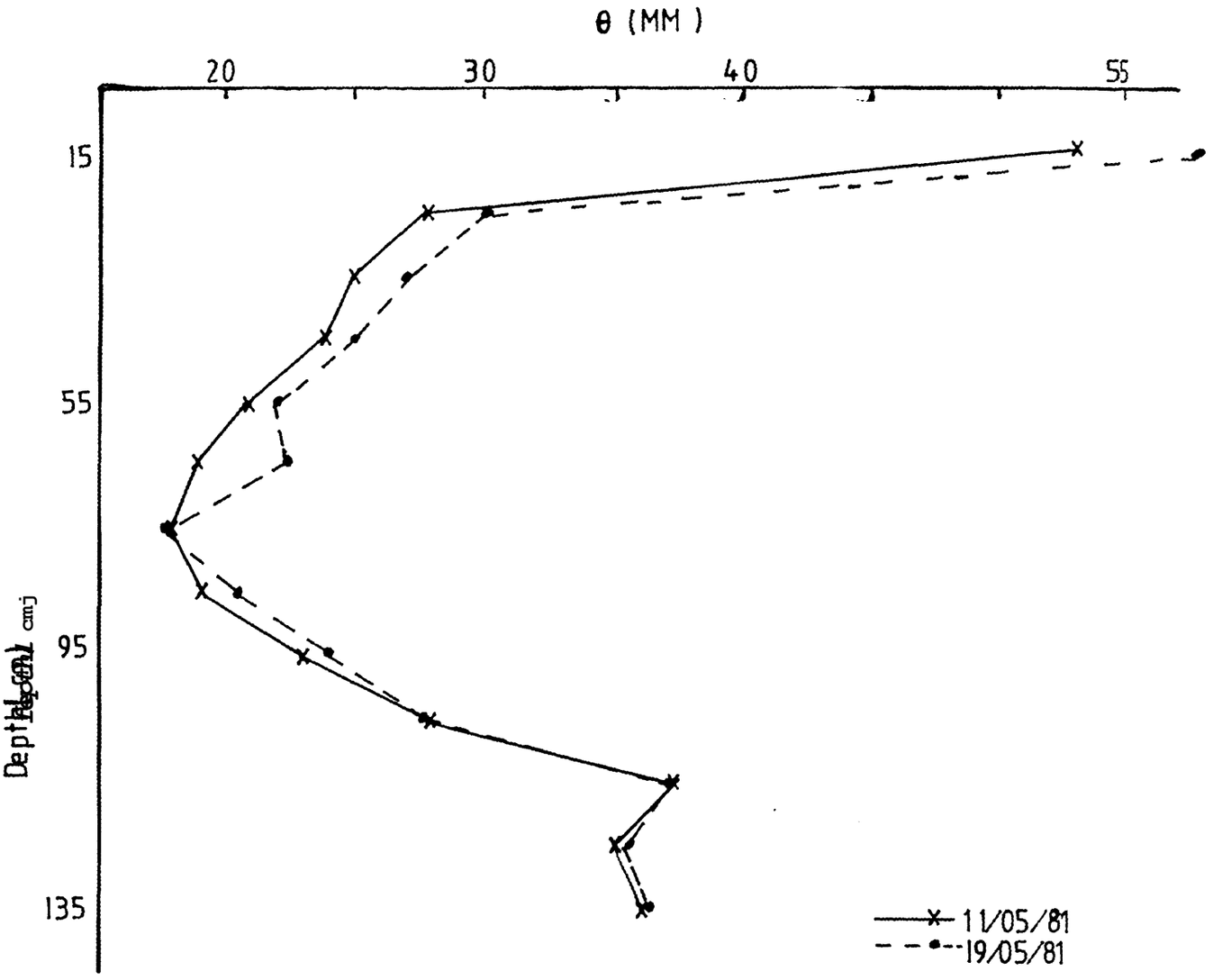

FIG. 6·18 MOISTURE PROFILES
WETTING CYCLE - GRASS

The values of unsaturated hydraulic conductivity used for the various layers and corresponding average volumetric moisture contents are presented in Table 6.4 (Figures 6.19-6.21). The constants in the linear regression equation of the form log k = log a + bθ and corresponding correlation coefficients are shown in Table 6.5.

Generally, there is a fairly good correlation between the unsaturated hydraulic conductivity and volumetric moisture content values ranging from 0.60 to 0.99. It is worth mentioning that although the data points are at most five in some layers, the minimum number of data points is three, and this was obtained for only one layer, the 55-65 cm layer. Unfortunately though, the k(θ) relationship for the 0-15 cm layer could not be obtained by the technique. This is attributable to the calculation procedure adopted. This involved obtaining the average change in storage between layers to coincide with the change in moisture storage occurring at the corresponding depth of measurement of the moisture content and soil water potential readings.

The 15-25 cm and 25-35 cm layers were observed to have similar characteristics as shown in Table 6.4 and Figure 6.19. For the 0-15 cm layer however, it was decided to extrapolate the 15-25 cm layer k(θ) values, since k(θ) values obtained for those layers for a similar soil type by Lawlor (1972) were very similar.

A noticeable feature observed in the k(θ) value for the permanent grass (Table 6.4, Figures 6.19-6.21) is the variability in k(θ) values between the layers particularly at 65-75 and 75-85 cm layers, where high k(θ) values were obtained despite the relative lower volumetric moisture content prevalent at these layers. This suggests that an impeding layer might be present especially when lower k(θ) values were obtained below these layers for relatively higher moisture contents. The latter confirms what has been suggested earlier in Chapter 5 on site description. The occurrence of the impeding layer adds another complexity to model result interpretation especially when temporary saturation occurs at the impeding layer. This may lead to capillary rise and lateral flow thus invalidating the inherent assumption of one-dimensional flow in the model operation. However since the model testing was carried out predominantly for summer periods when zero flux-planes were observed, the restriction of subsoil per-

TABLE 6.4 : Unsaturated hydraulic conductivity data (permanent grass)

Depth (cm)	q	$\overline{(\frac{dH}{dz})}$	K (mm/day)	$\overline{\theta}$ Mean Moisture Content cm/cm
	1.09	0.79	1.38	0.292
	0.88	0.52	1.69	0.277
15-25	0.85	0.99	0.27	0.241
	0.34	1.39	0.25	0.233
	0.53	6.33	0.08	0.219
	0.86	0.54	1.59	0.260
	0.60	0.52	1.15	0.248
25-35	0.37	3.00	0.12	0.201
	0.68	9.00	0.08	0.189
	0.65	1.14	0.57	0.245
	0.34	1.13	0.30	0.232
35-45	0.30	1.71	0.17	0.188
	0.42	3.05	0.13	0.175
	0.59	0.42	1.40	0.195
	0.38	0.49	0.77	0.193
45-55	0.21	0.42	0.50	0.178
	0.16	1.13	0.14	0.186
	0.29	1.72	0.16	0.176
	0.66	0.51	1.29	0.185
55-65	0.48	0.41	1.27	0.184
	0.19	0.92	0.20	0.178
	0.70	0.32	2.19	0.176
	0.60	0.16	3.75	0.173
65-75	0.73	0.30	2.44	0.173
	0.30	0.13	2.30	0.169
	0.76	0.38	2.00	0.174
	0.67	0.33	2.03	0.174
75-85	0.25	0.11	2.27	0.173
	0.11	0.33	0.33	0.171
	0.76	0.53	1.43	0.209
	0.79	0.49	1.61	0.205
85-95	0.54	0.52	1.03	0.203
	0.14	0.42	0.33	0.196
	0.27	0.62	0.43	0.194
	1.05	0.68	1.54	0.279
	0.92	0.82	1.12	0.272
95-105	0.42	0.83	0.50	0.262
	0.33	1.00	0.33	0.256
	0.06	0.67	0.08	0.254

Table 6.4 Continued

Depth (cm)	q	$(\frac{\overline{dH}}{dZ})$	K (mm/day)	$\overline{\theta}$ Mean Moisture Content cm/cm
	1.15	0.98	1.17	0.359
	1.78	1.39	1.28	0.358
105-115	1.12	1.41	0.79	0.358
	0.27	1.14	0.23	0.355
	0.25	1.64	0.15	0.354
	1.17	1.30	0.90	0.349
	0.50	1.58	0.32	0.345
115-125	1.29	2.20	0.58	0.332
	0.38	2.25	0.17	0.323

TABLE 6.5 : Regression constants describing $K(\theta)$ for different layers

Depth (cm)	log a	b	Correlation Coefficient
15-25	-4.77	17.38	0.96
25-35	-4.72	19.08	0.99
35-45	-2.32	8.16	0.97
45-55	-6.79	34.52	0.68
55-65	-22.40	121.98	0.99
65-75	-4.67	29.75	0.60
75-85	-60.94	352.45	0.84
85-95	-9.39	46.17	0.93
95-105	-11.73	43.09	0.91

FIG.6.19 UNSATURATED HYDRAULIC CONDUCTIVITY-WETNESS RELATIONSHIPS

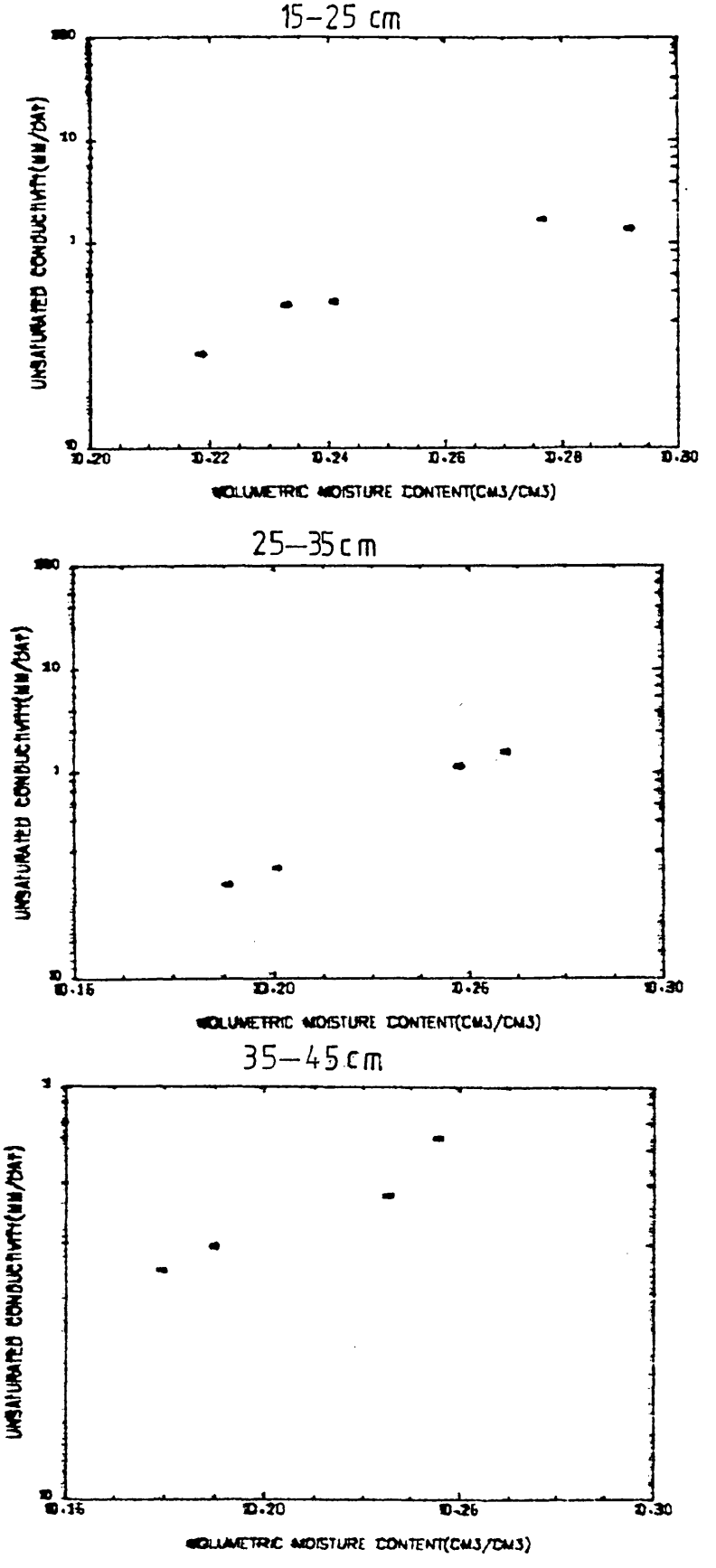

FIG.6.20 UNSATURATED HYDRAULIC CONDUCTIVITY-WETNESS RELATIONSHIPS

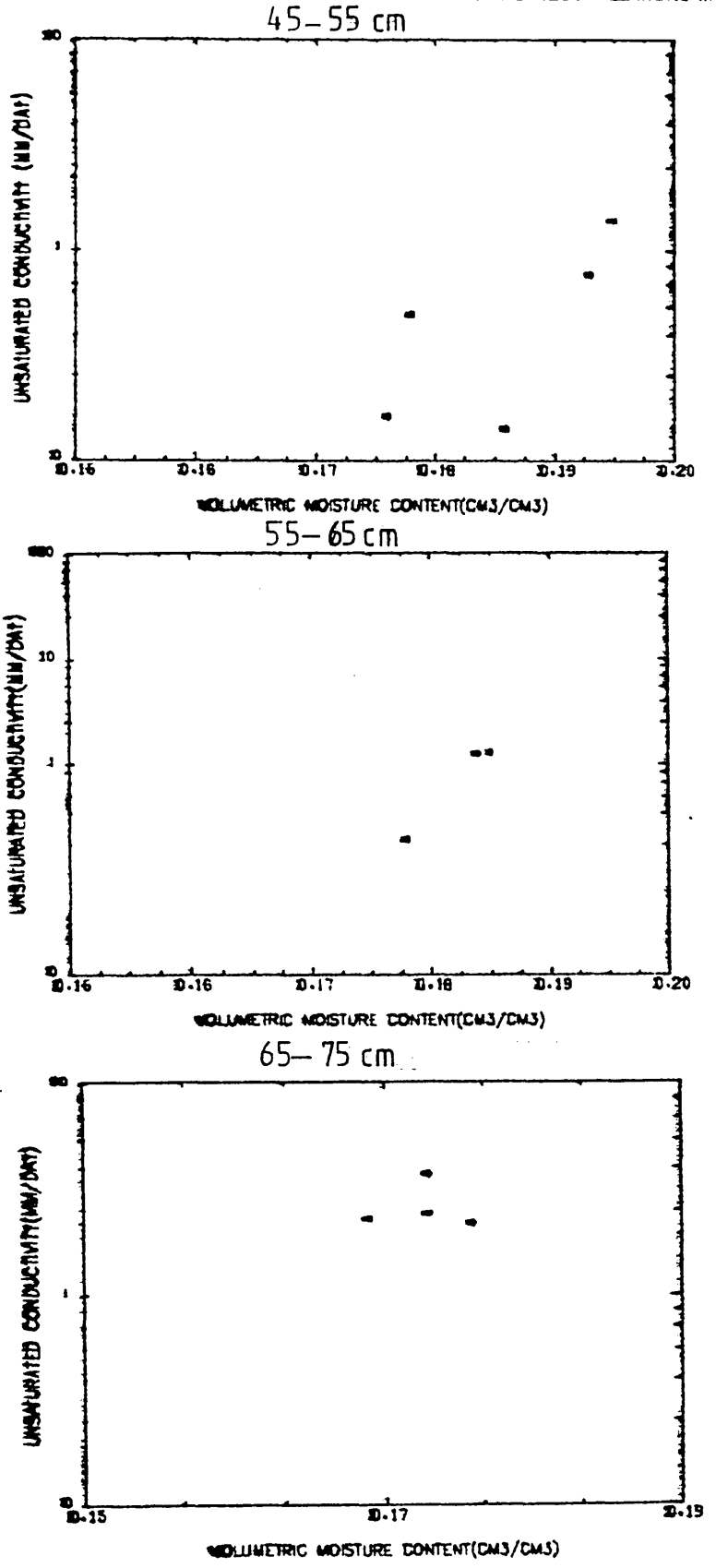

FIG.6.21 UNSATURATED HYDRAULIC CONDUCTIVITY–WETNESS RELATIONSHIPS

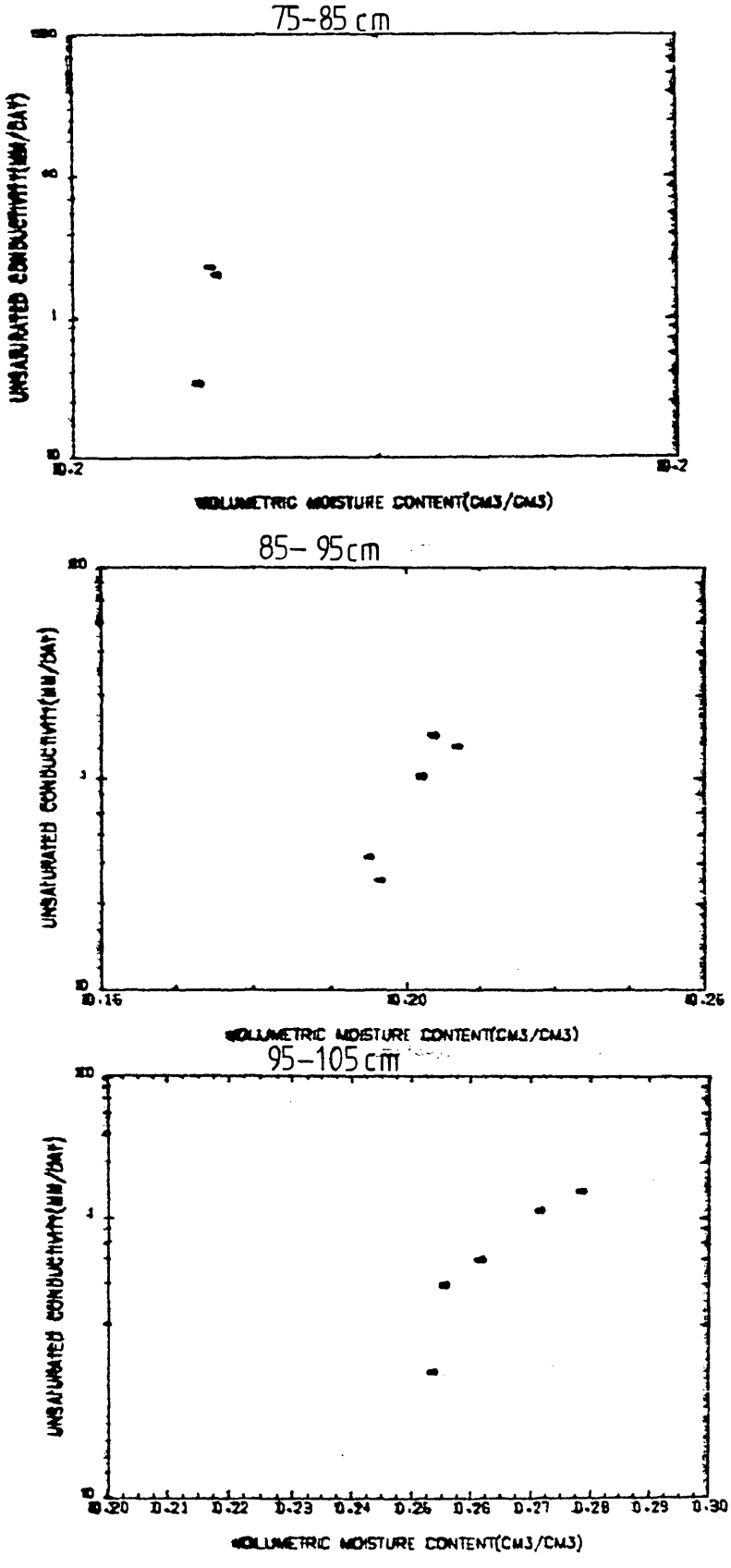

meability may not be too great a factor to significantly interfere with model predictions at these lower depths.

Between the 15-45 cm layers (Table 6.4) a wider range of moisture contents are obtained than at lower layers. This indicates the effects of evapo-transpiration at these shallower depths, since more moisture is being lost relative to deeper layers as a result of root abstraction.

Similar analyses carried out for the wheat plot showed greater variability in the $k(\theta)$ values. The data obtained is scanty for meaningful deductions to be made. Consequently, the physically based soil water model evaluation is concentrated on the permanent grass plot.

6.5.2 Soil Moisture Characteristics

Figures 6.22a, 6.22b, 6.22c and 6.22d show the matric potential/volumetric moisture content relationships for the different layers. It is evident from the correlation coefficients obtained that the 0-15 and 15-25 cm layers can be represented by the same soil moisture characteristic curve. The latter is true also of the 25-35 and 35-45 cm layers and the 45-75 cm layer. The corresponding correlation coefficients are 0-25 cm (R^2 = 0.68), 25-45 cm (R^2 = -0.74) and 45-75 cm (R^2 = -0.80). The results indicate that the variations in soil moisture characteristics are not as pronounced as those obtained in the $k(\theta)$ relationship.

6.6 Conclusions

On the whole, the natural balance technique has been shown to offer promise for future use. Although certain errors have been shown to affect the derived $k(\theta)$ values, the results obtained reveal that the moisture content range is low for the soil in the permanent grass plot. The above is an indication of the sandy nature of the profile. The $k(\theta)$ values in the 15-65 cm layer at most volumetric moisture contents are below 1.5 mm/day which indicates a low unsaturated hydraulic conductivity at the given moisture contents. This latter characteristic probably accounts for the occasional ponding observed during and immediately after precipitation in the permanent grass plot.

FIG 6 22 SOIL MOISTURE CHARACTERISTICS

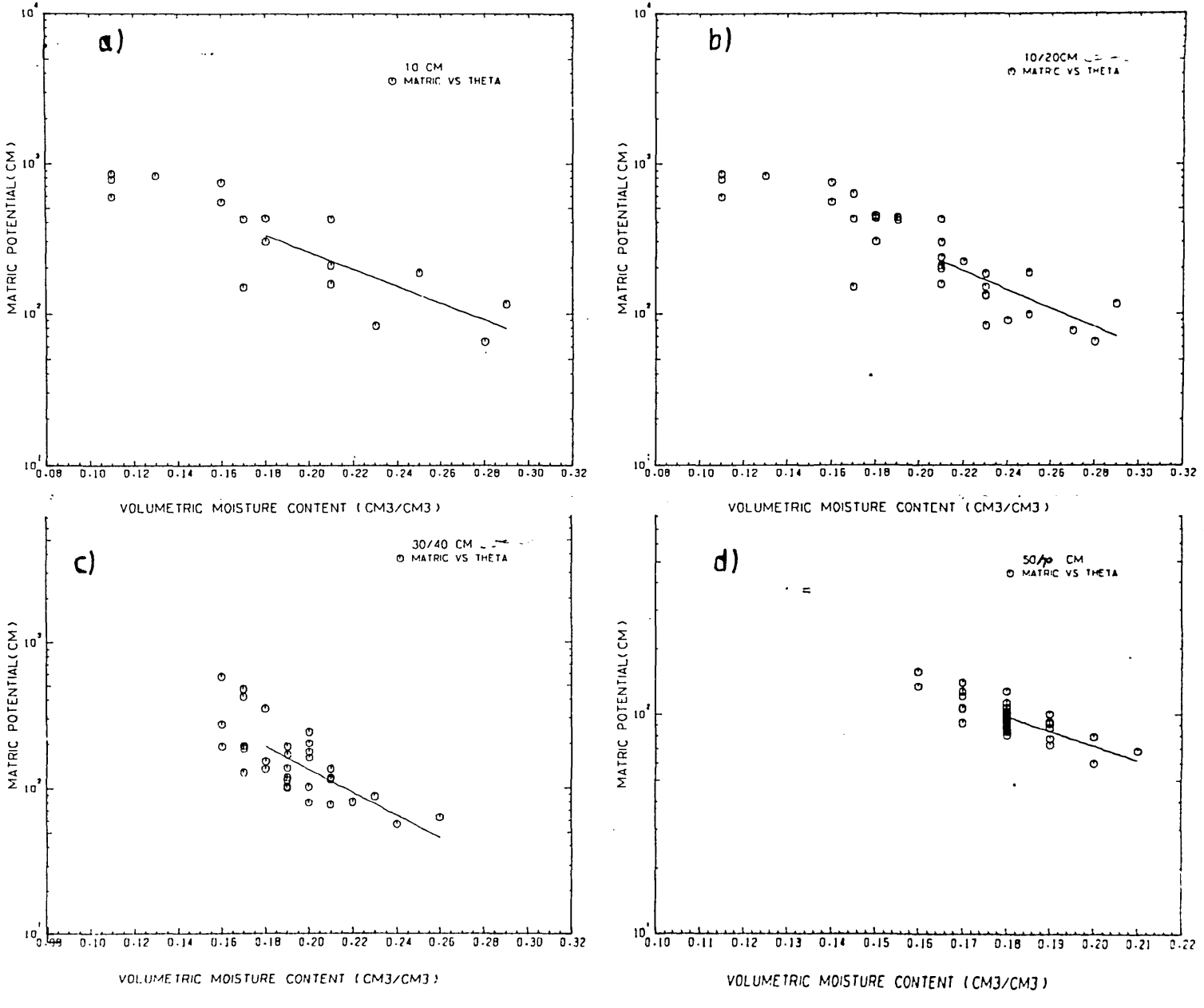

The variations in soil moisture characteristics on the other hand are low. In actual fact, a single moisture characteristic has been shown to be applicable to several layers.

CHAPTER 7

EVALUATION OF THE PHYSICAL SOIL WATER MODEL

7.1 Introduction

Earlier discussion in Chapter 4 focussed on the details of the computational techniques involved in the field application of a physically based soil water model adopted for performance testing in this study.

The significance of the soil and root hydraulic parameters in the efficient operation of dynamic simulation models has also been highlighted in Chapters 3 and 6.

This chapter presents the results obtained from the adopted physically-based soil water model outlined in Chapter 4 when applied for validation testing under the permanent grass plot. The methodologies utilised for assigning the soil and root hydraulic resistance values and the iterative technique for deriving appropriate crown potential values are discussed. Finally, the simulation results that were obtained and their subsequent comparisons with observed layer moisture contents are presented.

7.2 Soil Hydraulic Resistance

This is the component of the total resistance encountered by moisture movement through the soil (Feddes and Rijtema, 1972 and Hillel, 1977). Essentially, the soil resistance is inversely proportional to the unsaturated hydraulic conductivity and the length of the roots per unit volume of soil (Gardner, 1964) as presented in equation 3.19

A prime consideration in the utility of the preceding expression to describe the soil hydraulic resistance involves the evaluation of the length of roots per unit volume of soil. This evaluation has been approached in different ways by several workers (Cowan, 1965; Lawlor, 1972; and Tinker, 1976) usually from the microscopic perspective of the root system as idealised by Gardner (1964). The latter normally involves an assessment of the root radius

(Federer, 1979) and the determination of the relative root length as a fraction of active roots under a given area of soil surface (Hillel et al., 1976) or an assessment of rooting density as a fraction of the total density in the root profile (De Jong and Cameron, 1979). Whatever approach is adopted, it becomes apparent that an estimate of the actual rooting depth of the test crop should be carried out in order to ascertain the root abstraction layers. During the summer months of 1981 and 1982, samplings of rooting depths were carried out under the various crops in which moisture content data are recorded. The results obtained have earlier been presented in Chapter 5, Table 5.3. The maximum observed depth of rooting was 28.8 cm for the permanent grass. The relative constancy in observed rooting depth for the two-year period, despite the random nature of the sampling confirms the observation made by Feddes and Rijtema (1972), that a grass root system does not change significantly with time. An identical result was also obtained by Lawlor (1972) under laboratory conditions in a similar soil type to that used in this study. Lawlor measured the total length of grass roots under unit surface area and obtained 1,400 cm roots per cm^2 of soil surface. This value falls within the range given by Newman (1969) for perennial grass crops of 100-4,000 cm/cm^2. Table 7.1 gives the root length results obtained by Lawlor under grass for the different rooting depths. Classificiation into large and small roots was carried out on the basis of root radius; 0.1 cm for large roots and 0.005 cm for the small roots.

TABLE 7.1 : Root density distribution (cm/cm^3)

Depth (cm)	Large Roots	Small Roots	Total	Relative Distribution
0-5	9.0	40.0	49.0)	0.45
5-10	4.0	19.0	23.0)	
10-15	2.5	15.0	17.5)	0.23
15-20	2.5	16.5	19.0)	
20-25	1.5	17.5	19.0)	0.32
25-35	2.0	30.0	32.0)	

Considering the labour and time required to obtain representative root counts under the different test crops, coupled with the non-availability of the laboratory resources needed to assess the root distribution pattern, it was decided to use Lawlor's results in Table 7.1 as an approximation of the root distribution pattern of the grass root system in the study area. This is because Lawlor's values were obtained from a similar soil type under grass. Subsequently, a procedure similar to De Jong and Cameron (1979) was used to derive appropriate root density as a fraction of the total root length within the profile from results in Table 7.1. The values obtained and later used for the simulation of the physical soil water model are also shown in Table 7.1.

7.3 Root Hydraulic Resistance

The application of equation 4.7 requires estimated values of the specific hydraulic resistance of the cortex. The conductive component of the root hydraulic resistance is important in tall crops but is often neglected in low growing crops like grass (Feyen *et al.*, 1980). However, the measurement of the root hydraulic resistance under *in situ* conditions has generally been elusive. This is because there are no techniques currently available to monitor *in situ* the changing hydraulics of growing roots in the soil. In order to circumvent the measurement of this parameter, previous workers (Hillel *et al.*, 1976 and Belmans *et al.*, 1979) have attempted to assign values to the hydraulic resistance of the cortex in equation 4.7 by assuming various values to depict sparse and dense rooting systems. For the purpose of validation, the following procedure was used to provide a range in which the cortex hydraulic resistance may lie.

7.3.1 Procedure for Estimating Cortex Hydraulic Resistance

Equation 4.12 gives the expression for the root abstraction term in equation 3.17. For the purpose of clarity, equation 4.12 is reproduced below:

$$ABST(I) = \frac{POTH(I) - POCR}{RS(I) + RR(I)} \qquad (7.1)$$

RR represents the root hydraulic resistance which is proportional to the hydraulic resistance of the cortex and inversely proportional to the length of roots per unit volume of soil (Feyen *et al.*, 1980). The

application of the above equation requires an estimate of two unknown terms, the crown potential (POCR) and RR. Soil hydraulic resistance (RS) can be obtained from the unsaturated hydraulic conductivity-wetness relationship while the total soil water head (POTH) can be obtained from tensiometer data. In order to solve equation 7.1 the following steps were deemed necessary:

7.3.1.1 Water Balance

The sink term (ABST) in the above equation 7.1 is synonymous with the actual evapotranspiration of the plant. Consequently, if appropriate values of POCR and RR are to be obtained, optimisation of the actual flux with the calculated flux from the above equation must be carried out.

In order to obtain the actual evapotranspiration occurring in the grass plot, it is necessary that a water balance be carried out. It is evident that the estimation of the actual evapotranspiration component of the water balance equation hinges primarily on the precise location of the depth in the soil that separates the upward and downward fluxes occurring within the soil profile. This separation is often difficult to attain during the winter months since the gravitational gradient is dominant. However, in the summer months when sparse rainfall occurs, tensiometric readings facilitate the location of zero flux planes (Section 6.2.3) or, alternatively, a graphical inspection of the temporal variation of layer moisture contents could reveal a depth of acute change of slope, signalling the presence of a drying front (McGowan and Williams, 1980).

In the summer months of 1981 (May-July), the plots of the hydraulic head profiles under the permanent grass revealed the occurrence of zero-flux plane depths. The hydraulic head profiles are shown in Figures 7.1a - 7.1d. Figures 7.1a and 7.1b show that a draining profile obtains between day 121 and day 149. Beyond day 149, a drying profile ensues as evidenced by the occurrence of zero flux plane on day 156 at 30 cm depth, and its progression through the 40 cm depth on day 166 and ultimately reaching a depth of 90 cm on day 173. This latter depth was retained until day 201, beyond which convergent zero flux planes were noticeable on days 205 and 208. It is however worth mentioning that the interpretation of the zero flux plane is

FIG.7-1a HYDRAULIC HEAD PROFILES PERM. GRASS(1981)

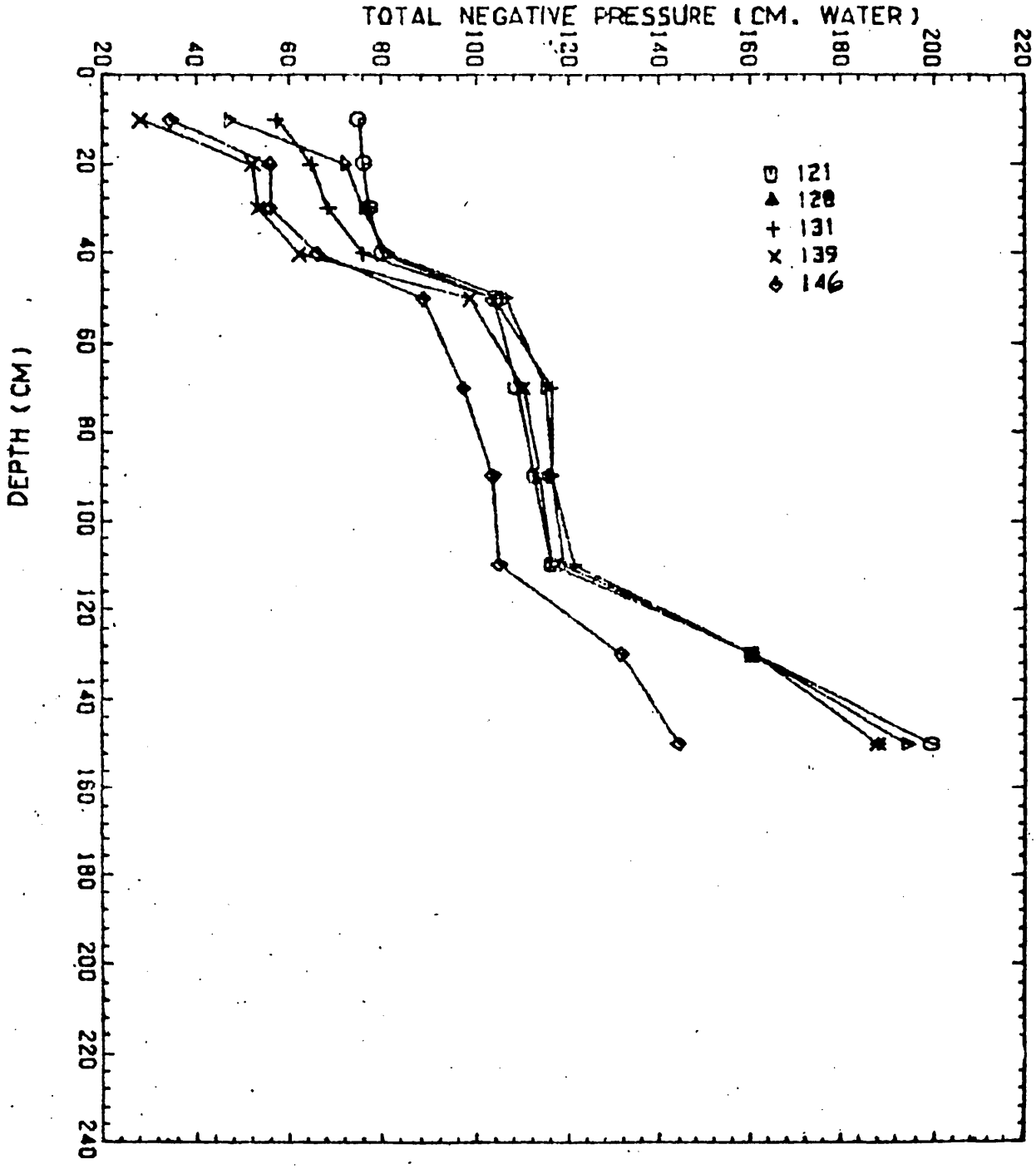

FIG.7·1b HYDRAULIC HEAD PROFILES PERM. GRASS (1981)

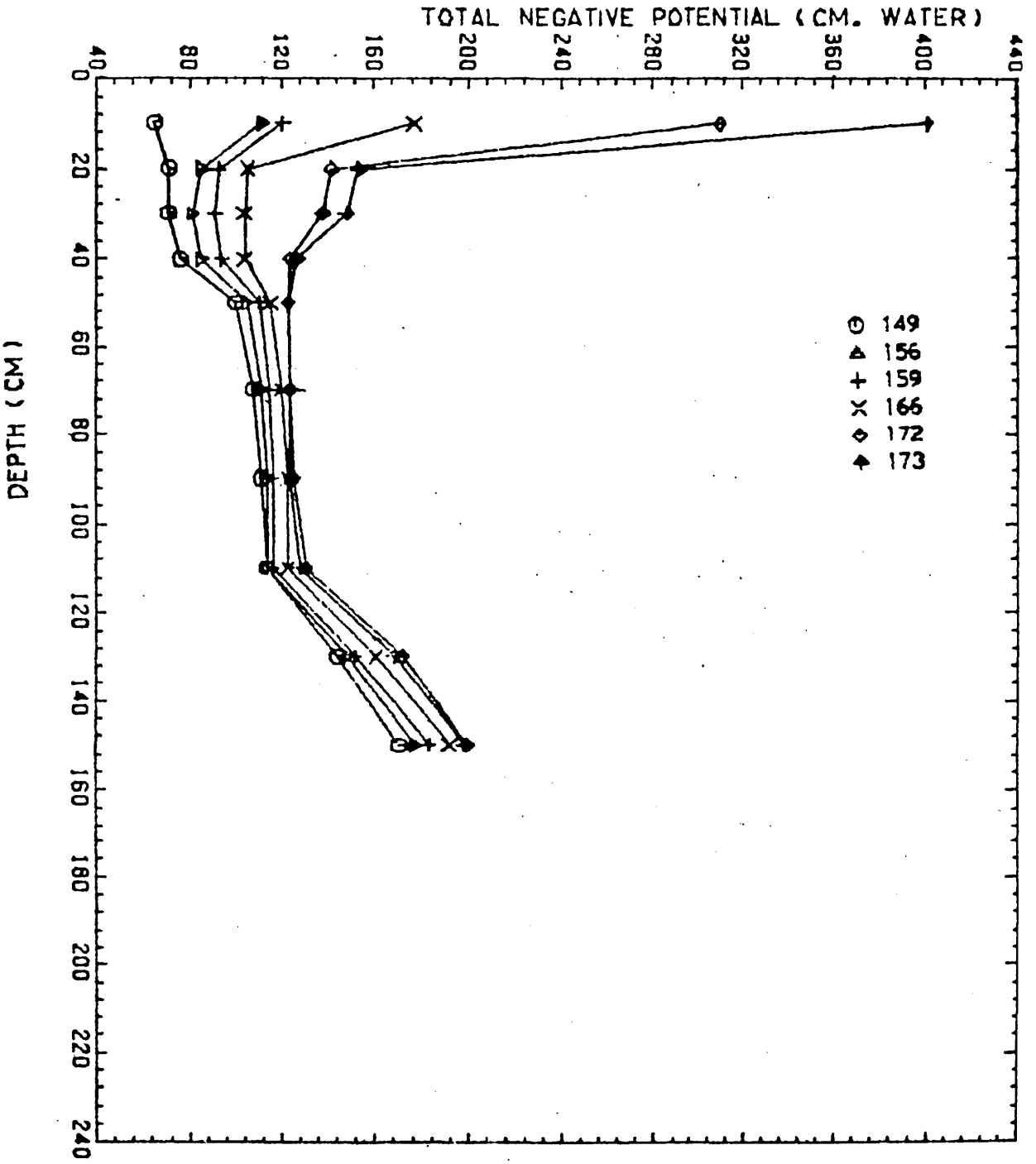

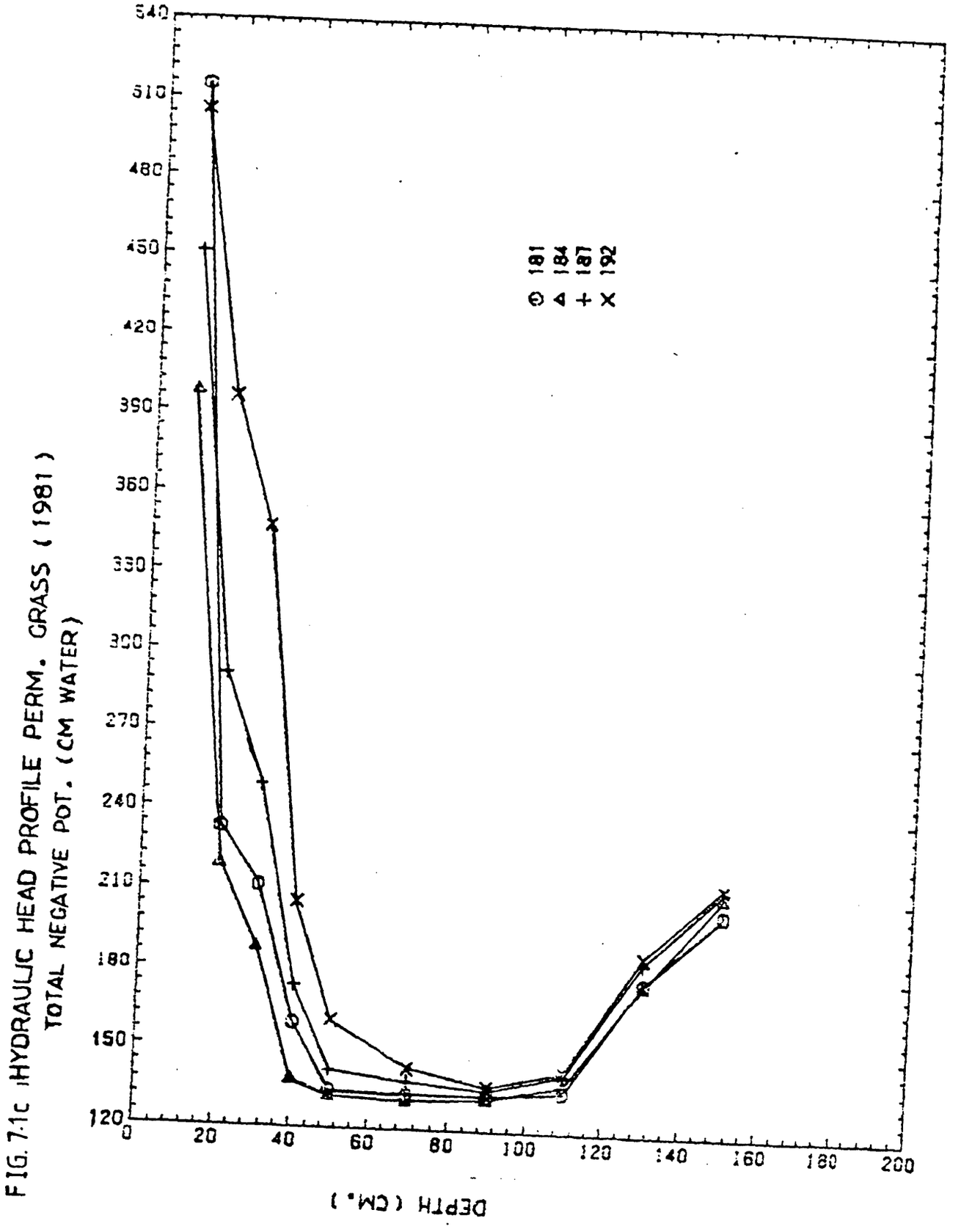

FIG. 7.1c HYDRAULIC HEAD PROFILE PERM. GRASS (1981)
TOTAL NEGATIVE POT. (CM WATER)

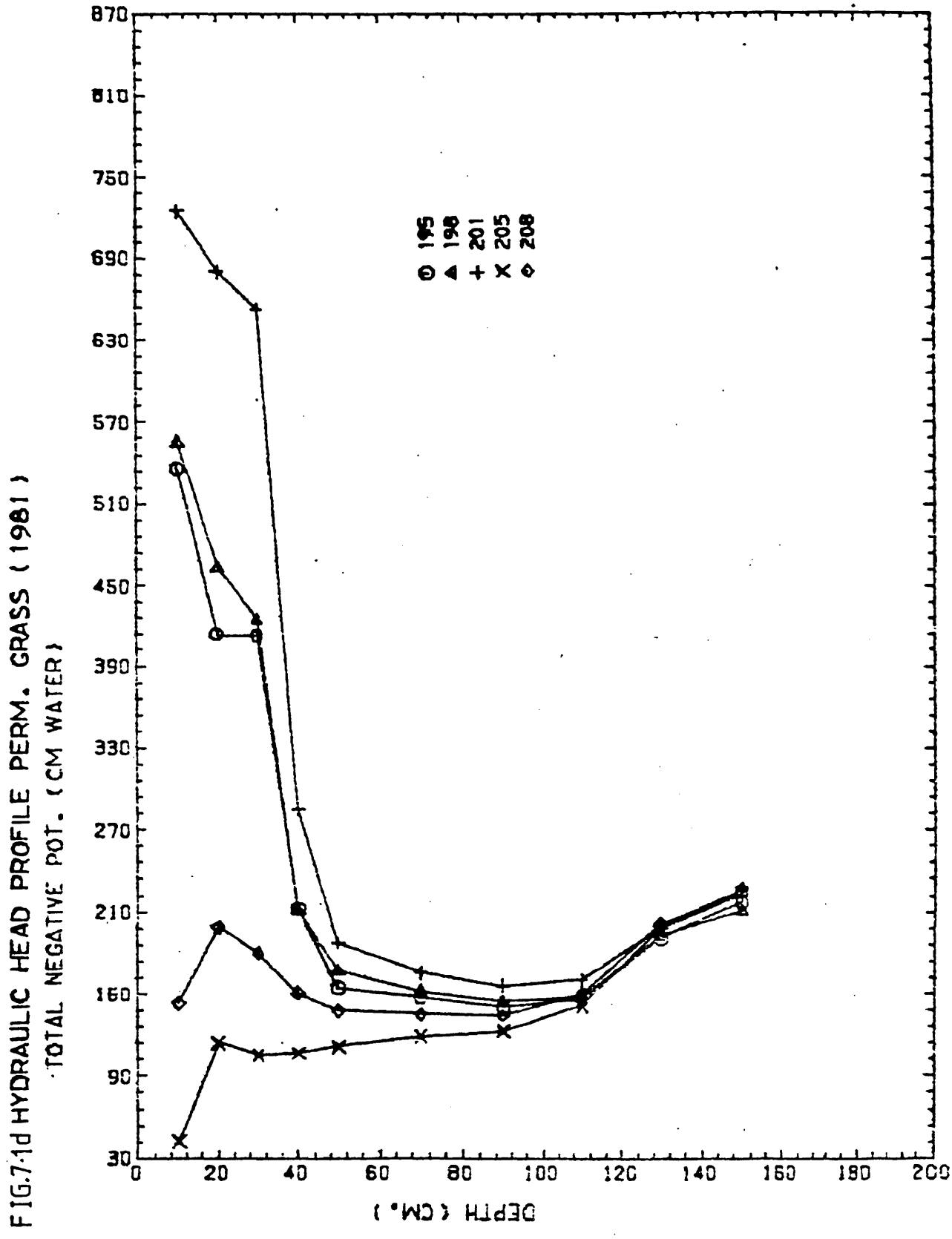

FIG.7.1d HYDRAULIC HEAD PROFILE PERM. GRASS (1981)
TOTAL NEGATIVE POT. (CM WATER)

difficult on days 181 and 184 because the gradient at 70 cm and 90 cm is not too apparent. However, from the zero flux plane estimates, actual evapotranspiration estimates were calculated as a residual from the water balance equation for the period between day 156 and day 208. The latter was carried out in a similar manner to that described in section 6.2.3 under the natural balance technique. The corresponding actual evapotranspiration values obtained are presented in Table 7.2. Having obtained the actual evapotranspiration values for the interval between readings, the average daily actual evapotranspiration rates were computed for the period between day 156 and day 208 according to the expression given in equation 4.14.

TABLE 7.2 : Observed actual evapotranspiration

Day No.	Rainfall (mm)	Actual Evapotranspiration (mm)
156-166	11.1	24.7
167-173	0.7	16.1
174-177	1.7	2.0
178-181	0.0	13.14
182-184	3.7	2.58
185-187	0.1	5.03
188-192	0.0	10.57
193-195	0.6	6.33
194-198	0.8	5.10
199-201	0.1	2.96
202-*205	24.1	2.73
204-*208	0.1	9.25

* Convergent zero flux plane depths

7.3.1.2 Calculation of Crown Potential

The estimation of daily actual evapotranspiration values allows the use of equation 7.1 to estimate crown potential values for days in which simultaneous moisture content and tension profiles were monitored. This latter potential was assumed to sustain the imposed evapotranspiration rate. In order to estimate the actual crown potential necessary to satisfy the actual evapotranspiration rates, arbitrary values of the cortex hydraulic resistance were assigned to equation 4.7. The optimisation of the crown potential values was then carried out following the procedure delineated in Chapter 4 (Section 4.3.5). for different values of the cortex hydraulic resistance, by minimising

the difference between the calculated flux and actual evapotranspiration rate for corresponding days.

Figures 7.2, 7.3 and 7.4 present the plots of the temporal distributions of the calculated crown potentials for varying arbitrary values of the cortex hydraulic resistance ranging from 0 to 10,000 days. The plots reveal a decreasing crown potential as the soil progressively dries out, attaining the minimum at day 201, this coinciding with the day on which the maximum depth of extraction was observed. This pattern of decreasing crown potential was constant for cortex hydraulic resistance values lying between zero and 2,000 days. For higher values, a reversal in minimum crown potential was noticed, from minimum on day 201 to minimum on day 181. This latter observation provides an interesting qualitative picture when considered from the point of view of plant physiological response to progressive drying of the soil. Previously, it has been recognised that the ZFP depth increased with time until day 201 when maximum depth was developed at 90 cm. Federer (1979) showed that increasing drying of the soil leads to a corresponding decrease in plant water potential. Also van Bavel (1976) intimated that a decreasing soil water potential is accompanied by a reduction in transpiration because of an increase in rhizosphere resistance that results. Subsequently, the crown potential response relative to the actual evapotranspiration rates occurring on days 181 and 201 was considered. The actual evapotranspiration rates as obtained from water balance on days 181 and 201 are 1.36 mm/day and 0.51 mm/day respectively. The corresponding potential evapotranspiration rates are 3.80 mm/day for day 181 and 3.90 mm/day for day 201. As such, if the observations of Federer and van Bavel are judged correct, it follows that the cortex hydraulic resistance must lie between zero and 2,000 days. Consequently, for the purpose of validation of the physical soil water model, it was decided to adopt a value of 1000 days for the cortex hydraulic resistance values for all the layers within the rooting profile. The value of 1000 days when applied to the root profile in conjunction with the root density for each layer within the root profile gives a total root hydraulic resistance of 9.7×10^3 days. This latter value of root hydraulic resistance is in close agreement with that of Rijtema (1965) for grass growing in a loamy sand (10.4×10^3 days). Although the cortex hydraulic resistance of 1000 days was assumed for the pur-

SIMULATED OPTIMISED CROWN POTENTIALS USING DIFFERENT CORTEX HYDRAULIC RESISTANCES

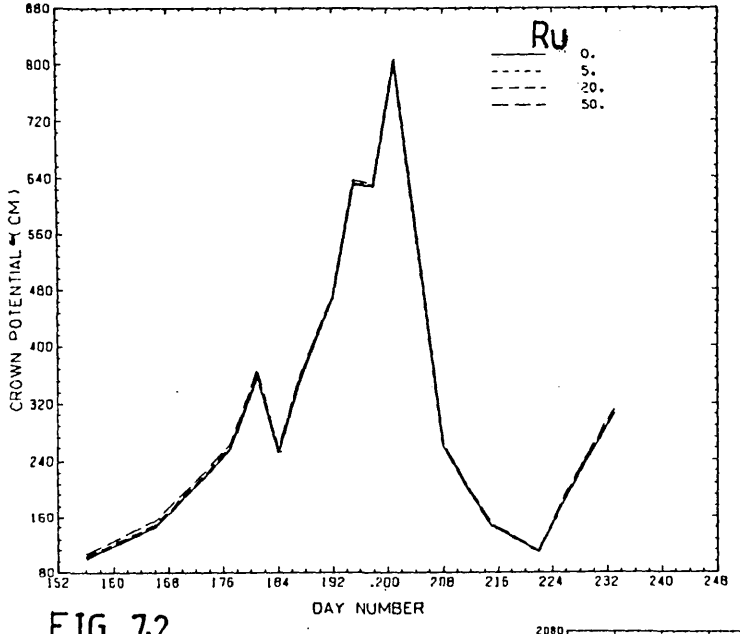

FIG. 7.2

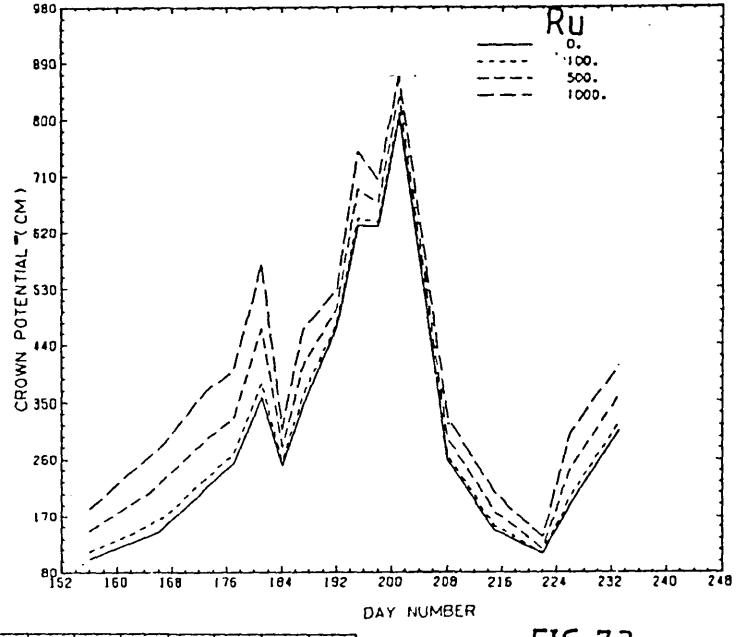

FIG. 7.3

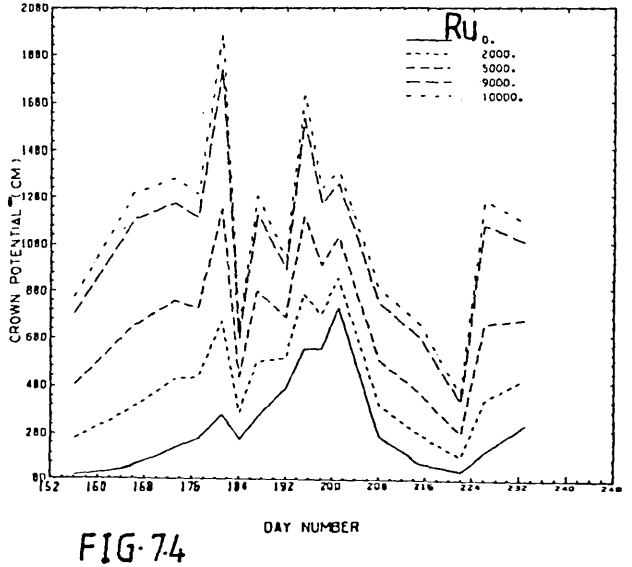

FIG. 7.4

pose of this test, it was borne in mind that in general cortex hydraulic resistance may possess changing values. This is because the cortex resistance depends on root proliferation and soil moisture content availability, both of which are changing temporally and spatially within the soil profile.

7.4 Description of Input Data to Physical Soil Water Model

The numerical solution of equation 3.17 requires the measurement of soil hydraulic properties $h(z,\theta)$ and $k(z,\theta)$. The evaluation of these parameters has been earlier discussed in Chapter 6. The use of these soil water hydraulic characteristics normally requires the description of the results by a functional relationship or their reduction into a tabular form (Wang and Lakshiminarayana, 1968). For the purpose of this study, the empirical relationships given in equations 4.3 and 4.4 were used to describe the $h(z,\theta)$ and $k(z,\theta)$ by fitting a regression line through the data points to obtain the relevant constants. These constants were given as input data, because they afford better ease of handling and facilitate programming for numerical analysis.

Further input data are the initial volumetric moisture content existing in the soil profile and the boundary conditions at the surface and at the bottom of the profile. At the surface, the boundary conditions imposed are daily rainfall values and daily evapotranspiration rates. For the bottom of the profile, unit hydraulic gradient is assumed, since the potential gradient at the bottom of a profile draining to a water table at a still greater depth is generally close to unity (Van Bavel *et al.*, 1968; Davidson *et al.*, 1969 and Hillel, 1977).

7.5 Computer Program (Appendix A)

The general concept behind the physical soil water model utilised for validation has been introduced in Chapter 3. The soil hydraulic characteristic algorithm and the computational procedure utilised for the estimation of crown potentials have been discussed in Chapter 4. Consequently, the abstraction algorithm coupled with the Darcian flux component of the model were translated into a FORTRAN IV program following the lines suggested by Hillel (1977) for use with the Imperial College CDC Cyber 6400 computer.

The flow chart which indicates the sequence in which the numerical solution of equation 4.2 is performed is displayed in Figure 4.3.

The following results are obtained:- the time distribution of the layer moisture contents; the successive daily profiles of the hydraulic head, the daily patterns of cumulative root abstraction, the crown potential distribution with time and soil water flux at bottom of the profile. It will be noted that the values of evapotranspiration are deduced from soil water data. The objective here is to compare the simulation results obtained from the physically-based soil water model with those observed in the field. The latter also involves the identification of the more sensitive components of the adopted soil water model.

7.6 The Model Behaviour

Rijtema (1965) intimated that the plant possesses a potential leaf suction which is defined as the theoretical suction which the leaf must have to be able to sustain the potential evaporative demand of the atmosphere. This latter suction is expected to prevail at very low soil moisture deficit conditions. However, at high soil moisture deficit conditions, the leaves may not be able to satisfy the potential demand, hence the actual leaf suction will not be equal to the potential suction. The physical model results allow for the examination of the actual crown potential relative to the potential crown potential that is required to maintain the atmospheric demand. Figure 7.5 shows the temporal distribution of the potential crown and actual crown potentials simulated during the test period. These values were obtained by optimising the combined flux obtained by the sink term with the potential evapotranspiration and actual evapotranspiration rates respectively. Apparent in Figure 7.5 is the equivalence of the potential and actual crown potentials in the early days of the drying process, between day 156 and day 164. The latter shows that the leaves at this early stage are capable of satisfying the potential evaporative demand. Beyond day 166, divergences between actual and potential crown potentials are observed, thus indicating that the stomata in the leaves can no longer guarantee transpiration at the potential rate. This is a consequence of progressive drying out of the

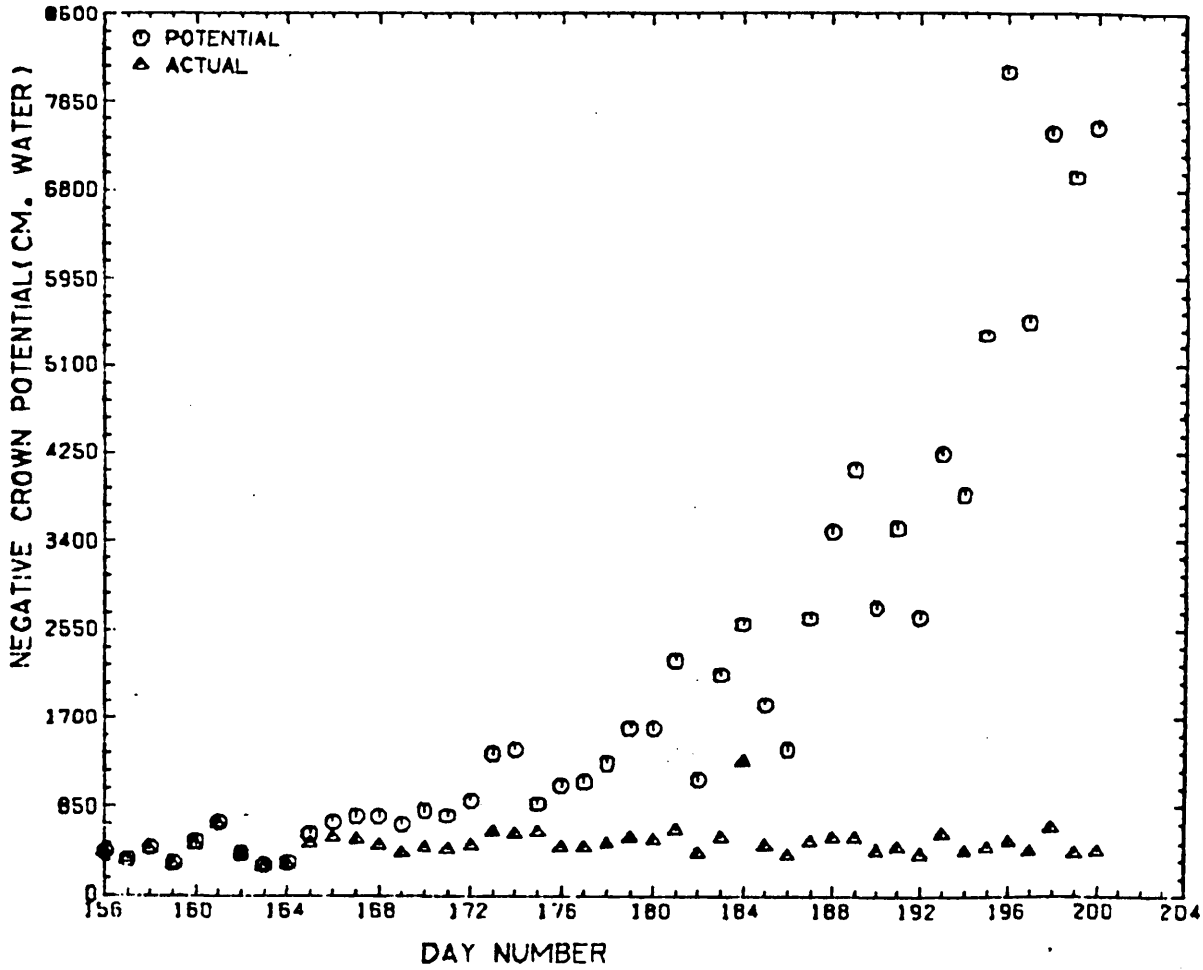

FIG. 75 TEMPORAL DISTRIBUTION OF POTENTIAL AND ACTUAL CROWN POTENTIALS

soil as evidenced by ZFP displacement to lower depths (Figures 7.1a-7.1c). The maximum actual crown potential obtained is -689 cm water as opposed to -7940 cm water for the potential crown potential. This shows a difference of twelve orders of magnitude. This latter observation accords with the observation of Rijtema (1965) that much reduction occurs in actual potential relative to the potential crown potential. This was also supported by Walley and Hussein (1982) as shown in the form of relationship selected to describe the actual crown potential. Also apparent in Figure 7.5 is the fact that while the potential crown potential is decreasing at an exponential rate, the daily actual crown potential shows no appreciable difference during the test period. This observation is in agreement with Feyen et al. (1980) who observed from potted ryegrass that there are no significant fluctuations in leaf water potential, either under high evaporativity or low evaporativity until moisture stress became very severe. Further observation shows that the simulated actual crown potentials range between -300 cm water and -700 cm water. This latter indicates that the actual crown potential can actually be assigned a single value for the test period. This single value was obtained by estimating the mean of the simulated actual crown potentials for the test period. The mean obtained is -493.46 cm water, and this value was later used to simulate the abstraction from each layer within the rooting profile.

7.6.1 The Relationship of Actual/Potential Crown Potential and Soil Hydraulic Resistance

An indication of the degree of soil dryness is the soil hydraulic resistance to moisture movement within the soil profile which depends on the unsaturated hydraulic conductivity-wetness relationship. The soil hydraulic resistance can therefore be equated to the prevailing soil moisture deficit at any given time and depth.

The previous discussion in section 7.6 indicated the occurrence of a divergence between actual and potential crown potentials beyond day 166. This latter observation should allow the testing of the simulated potentials as this will show whether they have any physical relevance to what obtained under field conditions. Consequently, an attempt was made to relate the ratio of actual/potential crown poten-

tial to the soil hydraulic resistance values obtained within the rooting zone.

Figure 7.6 presents this relationship, revealing a decreasing exponential relationship from unit ratio for successive increases in soil hydraulic resistance. The curve obtained in Figure 7.6 is similar to empirical drying curves that relate either AE/PE ratio to soil dryness (Penman, 1949) or that relating AE/PE ratio to soil moisture matric potential (Feddes et al., 1976).

7.6.2 Simulation of Layer Moisture Contents

The predictions of the physical soil water model with the root cortex hydraulic resistance of 1000 days and actual crown potential of -493.46 cm water are compared with observed field measurements of soil water content obtained by the neutron probe during the growing season of 1981. Figure 7.7a-7.7h show the temporal distribution of the observed and predicted layer moisture contents. The neutron probe readings were not obtained on a daily basis, consequently they do not allow a more critical comparison of the predicted moisture content for the different layers. The predicted values for the 10 cm layer (0-15 cm) simulated the effect of precipitation on this layer throughout the test period. There is a fairly good agreement between day 156 and 184 beyond which agreement became poor; the predicted results became higher than the observed showing lower abstraction. The 0-15 cm layer is the zone mainly affected by irregular and alternating drying and wetting patterns. As such the level of variations that occur up to day 184 may be regarded as reasonable. The systematic overestimate after day 184 can be attributed to several factors. Firstly, the unsaturated hydraulic conductivity-wetness ($k(\theta)$) relationships used in the 0-15 cm layer may not reflect the actual $k(\theta)$ relationship. This is because, in the model simulation, the $k(\theta)$ relationship obtained for the 15-25 cm layer was used for the 0-15 cm layer. Secondly, the soil moisture characteristic obtained for this layer may not match with the $k(\theta)$ relationship used; and this is likely to introduce errors into the simulation results. Other factors that may account for this discrepancy are inherent in the assumptions made in the model operations. This includes the assumption that all rainfall infiltrate the profile in one-time step.

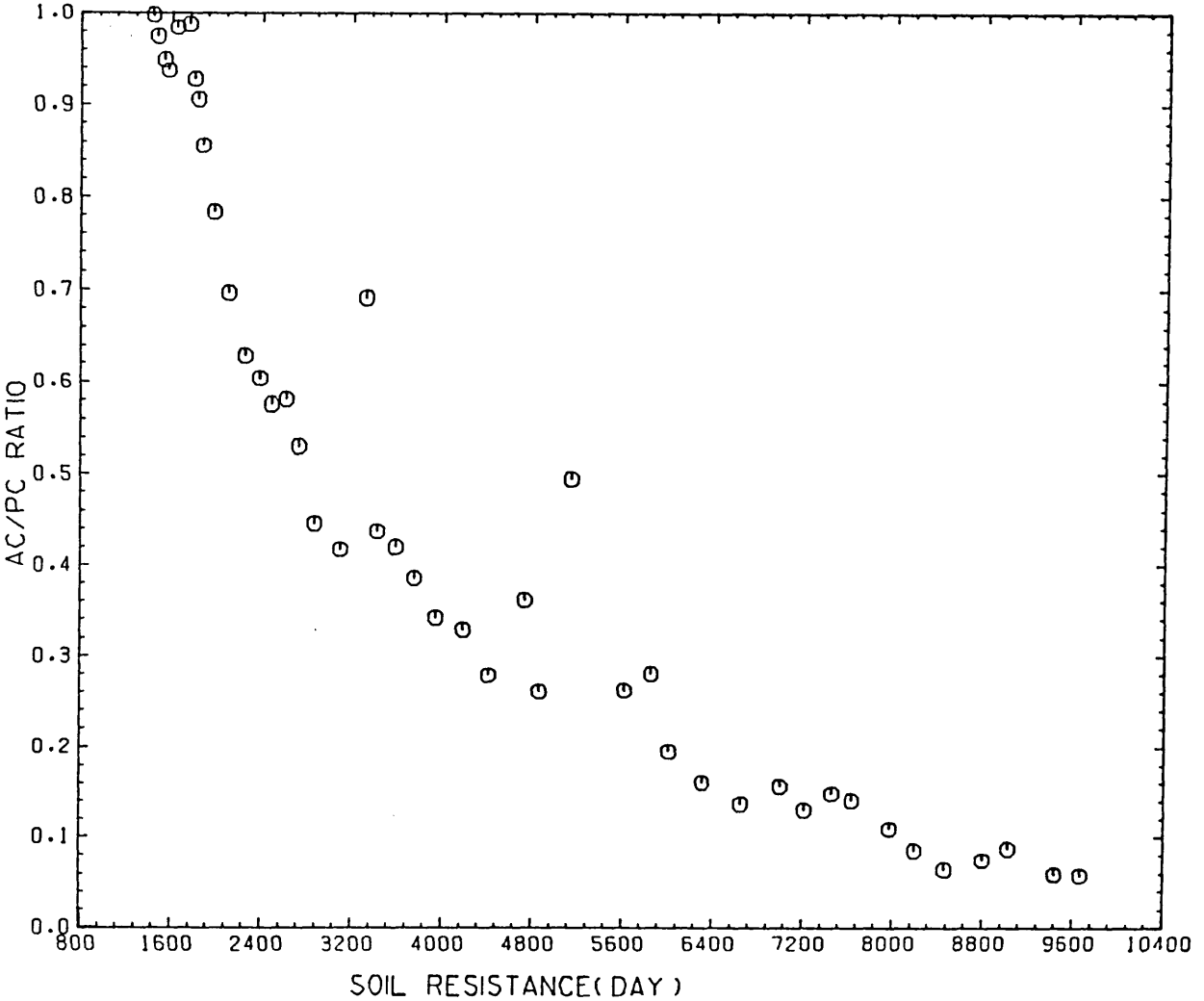

FIG. 7.6 RELATIONSHIP OF ACTUAL/POTENTIAL CROWN POTENTIAL RATIO VS SOIL HYDRAULIC RESISTANCE

FIG 77 SIMULATED VS OBSERVED MOISTURE CONTENT

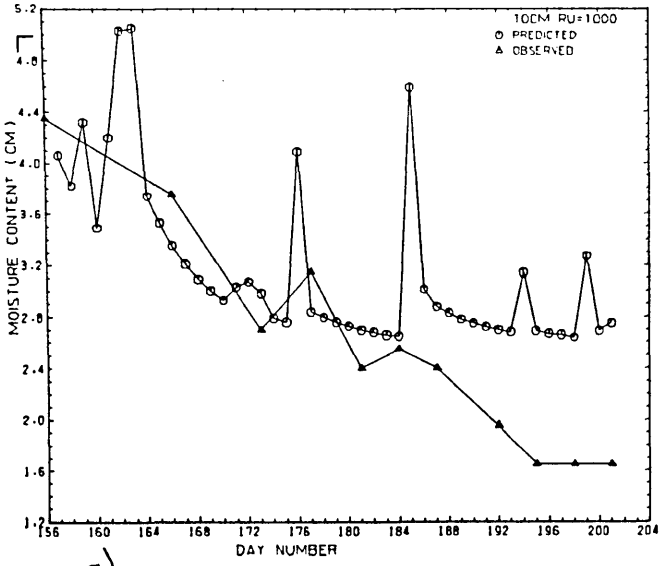

a) SIMULATED VS OBSERVED MOISTURE CONTENT

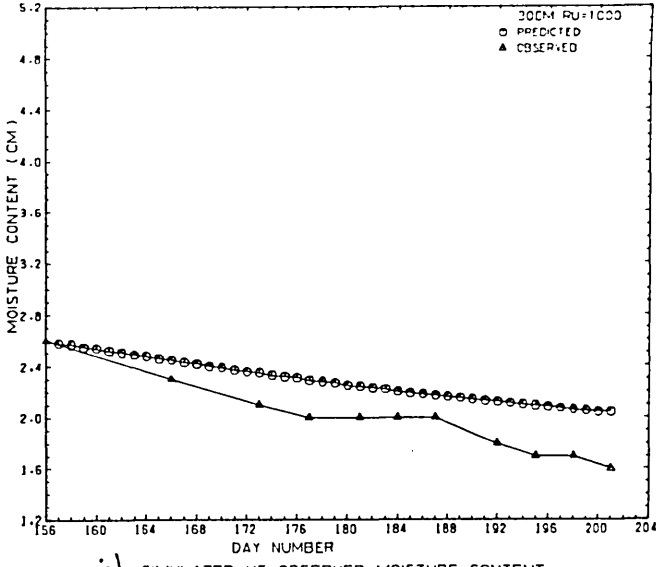

c) SIMULATED VS OBSERVED MOISTURE CONTENT

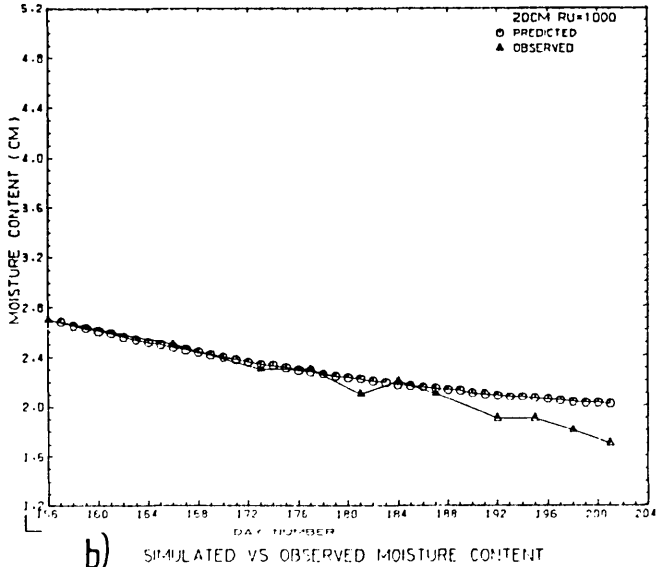

b) SIMULATED VS OBSERVED MOISTURE CONTENT

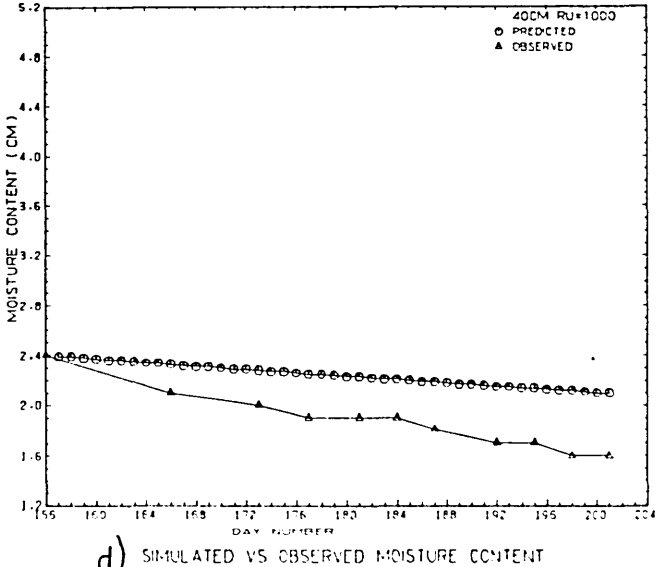

d) SIMULATED VS OBSERVED MOISTURE CONTENT

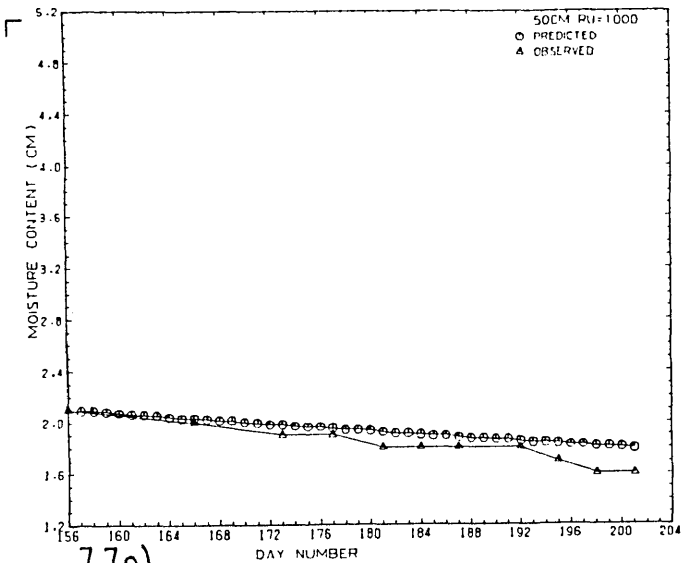

77e) SIMULATED VS OBSERVED MOISTURE CONTENT

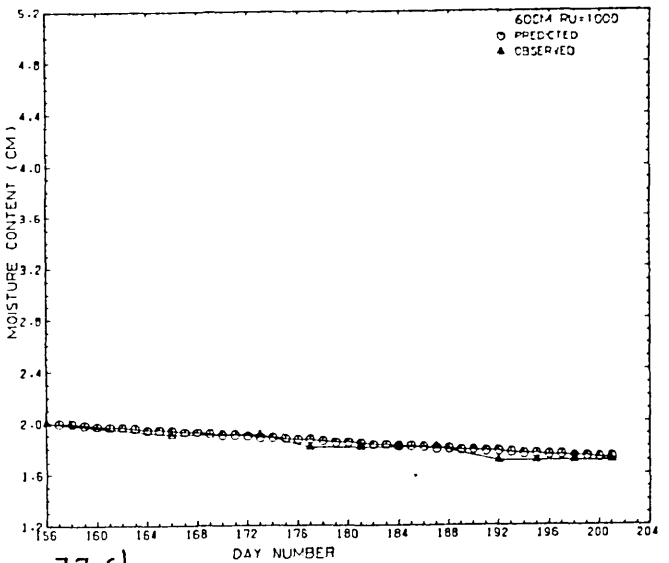

77 f) SIMULATED VS OBSERVED MOISTURE CONTENT

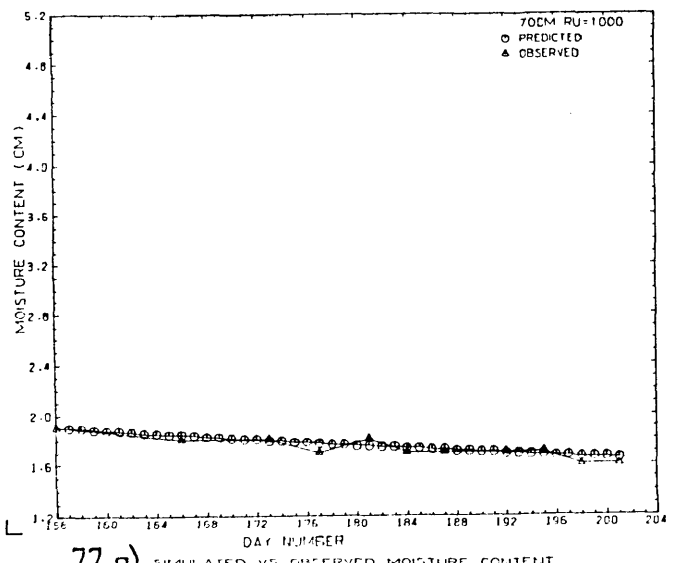

77 g) SIMULATED VS OBSERVED MOISTURE CONTENT

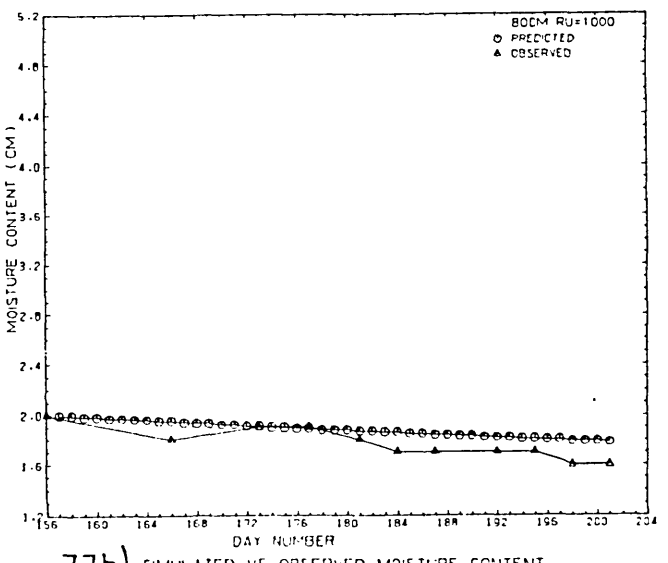

77h) SIMULATED VS OBSERVED MOISTURE CONTENT

Discrepancies were also observed for the 25-35 cm layer (Figure 7.7c) and the 35-45 cm layer (Figure 7.7d). In both layers, the computed layer moisture contents were higher at all sampling times than the measured moisture contents. The upward movement of water consequent upon suction gradients created by the roots may probably explain this observation; particularly as the 35-45 cm layer represents the lower boundary of the root profile. The discrepancies can also be explained by the fact that a constant root cortex hydraulic resistance was used throughout the simulation. The latter does not consider the fact that the root resistance will change according to soil moisture content and root proliferation. Also in the use of the model, one dimensional vertical flow was assumed to prevail. This does not account for lateral flow movement. Generally, there were good agreements between the predicted and measured values at deeper layers (Figures 7.7e, 7.7f, 7.7g and 7.7h). These deeper layers are the ones that are likely to be least affected by the inclusion of the root extraction term in the evaluation of the $k(\theta)$ by the natural balance technique.

7.6.3 Sensitivity of Model Ouput to Root Hydraulic Resistance

In the above simulation, cortex hydraulic resistance of 1000 days was assumed. The use of a constant actual crown potential allows for the ascertaining of the effects varying cortex hydraulic resistance values would have on the model predictions. Hence values of 500 days and 1500 days representing ±50% of the 1,000 days resistance values were assigned for running the model.

Figures 7.8 and 7.9 show the temporal variations of the predicted moisture contents as obtained for 500 days and 1500 days cortex hydraulic resistance values respectively. It is observed that better agreement is obtained by using 1500 days at the 0-15 cm layer between day 156 and 185 and also at the 15-25 cm layer. This latter observation is in agreement with Feddes and Rijtema (1972) who observed that at progressive drying out of the soil, the plant resistance increases considerably.

FIG. 7.8 SIMULATED VS OBSERVED MOISTURE CONTENT

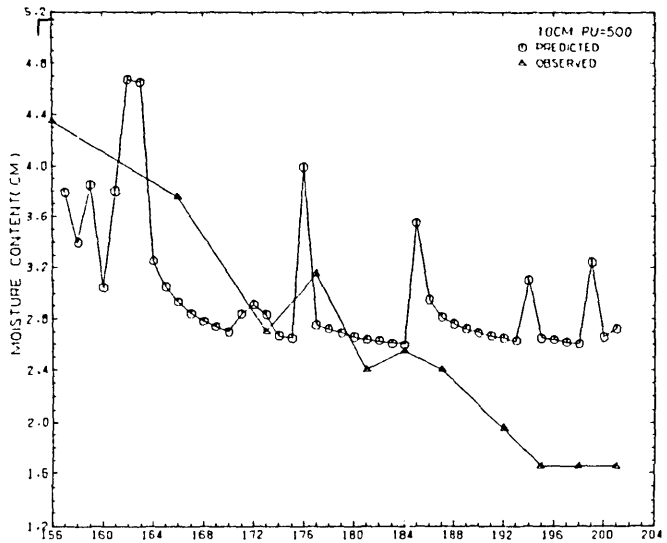

a) SIMULATED VS OBSERVED MOISTURE CONTENT

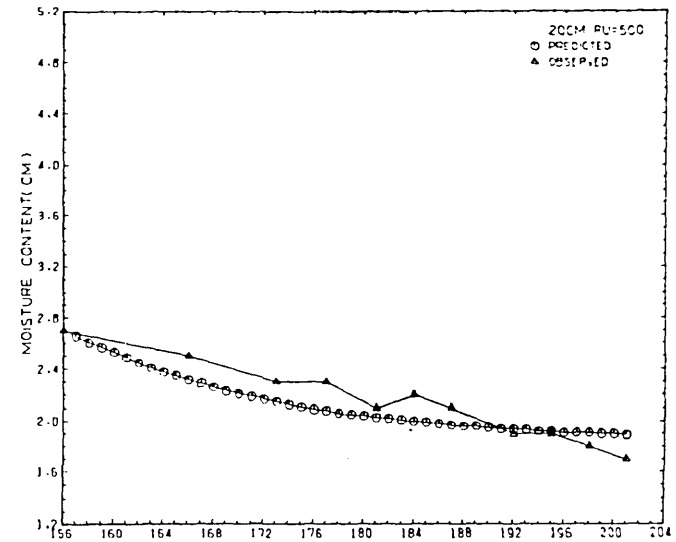

b) SIMULATED VS OBSERVED MOISTURE CONTENT

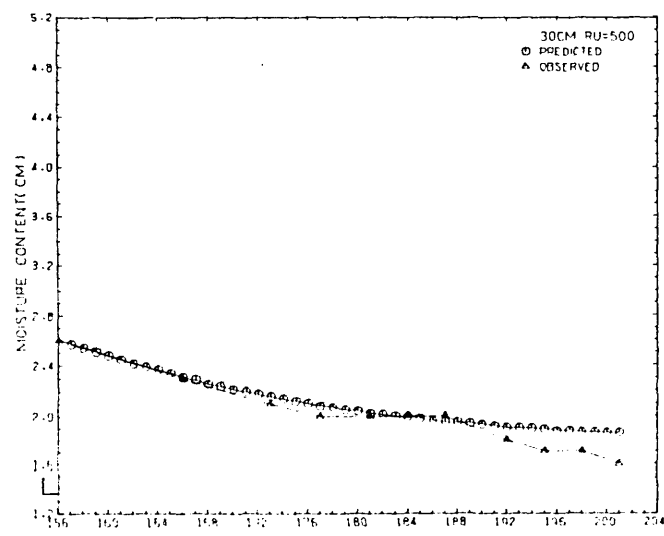

c) SIMULATED VS OBSERVED MOISTURE CONTENT

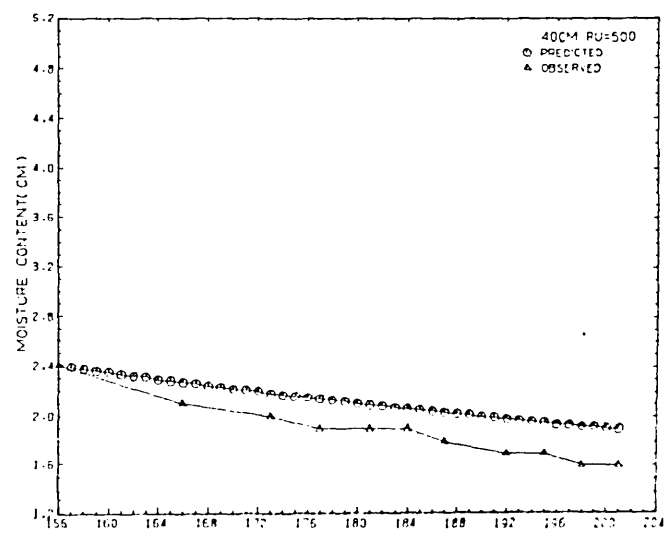

d) SIMULATED VS OBSERVED MOISTURE CONTENT

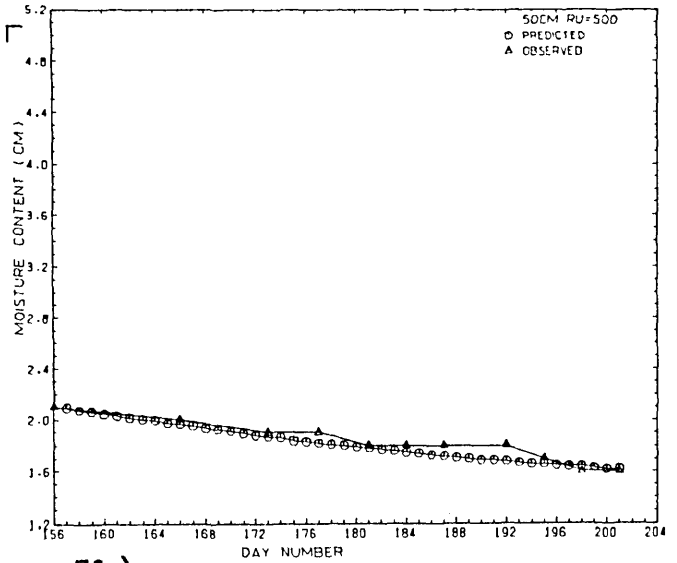

7.8e) SIMULATED VS OBSERVED MOISTURE CONTENT

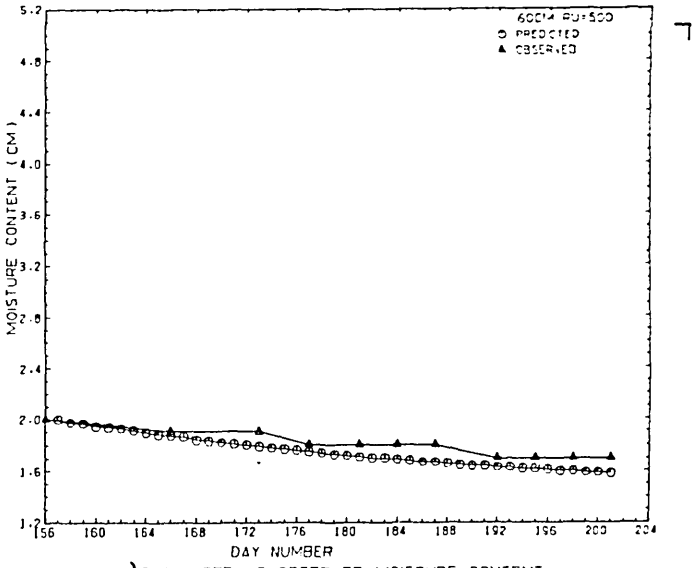

7.8 f) SIMULATED VS OBSERVED MOISTURE CONTENT

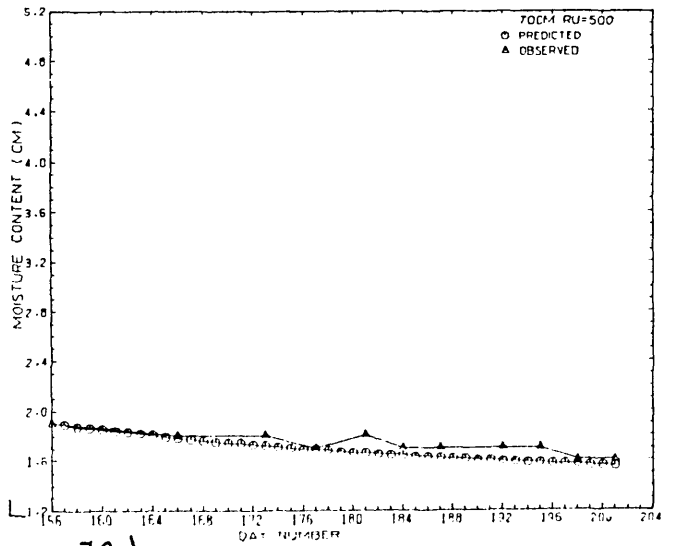

7.8g) SIMULATED VS OBSERVED MOISTURE CONTENT

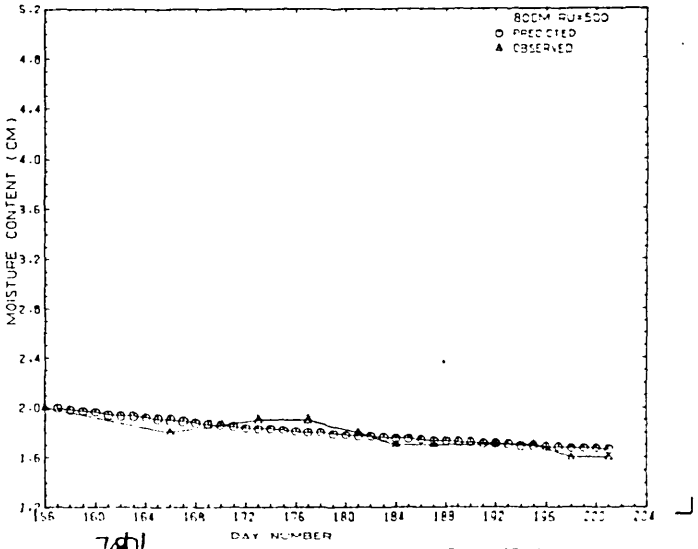

7.8h) SIMULATED VS OBSERVED MOISTURE CONTENT

FIG 7.9 SIMULATED VS OBSERVED MOISTURE CONTENT

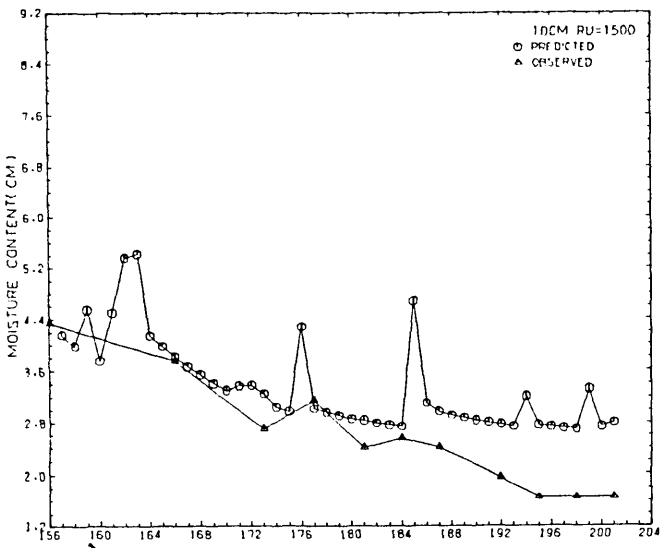

a) SIMULATED VS OBSERVED MOISTURE CONTENT

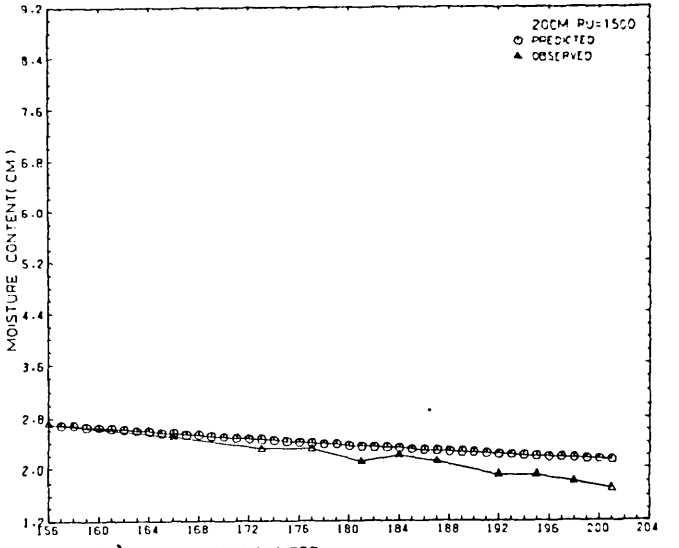

b) SIMULATED VS OBSERVED MOISTURE CONTENT

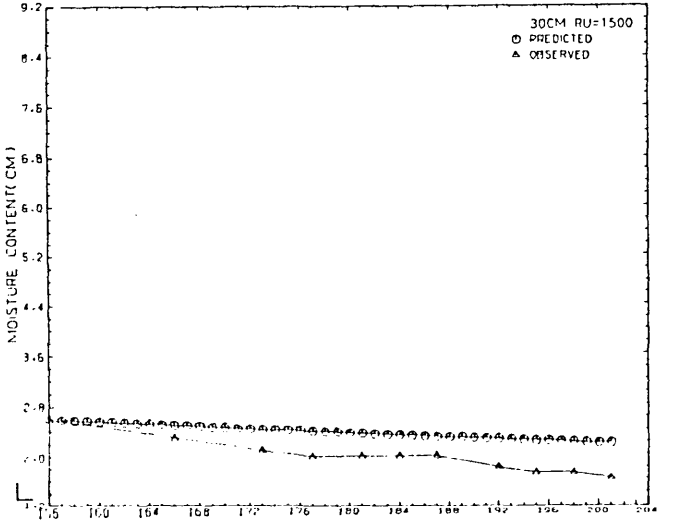

c) SIMULATED VS OBSERVED MOISTURE CONTENT

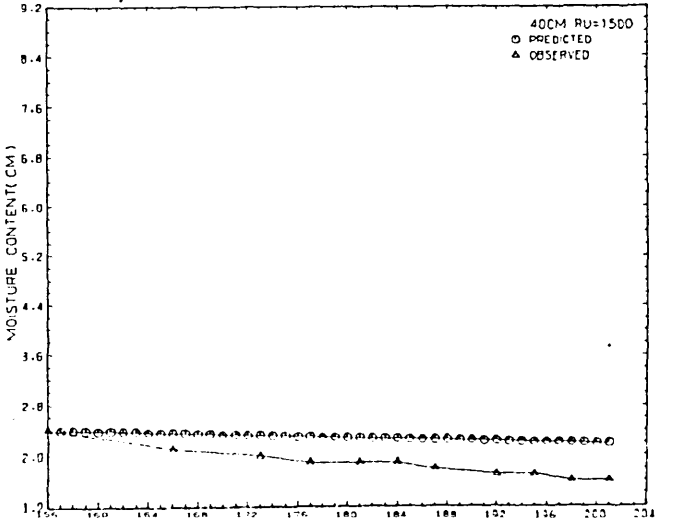

d) SIMULATED VS OBSERVED MOISTURE CONTENT

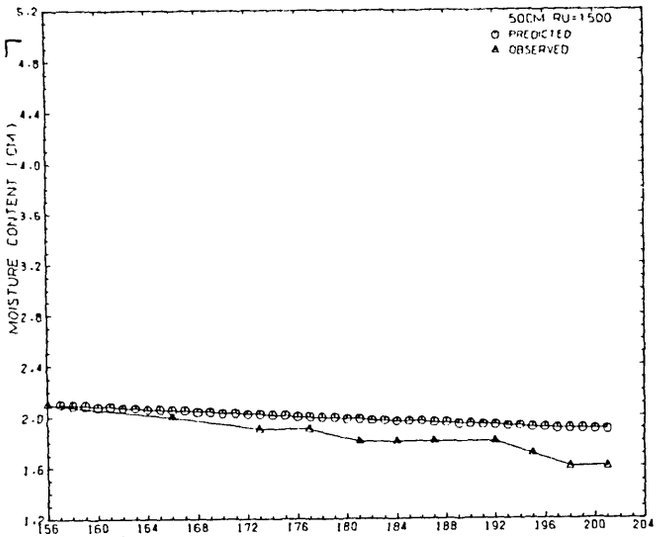

7.9e) SIMULATED VS OBSERVED MOISTURE CONTENT

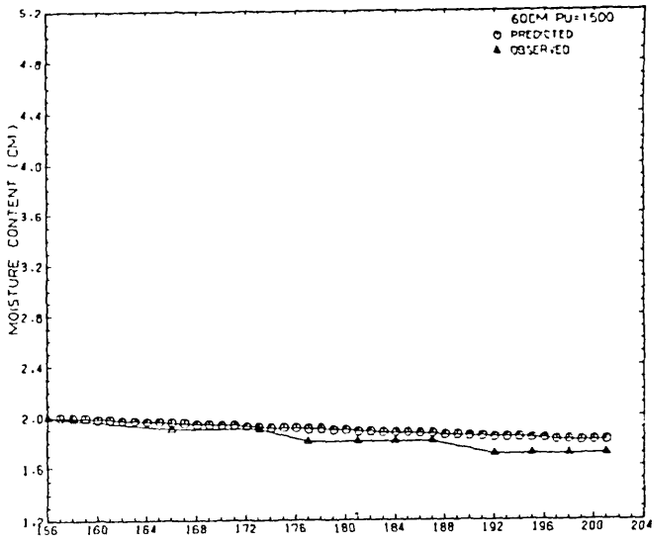

7.9f) SIMULATED VS OBSERVED MOISTURE CONTENT

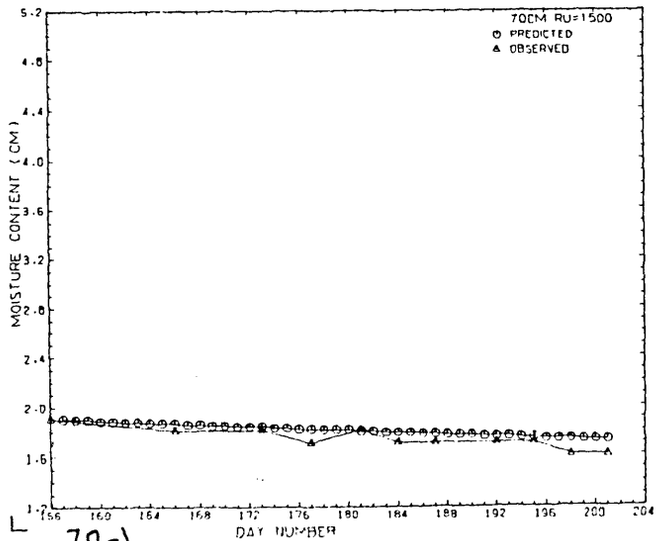

7.9g) SIMULATED VS OBSERVED MOISTURE CONTENT

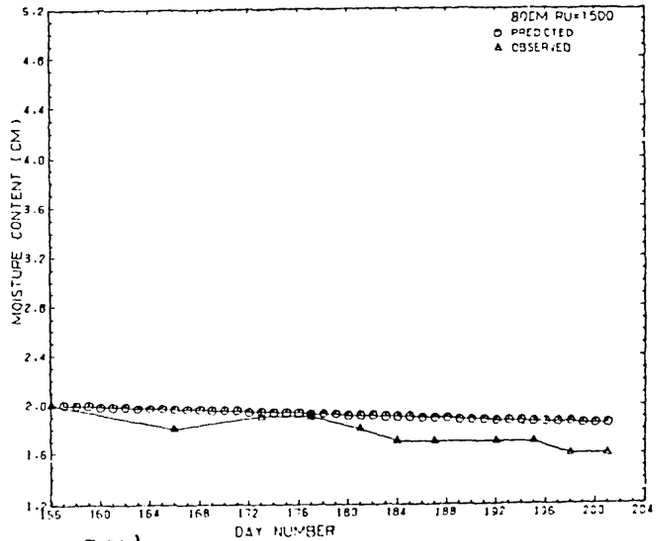

7.9h) SIMULATED VS OBSERVED MOISTURE CONTENT

7.6.4 Actual Evapotranspiration and Drainage

The cumulative actual evapotranspiration predicted by the model is compared with the cumulative evapotranspiration obtained from water balance computation (Figure 7.10). The total accumulated actual evapotranspiration for both water balance and calculated are 62.82 mm and 58.06 cm respectively, a difference of 4.76 mm. This latter result is very encouraging when considered in terms of errors which might have been caused by the use of a constant actual crown potential. Although the difference obtained is apparently insignificant, the results in Figure 7.10 show that initially, the accumulated actual evapotranspiration losses are in agreement. Disagreements were later observed to occur beyond day 172, when predicted fell below the observed.

Calculated drainage at 100 cm depth gave a cumulative drainage of 19.3 mm while the cumulative drainage obtained from measured changes of soil water content at depths below the ZFP is 16.4 mm. The difference is 2.9 mm. It is observed that the predicted drainage decreases gradually. This is expected since the assumption of unit hydraulic gradient implies that the flux at the bottom should be equal to the unsaturated hydraulic conductivity which decreases with time in a drying soil.

The consistent underestimation of the calculated actual evapotranspiration beyond day 172 in Figure 7.10 can be attributed to the use of a constant actual crown potential. The latter will cause lower abstraction with time as soil dries. This is because the crown potential used in the simulation is lower than that obtained by optimisation, especially with progressive drying of the soil. The latter point is believed to contribute to the systematic underestimation of the abstraction as evidenced in Figure 7.10.

7.6.5 Simulated Hydraulic Head Profiles

Another critical test for the validation of the adopted physical model is the simulation of the sequential hydraulic head profiles (Figures 7.11-7.14) during the test period. The evolution of the zero flux plane depth on day 157 at the 20 cm depth is shown in Figure 7.11 and the gradual displacement of this depth to 30 cm and 40 cm

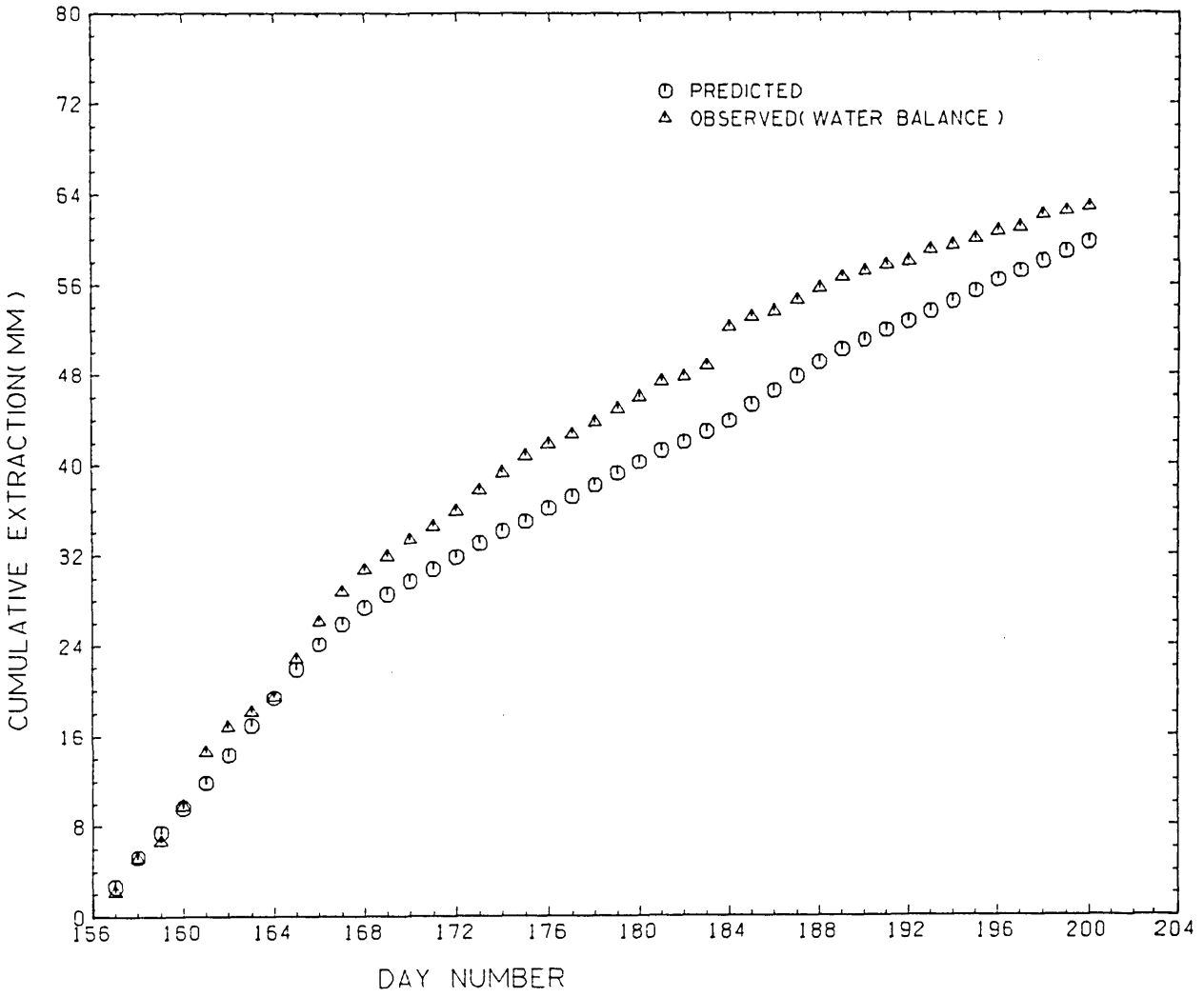

FIG. 7·10 CUMULATIVE EVAPOTRANSPIRATION

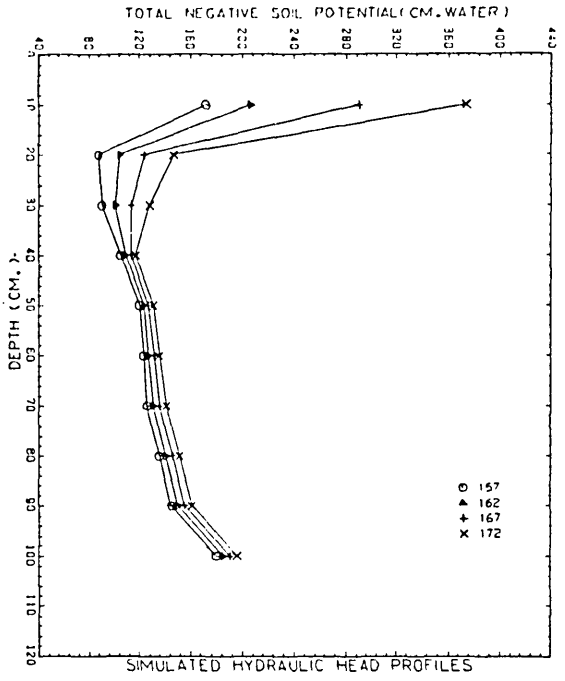

FIG.7-11

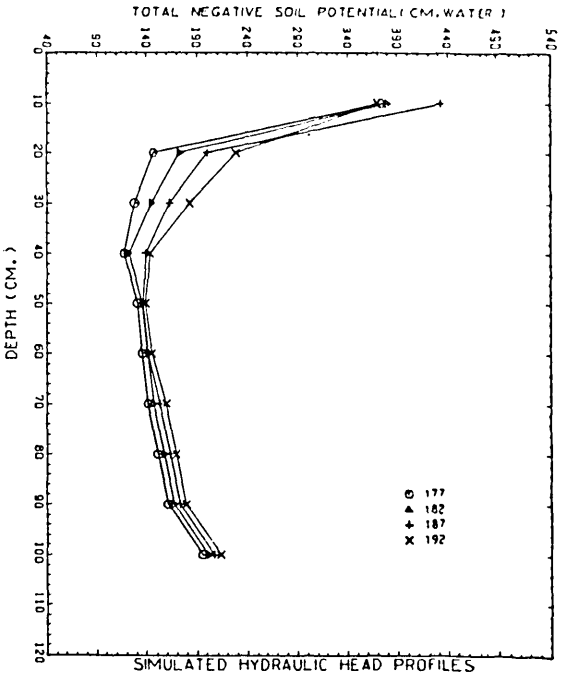

FI G.7-12

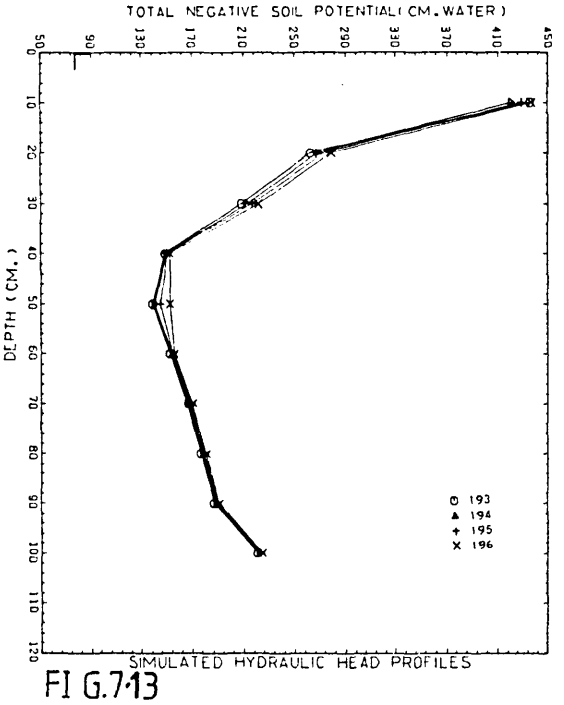

FI G.7-13

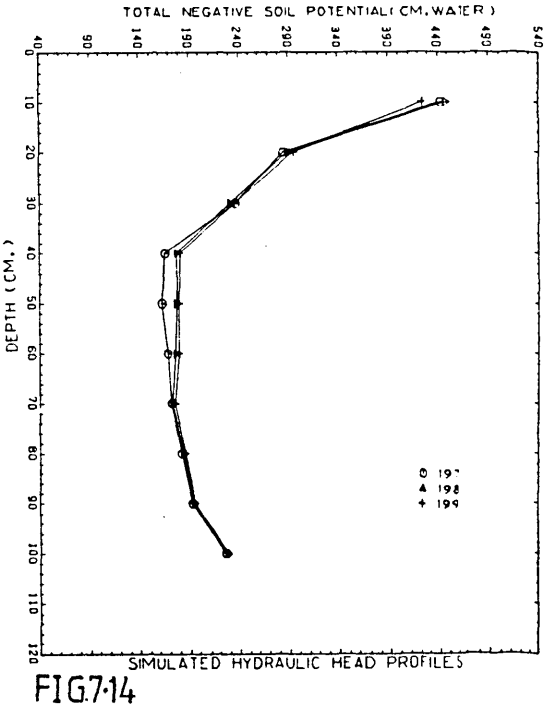

FIG.7-14

depths on days 162 and 167 respectively. The maximum depth of the zero-flux plane that was obtained by simulation is at 70 cm on days 198 and 199. This is in contrast to the 90 cm depth obtained from measured hydraulic head profiles (Figure 7.1c). The development of the simulated zero flux planes do not coincide with the measured zero flux depths beyond day 172. This latter point supports the observation that the observed zero flux plane data is very difficult to interpret in the particular site considered. This could be explained by the fact that tensiometer readings at deeper depths beyond 50 cm were obtained at 20 cm depth intervals. It is therefore important that the depth intervals be reduced to be able to obtain accurate interpretation of the ZFP depths.

There was persistence of the simulated ZFP depths at 40 cm depth between days 167 and 182, while the observed (Figures 7.1b and 7.1c) ZFP for the corresponding period has shifted to the 90 cm depth. This latter point obviously explains in part the underestimation of the accumulated actual evapotranspiration and the overestimation of the drainage as shown in Section 7.6.4.

7.7 Conclusions

It has been shown that the physical soil water model can be used to describe the changes in storage under the permanent grass plot during a 45-day period. The simulations of the respective soil water parameters and actual evapotranspiration and drainage losses are realistic considering that approximate plant hydraulic resistance value was utilised. It has also been shown that during the simulation period, the changes in actual crown potentials are not appreciable and can be assigned a single value. However, the physical soil water model fits are shown to be limited by the various assumptions inherent in its operation. Also of considerable importance is the methodology used in evaluating the unsaturated hydraulic conductivity-wetness relationship. The inclusion of the root extraction term in the latter and the extrapolation of the $k(\theta)$ relationship of the 15-25 cm to the 0-15 cm layer, and also the use of a constant actual crown potential are likely to have caused the errors in simulation. The simulations are shown to be improved if the cortex hydraulic resistance value is increased.

The interpretation of the observed zero flux plane data has been shown to be difficult as agreements with simulated hydraulic head profiles are not achieved. This interpretation has been shown to affect the simulated actual evapotranspiration and drainage losses. It is evident therefore that for significant improvements to be made to better the model fits, the following inadequacies inherent in the model operation should be rectified:-

(a) Apply the natural balance technique to evaluate the $k(\theta)$ of the profile by avoiding transpiration losses. This can be achieved by using a bare plot.

(b) A better interpretation of the zero-flux plane depths can be obtained if tensiometers are installed down the profile at smaller depth increments.

(c) Further efforts are needed to better the technique of assessing the plant hydraulic resistance. This is necesary to account for the effects of root growth and varying soil moisture contents.

(d) Further work (by others) could include exploring the sensitivity of model predictions to changing $k(\theta)$ relationships.

The results show that despite the inherent errors which might have accrued from parameter estimation, the physical soil water model used in this study is consistent with current knowledge of soil-plant-atmosphere hydraulics.

CHAPTER 8

THE EVALUATION OF EMPIRICAL DRYING CURVES

8.1 Introduction

The relative lack of experimental validation of both single and multi-layer soil water models has been discussed in Chapter 3. It has been apparent that this has contributed to the limited field application of both physical and empirical soil water models.

In Chapter 4, the choice of two single-layer models and their operational dynamics were discussed. This chapter focusses on the evaluation of these models. It presents the methodologies adopted for computing the soil moisture deficits and available water capacity from soil moisture data collected under different agricultural crops between 1980 and 1982. The simulation results associated with the observed soil moisture deficits from the various neutron probe access tubes are presented and the spatial variability of the results is discussed.

8.2 The Determination of Field Capacity and Soil Moisture Deficit

Schofield and Penman (1948) conceived soil moisture deficit (SMD) as the difference betwen observed drain flow and total rainfall on small plots. However, in the present state-of-the art of empirical soil moisture modelling, SMD is defined as the volume of water that is required to return a given soil to field capacity. SMD as a concept can be viewed as an index of the degree of soil dryness prior to rainfall or irrigation input.

From the preceding definition, it is evident that the field capacity represents a datum from which SMD can be evaluated. Consequently, the validity of the SMD concept will depend largely on the methodology used for determining the field capacity. This is because most empirical soil water models for predicting SMD consider only the inputs and outputs of water at the soil surface once the integrated profile water content is at or below the field capacity. Once the soil is at or drier than field capacity, there is no provision made for significant drainage or capillary rise across the base

of the profile. In order for an accurate assessment of the single-layer models to be made, it is therefore important that a systematic method for computing the field capacity and hence observed SMD be adopted. Hillel (1980) and Bell (1981) discussed the problems associated with field capacity determination. Some of these problems are inherent in the definition of the field capacity concept. Conventionally, the field capacity is defined as the water content of a profile which after having received excess water, drains within 2-3 days to a reproducible water content and thereafter further drainage is deemed negligible. From this definition, the controversy arises as to what extent the field capacity concept is valid for defining SMD's. This is because field capacity is not normally reproducible in most soil types. It is generally deemed to occur in two situations:-

(a) In soils whose matrix has poor conductivity and flow occurs predominantly through the macropores. This condition is represented by clay soils, and significant drainage may still occur long after 2-3 days.

(b) In highly conductive soils where the potential gradient tends towards zero and as such the profile may be in equilibrium with the water table. However since the water table depth is expected to vary in soils, it is apparent that each depth will have an associated field capacity value for a given profile. This latter condition presents a difficulty of depth to which field capacity applies.

The above two situations are extremes and are not often encountered in the field, rather, most soils possess intermediate conductivity and deep water tables. This adds complexity to field capacity determination since large and prolonged drainage may be released from the profile bottom while the upper part of the profile provides upward fluxes to evaporation and crop water abstraction. This leads to a zero flux plane development which changes according to rainfall input and rooting depth variation.

It is seen from the above that the field capacity of any given soil is influenced by a combination of factors. This then leads to the question of the validity or otherwise of the concept. Whatever the limitations that may be apparent in the concept, it is evident

that the field capacity presents a useful datum for which soil moisture data may be compared. In the utility of the concept, cognisance must be paid to the particular application. This is because while SMD computation using the concept may suffice for irrigation, since the deficit so predicted applies to the effective rooting zone, it may not fulfil the requirements of the hydrologist who may be more concerned about the lower component of the profile because of the drainage term. However, this study is primarily addressed to crop abstraction and the use of the field capacity may therefore be justified.

For the purpose of this study, integrated profile water content for the period under investigation (1980-1982) was determined to a depth of 1.5 m in the wheat and orchard sites and to depths of 1.3 m in the permanent grass and field beans/cabbage sites. In the former, the 1.5 m depth was used for computation to ensure that same profile depth was considered for all the access tubes within the respective sites in order to allow for comparative evaluation of the SMD's. However, the 1.3 m depth was the maximum depth to which the integrated moisture content could be computed; and this depth is believed to embrace the depth to which upward fluxes might apply in the plots.

Figure 8.1 shows the total profile moisture content distribution with time from the sites in which moisture content data were available throughout the period of investigation (1980-1982). Evident from the figure is the attainment of higher profile moisture contents during the winter months (December - March), which coincide with the period from day 361 to day 457, than obtained for subsequent periods. The same observation is noticed between days 724 and 814 which coincides with December - March 1982. In the latter period, few winter readings are obtained primarily because of the heavy snow storms that occurred between November 1981 and February 1982. Although higher moisture contents were obtained during the winter months, there were no discernible plateaux of readings which can represent field capacity values. As a result, the moisture contents obtained during these periods were inspected in conjunction with rainfall data such that the moisture contents obtained 2-3 days after given rainfall events were isolated. The arithmetic means of the moisture contents were then obtained for these isolated days for the different sites and were

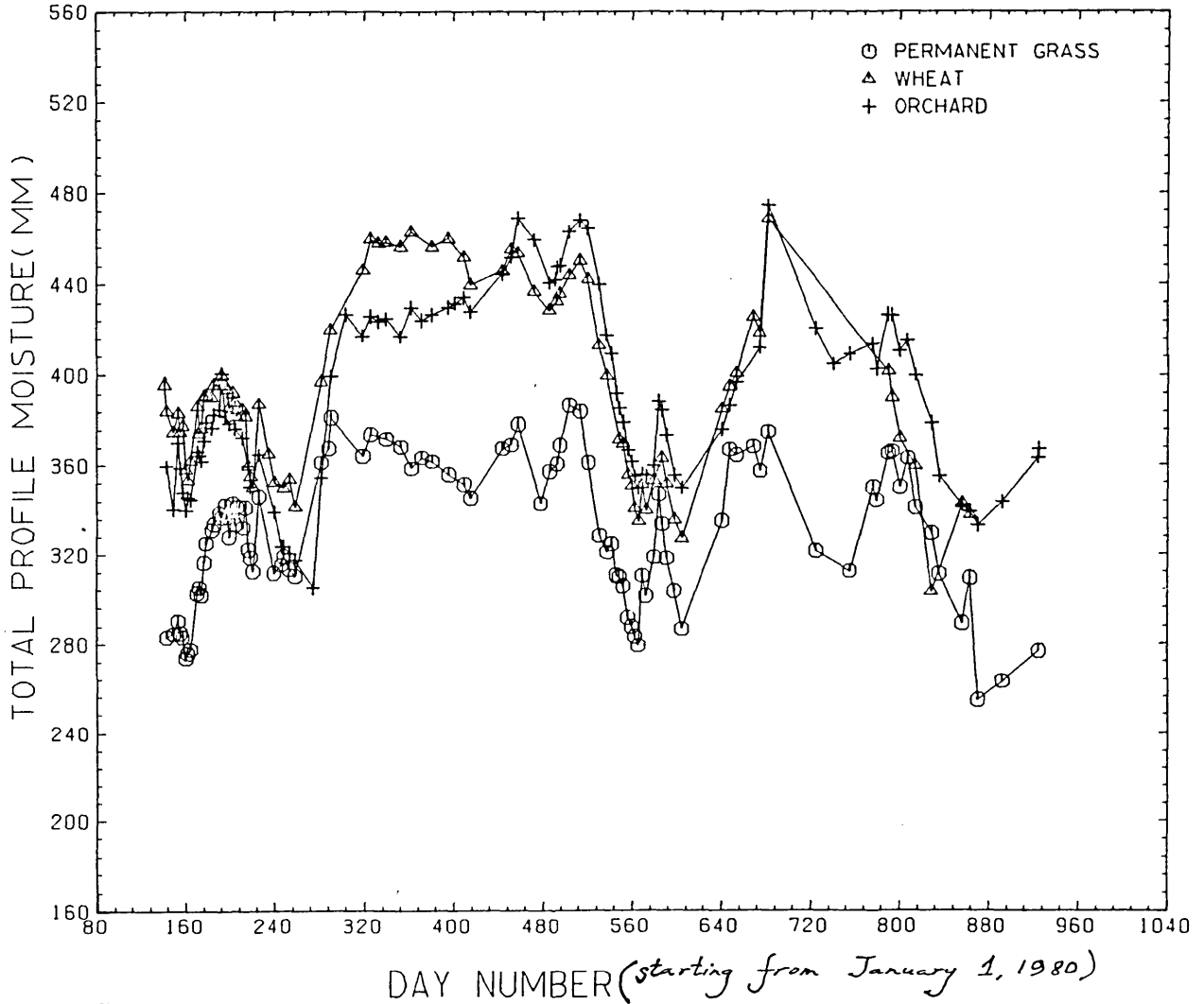

FIG 8.1 DISTRIBUTION OF TOTAL PROFILE MOISTURE WITH TIME

designated the field capacity values for the given profile. These values were subsequently utilised for SMD computation for each of the plots. Table 8.1 shows the field capacity values that were used for computing the soil moisture deficits for the period 1980-1982. Corresponding coefficients of variability associated with the individual values are also shown.

TABLE 8.1 : Field capacity values

Crop	Year	Number of Values	Field Capacity (mm)	Coefficient of Variation (%)
Grass	1980/1981	9	357.5	2.8
	1981/1982	4	365.6	0.9
Wheat	1980/1981	8	452.8	1.7
	1981/1982	4	419.9	7.9
Orchard	1980/1981	10	436.9	3.2
	1981/1982	4	426.5	1.02
Field Beans/ Cabbage	1980/1981	8	370.1	2.3
	-	-	-	-

8.3 Determination of Available Water Capacity

In order to assess the performance of the drying curve, represented by equation 4.21, it is essential to determine the available water capacity of the different sites. The available water capacity represents the total amount of water that is available to the plant and it takes into account the rooting depth. It thus ensures a specific range to which the available water to the crop and hence computed evapotranspiration applies. Conventionally, the available water is defined as the difference between the field capacity and permanent wilting percentage multiplied by the rooting depth. The permanent wilting percentage is normally obtained by using a pressure plate apparatus set at -15 bars to estimate the moisture content at this given pressure for a specified volume of soil. In common with other techniques which utilise disturbed soil samples, the latter technique suffers from lack of representativeness of the field soils coupled with the inability to resolve the problem of variability. Another technique that can be used employs a soil textural triangle (Salter and Williams, 1967). This assumes that most soils are grouped into

certain categories or classes which have corresponding available water capacities. Although the latter has enjoyed some applicability in the past, it still cannot account for heterogeneity which occurs in field soil profiles. As a result of the aforementioned problems, it was decided in this study to use an objective function technique to estimate the optimum available water capacity obtained by parameter optimisation of the soil moisture model. This was achieved by comparing model predictions with observed soil moisture deficits. The criterion of fit chosen was that of a non-dimensional form proposed by Nash and Sutcliffe (1970), the R^2 criterion. This criterion is based on the sum of the squares of the difference between observed and simulated ordinates, F^2, where

$$F^2 = \sum_{i=1}^{m} (q_i' - q_i)^2 \qquad (8.1)$$

where q_i' = simulated value at time i

q_i = observed value at time i

m = number of observed values

In the above equation (8.1) F^2 is similar to the residual variance of a regression analysis, and the initial variance F_o^2 is defined by:-

$$F_o^2 = \sum_{i=1}^{m} (q_i - \bar{q})^2 \qquad (8.2)$$

where $\bar{q}$ = mean of the observed ordinate.

The efficiency of the model, R^2, is therefore defined as the proportion of the initial variance which the model is able to reproduce such that:

$$R^2 = \frac{F_o^2 - F^2}{F_o^2} \qquad (8.3)$$

The significance of $R^2 = 1$ is that the fit is perfect while $R^2 < 0$ shows that the mean of the values gives a better result.

8.3.1 Linear Drying Curve

The form of the drying curve selected for model performance is similar to that in Figure 4.5.

This curve shows that at some range of the available water, the crop transpires at the potential evaporative demand until a threshold value, equivalent to the root constant is reached. Beyond this critical point, actual evapotranspiration falls below the potential evapotranspiration rate. In Figure 4.5 the points A and B are not known, consequently a computer program (Appendix B) was developed by this author which utilises the above objective function as a performance criterion to estimate values of available water at points A and B. The computer program requires as inputs daily rainfall data, initial SMD and daily potential evapotranspiration rates.

Trial and error values were assigned to represent points A and B in Figure 4.5, and simulated moisture deficits were obtained using the procedure described earlier in Figure 4.4. The simulated moisture deficits were then compared with the observed soil moisture deficits using the R^2 criterion. The optimum R^2 values obtained for the various crops are shown in Table 8.2. In assigning values to the root constant which is equivalent to point A in Figure 4.5, negative values were precluded since this would be inconsistent with the root constant concept. An interesting observation in the optimisation results for all sites is the development of a contouring ridge in the response surfaces obtained by plotting R^2 values as a function of the two parameters, the root constant (A) and available water capacity (B). The result for the permanent grass site using the 1980 soil moisture data set is shown in Figure 8.2. This shows that there is a linear relationship between the root constant values and the available water capacity. For all sites, the optimal R^2 values were obtained close to zero root constant as shown in Table 8.2. The implication of the latter is that once a deficit sets in, the actual evapotranspiration rate falls below the potential evapotranspiration rate at increasing soil moisture deficits. This observation can probably be explained by the nature of the soil prevalent in the field site. The soils are sandy and hence highly conductive at higher moisture contents. This property is likely to lead to greater losses of soil

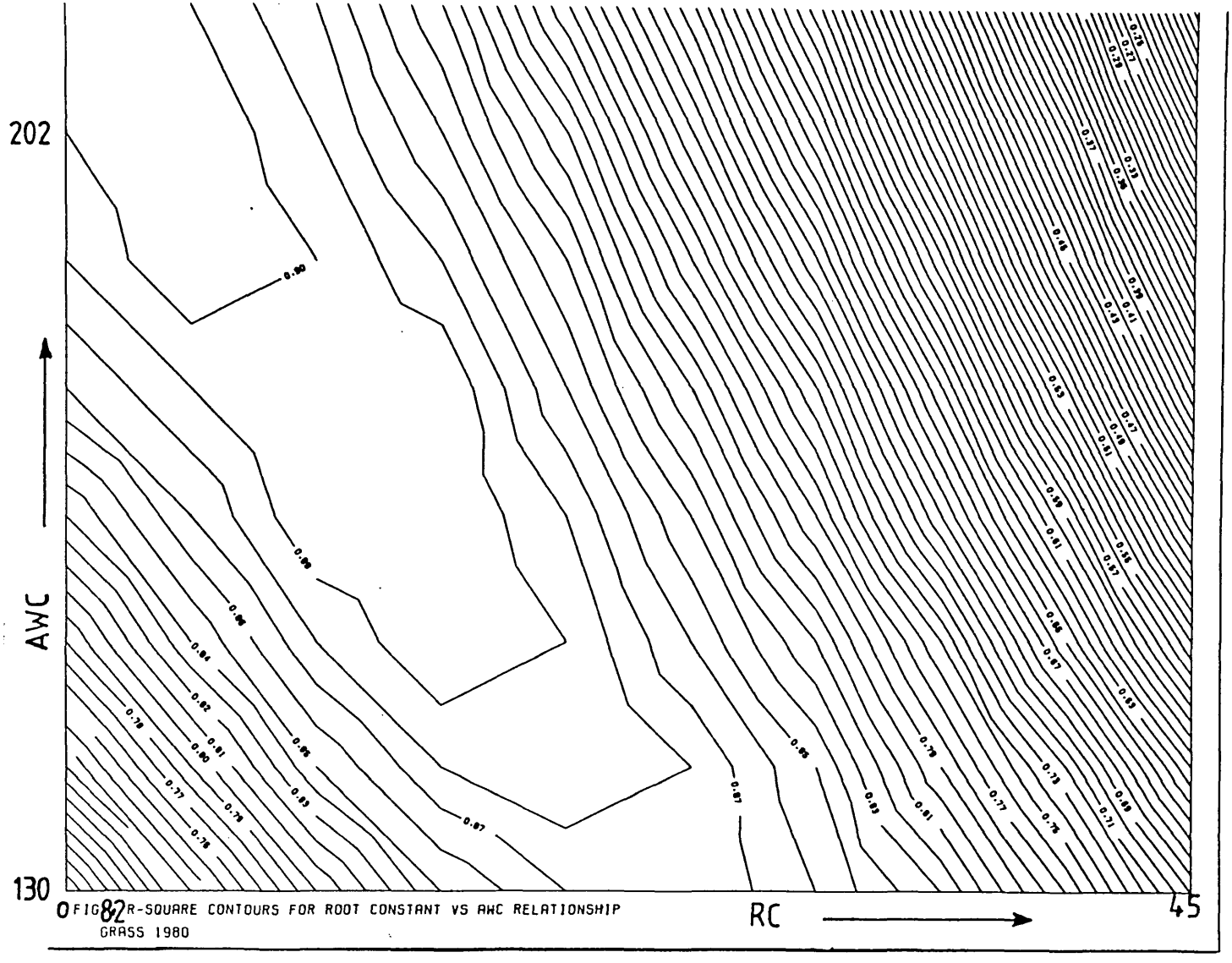

FIGURE 82 R-SQUARE CONTOURS FOR ROOT CONSTANT VS AWC RELATIONSHIP
GRASS 1980

moisture to deep percolation and thus little water retention in the rooting zone to satisfy the potential evaporative demand. For a beginning, the optimisation was confined to the 1980 data. However it is borne in mind that the available water capacity for individual sites may not be constant since it is subject to changes in the soil area that is exploited by the plant roots. Consequently, yearly opimisation of the available water capacities (AWC') for the different crops was carried out. Table 8.2 shows the corresponding R^2 values obtained coupled with the variations in available water capacities that resulted. The field beans/cabbage site showed the least available water capacity of 51 mm while the orchard site has the highest available water capacity of 280 mm. The result showed that in utilising the linear depletion curve, the available water capacity variation from year to year must be considered as this would have some influence on model output.

TABLE 8.2 : Linear depletion curve - available water optimisation

Crop	Year	RC (mm)	AWC (mm)	R^2	RC (mm)	AWC' (mm)	R'^2
Grass	1980	0	202	0.9099	0	202	0.9099
	1981	9	202	0.9088	0	207	0.9143
	1982	6	202	0.8562	0	194	0.8840
Wheat	1980	0	204	0.8326	0	204	0.8326
	1981	13	204	0.8089	0	211	0.8204
	1982	7	204	0.5835	0	172	0.6090
Orchard	1980	0	280	0.8196	0	280	0.8196
	1981	24	280	0.7252	0	220	0.7390
	1982	18	280	0.6049	0	252	0.6234
Field Beans/ Cabbage	1980	0	123	0.8277	0	123	0.8277
	1981	26	123	0.5130	0	51	0.7160
	1982	-	-	-	-	-	-

8.3.2 The Exponential Drying Curve

Prior discussion on the operational behaviour of the exponential drying curve in Chapter 4 has shown the necessity for estimating the critical point at which actual evaporation rate falls below the

potential evaporation rate. The R^2 criterion as discussed above was also utilised to obtain optimised values for the root constant. The R^2 values obtained for the exponential curve in the different crops and associated root constants are shown in Table 8.3. The variation of the optimised root constants with years is also demonstrated.

TABLE 8.3 : Exponential drying curve - optimised root constant

Crop	Year	Root Constant (mm)	R^2
Grass	1980	36.0	0.8641
	1981	31.0	0.9338
	1982	39.0	0.8464
Wheat	1980	74.0	0.8073
	1981	48.0	0.7817
	1982	60.0	0.6113
Orchard	1980	72.0	0.8167
	1981	51.0	0.5698
	1982	70.0	0.5983
Field Beans/ Cabbage	1980	27.0	0.7959
	1981	12.0	0.7131
	1982	-	-

An implication of the variation of root constants with years for the exponential curve is that the application of quoted fixed root constant values to simulate soil moisture deficits should be used with caution. This latter result is in agreement with Wheater et al. (1982) and Calder et al. (1983) findings that yearly variations of root constants produce better fits than the utility of quoted root constant values.

8.4 Simulation Results

The simulated optimised soil moisture deficits using the linear depletion curve compared with observed soil moisture deficits are shown in Figures 8.3a, 8.3b, 8.3c, 8.4a, 8.4b, 8.4c, 8.5a, 8.5b, 8.5c and 8.6a, 8.6b, for grass, wheat, orchard and field beans/cabbage sites respectively.

Generally, the simulations show that the linear model is able to reproduce the seasonal variations in soil moisture deficit,

FIG.8.3a SIMULATED Vs OBSERVED SMDs (GRASS 1980)

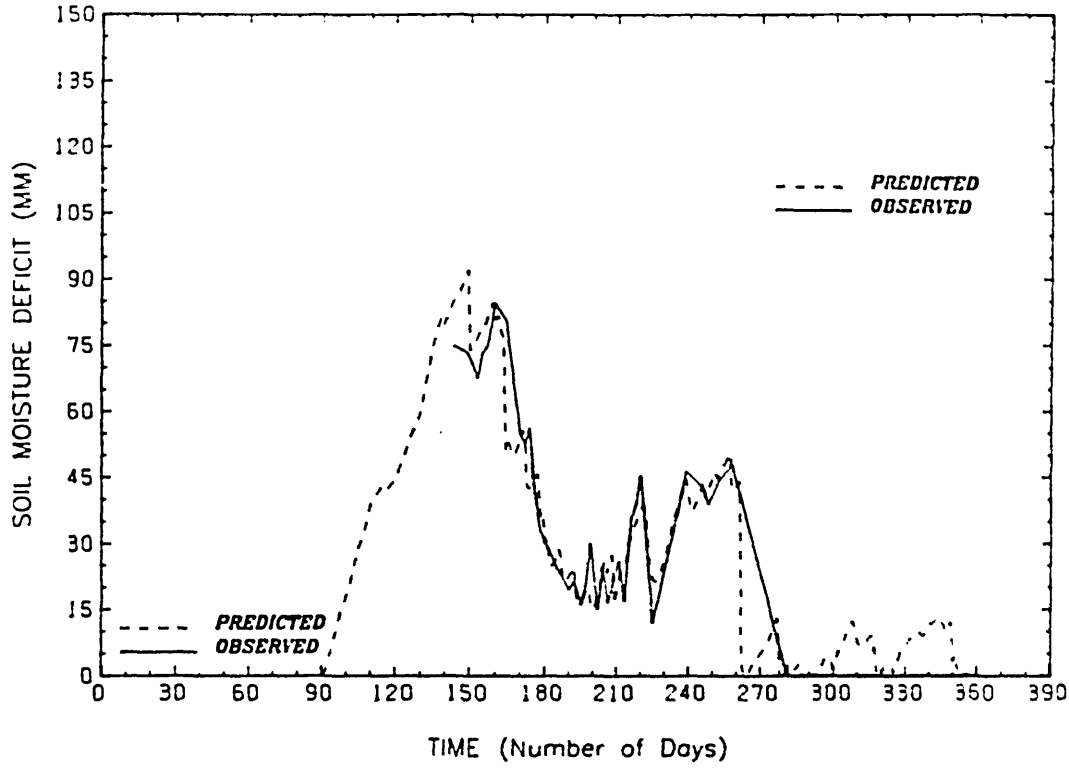

FIG. 8.3b SIMULATED Vs OBSERVED SMDs (GRASS 1981)

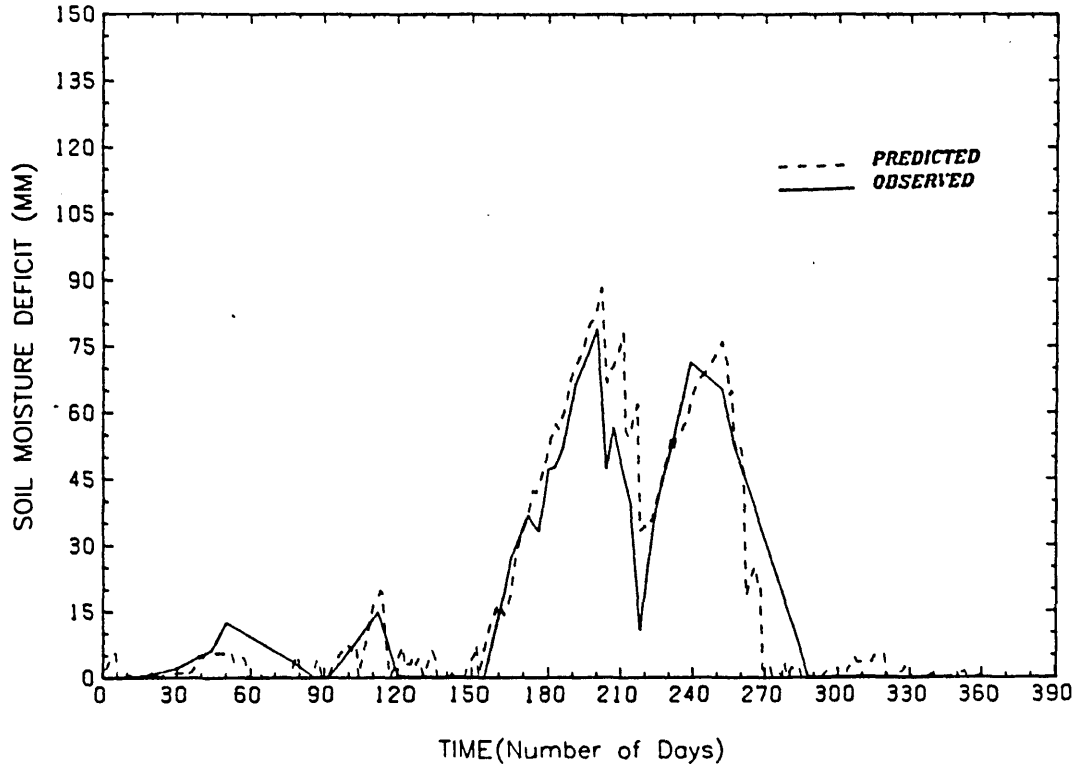

FIG.8.3c SIMULATED Vs OBSERVED SMDs (GRASS 1982)

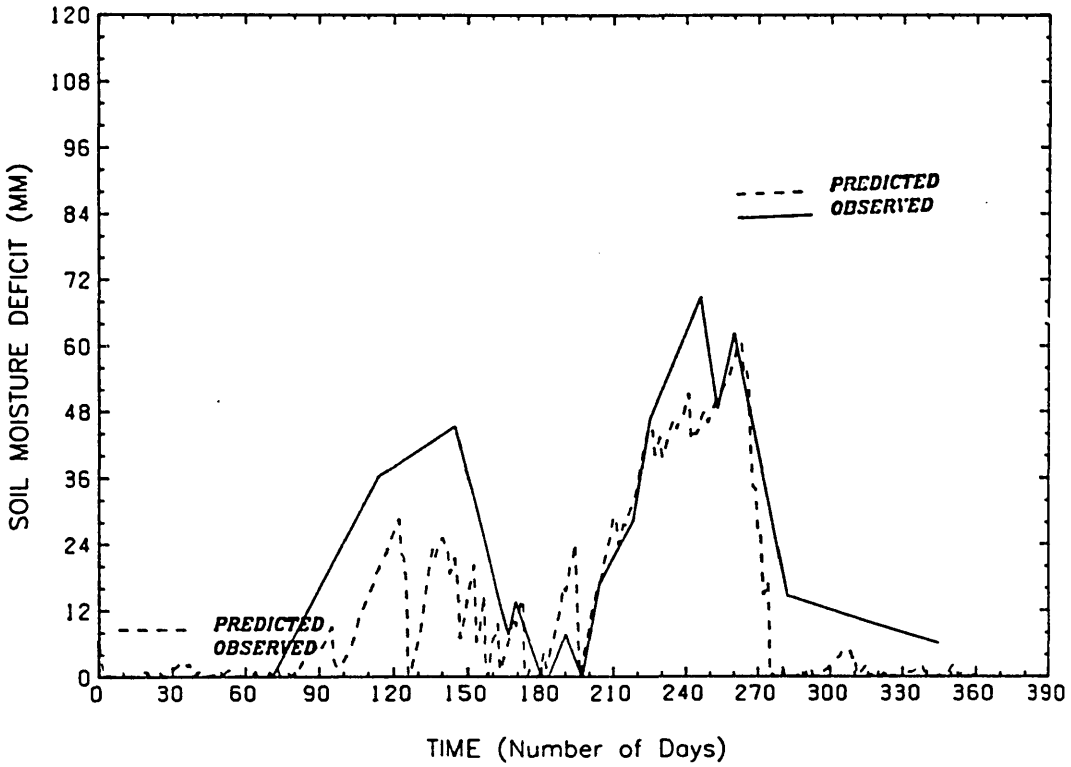

FIG.8.4c SIMULATED Vs OBSERVED SMDs (WHEAT 1980)

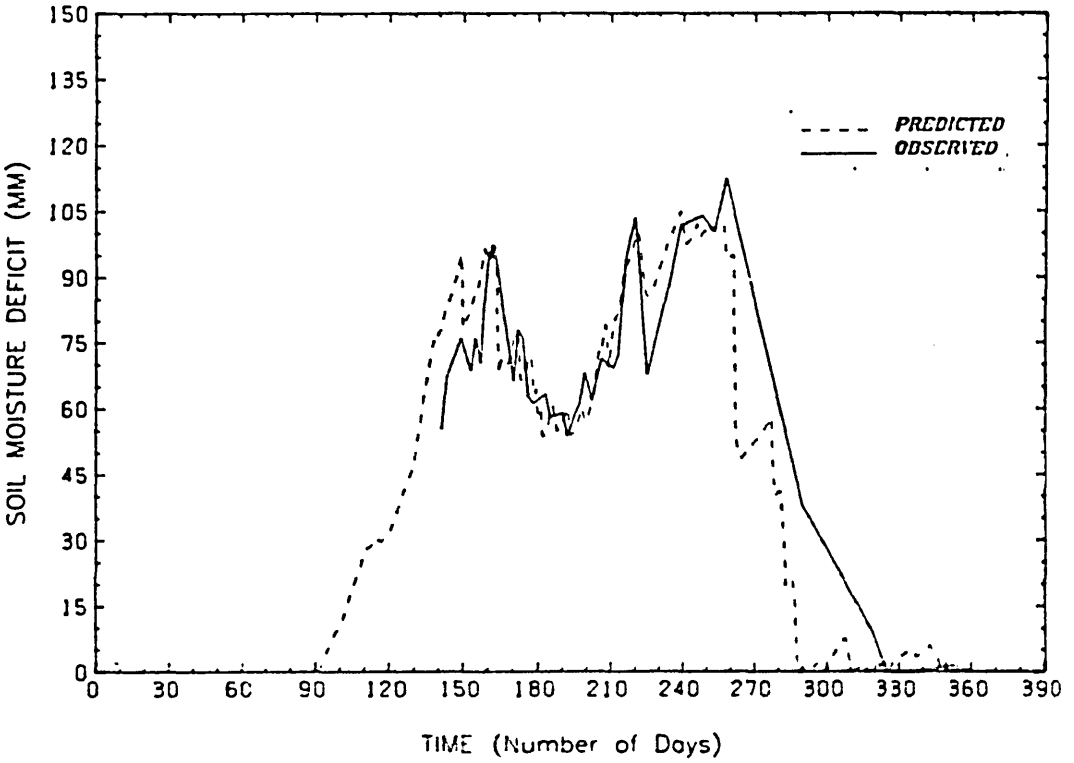

FIG.8.4b SIMULATED Vs OBSERVED SMDs (WHEAT 1981)

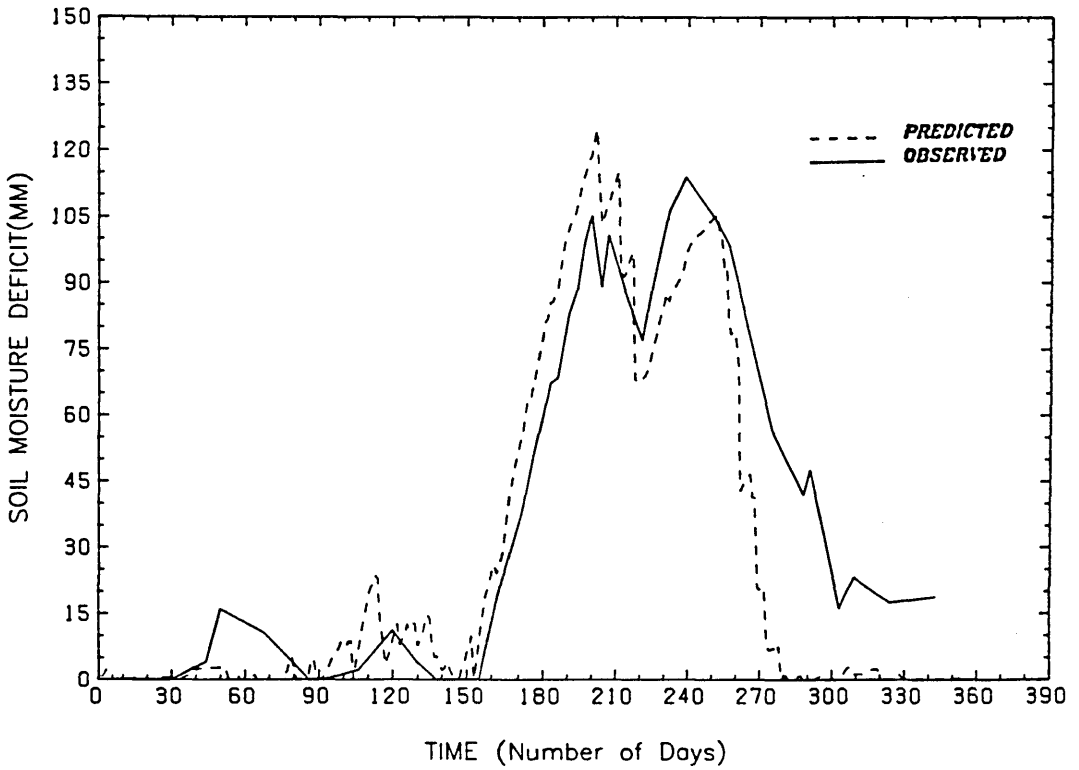

FIG.8.4c SIMULATED Vs OBSERVED SMDs (WHEAT 1982)

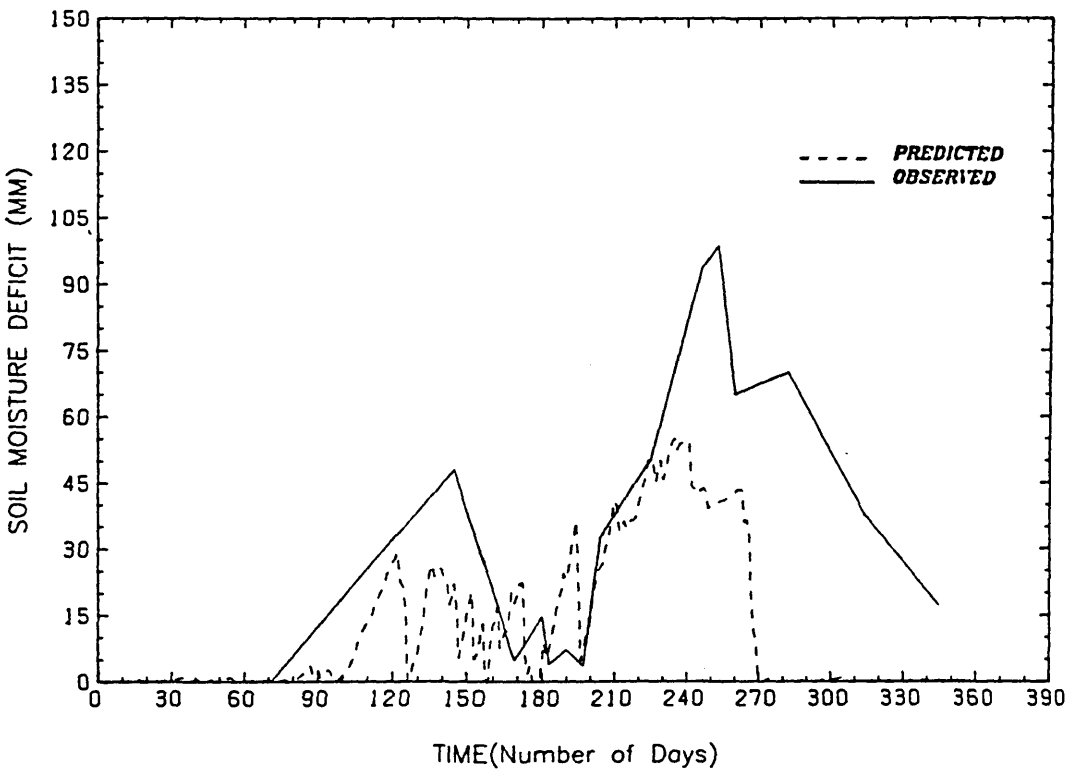

FIG. 8.5a SIMULATED Vs OBSERVED SMDs (ORCHARD 1980)

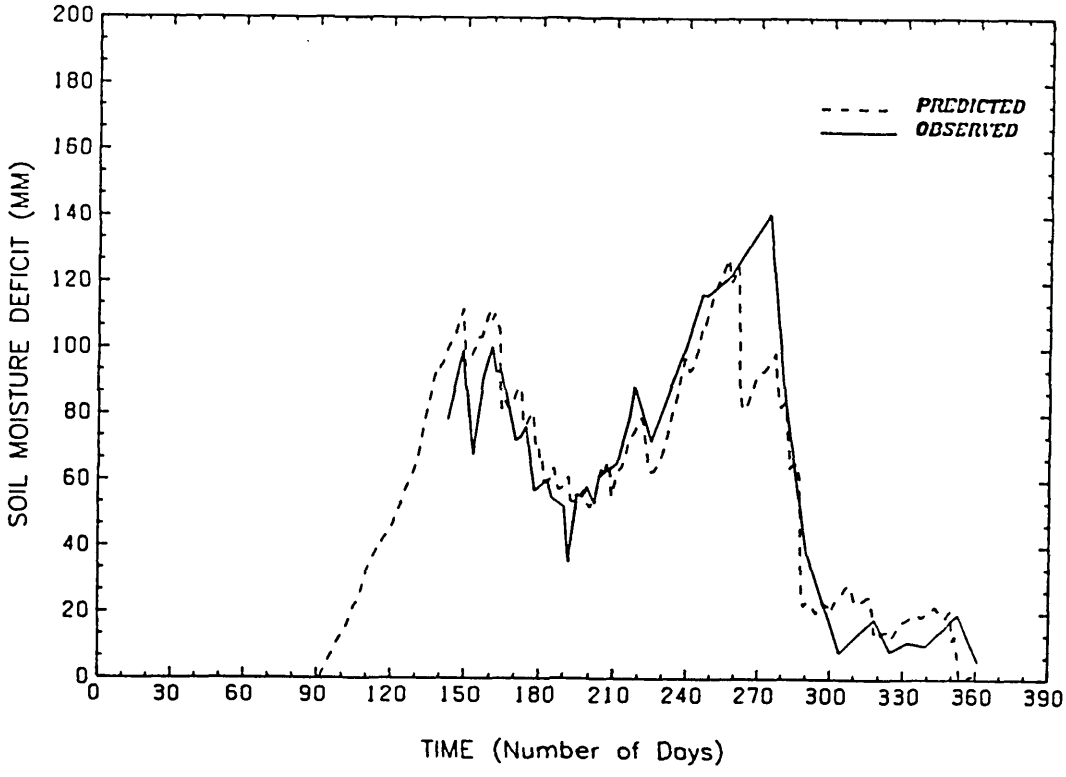

FIG. 8.5b SIMULATED Vs OBSERVED SMDs (ORCHARD 1981)

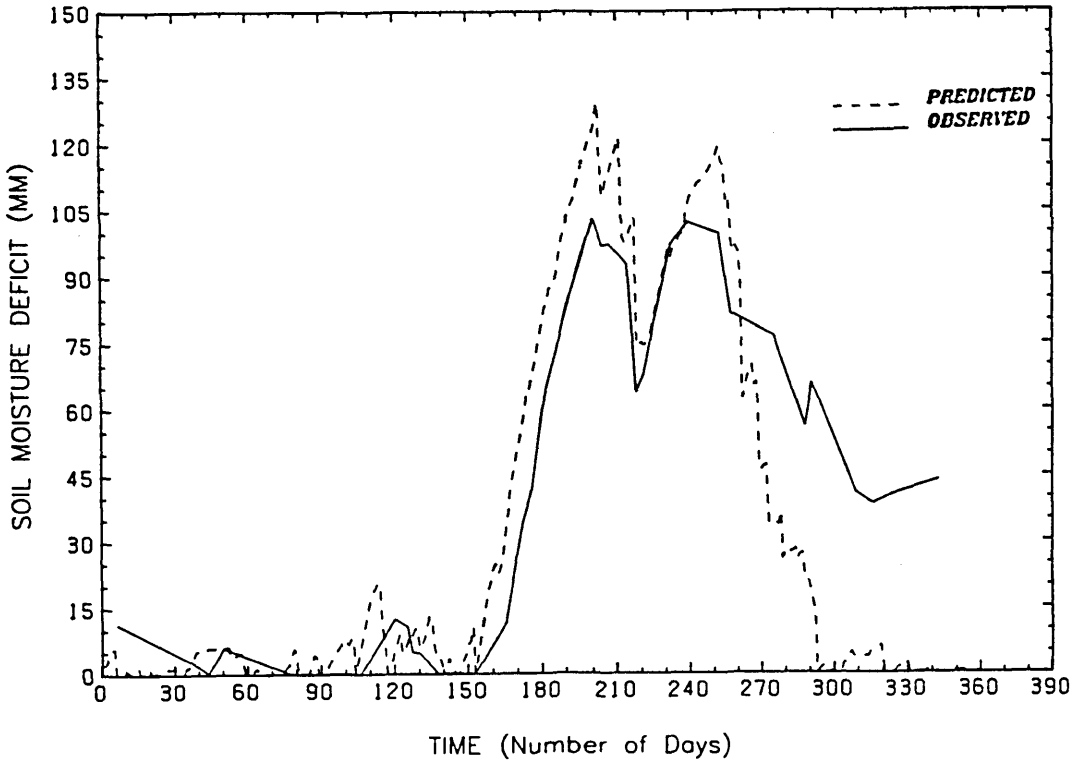

FIG. 8.5c SIMULATED Vs OBSERVED SMDs (ORCHARD 1982)

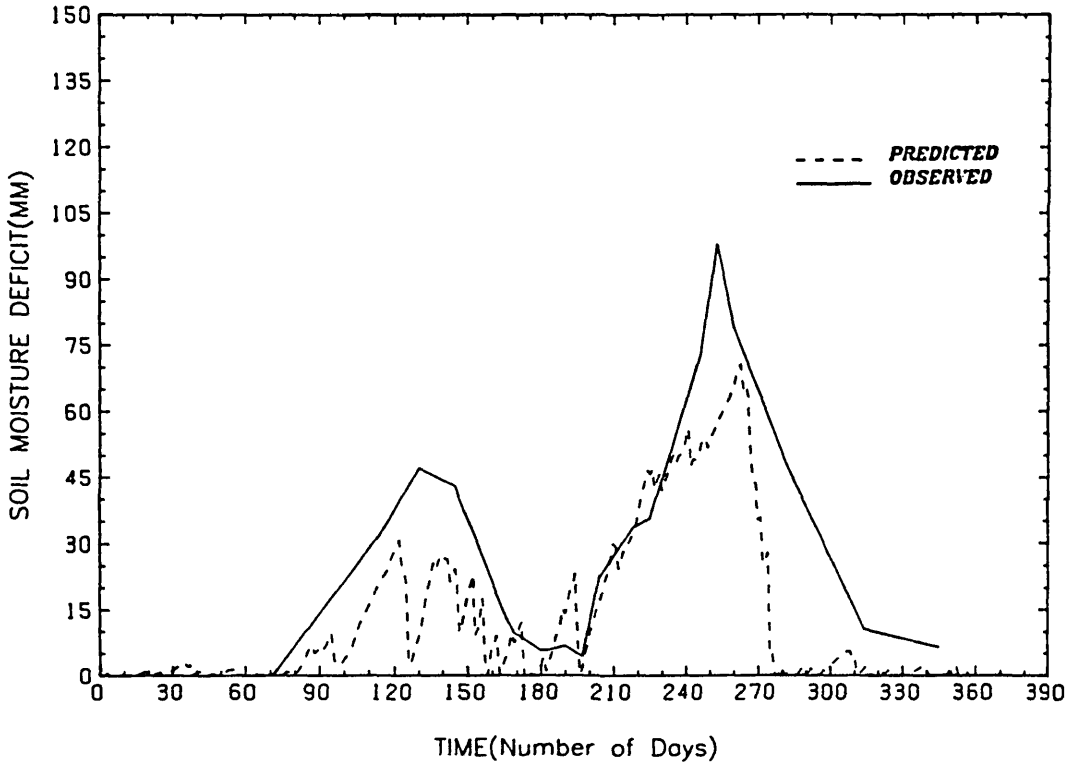

FIG. 8.6a SIMULATED Vs OBSERVED SMDs (FIELD BEAN 1980)

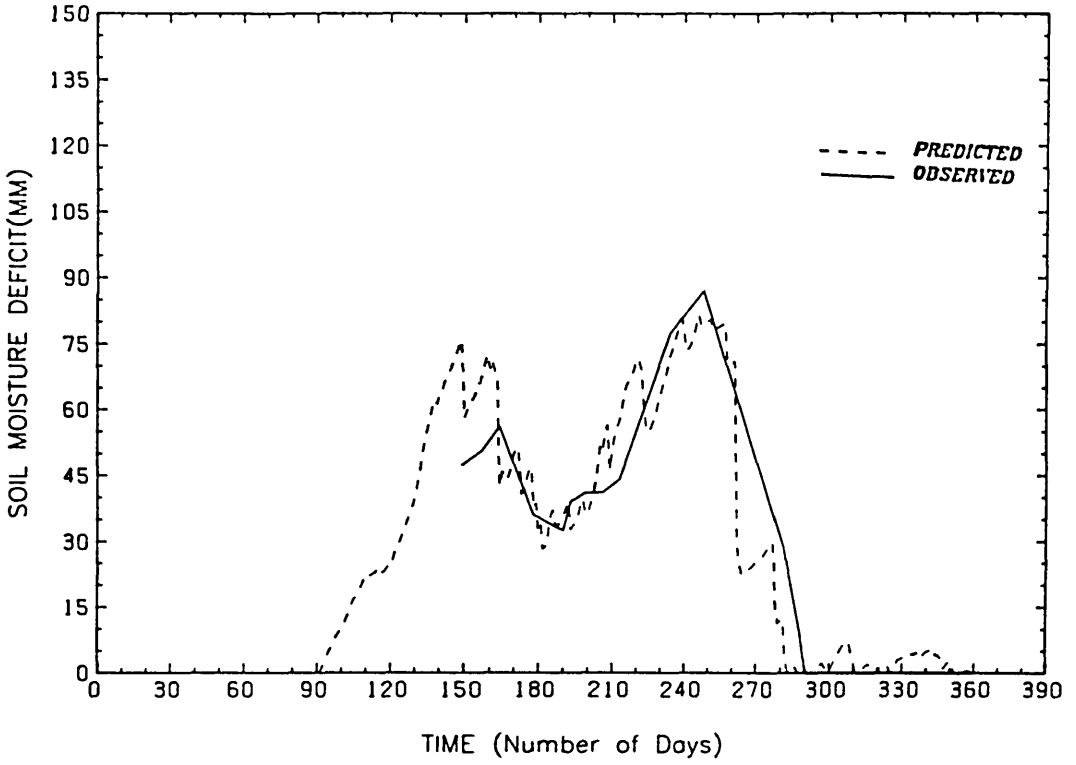

FIG. 8.6b SIMULATED Vs OBSERVED SMDs (CABBAGE 1981)

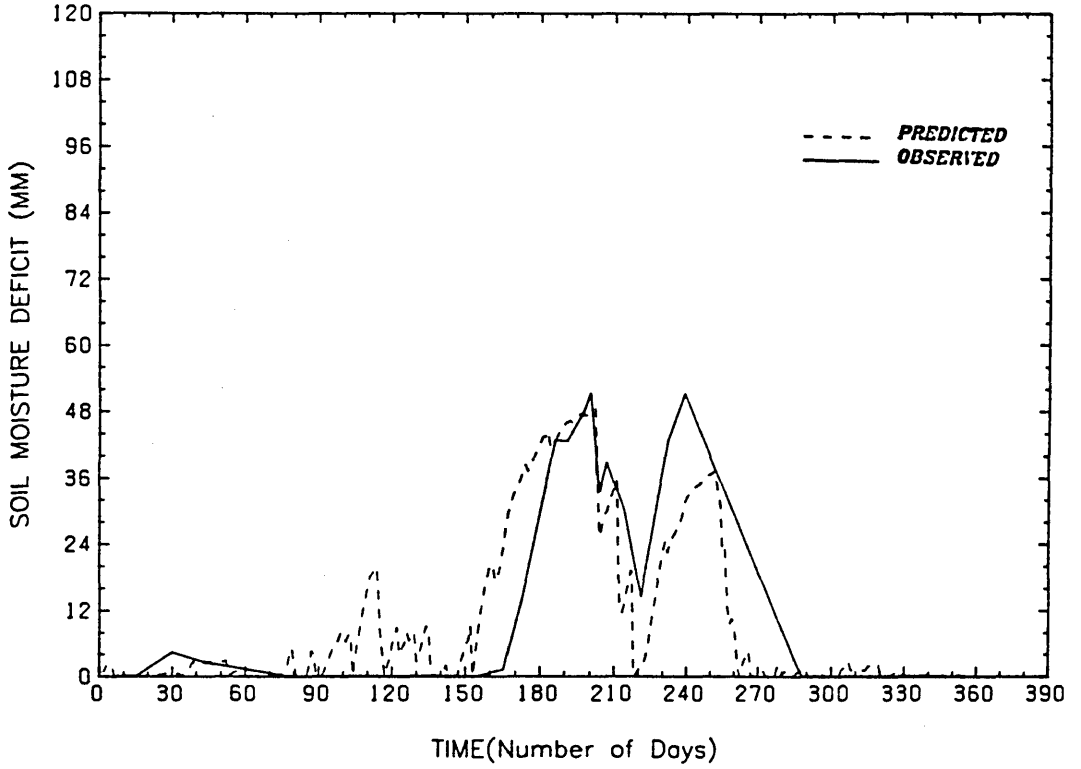

although some deficiencies in performance are apparent. It should also be noted that the interpretation of the data in some cases may be ambiguous. The latter is especially true during the autumn and winter months when the frequency of measured SMD is once weekly and sometimes once in every fortnight. This is also applicable to the 1982 cropping season where few measured data are collected compared to previous years.

In spite of the relatively good agreement obtained between predicted and observed soil moisture deficits for all crops, a consistent feature observed is an earlier prediction of return to field capacity by the linear model. This behaviour is demonstrated in Figures 8.3a and 8.3b for the permanent grass site, 1980 and 1981 autumn periods, this duration being 16 days coinciding with days 264 and 280 in Figure 8.3a. This latter observation may be ascribed to the methodology used in determining the field capacity. This is because specific profile depths were considered which in most cases will also include the drainage component of the unsaturated zone; and hence may lead to relatively higher field capacity values.

Figures 8.7a, 8.7b, 8.7c, 8.8a, 8.8b, 8.8c and 8.9a, 8.9b, 8.9c and 8.10a, 8.10b are the predicted soil moisture deficits obained from the exponential curve as compared with the observed. The simulations are similar to those obtained for the linear depletion curve. However when the R^2 values obtained by both linear and exponential curves are compared (Tables 8.1 and 8.2), the linear depletion curve has a superior performance. Certain definite assumptions in the operations of the models must have accounted for these differences in performance. These assumptions include the use of the available water capacity and the exponential decay curve. The former assigns a limit to the amount of water made accessible to the plant and must have made allowance for capillary movement to the roots. In the exponential curve however, there is no limit imposed on the amount of water available to the plant and an equation applicable to bare soil is assumed to prevail beyond the root constant for all crops. This equation should be expected to differ for differing soil types and for this study must have influenced the output of the model. Other factors which must have also affected the models' performance include the assumptions that there are no runoff and interception, as such all precipitation is assumed to percolate the soil profile.

FIG. 8.7a SIMULATED Vs OBSERVED SMDs (GRASS 1980)
(EXPONENTIAL CURVE)

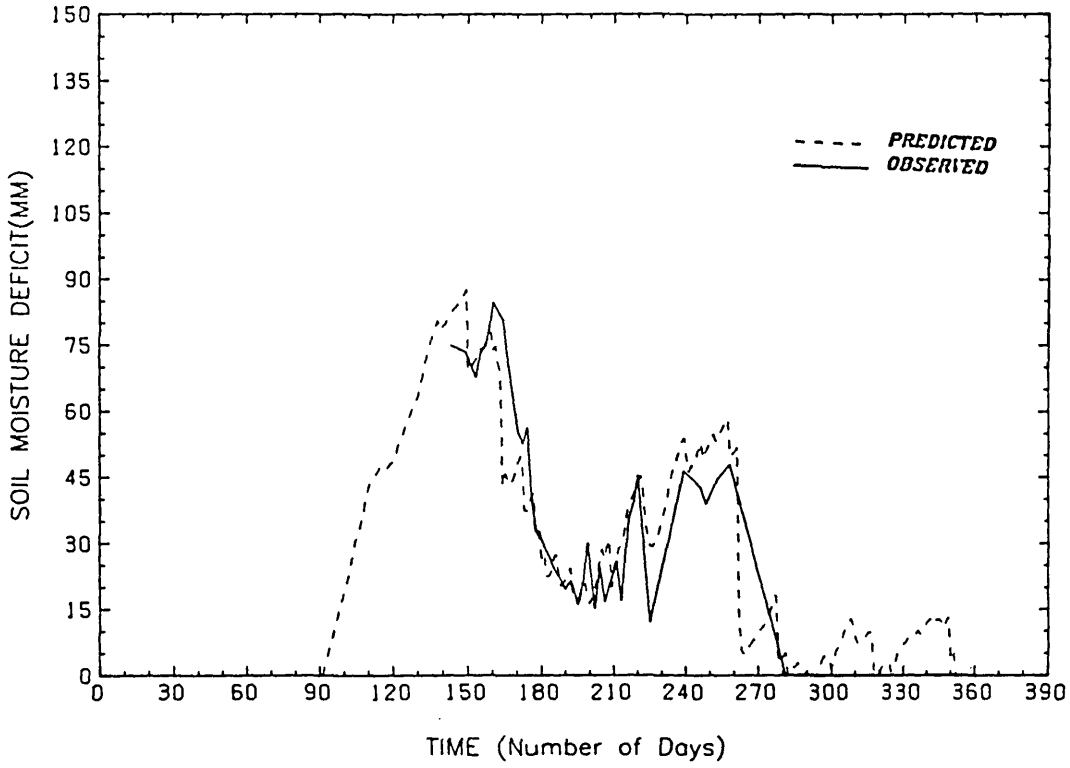

FIG. 8.7b SIMULATED Vs OBSERVED SMDs (GRASS 1981)
(EXPONENTIAL CURVE)

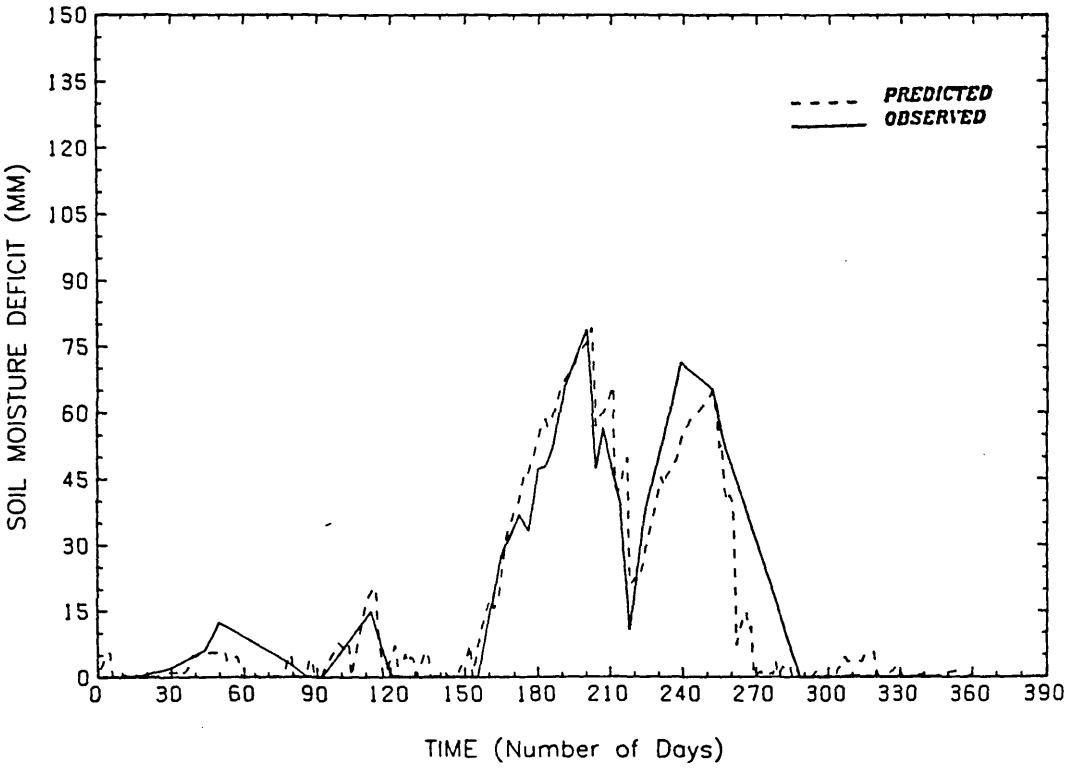

FIG. 8.7c SIMULATED Vs OBSERVED SMDs (GRASS 1982)

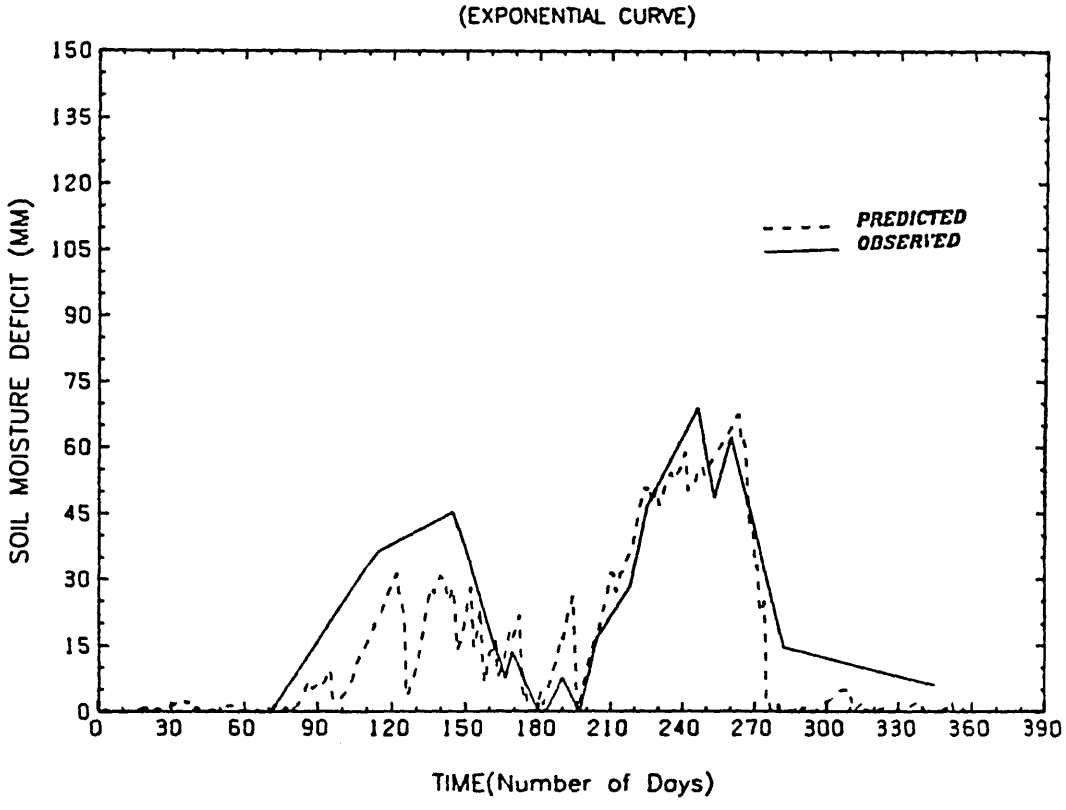

FIG. 8.8a SIMULATED Vs OBSERVED SMDs (WHEAT 1980)
(EXPONENTIAL CURVE)

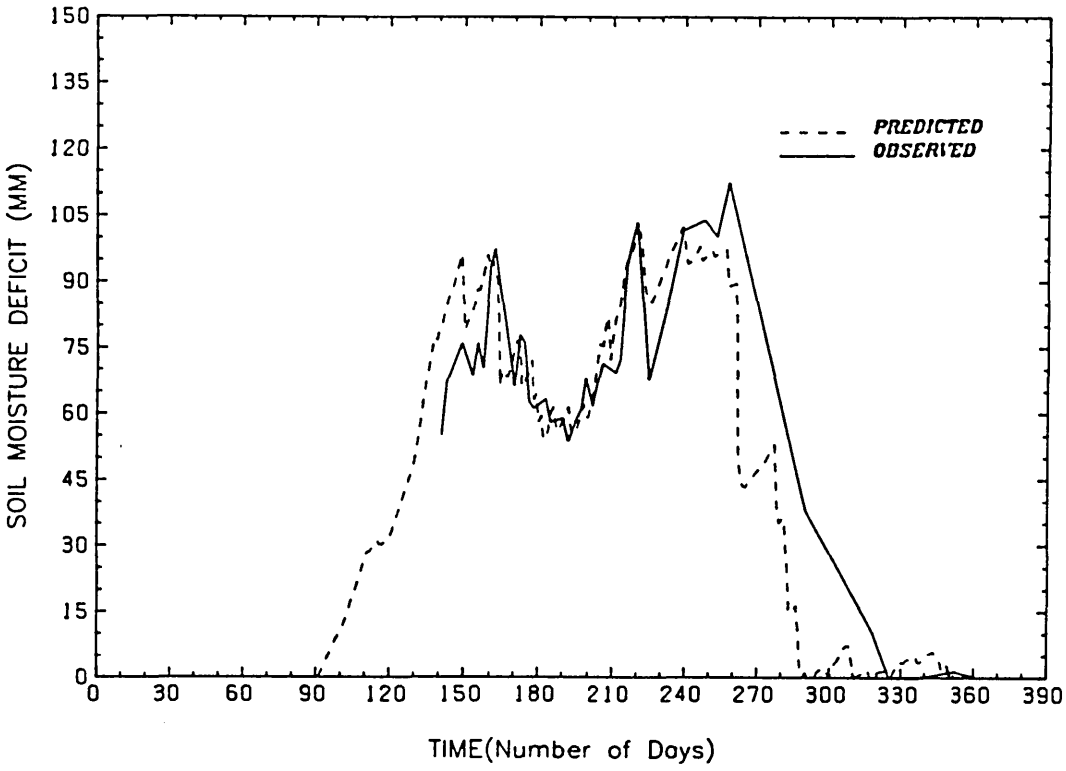

FIG. 8.8b SIMULATED Vs OBSERVED SMDs (WHEAT 1981)
(EXPONENTIAL CURVE)

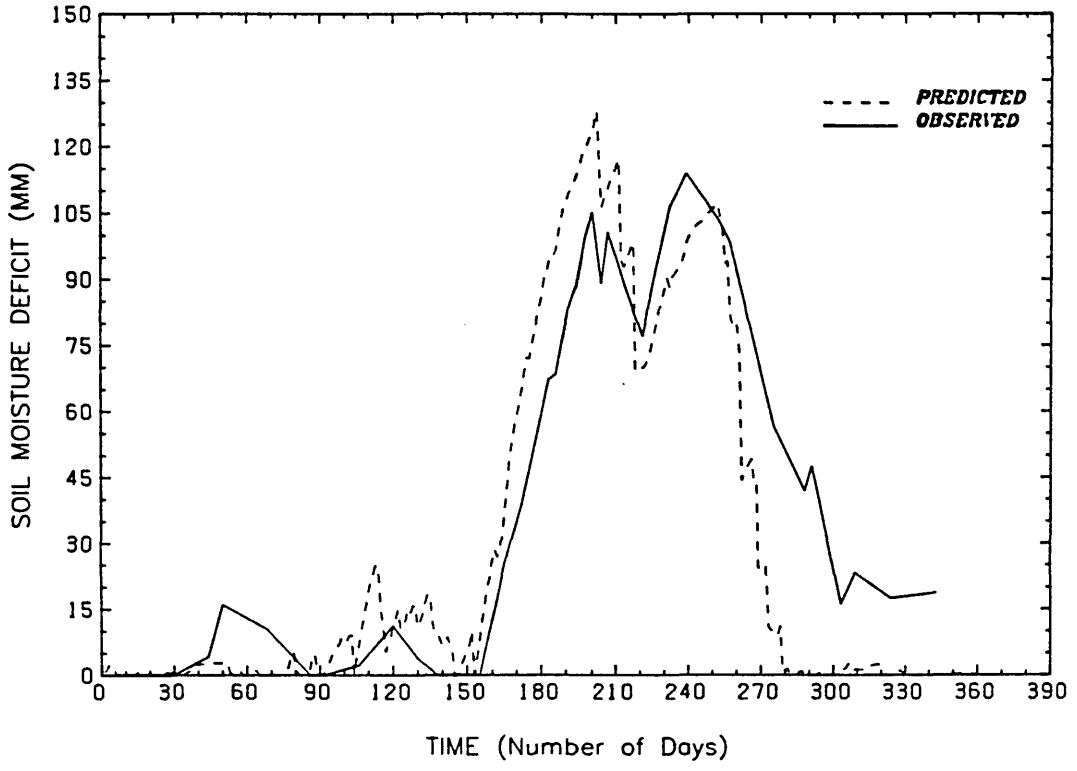

FIG. 8.8c SIMULATED Vs OBSERVED SMDs (WHEAT 1982)

(EXPONENTIAL CURVE)

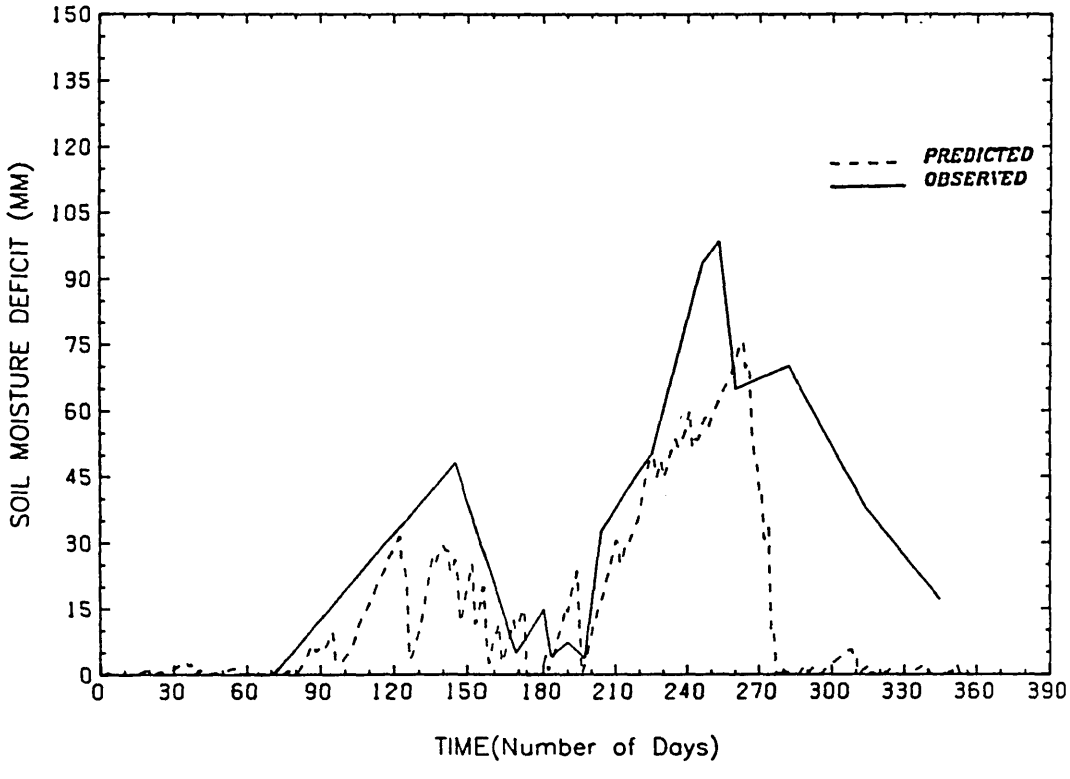

FIG. 8.9a SIMULATED Vs OBSERVED SMDs (ORCHARD 1980)
(EXPONENTIAL CURVE)

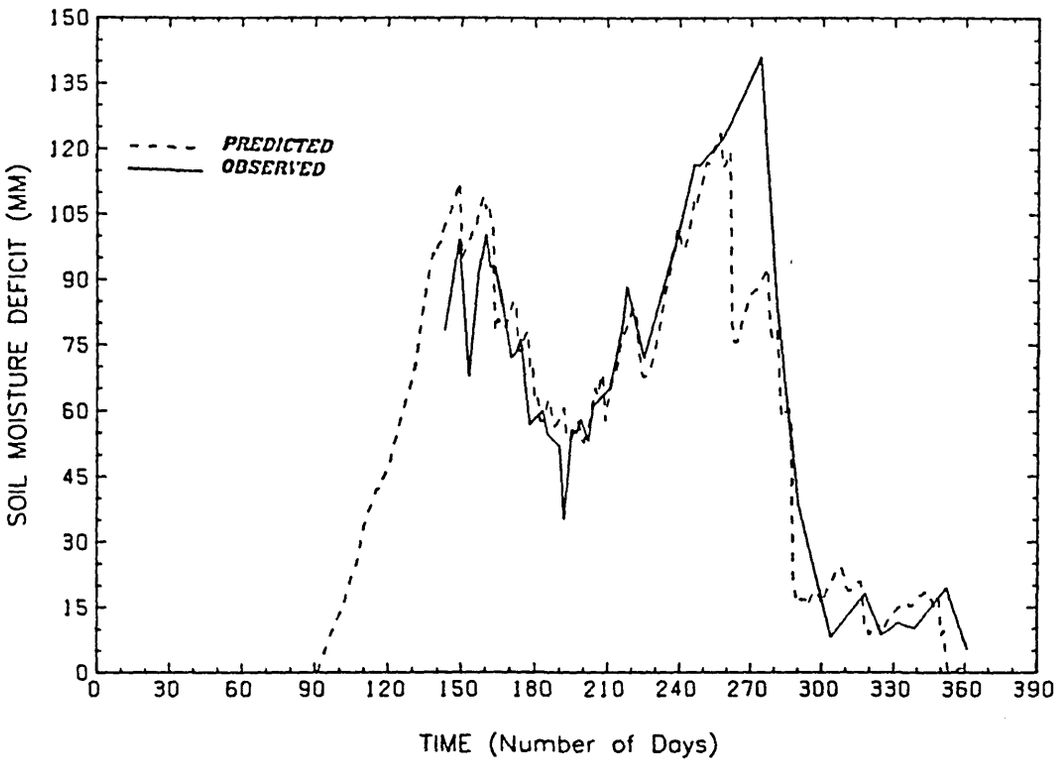

FIG. 8.9b SIMULATED Vs OBSERVED SMDs (ORCHARD 1981)
(EXPONENTIAL CURVE)

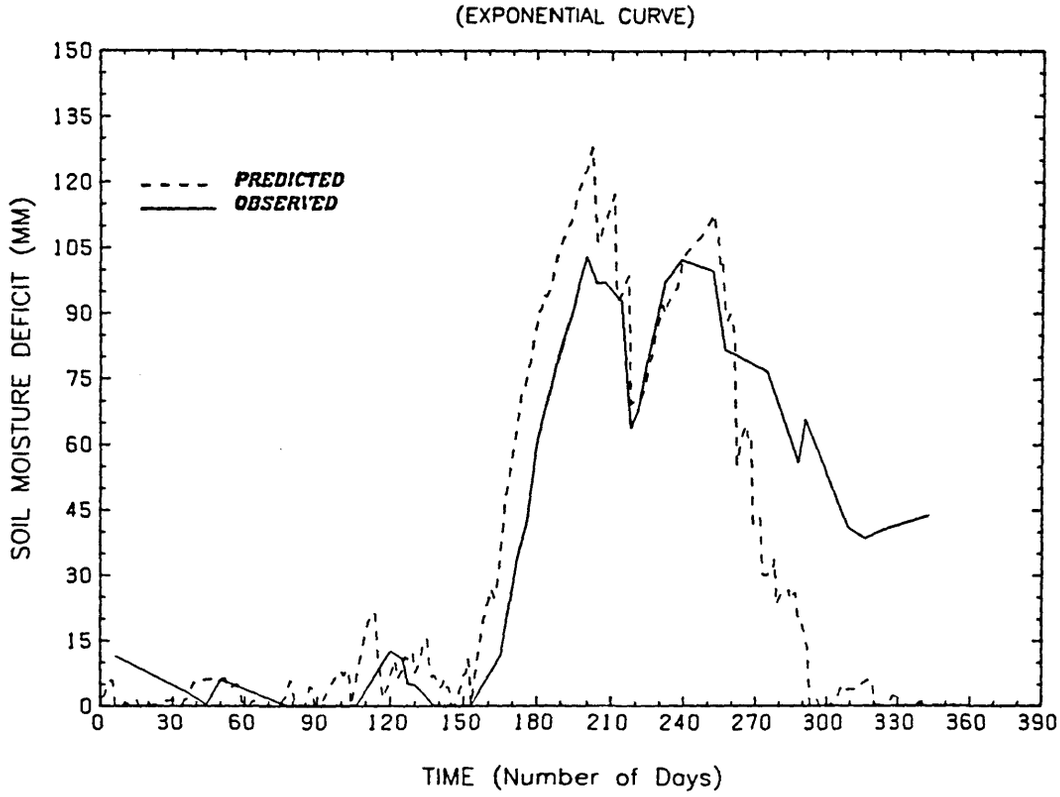

FIG. 8.9c SIMULATED Vs OBSERVED SMDs (ORCHARD 1982)

(EXPONENTIAL CURVE)

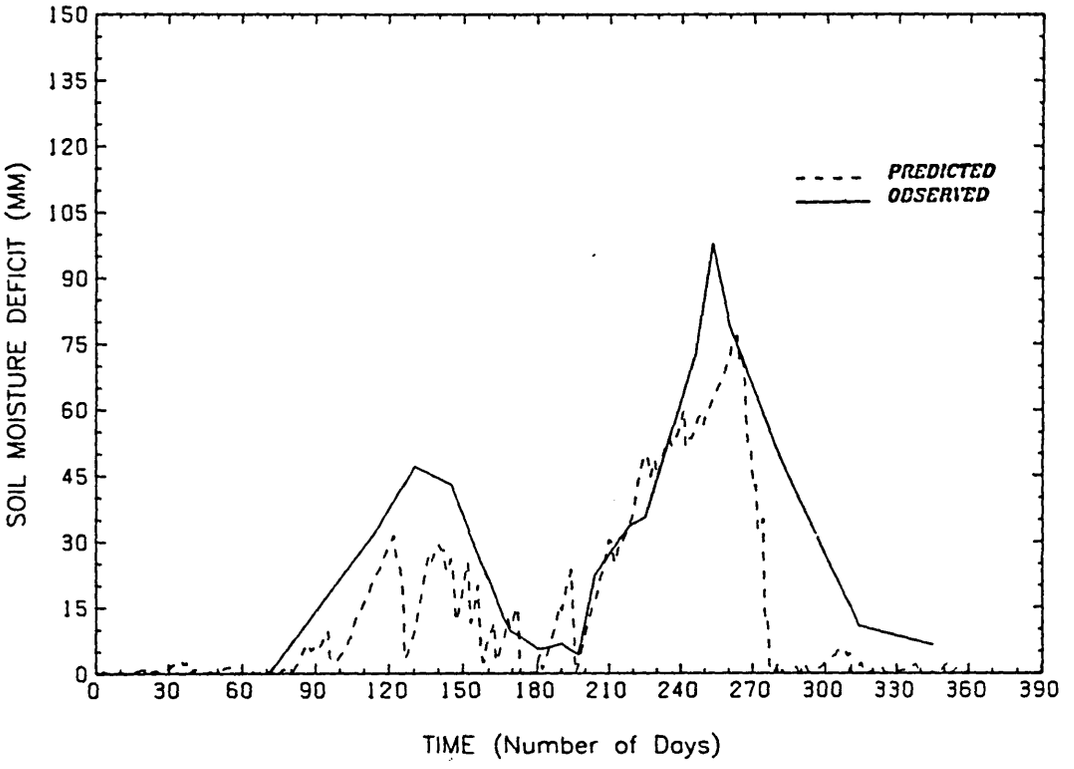

FIG. 8.10a SIMULATED Vs OBSERVED SMDs (FIELD BEAN 1980)
(EXPONENTIAL CURVE)

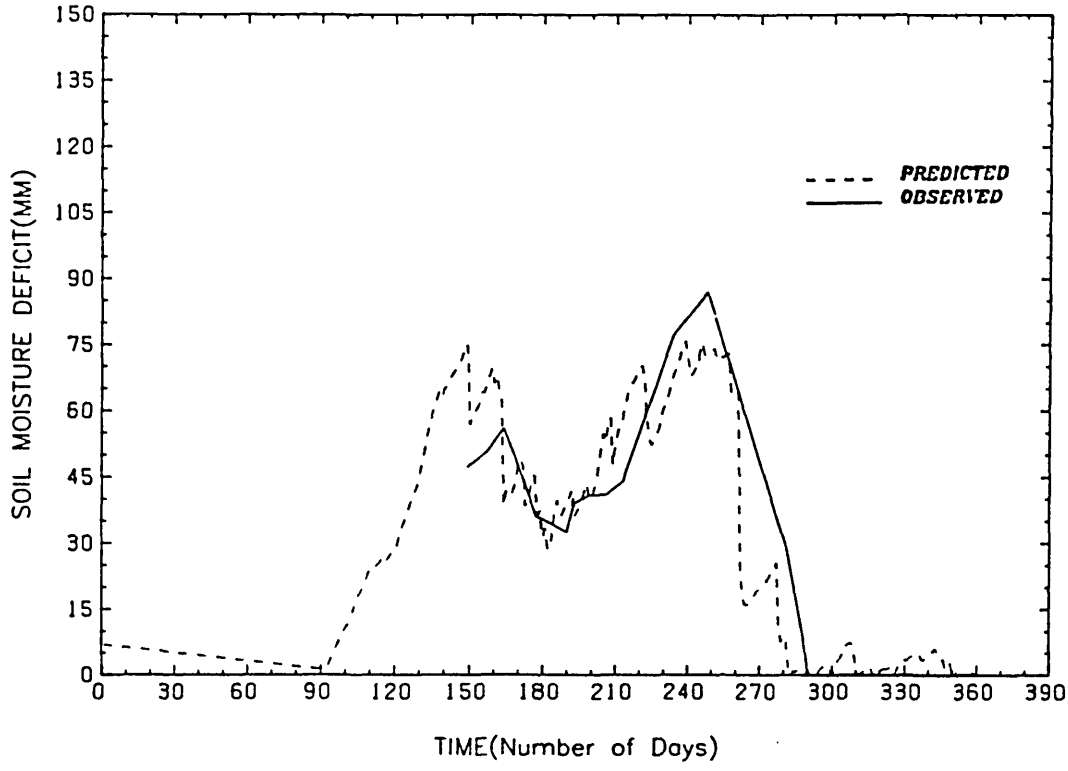

FIG. 8.10b SIMULATED Vs OBSERVED SMDs (CABBAGE 1981)
(EXPONENTIAL CURVE)

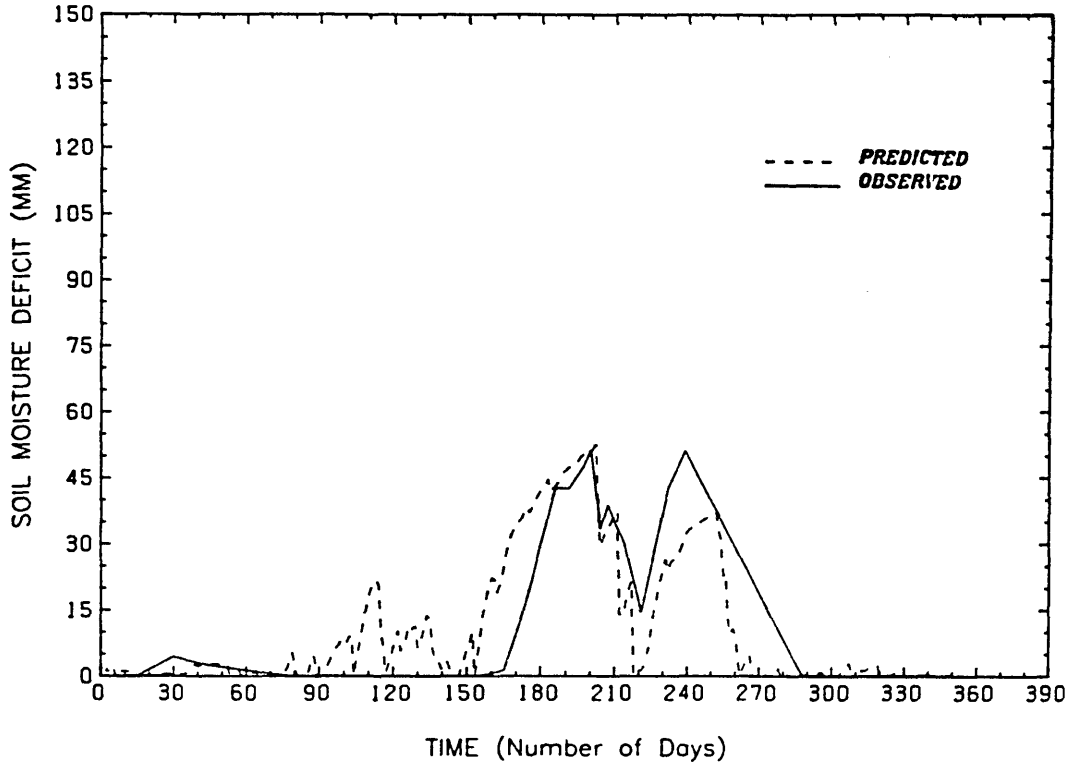

8.5 Recharge Estimation

As discussed earlier, the empirical models estimate actual evaporation and hence the residual from rainfall of recharge and runoff. In the experimental site, runoff is only observed in exceptional storms, as such the residual is assumed to reflect recharge only.

Table 8.4 shows the recharge estimates obtained for both models under the various crops. It should be noted that the 1980 recharge estimates do not include the recharge for the winter months January - March 1980 but for the spring, summer and autumn months. This is because climatic and soil moisture data were only available for the latter months. For the 1980 season, the field bean/cabbage gave the highest recharge of 104.29 mm for the linear model and orchard has the lowest of 11.59 mm. However for the 1981 season, although the pattern was repeated, it is observed that not much variation occurs between recharge estimated by both models.

TABLE 8.4 : Recharge estimates (mm)

Year	Crops							
	Grass		Wheat		Orchard		Field Beans/ Cabbage	
	Linear	Exponential	Linear	Exponential	Linear	Exponential	Linear	Exponential
1980	87.98	77.90	72.62	79.48	11.59	14.91	104.29	98.15
1981	293.19	289.81	290.56	282.06	215.06	211.88	369.72	348.50
1982	311.6	291.84	331.30	292.27	301.18	301.52	-	-

The recharge estimation is however limited by the conceptual basis of the model which does not recognise the existence of simultaneous recharge and deficit. However, it has become apparent at least in the permanent grass plot as demonstrated in Chapter 6, that even during deficit conditions, recharge does occur. This being evident in the hydraulic head profiles in Figure 7.1b. These profiles show that as drying continues, the zero flux plane moves down, but drainage continues at depth during the summer although at reduced rates. The concept of a single field capacity value for the profile is inappropriate for this response, which can only be represented in a

multilayer approach; as shown by the physical model simulations in previous chapter.

8.6 Spatial Variability of SMD's

In the evaluation of the empirical models, only the soil moisture data from one access tube in each of the crop sites was utilised. However, it is recognised that spatial variability occurs in soil moisture response to rainfall and also in the local plant population around each access tube. Consequently the observed soil moisture deficits computed for each access tube were analysed for their standard deviation during the period of the study using the following equation:-

$$\sigma_E = \sum_{i=1}^{n} [(q_i - \bar{q})^2/(n - 1)]^{\frac{1}{2}} \qquad (8.4)$$

where σ_E = standard deviation

q_i = measured SMD

$\bar{q}$ = mean of observed SMD's for a given tube

n = number of observations

Equations 8.4 as defined provides a measure of the variability of the SMD for the individual tubes. This gives an indirect measure of spatial variability when the standard deviations are compared.

Table 8.5 gives the standard deviations obtained for the various crops. The result shows the very high variability that occurs in soil moisture deficit in the experimental site. The difference in the variability at the wheat, permanent grass and field bean/cabbage sites access tubes can be explained by the large separation of the access tubes in each site, and also by the plant population around each access tube. This difference is particularly amplified in the permanent grass plot, which is about ±15 mm. In contrast the difference in the standard deviations for the orchard is 4.19 mm, which indicates that there is not much variability in the calculated standard deviation for the orchard. This is explained by the fact that the

access tubes are relatively more closely spaced, a maximum of 1 metre apart.

TABLE 8.5 : Standard deviation of measured SMD's

Crop	Year	Tube 1	Tube 2	Tube 3	Tube 4
		Standard Deviation (mm)			
Grass	1980-1982	24.92	40.13	-	-
Wheat	1980-1982	26.57	35.32	30.14	-
Orchard	1980-1982	36.19	37.84	33.65	37.20
Field Beans/ Cabbage	1980-1982	38.62	-	-	-

In general, the high variability in the experimental sites can be explained by medium scale inhomogeneities in the soil profile as evidenced by a more developed humus layer in the orchard profiles. This is likely to vary with depth and hence can influence the measured SMD. Also the observation of podsolisation below a depth of 1.2 m in the site might have caused the high variability due to capillary rise or lateral movement which could have resulted in times when the soil profile is still wet below and drying at the upper part.

8.7 Conclusions

The assessment of two single layer soil moisture models have been made regarding their predictive abilities. It has been shown that the models can give reasonable simulation of soil moisture when expressed as a deficit with respect to field capacity. The simulations are shown to be improved if the available water capacity and root constant values are allowed to vary for different years. However, the model fits are shown to be limited by the conceptual basis of the model.

The utility of the models for recharge estimation has been shown but it has been evident that serious limitations affect the reliability of the results. This is because tensiometer data indicate

recharge during deficit periods. Consequently, the use of a single field capacity to represent the soil profile is inappropriate for these profiles in which dynamic response of the profile is important for recharge. Recharge estimates from both models do not show significant difference. It has been shown that the field bean/cabbage plots give the maximum recharge while the orchard gives the lowest recharge. Significant variations with crop in 1980 and 1981 are shown, but not for 1982.

The high spatial variability in measured soil moisture deficit has been shown and calls into question the use of measured data from single access tubes. Little variability is observed within tubes that are closely spaced.

The results show that single-layer models can provide realistic simulation of soil moisture status and can be better improved if field capacity determination is modified to include the drainage term. However for irrigation prediction, the models might just suffice.

CHAPTER 9

CONCLUSIONS

The aim of this study has been the evaluation of physically-based and empirically-based soil water models. This was to provide a better understanding of the interplay of parameters used in predicting soil water status.

A review of plant water relations indicated the complex and interrelated processes involved in soil moisture loss through plants (Section 3.2.2). An account of postulated models showed that model validation has not in general been carried out to an appropriate extent (Section 3.4). This has been ascribed to the difficulty of instrumenting field soil profiles and the problem of field soil heterogeneity in the evaluation of soil hydraulic parameters. Hence, the need for high quality field data. However, before validation was carried out, field experimentation under different agricultural crops was carried out at Silwood Park (Section 5.4). It was shown that the Silwood soils were predominantly sandy and non-uniform with depth (Section 5.4.3). Restriction of subsoil permeability occasioned by podsolisation below the 120 cm depth was observed. This showed that lateral flow was likely to occur in the soils of the study site.

The neutron probe was shown to offer the best method for determining soil moisture content *in situ*, while mercury manometer tensiometers, if carefully constructed and maintained, would operate efficiently within the range of operation. A comparison of the Institute of Hydrology's neutron probe calibration curve for a similar soil type with the bulk calibration derived for the site indicated that the Institute of Hydrology's curve would give a calculated soil moisture content of 11.98% higher than that derived for the site. This emphasises the need to carry out field calibration in situations where absolute values of soil moisture content are required. A special surface calibration technique which considered neutron probe count readings at depths near the soil surface (Section 5.6.2) was employed and good correlation between count ratio and moisture volume fraction was obtained.

The soil moisture content and potential readings collected for the period 1980-1982 allowed the evaluation of the soil moisture characteristics and the k(θ) relationship. A "natural balance" procedure was proposed for the derivation of these hydraulic parameters (Section 6.2.3.3). Serious limitations were shown to affect the results obtained for the K(θ) relationships. These limitations are the neglect of transpiration and drainage losses during the drying and wetting cycles. It was shown that this neglect caused overestimation of the K(θ) values, especially for depths near the soil surface, because of preferential moisture uptake by plant roots at these depths (Section 6.2.3.3). However, the "natural balance" technique offers promise for future use if used on bare soil surfaces. The k(θ) values derived for the site were shown to be variable with depth. On the other hand, the variation of soil moisture characteristics was low. In actuality, a single moisture characteristic was shown to be applicable to several layers.

A physically-based model which embodied soil and plant hydraulic characteristics was chosen for validation study (Section 4.2) and empirically-based soil water models that utilise the root constant concept were also adopted (Section 4.5). The physically-based soil water model was shown to simulate soil water status during a 45-day period. However, the simulations were shown to be affected by a variety of factors. These include the use of a single constant crown potential, the use of approximate values for the root hydraulic resistance and the extrapolation of the k(θ) value for the 15-25 cm layer to the 0-15 cm layer. The simulations were improved when the root hydraulic resistance value was increased (Section 7.6.3). This indicated that the root hydraulic resistance may be more important than the soil hydraulic resistance in improving model fits.

The interpretation of the observed zero-flux plane data was shown to be difficult as agreements with simulated hydraulic head profiles were not achieved (Section 7.6.5). This interpretation was shown to affect model behaviour.

In order to improve the physically-based soil water model fits, the following are recommended for further investigation:-

(a) Apply the "natural balance" technique to a bare plot for the derivation of k(θ).

(b) Carry out careful and better interpretation of the zero-flux plane data. This can be obtained if tensiometers are installed at smaller depth increments down the profile.

(c) Efforts are still required to better the technique for assessing the plant hydraulic resistance. This is to account for root proliferation and ageing.

(d) Explore the sensitivity of model predictions to changing $K(\theta)$ relationships.

The assessment of two single-layer empirically based soil water models were also made regarding their predictive abilities. The models were shown to give reasonable simulation of soil moisture status when expressed as a deficit with respect to field capacity (Section 8.4). The constant/linear depletion model was shown to be superior to the exponential model for the data set considered. The simulations were improved for different years if the available water capacity and root constant values were allowed to vary for different years (Section 8.3.1). The models were shown to be inadequate for recharge estimation when deficit condition occurred. This was evidenced by tensiometer readings which indicated recharge during deficit periods (Section 7.3.1.1). Consequently, the use of the field capacity to represent the whole soil profile has been shown to be inappropriate for profiles in which dynamic response is important.

High spatial variability in measured soil moisture deficit was shown for access tubes which were widely spaced. This casts doubt on the use of single access tubes for model validation. In order for empirically-based models to be flexible in serving irrigation needs of crops and recharge estimates, the drainage term should be included in future studies. It is therefore believed that further efforts are required to evaluate multi-layer models which incorporate a redistribution component.

REFERENCES

Amerman, C.R., Hillel, D.I. and Peterson, A.E. (1970), "A Variable-Intensity Sprinkling Infiltrometer", Soil Sci. Soc. Am. Proc., 34, 830-832.

Arnott, J.A. and Wales-Smith, B.G. (1978), "Soil Moisture Extraction Model (SMEM); A Component of Morecs", An internal report of a discussion held at the Meteorological Office, London.

Arya, L.M., Farrell, D.A. and Blake, G.R. (1975), "A field study of soil water depletion patterns in presence of growing soybean roots:- I. Determination of hydraulic properties of the soil", Soil Sci. Soc. Am. Proc., 39, 424-430.

Baier, W. (1967), "Relationships between soil moisture, actual and potential evapotranspiration", Proc. Hydrol. Symp., No. 6, Univ. of Saskatchewan, 15-16 November.

Baier, W. and Robertson, G.W. (1966), "A new versatile soil moisture budget", Canadian Journal of Plant Science, 46, 299-315.

Bell, J.P. (1976), "Neutron probe practice", Inst. of Hydrol., Wallingford, Rep. 19.

Bell, J.P. (1981), "Problems arising from the field capacity concept in comparing measured soil moisture deficits with MORECS Predictions", The Morecs Discussion Meeting, Institute of Hydrology, Wallingford, Rep. No. 78.

Belmans, C., Feyen, J. and Hillel, D. (1979), "An attempt at experimental validation of macroscopic-scale models of soil Moisture Extraction by Roots", Soil. Sci., 127, 174-186.

Belmans, C., Wesseling, J.G. and Feddes, R.A. (1981), "Simulation model of the water balance of a cropped soil providing different types of boundary conditions (SWATRE)", Instituut voor cultuurtechniek en Waterhuishouding Nota 1257.

Black, T.A., Gardner, W.R. and Thurtell, G.W. (1969), "The prediction of evaporation, drainage and soil water storage for a bare soil", Soil Sci. Soc. Am. Proc., 33, 655-660.

Bodman, G.B. and Colman, E.A. (1944), "Moisture and energy conditions during downward entry of water into soils", Soil Sci. Soc. Am. Proc., 8, 116-122.

Boonyatharokul, W. and Walker, W.R. (1979), "Evapotranspiration under depleting soil moisture", Proc. A.S.C.E., J. of Irrig. and Drainage, 105, 391-402.

Bouma, J., Hillel, D.I., Hole, F.D. and Amerman, C.R. (1971), "Field measurement of unsaturated hydraulic conductivity by infiltration through artificial crusts", Soil Sci. Soc. Am. Proc., 32, 362-364.

Bouyoucos, G.J. and Mick, A. (1948), "A comparison of electrical resistance units for making continuous measurements of soil moisture under field conditions", Plant Phys., 23, 532.

Brady, N.C. (1974), "The nature and properties of soils", MacMillan, New York.

Brooks, R.H. and Corey, A.T. (1966), "Properties of porous media affecting fluid flow", Proc. Am. Soc. Civ. Eng., J. Irrigation Div., IR2, 61-88.

Brouwer, R. (1965), "Water movement across the root", In the State and Movement of Water in Living Organisms, Symp. Soc. Exptl. Biol., 19, 131-159.

Bruin, H.A.R. De and Labians, W.N. (1980), "Een test van een nieuwe berekeningswijze van de open-water verdamping volgens Penman ten behoeve van snelle voorlichting omtrent de verdamping", KNMI, Verslagen V-357, De Bitt.

Buckingham, E. (1907), "Studies on the measurement of soil moisture", U.S. Dept. of Agr. Bur. of Soils, Bull. 38.

Calder, I.R., Harding, R.J. and Rosier, P.T.W. (1983), "An objective assessment of soil-moisture deficit models", J. of Hydrol., 60, 329-355.

Carbon, B.A. and Galbraith, K.A. (1975), "Simulation of the water balance for plants growing on coarse textured soils", Aust. J. Soil. Res., 13, 21-31.

Childs, E.C. (1940), "The use of soil moisture characteristics in soil studies", Soil Sci., 50, 239-252.

Childs, E.C. (1969), "An introduction to the physical basis of soil water phenomena", Wiley (Interscience) New York.

Childs, E.C. and Collis-George, N. (1950), "The permeability of porous materials", Proc. R. Soc., London, Series A, 201, 392-405.

Colman, E.A. and Bodman, G.B. (1944), "Moisture and energy conditions during downward entry of water into moist and layered soils", Soil Sci. Soc. Am. Proc., 9, 3-11.

Cooper, J.D. (1980), "Measurement of moisture fluxes in unsaturated soil in Thetford Forest", Inst. of Hydrol., Wallingford, Rep. 66.

Cowan, I.R. (1965), "Transport of water in the soil-plant-atmosphere system", J. Appl. Ecol., 2, 221-239.

Darcy, H. (1856), "Les Fountaines Publique de la Ville de Dijon", Dalmont, Paris.

Davidson, J.M., Biggar, J.W. and Nielsen, D.R. (1963), "Gamma radiation attenuation for measuring bulk density and transient water flow in porous media", J. Geophys. Res., 68, 4477-4783.

Davidson, J.M., Stone, L.R., Nielsen, D.R. and Larue, M.E. (1969), "Field measurement and use of soil-water properties", Water Resources Research, 5, 1312-1321.

De Jong, R. and Cameron, D.R. (1979), "Computer simulation model for predicting soil water content profiles", Soil Sci., 128, 41-48.

Denmead, O.T. and Shaw, R.H. (1959), "Evapotranspiration in relation to the development of the corn crop", Agron. J., 51, 725-726.

Denmead, O.T. and Shaw, R.T. (1962), "Availability of soil water to plants as affected by soil moisture content and meteorological conditions", Agron. J., 54, 385-390.

Diment, G.A. and Watson, K.K. (1983), "Stability analysis of water movement in unsaturated porous materials", 2: Numerical studies, Water Resources Research, 19, 1002-1010.

Doorenbos, J. and Pruitt, W.O. (1977), "Crop water requirement", Irrigation and Drainage Paper No. 24, Food and Agriculture Organisation, Rome.

Dunin, F.X. (1969), "The evapotranspiration component of a pastoral experimental catchment", J. of Hydrol., 7, 147-157.

Eagleson, P.S. (1970), "Dynamic hydrology", McGraw Hill, New York.

Feddes, R.A. (1971), "Water, heat and crop growth", Thesis, Comm. Agr. Univ. Wageningen, 71-12.

Feddes, R.A. and Rijtema, P.E. (1972), "Water withdrawal by plant roots", J. of Hydrol., 17, 33-59.

Feddes, R.A., Kowalik, P., Kolinska-Malinka, K. and Zaradny, H. (1976), "Simulation of field water uptake by plants using a soil water dependent root extraction", J. of Hydrol., 31, 13-26

Feddes, R.A., Neuman, S.P. and Bresler, E. (1974), "Field test of a modified numerical model for water uptake by root systems", Water Resources Research, 10, 1199-1206.

Federer, C.A. (1979), "A soil-plant-atmosphere model for transpiration and availability of soil water", Water Resources Research, 15, 555-562.

Federer, C.A. (1982), "Transpirational supply and demand: plant, soil and atmosphere effects evaluated by simulation", Water Resources Research, 18, 355-362.

Ferguson, H. and Gardner, W. (1962), "Water content measurement in soil columns by gamma-ray absorption", Soil Sci. Soc. Am. Proc., 26, 11-14.

Feyen, J., Belmans, C., Hillel, D. (1980), "Comparison between measured and simulated plant water potential during soil water extraction by potted rye grass", Soil Sci., 129, 180-185.

Gardner, C.M.K. (1981), "Preliminary comparisons between Morecs and measured soil moisture deficits", In the Morecs discussion meeting, Institute of Hydrology Report, 78, 20-27.

Gardner, C.M.K. and Bell, J.P. (1980), "Comparison of measured soil moisture deficits with estimates by MORECS", Proc. UNESCO Conf.- The Effect of Man on the Hydrological Regime with Special Reference to Representative and Experimental Basins", IAHS-AISH, Publ. No. 130, 337-341.

Gardner, W.R. (1956), "Calculation of capillary conductivity from pressure plate outflow data", Soil Sci. Soc. Am. Proc., 20, 317-320.

Gardner, W.R. (1960a), "Soil water relations in arid and semi-arid conditions", UNESCO, 15, 37-61.

Gardner, W.R. (1960b), "Dynamic aspects of water availability to plants", Soil Sci., 89, 63-73.

Gardner, W.R. (1964), "Relation of root distribution to water uptake and availability", Agron. J., 56, 41-45.

Gardner, W.R. and Ehlig, C.F. (1962), "Impedance to water movement in soil and plant", Science, 138, 3539, 522-523.

Gardner, W.R. and Ehlig, C.F. (1963), "The influence of soil water on transpiration by plants", J. Geophys. Res., 68, 5719-5724.

Gardner, W.R., Hillel, D. and Benyamini, Y. (1970), "Post irrigation movement of soil water: I. Redistribution," Water Resources Research, 6, 851-861. II. "Simultaneous redistribution and evaporation", Water Resources Research, 6, 1148-1153.

Goodhew, R. (1970), "A flexible technique for the estimation of short-term actual evaporation and soil moisture deficit over diverse catchment areas", MSc Thesis, Imperial College, London.

Goutzamanis, J.J. and Connor, D.J. (1977), "A simulation of the wheat crop", Bulletin No. 1, School of Agriculture, La Trobe University.

Green, W.H. and Ampt, G.A. (1911), "Studies on soil physics: Flow of air and water through soils", J. Agr. Sci., 4, 1-24.

Green, R.E. and Corey, J.C (1971), "Calculation of hydraulic conductivity: a further evaluation of predictive methods", Soil Sci. Soc. Am. Proc., 35, 3-8.

Green, R.E., Hanks, R.J. and Larson, W.E. (1964), "Estimates of field infiltration by numerical solution of the moisture flow equation", Soil Sci. Soc. Am. Proc., 28, 15-23.

Grindley, J. (1967), "The estimation of soil moisture deficits", Meteorological Magazine, 96, 97-108.

Grindley, J. (1970), "Estimation and mapping of evaporation", I.A.H.S. Symp. on World Water Balance.

Haines, W.B. (1930), "Studies in the physical properties of soils, V. The Hysteresis effect in capillary properties and the modes of moisture distribution associated therewith", J. Agr. Sci., 20, 97-116.

Hall, D.G.M. and Heaven, F.W. (1979), "Comparison of measured and predicted soil moisture deficits", J. Soil Sci., 30, 225-237.

Hanks, R.J. and Bowers, S.A. (1962), "Numerical solution of the moisture flow equation for infiltration into layered soils", Soil Sci. Soc. Am. Proc., 26, 530-534.

Herkelrath, W.N., Miller, E.E. and Gardner, W.R. (1977), "Water uptake by plants. I. Divided root experiments", Soil Sci. Soc. Am. Proc., 41, 1033-1038. II. "The root contact model", Soil Sci. Soc. Am. Proc., 41, 1039-1043.

Hillel, D. (1977), "Computer simulation of soil-water dynamics". Int. Dev. Res. Centre, Ottawa, Canada.

Hillel, D. (1980a), "Fundamentals of soil physics", Academic Press, New York.

Hillel, D. (1980b), "Application of soil physics", Academic Press, New York.

Hillel, D. and Benyamini, Y. (1974), "Experimental comparison of infiltration and drainage methods for determining unsaturated hydraulic conductivity of a soil profile in situ", Proc. FAO/IAEA Symp. Isotopes and Radiation Techniques in Studies of Soil Physics, Vienna, 271-275.

Hillel, D. and Gardner, W.R. (1970), "Measurement of unsaturated conductivity diffusivity by infiltration through an impeding layer", Soil Sci., 109, 149.

Hillel, D., Krentos, V.D. and Stylianou, Y. (1972), "Procedure and test of an internal drainage method for measuring soil hydraulic characteristics in situ", Soil Sci., 114, 395-400.

Hillel, D., Talpaz, H. and van Keulen, H. (1976), "A macroscopic scale model of water uptake by a non-uniform root system and of water and salt movement in the soil profile", Soil Sci., 121, 242-255.

Hillel, D. and van Bavel, C.H.M. (1976), "Simulation of profile water storage as related to soil hydraulic properties", Soil Sci. Soc. Am. Proc., 40, 807-815.

Hillel, D., van Beek, C.G.E.M. and Talpaz, H. (1975), "A microscopic scale model of soil water uptake and salt movement to plant roots", Soil Sci., 120, 385-399.

Holmes, R.M. and Robertson, G.W. (1959), "A modulated soil moisture budget", Monthly Weather Review, 87, 101-106.

Holtan, H.N. (1961), "A concept for infiltration estimates in watershed engineering", U.S. Dept. Agr. Res. Service Publ. 41-51.

Horton, R.E. (1940), "An approach toward a physical interpretation of infiltration-capacity", Soil Sci. Soc. Am. Proc., 5, 399-417.

Huck, M.G., Klepper, B. and Taylor, H.M. (1970), "Diurnal variations in root diameter", Pl. Physiol., 45, 52-530.

Idso, S.B., Reginato, R.J. and Jackson, R.D. (1979), "Calculation of evaporation during the three stages of soil drying", Water Resources Research, 15, 2.

Israelsen, O.W. and Hansen, V.E. (1967), "Irrigation principles and practices", Wiley, New York.

Jackson, R.A. (1972), "On the calculation of hydraulic conductivity", Soil Sci. Soc. Am. Proc., 36, 380-383.

Kirkham, D. and Powers, W.L. (1972), "Advanced soil physics", Wiley-Interscience, New York.

Klute, A., Whisler, F.D. and Scott, E.H. (1965), "Numerical solution of the flow equation for water in a horizontal finite soil column", Soil Sci. Soc. Am. Proc., 29, 353-358.

Kohler, M.A. and Linsley, R.K. (1951), "Predicting runoff from storm rainfall", U.S. Weather Bureau Res., Pap. 34, Washington.

Kostiakov, A.N. (1932), "On the dynamics of the coefficient of water-percolation in soils and on the necessity of studying it from a dynamic point of view for purposes of amelioration", Trans. Com. Int. Soc. Soil Sci., 6th, Moscow, Part A, 17-21.

Kunze, R.J., Uehara, G. and Graham, K. (1968), "Factors important in the calculation of hydraulic conductivity", Soil Sci. Soc. Am. Proc., 32, 760-765.

Lawlor, D.W. (1972), "Growth and water use of Lolium perenne I. Water Transport", J. Appl. Ecol., 9, 79-98.

Lawless, G.P., MacGIllivray, N.A. and Nixon, P.R. (1963), "Soil moisture interface effects upon reading of neutron moisture probes", Soil Sci. Soc. Am. Proc., 27, 502.

Makkink, G.F. and van Heemst, H.D.J. (1975), "Simulation of the water balance of arable land and pastures", Centre for Agricultural Publishing and Documentation, Wageningen, Netherlands.

Marshall, T.J. (1958), "A relation between permeability and size distribution of pores", J. Soil Sci., 9, 1-18.

Marshall, J.J. and Holmes, J.W. (1979), "Soil Physics", Cambridge Univ. Press, Cambridge.

McGowan, M. and Williams, J.B. (1980), "The water balance of an agricultural catchment. 1. Estimation of evaporation from soil water records", J. of Soil Sci., 31, 217-230.

McNeil, D.D. and Shuttleworth, W.J. (1975), "Comparative measurements of energy fluxes over a pine forest", Boundary Layer Meteorol., 7, 297-313.

Mein, R.G. and Larson, C.L. (1973), "Modelling infiltration during a steady rain", Water Resources Research, 9, 384-394.

Miller, D.E. and Gardner, W.H. (1962), "Water infiltration into stratified soils", Soil Sci. Soc. Am. Proc., 26, 115-118.

Molz, F.J. (1971), "Interaction of water uptake and root distribution", Agron. J., 63, 608-610.

Molz, F.J. (1975), "Potential distributions in the soil-root system", Agron. J., 67, 726-729.

Molz, F.J. (1981), "Models of water transport in the soil-plant system - a review", Water Resources Research, 17, 1245-1260.

Molz, F.J. and Remson, I. (1970), "Extraction term models of soil moisture use by transpiring plants", Water Resources Research, 6, 1346-1356.

Molz, F.J., Remson, I., Fungaroli, A.A. and Drake, R.L. (1968), "Soil moisture availability for transpiration", Water Resources Research, 4, 1346-1356.

Monteith, J.L. (1965), "Evaporation and environment", Symp. Soc. Exptl. Biol., 19, 205-234.

Nash, J.E. and Sutcliffe, J.V. (1970), "River flow forecasting through conceptual models: Part I - A discussion of principles, J. Hydrol., 10, 282-290.

Newman, E.I. (1969), "Resistance to water flow in soil and plant - 1. Soil resistance in relation to amount of roots: theoretical estimates", J. Appl. Ecol., 6, 1-22.

Nimah, M.N. and Hanks, R.J. (1973), "Model for estimating soil water, plant and atmospheric interrelations - I. Description and sensitivity", Soil Sci. Soc. Am. Proc., 37, 522-527.

Olgard, P.L. (1965), "On the theory of the neutronic method for measuring the water content in soil", Danish Atomic Energy Commission, Roskilde, Denmark, Riso Rep. 97, 1-74.

Ogata, G. and Richards, L.A. (1957), "Water content changes following irrigation of bare field soil that is protecetd from evaporation", Soil Sci. Soc. Am. Proc., 21, 355-356.

Parkes, M.E. and O'Callaghan, J.R. (1980), "Modelling soil water changes in a well-structured, freely draining soil", Water Resources Research, 16, 755-761.

Peck, A.J. (1964), "The diffusivity of a water in a porous material", Austr. J. of Soil Research, 2:1-7.

Pegg, R.K. and Ward, R.C. (1972), "Evaporation from a small clay catchment", J. Hydrol., 15, 149-165.

Penman, H.L. (1948), "Natural evaporation from open water, bare soil and grass", Proc. Roy. Soc., London (A), 193, 120-145.

Penman, H.L. (1949), "The dependence of transpiration on weather and soil conditions", J. Soil Sci., 1, 74-89.

Penman, H.L. (1956), "Evaporation: an introductory survey", Neth. J. Agr. Sci., 4, 9-29.

Penman, H.L. and Schofield, R.K. (1951), "Some physical effects of assimilation and transpiration", Symp. Soc. Exptl. Biol., 5, 115-129.

Philip, J.R. (1957a), "The theory of infiltration. I. The infiltration equation and its solution", Soil Sci., 83, 345-357.

Philip, J.R. (1957b), "The physical principles of water movement during the irrigation cycle", Proc. 3rd Int Cong. Irrig. Drainage, 8, 125-128.

Philip, J.R. (1966), "Plant water relations - some physical aspects", Ann. Rev. Plant Physiol., 17, 245-268.

Pierce, L.T. (1958), "Estimating seasonal and short-term fluctuations in evapotranspiration from meadow crops". Bull. Amer. Meteorol. Soc., 39, 73-78.

Poulovassilis, A., Krentos, V.D., Stylianou, Y. and Metochis Ch. (1974), "Soil water properties of a layered soil determined in situ", Isotope and Radiation Tech. in Soil Physics and Irrigation Studies Proceedings, 205-224.

Raats, P.A.C. (1973), "Unstable wetting fronts in uniform and non-uniform soils", Soil Sci. Soc. Am. Proc., 37, 681-685.

Rawitz, E., Margolin, M. and Hillel, D. (1972), "An improved variable intensity sprinkling infiltrometer", Soil Sci. Soc. Am. Proc., 36, 533-535.

Remson, I., Drake, R.L., McNeary, S.S. and Walls, E.M. (1965), "Vertical drainage of an unsaturated soil", Am. Soc. Civil Eng. Proc., J. Hyd. Div., 9, 55-74.

Reynolds, S.G. (1970), "The gravimetric method of soil moisture determination", J. Hydrol., Parts I, II, III, 11, 258-300.

Richards, L.A. (1931), "Capillary conduction of liquids in porous media", Physics, 1, 318-333.

Richards, L.A. and Gardner, W.A. (1936), "Tensiometers for measuring the capillary tension of soil water", J. Amer. Soc. Agron., 28, 352-358.

Rijtema, P.E. (1965), "An analysis of actual evaporation", Agric. Res. Report, 659, Pudoc, Wageningen.

Rijtema, P.E. (1966), "Transpiration and production of crops in relation to climate and irrigation". Intl. Comm. on Irrigation and Drainage, Special Session.

Rijtema, P.E. (1969), "On the relation between transpiration, soil physical properties and crop production as a basis for water supply plans", Committee for Hydrol. Res. (T.N.O.), 15, 28-58.

Ritchie, J.T. (1972), "Model for predicting evaporation from a row crop with incomplete cover", Water Resources Research, 8, 1024-1213.

Rose, C.W. (1966), "Agricultural physics", Pergamon Press, Oxford.

Rose, C.W., Stern, W.R. and Drummond, J.E. (1965), "Determination of hydraulic conductivity as a function of depth and water content for soil in situ", Austr. J. of Soil Res., 3, 1-9.

Rowse, H.R., Stone, D.A. and Gerwitz, A. (1978), "Simulation of water distribution in soil and its comparison with experiment", Plant Soil, 49, 534-550.

Rubin, J. (1966), "Theory of rainfall uptake by soils initially drier than their field capacity and its applications", Water Resources Research, 2, 739-749.

Rubin, J. (1967), "Numerical method for analysing hysteresis - affected, post-infiltration reditribution of soil moisture", Soil Sci. Soc. Am. Proc., 31, 13-20.

Russell, G. (1980), "Crop evaporation, surface resistance and soil water status", Agric. Met., 21, 213-226.

Rutter, A.J. (1975), "The hydrological cycle in vegetation", In "Vegetation and the atmosphere, Vol. 1 : Principles" (edited by J.L. Monteith), Academic Press, London, 111-150.

Rutter, A.J. (1980), Personal Communications, Imperial College, London.

Salter, P.J. and Williams, J.B. (1967), "The influence of texture on the moisture characteristics of soils - IV : A method of estimating the available water capacity of profiles in the field", J. Soil Sci., 18, 174-181.

Saxton, K.E., Johnson, H.P. and Shaw, R.H. (1974), "Modelling evapotranspiration and soil moisture", Trans. ASAE, 17, 673-677.

Schofield, R.K. and Penman, H.L. (1948), "The concept of soil moisture deficit", Proc. 2nd Int. Conference on Soil Mechanics, Rotterdam, Vol. I, 132-136.

Schmugge, T.J. (1978), "Remote sensing of surface soil moisture", J. Appl. Meteorol., 17, 1549.

Schmugge, T.J., Jackson, T.J. and McKim, H.L. (1980), "Survey of methods for soil moisture determination", Water Resources Research, 16, 961-979.

Shaw, R.H. (1963), "Estimating soil moisture under corn", Iowa State Univ. Res. Bull., 520, 969-980.

Shuttleworth, W.J. (1976), "A one-dimensional theoretical description of the vegetation - atmosphere interaction", Boundary Layer Meteorol., 10, 273-302.

Shuttleworth, W.J. (1978), "A simplified one-dimensional theoretical description of the vegetation-atmosphere interaction", Boundary Layer Meteorol., 14, 3-27.

Shuttleworth, W.J. (1979), "Evaporation", Institute of Hydrology Report, 56, Wallingford, Oxon.

Slayter, R.O. (1956), "Evapotranspiration in relation to soil moisture", Neth. J. Agric. Sci., 4, 73-76.

Slayter, R.O., Bierhuizen, J.F. and Rose, C.W. (1965), "A porometer for laboratory and field operation", J. Exp. Bot., 16, 182.

Slichter, C.S. (1899), "Theoretical investiations of the motion of groundwater", U.S. Geol. Survey Ann. Rep., 19, 295-384.

Smith, K. (1964), "A long-period assessment of the Penman and Thornthwaite P.E. Formulae", J. Hydrol., 2, 277-290.

Soil Survey of England and Wales (1983), Rothamsted Experimental Station, Harpendon, Herts, England.

Staple, W.J. (1969), "Comparison of computed and measured moisture redistribution following infiltration", Soil Sci. Soc. Am. Proc., 33, 206.

Stark, N. (1968), "Spring transpiration of three desert species", J. Hydrol., 6, 297-305.

Stewart, J.B. and Thom, A.S. (1973), "Energy budgets in a pine forest", Quart. J. Roy. Meteorol. Soc., 99, 154-170.

Swinbank, W.C. (1951), "The measurement of vertical transfer of heat and water vapour by eddies in the lower atmosphere", J. Meteorol., 8, 135-145.

Szeicz, G. and Long, I.F. (1969), "Surface resistance of crop canopies", Water Resources Research, 5, 622-633.

Tachjman, S. (1971), "Evaporation and energy balance of forest and field", Water Resources Research, 7, 511-523.

Tanner, C.B. (1968), "Evaporation of water from plants and soil", In "Water Deficits and Plant Growth", Academic Press, New York.

Taylor, H.M. and Klepper, B. (1975), "Water uptake by cotton root systems", An examination of assumptions in the single root model", Soil Sci., 120, 57-70.

Thom, A.S. and Oliver, H.R. (1977), "On Penman's equation for estimating regional evaporation". Quart. J. Roy. Meteorol. Soc., 105, 345-357.

Thom, A.S., Stewart, J.B. and Oliver, H.R. (1975), "Comparison of aerodynamic and energy budget estimates of fluxes over a pine forest", Quart. J. Roy. Meteorol. Soc., 101, 93-105.

Thompson, N. (1981), "MORECS", the Morecs discusison meeting, Institute of Hydrology, Report, 78, 1-10.

Thompson, N. (1982), "A comparison of formulae for the calculation of water loss from vegetated surfaces", Agric. Meteorol., 26, 265-272.

Thompson, N., Barne, I.A. and Ayles, M. (1981), "The Meteorological Office rainfall and evaporation calculation system (MORECS)", Hydrology Memo No. 45, Meteorological Office.

Thomson, R.I. (1981), "In situ measurement of the unsaturated hydraulic conductivity function of a soil profile at Silwood Park", MSc Thesis, Dept of Civil Eng., Imperial College, London.

Thornthwaite, C.W. (1948), "An approach towards a rational classification of climate", Geog. Review, 38, 85-94.

Thornthwaite, C.W. and Mather, J.R. (1955), "The water balance", Publ. in Climatology VIII, 1, Drexel Inst. of Tech., New Jersey.

Tinker, P.B. (1976), "Roots and water", Phil. Trans. Roy. Soc. Lond., B, 273, 445-461.

Van Bavel, C.H.M. (1966), "Potential evaporation: the combination concept and its experimental verification", Water Resources Research, 2, 455-467.

Van Bavel, C.H.M. (1976), "Stomatal control of root water uptake dynamics, Agron. Abstr., 124.

Van Bavel, C.H.M., Stirk, G.B. and Brust, K.J. (1968), "Hydraulic properties of a clay loam soil and the field measurement of water uptake by roots", Parts I, II and III, Soil Sci. Soc. Am. Proc., 32, 310-326.

Van den Honert, T.H. (1948), "Water transport as a catenary process", Faraday Soc. Discuss., 3, 146-153.

Veihmeyer, F.J. and Hendrickson, H.H. (1955), "Does transpiration decrease as soil moisture decreases?" Trans. Am. Geophys. Union, 36, 425-448.

Visser, W.C. (1966), "Progress in the knowledge about the effect of soil moisture content on plant production", Inst. Land Water Management, Wageningen, Netherlands, Tech. Bull. 45.

Walley, W.J. and Hussein, D.E.D.A. (1982), "Development and testing of a general purpose soil-moisture-plant model", Hydrol. Sciences, 27, 1-17.

Wang, F.C. and Lakshminarayana, V. (1968), "Mathematical simulation of water movement through unsaturated non-homogenous soil", Soil Sci. Soc. Am. Proc., 32, 329-334.

Ward, R.C. (1963), "Observation of P.E. on Thames flood plain 1959-60", J. Hydrol., 1, 183-194.

Watson, K.K. (1966), "An instantaneous profile method for determining the hydraulic conductivity of unsaturated porous mterials", Water Resources Research, 2, 709-715.

Weatherley, P.E. (1976), "Introduction : Water movement through plants", Phil. Trans. Roy. Soc. Lond., B, 273, 435-444.

Wellings, S.R. and Bell, J.P. (1980), "Movement of water and nitrate in the unsaturated zone of upper chalk near Winchester, Hants, England", J. of Hydrol., 48, 119-136.

Wheater, H.S. (1977), "Flood runoff from small rural catchments", Ph.D. Thesis, Univ. of Bristol, England.

Wheater, H.S. and Weaver, E. (1980), "A soil moisture model for catchment analysis", In the Influence of Man on the Hydrological Regime, Proc. Helsinki Symp., IAHS Publ. No. 130, 377-384.

Wheater, H.S., Sherratt, D.J. and Nwabuzor, S.S. (1982), "Assessment of effects of land use on groundwater recharge", In Improvement of methods of long-term prediction of variations in groundwater resources and regimes due to human activity, Proc. Exeter Symp., IAHS Publ. No. 136, 135-147.

Whisler, F.D., Klute, A. and Millington, R.J. (1968), "Analysis of steady-state evapotranspiration from a soil column", Soil Sci. Soc. Am. Proc., 32, 167-174.

Wind, G.P. and van Doorne, W. (1975), "A numerical model for the simulation of unsaturated vertical flow of moisture in soils", J. of Hydrol., 24, 1-20.

Woodhead, T. (1976), "Annual Report, Part 1", Rothamstead Exp. Stn., Harpenden, Herts.

Youngs, E.G. (1958), "Redistribution of moisture in porous materials after infiltration", Soil Sci., 86, 117-125.

Youngs, E.G. (1964), "An infiltration method of measuring the hydraulic conductivity of unsaturated porous materials", Soil Sci., 109, 307-311.

Zahner, R. (1967), "Refinement in empirical functions for realistic soil moisture regimes under forest cover", Int. Symp. on Forest Hydrology (edited by W.E. Sopper and H.W. Lull).